Theoretical Solid State Physics

Sommersemester 2018
Technische Universität Berlin

PD Dr. Gernot Schaller

July 18, 2020

This is my first lecture on solid state physics, and the script should therefore be considered as being in construction. It will be extended and modified throughout the course and it would therefore be wise not to print it in the beginning but rather for later reference. The script represents an excerpt of other lecture notes and books. Figures – if not otherwise noted – are originals, though. A significant portion of the material treated has been taken from lecture notes of Tobias Brandes. The lecture script will be made available online at `http://www1.itp.tu-berlin.de/schaller/lectures.html`.

Corrections and suggestions for improvements should be addressed to me gernot.schaller@tu-berlin.de. Special thanks go to Dr. Javier Cerrillo and Philipp Stammer for turned-in corrections.

The lecture will take place on Thursdays 10:15–11:45 and Fridays 8:30–10:00. In addition to the lecture, students should attend the seminar on Tuesdays 14:15–16:00 in EW 114. To earn the credit points, students should turn in the regular homework assignments in the seminar and score at least 60% there.

some useful literature for the lecture:

- lecture script: `http://www1.itp.tu-berlin.de/schaller/lectures.html`
- G. Czycholl, Theoretische Festkörperphysik, Springer, Heidelberg (2008)
- C. Kittel, Quantum Theory of Solids, Wiley, (1987)
- Ashcroft/Mermin, Solid State Physics, Holt Saunders (1981)
- Haken: Quantenfeldtheorie des Festkörpers, Teubner
- Ibach, Lüth: Festkörperphysik, Springer
- Kittel: Quantentheorie der Festkörper, Oldenbourg
- Scherz: Quantenmechanik, Teubner

The tentative content of the lecture includes

- crystal structures
- phonons
- free electrons
- interacting electrons
- electron-phonon interactions
- superconductivity
- magnetism

Contents

Chapter 1

Crystals

In this chapter, we mainly follow Ref. [3].

Crystals can be seen as extremely large molecules. Whereas the number of constituents in normal molecules can range up to a few thousand atoms e.g. in case of amino acids, crystals extend into the macroscopic regime and can thus contain in the order of 10^{23} atoms. To understand the phenomena occurring in crystals, it is often enough to understand the electron-electron interactions only, as the positions of the atoms are roughly fixed. We only have to take care of the atomic displacements from their equilibrium positions, leading to the concept of phonons. The regularity present in many crystals is helpful in the theoretical treatment. We will start as usual from this phenomenologic perspective and will therefore consider the presence of a lattice structure as given. From this perspective, we will first review possible classification schemes for lattices and crystal systems. Roughly speaking, crystal systems are defined by point symmetries such as rotation, whereas lattices are defined by translational invariance.

1.1 Definitions

Most lattices in solid state systems can be described with the help of crystals.

Box 1 (crystal lattice/elementary cell) *A* **crystal lattice** *consists of abstract points* $\boldsymbol{R_n}$ *that are fully defined by integer combinations of d linearly independent basis vectors*

$$\boldsymbol{R_n} = \sum_{i=1}^{d} n_i \boldsymbol{a}_i \,, \qquad n_i \in \mathbb{Z} \,, \qquad \boldsymbol{n} = (n_1, \ldots, n_d) \,. \tag{1.1}$$

The basis vectors $\boldsymbol{a}_i$ *span the* **conventional elementary cell**, *which by periodic continuation covers the full space.*

From this it follows that such lattices need to obey some translational invariance: When shifted along the basis vectors, the lattice must look the same. They are infinitely large and are therefore rather a theoretical construct. Beyond the translation, crystals also obey further discrete rotational symmetries, which allows one to classify them.

We note that the definition of a crystal lattice does not imply that the basis vectors are orthonormal and neither is the choice of a basis unique. Given the basis vectors, we can compute for $d = 2$ and $d = 3$ the volume of the elementary cell via

$$\begin{aligned} V_{\rm ec}^{(2)} &= \left|\boldsymbol{a}_1 \times \boldsymbol{a}_2\right| \,, \\ V_{\rm ec}^{(3)} &= \left|\boldsymbol{a}_1 \cdot (\boldsymbol{a}_2 \times \boldsymbol{a}_3)\right| \,. \end{aligned} \tag{1.2}$$

However, when we think about realistic systems, the lattice points need not always coincide with the physical positions of all atoms. For example, some lattices may be constructed from atoms of different species and thereby loose the translational invariance. To account for this, a **Bravais lattice** [1] can be constructed from a crystal lattice by adding additional lattice points to the elementary cell. These additional points can either lie in the center of the elementary cell (body-centered), in the centers of the surfaces of the elementary cell (face-centered), or in the centers of two opposing surfaces of the elementary cell (base-centered). Thus, for every crystal lattice (defined by symmetry), one has at least one Bravais lattice. In the following, we will exemplify this in two and three dimensions (as the one-dimensional case is rather trivial).

1.1.1 Crystals in 2 dimensions

In two dimensions $d = 2$, there are four crystal systems and five Bravais lattices. In particular, we have the crystal systems:

1. The **quadratic system**, which is characterized by $\boldsymbol{a}_1 \cdot \boldsymbol{a}_2 = 0$ and $|\boldsymbol{a}_i| = a$. The quadratic system has a four-fold rotational symmetry, a mirror symmetry along two axes, and the inversion $\boldsymbol{r} \to -\boldsymbol{r}$ as symmetry operations that leave it invariant. The corresponding Bravais lattice is defined by $n_i \in \mathbb{Z}$ and $\boldsymbol{a}_1 = a\boldsymbol{e}_x$ and $\boldsymbol{a}_2 = a\boldsymbol{e}_y$. Its elementary cell has again the shape of a square.

2. The **rectangular system**, where one can choose $\boldsymbol{a}_1 \cdot \boldsymbol{a}_2 = 0$ but basis vectors of different lengths. It is only invariant with respect to a mirror symmetry with respect to two axes and inversion. The Bravais lattice is defined as before, just with two lattice constants accounting for the two directions, and the elementary cell is a rectangle. Alternatively, we can also choose the basis vectors having the same lengths but then they are not orthogonal to each other, see the second column in Fig. 1.1. In this case, the elementary cells become parallelograms.

3. The **hexagonal system**, defined by basis vectors of equal length but enclosing a 120 degree angle $\boldsymbol{a}_1 \cdot \boldsymbol{a}_2 = 1/2$. It has a six-fold rotational symmetry, a mirror symmetry along three axes, and the inversion. Its elementary cells are rhombuses.

4. The **oblique system**, where the angle between the basis vectors is not rectangular and also their length is different. Here, inversion is the only remaining symmetry operation, and the elementary cells are parallelograms.

These crystal systems and Bravais lattices are also visualized in Fig. 1.1.

When analyzing these lattice structures a bit, one may come to the conclusion that the body-centered rectangular lattice could also simply be considered a special oblique system. However, since it has all the symmetries of the rectangular crystal system, it is usually considered an own class.

1.1.2 Crystals in 3 dimensions

In three dimensions, there are seven crystal systems and 14 Bravais lattices:

1. The **cubic system** now includes three Bravais lattices: The simple cubic lattice (sc), the body-centered cubic lattice (bcc), and the face-centered cubic lattice (fcc). The conventional elementary cell is a cube.

---

[1] Auguste Bravais (1811–1863) did research on crystal physics and optics.

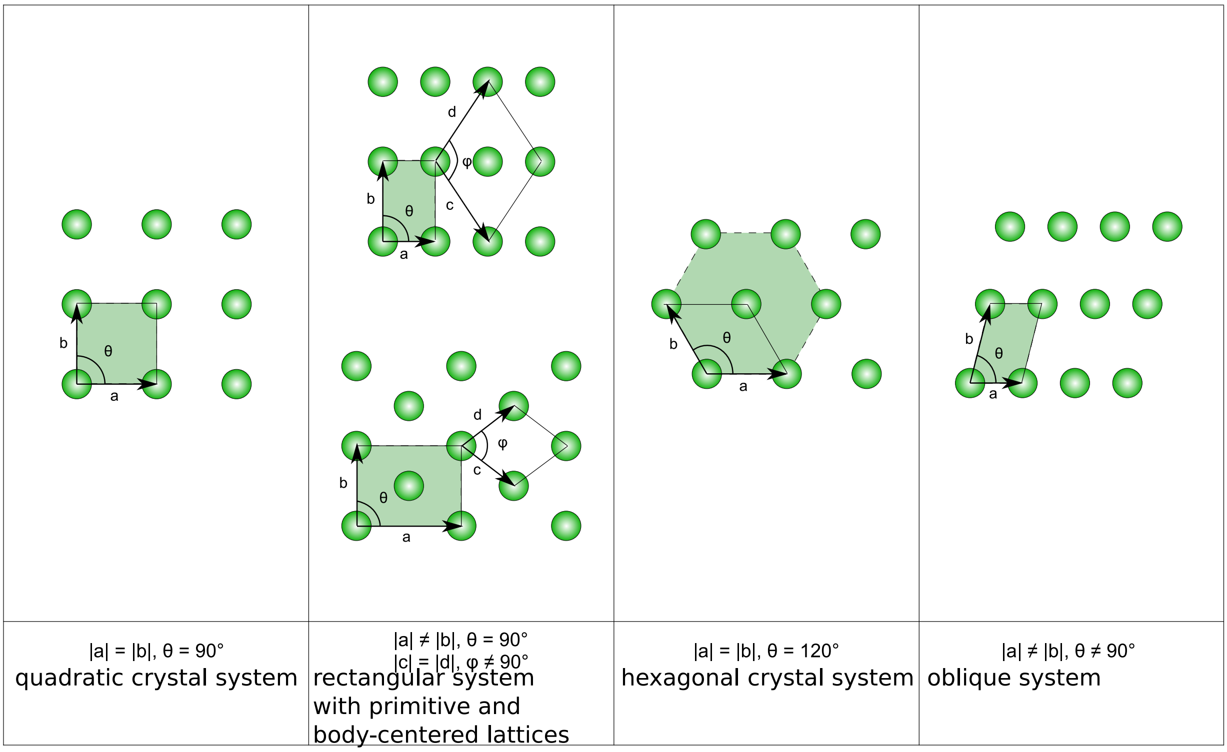

Figure 1.1: Visualization of the four different crystal systems quadratic, rectangular, hexagonal, and oblique (from left to right) [adapted from Wikipedia `https://commons.wikimedia.org/w/index.php?curid=3912829`]. The rectangular system can be classified with orthogonal basis vectors of different length a, b or non-orthogonal basis vectors of equal length c, d, and it has two Bravais lattices (primitive, top, and body-centered, bottom).

2. The **tetragonal system** has a square base but its height is different from the base lattice constant. All angles remain rectangular. It has two Bravais lattices: The simple tetragonal one and the body-centered tetragonal lattice.

3. The **orthorhombic system** can have different lattice constants, but all angles still remain rectangular. It has four different Bravais lattices, simple, base-centered, body-centered, and face-centered.

4. The **monoclinic system** has a rectangular base and two Bravais lattices: simple and base-centered.

5. The **rhombohedral system** has equal lattice constants and equal angles and only one Bravais lattice.

6. The **hexagonal system** is formed by piling hexagonal 2d lattices on top of each other.

7. The triclinic system.

An overview of these lattices and crystal systems is visualized in Fig. 1.2. Again, we see that a crystal system can have multiple Bravais lattices that however obey the same symmetry operations. For example, all lattices of the cubic crystal system have four-fold rotational symmetries around three different axes (passing throught the centers of the cube faces), three-fold rotational symmetries around four different axes (body diagonals), two-fold rotational symmetries around 6 axes (diagonals through opposing edge centers) and inversion symmetry.

The classification into crystal groups is important because many reasonable Hamilton operators have the same symmetry as the crystal. This means that they will commute with the

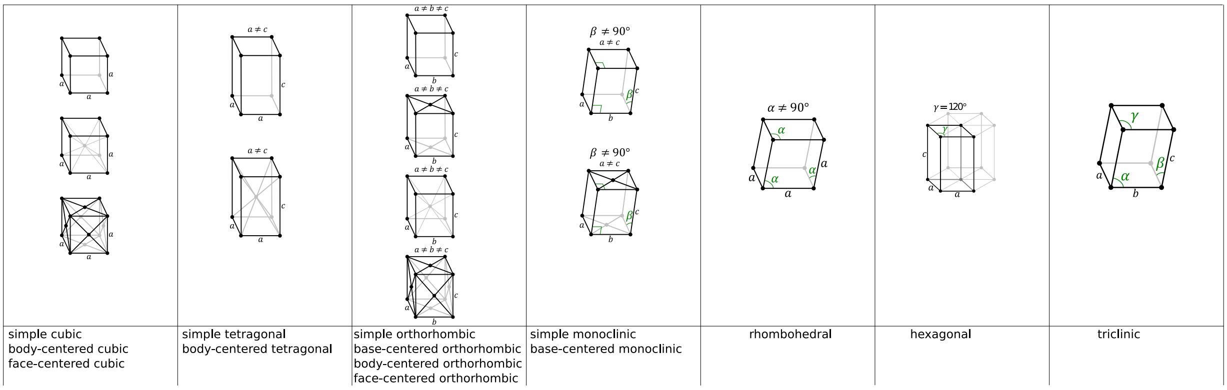

Figure 1.2: Visualization of the seven different crystal systems cubic, tetragonal, orthorombic, monoclinic, rhombohedral, hexagonal, triclinic (from left to right) [adapted from Wikipedia]. For many crystal systems there exist different Bravais lattices but all of them obey the symmetries of the crystal system.

corresponding symmetry operations, and just by finding the correct lattice classification one may therefore identify conserved quantities.

1.1.3 The cubic crystal system

Due to its simple structure and widespread application, we will here only discuss the cubic crystal system in greater detail.

- Each lattice point in the simple-cubic lattice has six next neighbours (each at distance a). A suitable choice of basis vectors is then

$$\boldsymbol{a}_1 = a \begin{pmatrix} 1 \\ 0 \\ 0 \end{pmatrix}, \qquad \boldsymbol{a}_2 = a \begin{pmatrix} 0 \\ 1 \\ 0 \end{pmatrix}, \qquad \boldsymbol{a}_3 = a \begin{pmatrix} 0 \\ 0 \\ 1 \end{pmatrix}, \qquad V_{\rm ec}^{(sc)} = a^3 \,. \tag{1.3}$$

  Thus, the conventional elementary cell is associated with each node of the simple cubic lattice. For this Bravais lattice, the conventional elementary cell is also the smallest one that is needed to cover the full space.

- For a face-centered cubic lattice we have 12 next neighbours (at distance $a/\sqrt{2}$). We could now take the basis vectors of the simple cubic lattice in Eq. (1.3). These would span the conventional elementary cell, which however is not the smallest one. Alternatively, we can choose the connection to three of the the next neighbours to define the basis vectors spanning the **primitive elementary cell** (which is the smallest possible one)

$$\boldsymbol{a}_1 = \frac{a}{2} \begin{pmatrix} 1 \\ 1 \\ 0 \end{pmatrix}, \qquad \boldsymbol{a}_2 = \frac{a}{2} \begin{pmatrix} 1 \\ 0 \\ 1 \end{pmatrix}, \qquad \boldsymbol{a}_3 = \frac{a}{2} \begin{pmatrix} 0 \\ 1 \\ 1 \end{pmatrix}, \qquad V_{\rm pec}^{(fcc)} = \frac{a^3}{4} \,. \tag{1.4}$$

  The corresponding primitive elementary cell has the shape of a diamond and by periodically continuing it, the complete space is covered.

- Finally, for a body-centered cubic one has 8 next neighbours (at distance $\sqrt{3}a/2$), and we to find the primitive elementary cell we can form a basis by choosing the connection to three of them

$$\boldsymbol{a}_1 = \frac{a}{2} \begin{pmatrix} 1 \\ 1 \\ 1 \end{pmatrix}, \qquad \boldsymbol{a}_2 = \frac{a}{2} \begin{pmatrix} 1 \\ -1 \\ 1 \end{pmatrix}, \qquad \boldsymbol{a}_3 = \frac{a}{2} \begin{pmatrix} -1 \\ 1 \\ 1 \end{pmatrix}, \qquad V_{\rm pec}^{(bcc)} = \frac{a^3}{2} \,. \tag{1.5}$$

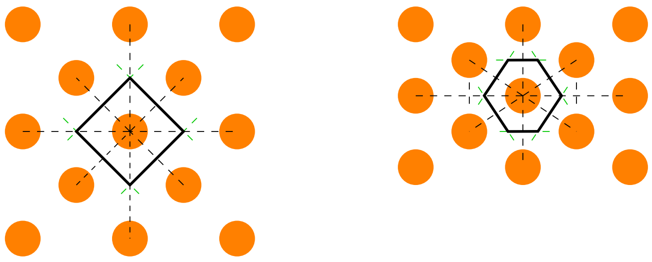

Figure 1.3: Visualization of the Wigner-Seitz construction for two different (left and right) 2d body-centered rectangular lattices. Connection lines to next neighbors and perpendicular lines are shown with black and green dashed lines, respectively, and the resulting Wigner-Seitz cell is shown with bold lines.

Thus, an elementary cell is associated with each node of the simple cubic lattice.

It is visible that the volume of the primitive elementary cells for the fcc and bcc lattices is much smaller than for the sc lattice, where one has one elementary cell per lattice node. However, one has to keep in mind that the lattice nodes in fcc and bcc lattices take part in many different elementary cells. For example, for an fcc lattice the cube corners belong to 8 elementary cells each and the points on the cube faces belong to two elementary cells. Therefore, in total we have $8 * 1/8 + 6 * 1/2 = 4$ lattice nodes per elementary cell, which yields the same ratio as for the simple cubic lattice.

We have seen that by identifying the next neighbours, one can find alternative bases and alternative elementary cells. A further way to find an elementary cell is the **Wigner-Seitz** [2] construction:

Box 2 (Wigner-Seitz cell) *The Wigner-Seitz cell around one lattice point is the smallest volume enclosed by the perpendicular planes placed at half-distance of the connection lines to all neighbours. It is a primitive elementary cell.*

Typically, one will of course start with the next neighbours in this construction, then add the next-to-next neighbours and so on until the enclosed volume does no longer become smaller, as depicted in Fig. 1.3. Again, the Wigner-Seitz cell is also an elementary cell in the sense that by periodic continuation of it the full space is covered. In addition, we see that by construction each of these particular elementary cells contains exactly one lattice node.

We see that if we would apply this construction to non-periodic structures, it is equivalent to a Voronoi [3] tessellation.

1.2 Realistic crystal structures

So far, we have defined all lattices as abstract nodes. When we talk about realistic solid bodies, these nodes can often be identified with the physical position of atoms or ions. However, this is not always the case. As a counterexample, consider e.g. a crystal made of amino acids, where we put a specific amino acid at each lattice node in the same orientation. Now, besides the lattice classification, the position of the atoms is given by

$$R_{\boldsymbol{n}\mu} = R_{\boldsymbol{n}} + R_{\boldsymbol{\mu}}\,, \tag{1.6}$$

where $R_{\boldsymbol{n}}$ denotes the lattice node as in Eq. (1.1) and $R_{\boldsymbol{\mu}}$ is constrained (normally to the elementary cell). This now allows one to describe the most general lattice structures.

We will just summarize a few popular lattices here:

---

[2] E.P. Wigner (1902–1995) was a theoretical physicist who won the Nobel price in 1963 and F. Seitz was one of his co-workers.

[3] Georgi Feodosjewitsch Voronoi (1868–1908) was a russian-ukrainian mathematician.

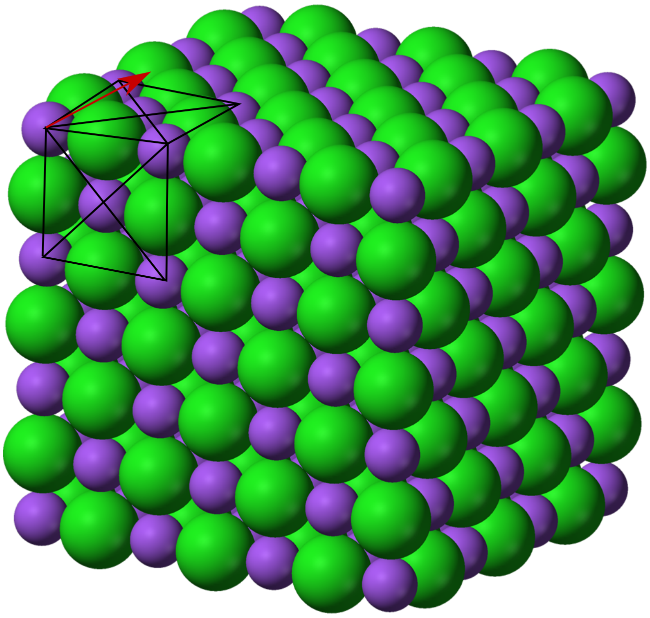

Figure 1.4: Crystal of sodium chloride – NaCl (adapted from Wikipedia). The sodium atoms (purple) are put on an fcc lattice (shown are just two faces with black lines), the chloride atoms are displaced: The arrow points to a Cl atom (not shown) at the center of the cube. The species can also be exchanged. If sodium and chloride were identical, we would have a simple cubic lattice with half the lattice constant.

- salt (NaCl) crystallizes in an fcc structure, where one has Na atoms at the original fcc lattice, and additionally Cl atoms displaced at $1/2\boldsymbol{a}_1 + 1/2\boldsymbol{a}_2 + 1/2\boldsymbol{a}_3$, see Fig. 1.4. If both atoms were identical, one would obtain an sc lattice with half the lattice constant.

- The structure of CsCl is simple cubic. At the corners of the cube one has Cs atoms, but at $1/2\boldsymbol{a}_1 + 1/2\boldsymbol{a}_2 + 1/2\boldsymbol{a}_3$ one has an additional Cl atom. If these atoms were identical, one would end up with an bcc lattice.

- Many elements condense in a hexagonally closed packed structure, e.g. Mg, Zn, Cd. This lattice structure is special in the sense that it usses the smallest volume per atom.

1.3 The reciprocal lattice

In the end, we want to apply these lattice classifications e.g. by performing Fourier transforms. For this, it is useful to introduce the reciprocal lattice

Box 3 (Reciprocal lattice) *For every Bravais lattice with basis vectors $\boldsymbol{a}_i$ and primitive elementary cell volume $V_{\rm pec} = |\boldsymbol{a}_1 \cdot (\boldsymbol{a}_2 \times \boldsymbol{a}_3)|$ one can define a reciprocal lattice via the new basis vectors*

$$\boldsymbol{b}_1 = \frac{2\pi}{V_{\rm pec}} (\boldsymbol{a}_2 \times \boldsymbol{a}_3) \,, \qquad \boldsymbol{b}_2 = \frac{2\pi}{V_{\rm pec}} (\boldsymbol{a}_3 \times \boldsymbol{a}_1) \,, \qquad \boldsymbol{b}_3 = \frac{2\pi}{V_{\rm pec}} (\boldsymbol{a}_1 \times \boldsymbol{a}_2) \,. \tag{1.7}$$

Each lattice point of the reciprocal lattice is then defined by integer multiples of the reciprocal basis vectors

$$\boldsymbol{G}_{\boldsymbol{k}} = k_1 \boldsymbol{b}_1 + k_2 \boldsymbol{b}_2 + k_3 \boldsymbol{b}_3 \,, \qquad \boldsymbol{k} = (k_1, k_2, k_3) \,. \tag{1.8}$$

In two dimensions, these definitions apply with $\boldsymbol{a}_3 = \boldsymbol{e}_z$.

From this definition, it follows that the basis vectors of the reciprocal lattice are orthogonal to the original Bravais lattice

$$|\boldsymbol{a}_i \cdot \boldsymbol{b}_j| = 2\pi\delta_{ij} \,. \tag{1.9}$$

This also implies that products of original and reciprocal lattice vectors are always an integer multiple of 2π

$$\boldsymbol{R_n} \cdot \boldsymbol{G_k} = \sum_i n_i \boldsymbol{a}_i \cdot \sum_j k_j \boldsymbol{b}_j = \pm 2\pi \sum_i n_i k_i \,. \tag{1.10}$$

We can even invert this statement: Given that the product of a vector $\boldsymbol{G}$ with all lattice vectors $\boldsymbol{R_n}$ is an integer multiple of 2π, we can conclude that $\boldsymbol{G}$ must specify a point of the reciprocal lattice.

Furthermore, one can show that the volume of the reciprocal elementary cell becomes the inverse of the primitive elementary cell volume (exercise)

$$V_{\text{rec}} = |\boldsymbol{b}_1 \cdot (\boldsymbol{b}_2 \times \boldsymbol{b}_3)| = \frac{(2\pi)^3}{V_{\text{pec}}} \,. \tag{1.11}$$

For the reciprocal lattice one can use the same classification schemes as for the original one. For example, the reciprocal lattice of the simple cubic lattice is obviously also simple cubic, the reciprocal of the fcc is bcc and vice-versa and the reciprocal of the reciprocal is the original. In particular, we can again define special elementary cells in the reciprocal lattice such as the Brillouin [4] zone.

Box 4 (Brillouin zone) *The* **first Brillouin zone** *is defined as the Wigner-Seitz cell of the reciprocal lattice.*

Just to practice a bit, we will discuss the reciprocal lattice for the cubic crystal system, cf. Sec. 1.1.3, in more detail.

- For the simple cubic lattice we can infer from Eq. (1.3) the reciprocal lattice basis vectors

$$\boldsymbol{b}_1 = \frac{2\pi}{a}\begin{pmatrix}1\\0\\0\end{pmatrix}, \qquad \boldsymbol{b}_2 = \frac{2\pi}{a}\begin{pmatrix}0\\1\\0\end{pmatrix}, \qquad \boldsymbol{b}_3 = \frac{2\pi}{a}\begin{pmatrix}0\\0\\1\end{pmatrix}. \tag{1.12}$$

  Thus, the reciprocal lattice of the simple cubic lattice is again simple cubic.

- For the reciprocal lattice of a face-centered cubic we get from Eq. (1.4) the basis vectors

$$\boldsymbol{b}_1 = \frac{2\pi}{a}\begin{pmatrix}-1\\-1\\+1\end{pmatrix}, \qquad \boldsymbol{b}_2 = \frac{2\pi}{a}\begin{pmatrix}-1\\+1\\-1\end{pmatrix}, \qquad \boldsymbol{b}_3 = \frac{2\pi}{a}\begin{pmatrix}+1\\-1\\-1\end{pmatrix}. \tag{1.13}$$

  By comparing with Eq.(1.5) we conclude that the reciprocal lattice of the face-centered cubic is a body-centered cubic lattice (we had chosen a different elementary cell, but these three vectors also point to three next neighbours of a body-centered cubic lattice).

---

[4] L. Brillouin (1889–1969) was a french physicist, also known for the WKB method.

- Finally, for a body-centered cubic lattice (1.5) one obtains a face-centered cubic basis

$$\boldsymbol{b}_1 = \frac{2\pi}{a}\begin{pmatrix} -1 \\ -1 \\ 0 \end{pmatrix}, \qquad \boldsymbol{b}_2 = \frac{2\pi}{a}\begin{pmatrix} 0 \\ +1 \\ -1 \end{pmatrix}, \qquad \boldsymbol{b}_3 = \frac{2\pi}{a}\begin{pmatrix} +1 \\ 0 \\ -1 \end{pmatrix}. \tag{1.14}$$

  These point to three different next neighbours in a face-centered cubic crystal. This must be expected from our previous result as the reciprocal lattice of the reciprocal lattice is the original lattice.

1.4 Periodic Functions

In a lattice, many functions such as e.g. the potential felt by the electrons inherit the underlying periodicity. This can be exploited in computing their Fourier transform with the help of the reciprocal lattice. To avoid ambiguities, we will in the following assume that we have ordered our basis vectors such that $V_{\rm ec} = \boldsymbol{a}_1 \cdot (\boldsymbol{a}_2 \times \boldsymbol{a}_3) > 0$, and similar for the reciprocal lattice, such that we have

$$\boldsymbol{a}_i \boldsymbol{b}_j = +2\pi\delta_{ij}\,. \tag{1.15}$$

First, let us recall that when in one dimension one has a periodic function with period X, it is clear that we can represent this function as a discrete Fourier series

$$f(x+X) = f(x) \Longrightarrow f(x) = \sum_k f_k e^{\mathrm{i}kx}\,, \qquad f_k = \frac{1}{X}\int_0^X f(x) e^{-\mathrm{i}kx} dx\,. \tag{1.16}$$

Here, k runs over discrete values determined by the periodicity: From $e^{\mathrm{i}kX} \overset{!}{=} 1$ we can conclude that

$$k = \frac{2\pi n}{X}\,, \qquad n \in \mathbb{Z}\,. \tag{1.17}$$

In one dimension, the X can be interpreted as the volume of the (only possible) elementary cell.

In complete analogy we can write for the lattice periodicity

$$f(\boldsymbol{r}) = f(\boldsymbol{r}+\boldsymbol{R})\,, \tag{1.18}$$

where $\boldsymbol{R}$ is some vector of the real lattice. This implies that the function is representable by a similar Fourier series

$$f(\boldsymbol{r}) = \sum_{\boldsymbol{G}} f_{\boldsymbol{G}} e^{+\mathrm{i}\boldsymbol{G}\cdot\boldsymbol{r}}\,, \tag{1.19}$$

where $\boldsymbol{G}$ runs through different discrete values. The expansion coefficients are given by an integral over the primitive elementary cell (periodicity implies that it suffices to consider just one)

$$f_{\boldsymbol{G}} = \frac{1}{V_{\rm ec}}\int_{\rm ec} f(\boldsymbol{r}) e^{-\mathrm{i}\boldsymbol{G}\cdot\boldsymbol{r}} d^3r\,. \tag{1.20}$$

Here, the periodicity condition implies

$$e^{+\mathrm{i}\boldsymbol{G}\cdot\boldsymbol{R}} = 1\,, \tag{1.21}$$

such that eventually we conclude that $\boldsymbol{G}\cdot\boldsymbol{R} = 2\pi n$. This has to hold whenever $\boldsymbol{R}$ is a lattice vector, and consequently $\boldsymbol{G}$ must be a vector of the reciprocal lattice.

Box 5 (basis on the elementary cell) *The functions* $\frac{1}{\sqrt{V_{\rm ec}}}e^{+{\rm i}\boldsymbol{G}\cdot\boldsymbol{r}}$ *form a basis on the elementary cell of the real lattice over the square-integrable functions, where* $\boldsymbol{G}$ *passes through all points of the reciprocal lattice. We have the relations*

$$\delta_{\boldsymbol{G},\boldsymbol{G}'} = \frac{1}{V_{\rm ec}} \int_{\rm ec} e^{+{\rm i}(\boldsymbol{G}-\boldsymbol{G}')\cdot\boldsymbol{r}} d^3r\,, \qquad \sum_{\boldsymbol{G}} e^{+{\rm i}\boldsymbol{G}\cdot\boldsymbol{r}} = V_{\rm ec} \sum_{\boldsymbol{R}} \delta(\boldsymbol{r}-\boldsymbol{R})\,. \tag{1.22}$$

These definitions essentially tell us how to represent lattice-periodic functions with a discrete Fourier series.

The first (orthogonality) relation can be seen by representing the real vector in the elementary cell as $\boldsymbol{r} = \sum_i \alpha_i \boldsymbol{a}_i$, where $0 \le \alpha_i \le 1$ as the vector should be inside the elementary cell, and the reciprocal lattice vector as $\boldsymbol{G} = \sum_i \beta_i \boldsymbol{b}_i$ with $\beta_i \in \mathbb{Z}$. Inserting and using Eq. (1.10) eventually shows the orthogonality:

$$\begin{aligned} \frac{1}{V_{\rm ec}} \int_{\rm ec} e^{+{\rm i}\sum_j \Delta\beta_j \boldsymbol{b}_j \sum_i \alpha_i \boldsymbol{a}_i} d^3r &= \frac{1}{V_{\rm ec}} \int_{\rm ec} e^{+{\rm i}\sum_j 2\pi\Delta\beta_j\alpha_j} d^3r = \prod_{j=1}^{3} \int_0^1 d\alpha_j e^{2\pi{\rm i}(\Delta\beta_j)\alpha_j} \\ &= \left\{ \begin{array}{ccc} 1 & : & \Delta\beta_j = 0 \;\; \forall j \\ 0 & : & \text{else} \end{array} \right. \end{aligned} \tag{1.23}$$

To see the second (completeness) relation, we start from an arbitrary function $\tilde{f}(\boldsymbol{r})$, which need not have any periodicity. However, we can define for each lattice point $\boldsymbol{R}$ the function $f^{\boldsymbol{R}}(\boldsymbol{r})$ as the periodic continuation of the function $\tilde{f}(\boldsymbol{r})$ from an elementary cell $EC(\boldsymbol{R})$ associated to $\boldsymbol{R}$ (e.g. the Wigner-Seitz cell) to the complete space, i.e.,

$$f^{\boldsymbol{R}}(\boldsymbol{r}) = \left\{ \begin{array}{ccc} \tilde{f}(\boldsymbol{r}) & : & \boldsymbol{r} \in EC(\boldsymbol{R}) \\ \tilde{f}(\boldsymbol{r}-\boldsymbol{R}') & : & \boldsymbol{r}-\boldsymbol{R}' \in EC(\boldsymbol{R}) \end{array} \right. . \tag{1.24}$$

Here, $\boldsymbol{R}'$ is a lattice vector that needs to be subtracted such that $\boldsymbol{r}-\boldsymbol{R}'$ is again in the elementary cell. By construction, $f^{\boldsymbol{R}}(\boldsymbol{r})$ is then periodic over the full lattice and has a Fourier expansion. Then, we can partition an integral over the complete space into integrals over individual elementary cells (e.g. Wigner-Seitz-cells) associated to each lattice node

$$\begin{aligned} \int \tilde{f}(\boldsymbol{r}) \sum_{\boldsymbol{G}} e^{+{\rm i}\boldsymbol{G}\boldsymbol{r}} d^3r &= \sum_{\boldsymbol{R}} \sum_{\boldsymbol{G}} \int_{EC(\boldsymbol{R})} \tilde{f}(\boldsymbol{R}+\boldsymbol{r}') e^{+{\rm i}\boldsymbol{G}(\boldsymbol{R}+\boldsymbol{r}')} d^3r' = \sum_{\boldsymbol{R}} \sum_{\boldsymbol{G}} \int_{EC(\boldsymbol{R})} f^{\boldsymbol{R}}(\boldsymbol{r}') e^{+{\rm i}\boldsymbol{G}\boldsymbol{r}'} d^3r' \\ &= \sum_{\boldsymbol{R}} \sum_{\boldsymbol{G}} V_{\rm ec} f^{\boldsymbol{R}}_{-\boldsymbol{G}} = V_{\rm ec} \sum_{\boldsymbol{R}} f^{\boldsymbol{R}}(\boldsymbol{0}) = V_{\rm ec} \sum_{\boldsymbol{R}} \tilde{f}(\boldsymbol{R})\,. \end{aligned} \tag{1.25}$$

In the second line, we have used Eq. (1.20) and Eq. (1.19) at $\boldsymbol{r} = 0$. Since the above relation has to hold for arbitrary functions, we have thus also shown the completeness relation.

Further, we note that an equivalent orthogonality relation holds for the reciprocal lattice.

Example: X-ray diffraction

As an example, we can treat the diffraction of X-rays. Assuming that in a crystal we have a lattice-periodic potential $V(\boldsymbol{r}) = V(\boldsymbol{r}+\boldsymbol{R})$ we can ask for the probability for an incoming wave with momentum $\boldsymbol{k}$ to be scattered into the outgoing momentum $\boldsymbol{k'}$. To lowest order, we can use Fermis golden rule, which requires to compute the matrix element

$$\begin{aligned} \langle \boldsymbol{k'}| V(\boldsymbol{r}) |\boldsymbol{k}\rangle &= \frac{1}{V_{\rm ec}} \int e^{-{\rm i}\boldsymbol{k'}\boldsymbol{r}} V(\boldsymbol{r}) e^{+{\rm i}\boldsymbol{k}\boldsymbol{r}} d^3r = \frac{1}{V_{\rm ec}} \int \sum_{\boldsymbol{G}} V_{\boldsymbol{G}} e^{+{\rm i}(\boldsymbol{k}+\boldsymbol{G}-\boldsymbol{k'})\boldsymbol{r}} d^3r \\ &= \sum_{\boldsymbol{G}} V_{\boldsymbol{G}} \delta_{\boldsymbol{k'}-\boldsymbol{k},\boldsymbol{G}} \,. \end{aligned} \tag{1.26}$$

This means that for these kinds of processes we will have to obey the selection rule that in- and outgoing wave vectors must be related by a reciprocal lattice vector

$$\boldsymbol{k'} = \boldsymbol{k} + \boldsymbol{G} \,. \tag{1.27}$$

That is, by considering the patterns created by diffracted X-rays we can conclude the reciprocal lattice and from that the real lattice structure of the diffracting crystal.

We will discuss this with the help of a simple example: Suppose the basis vectors $\boldsymbol{a}_1$ and $\boldsymbol{a}_2$ parametrize one plane of the real lattice. Then, a corresponding reciprocal lattice vector perpendicular to that plane can be written as $\boldsymbol{G} = n\boldsymbol{b}_3$ with integer n, and it has to obey

$$\boldsymbol{a}_3 \cdot \boldsymbol{G} = a_3 G \cos(\theta') = dG = 2\pi n \,. \tag{1.28}$$

Here, $d = a_3 \cos(\theta')$ is the perpendicular distance between the lattice planes spanned by $\boldsymbol{a}_1$ and $\boldsymbol{a}_2$. We can therefore conclude that $G = \frac{2\pi n}{d}$ with integer n. Furthermore, for the case of elastic scattering, where $\boldsymbol{k}^2 = \boldsymbol{k'}^2$, the selection rule can be written as

$$+2\boldsymbol{k} \cdot \boldsymbol{G} + \boldsymbol{G}^2 = 0 = +2kG\cos\alpha + G^2 \,. \tag{1.29}$$

Here, α is the angle between $\boldsymbol{G}$ and $\boldsymbol{k}$. Now inserting that the modulus of the photon wave vector is given by $k = 2\pi/\lambda$ with wavelength λ, we write this as

$$0 = +2d\cos(\alpha) + n\lambda \,, \tag{1.30}$$

and upon using that $\cos(\alpha) = \cos(\pi/2 + \theta) = -\sin(\theta)$, where θ is now the angle between the plane and the incoming wave vector $\boldsymbol{k}$, this implies the Bragg [5] reflection condition

$$2d\sin(\theta) = n\lambda \,. \tag{1.31}$$

By rotating the crystal or the incoming light, one can maximize $\sin(\theta) \to 1$, which allows one to infer the plane distance d. The whole setup is illustrated in Fig. 1.5.

---

[5] The british physicist W. H. Bragg (1862–1942) and his son W. L. Bragg (1890–1971) earned the Nobel price for this method.

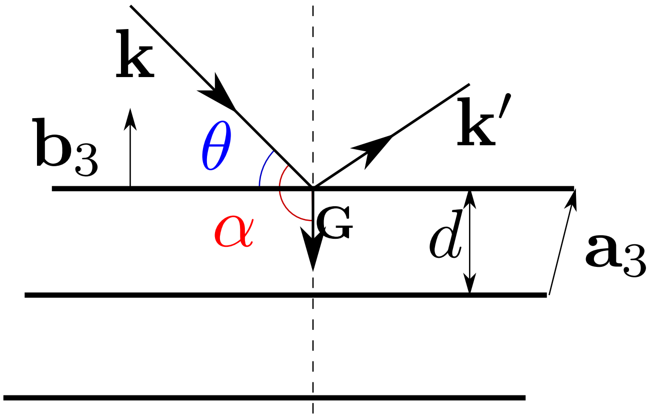

Figure 1.5: Visualization of the Bragg reflection scheme. An incoming wave k is reflected into k', and elastic scattering allows to determine the plane distance d.

Chapter 2

Phonons

2.1 The many-body Hamiltonian

For the energy scales at which solid crystals exist as such, we can safely treat nuclei as elementary objects. Then, the many-body Hamiltonian in a solid crystal contains the kinetic terms of electrons and nuclei, the electron-electron, nucleus-nucleus, and the electron-nuclei interactions. For example, for a crystal composed of N_e electrons and N_n identical nuclei with charge Z the Hamiltonian would read

$$H = \sum_{k=1}^{N_e} \frac{\boldsymbol{p}_k^2}{2m} + \sum_{K=1}^{N_n} \frac{\boldsymbol{P}_K^2}{2M} + \sum_{k<q} \frac{e^2}{|\boldsymbol{r}_k - \boldsymbol{r}_q|} + \sum_{K<Q} \frac{e^2 Z^2}{|\boldsymbol{R}_K - \boldsymbol{R}_Q|} - \sum_{k,Q} \frac{e^2 Z}{|\boldsymbol{r}_k - \boldsymbol{R}_Q|} \,. \tag{2.1}$$

Here, m and M denote the electron and nucleus masses, respectively, $\boldsymbol{p}$ and $\boldsymbol{P}$ their momenta, and $\boldsymbol{r}_k$ and $\boldsymbol{R}_K$ their positions. We have used the convention that small indices label electrons and capital ones the nuclei. Furthermore, when the whole system is electrically neutral, we can safely assume that $\sum_{K=1}^{N_n} Z_K = N_e$. However, one should be aware that the "nuclei" may not be naked, i.e., they might actually be ions that consist of the actual nuclei and tightly bound electrons. Then, Z and N_e have to be adapted accordingly.

To see which of the terms in the Hamiltonian are most relevant, it is useful to write the full Hamiltonian in a dimensionless form. We can use the Bohr radius as a natural length scale

$$a_0 = \frac{\hbar^2}{me^2} = 0.5 \times 10^{-10}\text{m} \tag{2.2}$$

and the Rydberg as a natural energy scale

$$E_0 = \frac{me^4}{\hbar^2} = \frac{e^2}{a_0} = 2\text{Ry} = 27.2\text{eV}\,. \tag{2.3}$$

Dividing by the energy scale, we see that by introducing the dimensionless positions $\boldsymbol{r} = a_0 \boldsymbol{x}$ and $\boldsymbol{R} = a_0 \boldsymbol{X}$, the dimensionless Hamiltonian can be written as

$$\begin{aligned}
\frac{H}{E_0} &= -\frac{\hbar^2}{2m}\frac{1}{E_0 a_0^2}\sum_k \nabla^2_{\boldsymbol{x}_k} - \frac{\hbar^2}{2M}\frac{1}{E_0 a_0^2}\sum_k \nabla^2_{\boldsymbol{X}_k} \\
&\quad + \frac{e^2}{a_0 E_0}\left[\sum_{k<q}\frac{1}{|\boldsymbol{x}_k - \boldsymbol{x}_q|} + \sum_{K<Q}\frac{Z^2}{|\boldsymbol{X}_K - \boldsymbol{X}_Q|} - \sum_{k,Q}\frac{Z}{|\boldsymbol{x}_k - \boldsymbol{X}_Q|}\right] \\
&= -\frac{1}{2}\sum_{k=1}^{N_e}\nabla^2_{\boldsymbol{x}_k} - \frac{m}{M}\frac{1}{2}\sum_{K=1}^{N_n}\nabla^2_{\boldsymbol{X}_K} + \sum_{k<q}\frac{1}{|\boldsymbol{x}_k - \boldsymbol{x}_q|} + \sum_{K<Q}\frac{Z^2}{|\boldsymbol{X}_K - \boldsymbol{X}_Q|} - \sum_{k,Q}\frac{Z}{|\boldsymbol{x}_k - \boldsymbol{X}_Q|}\,,
\end{aligned} \tag{2.4}$$

where we have used that $E_0 a_0^2 = \frac{\hbar^2}{m}$ and $E_0 a_0 = e^2$.

We see that the kinetic term for the nuclei is suppressed by a factor of m/M. Already the proton is 1800 times as heavy as an electron, and depending on the element, for typical solid crystals this factor is in the order of $10^{-4} \dots 10^{-5}$. The huge difference in electron and nucleus masses allows one to treat the nuclei to lowest order just as fixed, i.e., pinned to the lattice positions, which can be seen as a phenomenologic ingredient to the model.

2.2 Born-Oppenheimer approximation

The previous considerations tell us that it should be safe to neglect the kinetic part of the nucleus contribution, but we cannot neglect all nucleus contributions. For example, if we would neglect the attractive electron-nucleus interaction, the whole crystal would fall apart. Treating the kinetic part of the nuclei as the perturbation, i.e., we split $H = H_0 + H_1$ with

$$H_0 = T_e(\hat{\boldsymbol{p}}) + V_{ee}(\hat{\boldsymbol{r}}) + V_{nn}(\hat{\boldsymbol{R}}) + V_{en}(\hat{\boldsymbol{r}}, \hat{\boldsymbol{R}})\,, \qquad H_1 = T_n(\hat{\boldsymbol{P}})\,. \tag{2.5}$$

Here, $\boldsymbol{r}$ and $\boldsymbol{R}$ are the position operators for the electrons and nuclei, respectively and similar for $\boldsymbol{p}$ and $\boldsymbol{P}$.

In general, we would like to solve the time-independent Schrödinger equation

$$\left[T_e(\hat{\boldsymbol{p}}) + V_{ee}(\hat{\boldsymbol{r}}) + V_{nn}(\hat{\boldsymbol{R}}) + V_{en}(\hat{\boldsymbol{r}}, \hat{\boldsymbol{R}}) + T_n(\hat{\boldsymbol{P}})\right] \Psi(\boldsymbol{r}, \boldsymbol{R}) = E\Psi(\boldsymbol{r}, \boldsymbol{R}) \tag{2.6}$$

for the full wave function $\Psi(\boldsymbol{r}, \boldsymbol{R})$ and the energy E. Motivated by the observation that in the unperturbed problem described by H_0, the positions of the ions are stationary, we use the product ansatz

$$\Psi(\boldsymbol{r}, \boldsymbol{R}) = \chi(\boldsymbol{R})\phi(\boldsymbol{r}, \boldsymbol{R})\,. \tag{2.7}$$

Here, χ can be interpreted as a wave function of the nuclei and ϕ the electronic part, which implicitly depends on the nuclei positions. We demand that the electronic part is a solution of the simplified electronic Schrödinger equation

$$\left[T_e(\hat{\boldsymbol{p}}) + V_{ee}(\hat{\boldsymbol{r}}) + V_{nn}(\boldsymbol{R}) + V_{en}(\hat{\boldsymbol{r}}, \boldsymbol{R})\right] \phi(\boldsymbol{r}, \boldsymbol{R}) = E_0(\boldsymbol{R})\phi(\boldsymbol{r}, \boldsymbol{R})\,. \tag{2.8}$$

Here, the positions of the nuclei just enter as classical variables $\boldsymbol{R}$, and also the energies $E_0(\boldsymbol{R})$ depend parametrically on them. We see that $V_{nn}(\boldsymbol{R})$ is just a constant, which leads to a trivial shift of the energies (we will keep it here).

Using this in the full problem

$$\begin{aligned}
H\chi(\boldsymbol{R})\phi(\boldsymbol{r}, \boldsymbol{R}) &= \left[T_e(\hat{\boldsymbol{p}}) + V_{ee}(\hat{\boldsymbol{r}}) + V_{nn}(\hat{\boldsymbol{R}}) + V_{en}(\hat{\boldsymbol{r}}, \hat{\boldsymbol{R}}) + T_n(\hat{\boldsymbol{P}})\right] \chi(\boldsymbol{R})\phi(\boldsymbol{r}, \boldsymbol{R}) \\
&= \left[T_e(\hat{\boldsymbol{p}}) + V_{ee}(\hat{\boldsymbol{r}}) + V_{nn}(\boldsymbol{R}) + V_{en}(\hat{\boldsymbol{r}}, \boldsymbol{R})\right] \chi(\boldsymbol{R})\phi(\boldsymbol{r}, \boldsymbol{R}) \\
&\quad + \left[V_{nn}(\hat{\boldsymbol{R}}) - V_{nn}(\boldsymbol{R}) + V_{en}(\hat{\boldsymbol{r}}, \hat{\boldsymbol{R}}) - V_{en}(\hat{\boldsymbol{r}}, \boldsymbol{R}) + T_n(\hat{\boldsymbol{P}})\right] \chi(\boldsymbol{R})\phi(\boldsymbol{r}, \boldsymbol{R}) \\
&= \left[E_0(\boldsymbol{R}) + V_{nn}(\hat{\boldsymbol{R}}) - V_{nn}(\boldsymbol{R}) + V_{en}(\hat{\boldsymbol{r}}, \hat{\boldsymbol{R}}) - V_{en}(\hat{\boldsymbol{r}}, \boldsymbol{R}) + T_n(\hat{\boldsymbol{P}})\right] \chi(\boldsymbol{R})\phi(\boldsymbol{r}, \boldsymbol{R}) \\
&= \phi(\boldsymbol{r}, \boldsymbol{R}) \left[E_0(\boldsymbol{R}) + V_{nn}(\hat{\boldsymbol{R}}) - V_{nn}(\boldsymbol{R}) + T_n(\hat{\boldsymbol{P}})\right] \chi(\boldsymbol{R}) \\
&\quad + \underline{\left[V_{en}(\hat{\boldsymbol{r}}, \hat{\boldsymbol{R}}) - V_{en}(\hat{\boldsymbol{r}}, \boldsymbol{R})\right] \phi(\boldsymbol{r}, \boldsymbol{R})\chi(\boldsymbol{R})} = E\phi(\boldsymbol{r}, \boldsymbol{R})\chi(\boldsymbol{R})\,.
\end{aligned} \tag{2.9}$$

When we now neglect the underlined term, we can divide by the electronic wavefunction and obtain a Schrödinger equation for the nuclei only

$$\left[E_0(\boldsymbol{R}) + V_{nn}(\hat{\boldsymbol{R}}) - V_{nn}(\boldsymbol{R}) + T_n(\hat{\boldsymbol{P}})\right] \chi(\boldsymbol{R}) = E\chi(\boldsymbol{R})\,. \tag{2.10}$$

We see that the trivial shift of the electronic energies due to the $V_{nn}(\boldsymbol{R})$ term will always cancel.

To summarize, the Born [1]- Oppenheimer [2] approximation consists of first solving the electronic Schrödinger equation (2.8) as if the nuclei were fixed. Then, the eigenvalues $E_0(\boldsymbol{R})$ of the electronic solution pose an effective potential in the eq. (2.10) for the nuclei. In practice, one will find that this approach leads to quantized eigenvalues for electronic and nuclei degrees of freedom, i.e., one will have to solve the two equations

$$\begin{aligned}
\left[T_e(\hat{\boldsymbol{p}}) + V_{ee}(\hat{\boldsymbol{r}}) + V_{nn}(\boldsymbol{R}) + V_{en}(\hat{\boldsymbol{r}}, \boldsymbol{R})\right] \phi_\alpha(\boldsymbol{r}, \boldsymbol{R}) &= E_\alpha(\boldsymbol{R}) \phi_\alpha(\boldsymbol{r}, \boldsymbol{R}) \,, \\
\left[E_\alpha(\boldsymbol{R}) + V_{nn}(\hat{\boldsymbol{R}}) - V_{nn}(\boldsymbol{R}) + T_n(\hat{\boldsymbol{P}})\right] \chi_{\beta\alpha}(\boldsymbol{R}) &= E_{\beta\alpha} \chi_{\beta\alpha}(\boldsymbol{R}) \,.
\end{aligned} \tag{2.11}$$

Example: Coupled Oscillators

As a lightweight example for illustration, we can consider the Hamiltonian of two coupled oscillators

$$H = \frac{P^2}{2M} + \frac{p^2}{2m} + \frac{K}{2} X^2 + \frac{k}{2} (x - X)^2 \,. \tag{2.12}$$

As is indicated by the letters, the capital quantities denote the heavy oscillator and the small letters the little one, and x, X, p, and P are operators. Due to its low dimensionality, the problem can be solved exactly with a mode transformation, which only has to preserve the commutation relations

$$[x, p] = \mathrm{i} = [X, P] \,, \qquad [x, P] = [X, p] = 0 \,. \tag{2.13}$$

For the model at hand, this is quite simple to find. First, we write

$$\begin{aligned}
p &= \tilde{p}\sqrt{m} \,, \qquad & x &= \frac{\tilde{x}}{\sqrt{m}} \,, \\
P &= \tilde{P}\sqrt{M} \,, \qquad & X &= \frac{\tilde{X}}{\sqrt{M}} \,.
\end{aligned} \tag{2.14}$$

This clearly leaves the commutation relations invariant. The idea behind this is to make the kinetic terms appear like identical particles. With the new coordinates, the Hamiltonian becomes

$$\begin{aligned}
H &= \frac{\tilde{P}^2}{2} + \frac{\tilde{p}^2}{2} + \frac{K}{2M} \tilde{X}^2 + \frac{k}{2} \left(\tilde{x} \frac{1}{\sqrt{m}} - \tilde{X} \frac{1}{\sqrt{M}} \right)^2 \\
&= \left(\tilde{P}, \tilde{p} \right) \frac{1}{2} \begin{pmatrix} 1 & 0 \\ 0 & 1 \end{pmatrix} \begin{pmatrix} \tilde{P} \\ \tilde{p} \end{pmatrix} + \left(\tilde{X}, \tilde{x} \right) \frac{1}{2} \begin{pmatrix} \frac{K+k}{M} & -\frac{k}{\sqrt{mM}} \\ -\frac{k}{\sqrt{mM}} & \frac{k}{m} \end{pmatrix} \begin{pmatrix} \tilde{X} \\ \tilde{x} \end{pmatrix} \,.
\end{aligned} \tag{2.15}$$

Second, we now choose an orthogonal transformation (which also preserves the commutation relations)

$$\begin{pmatrix} \tilde{X} \\ \tilde{x} \end{pmatrix} = \begin{pmatrix} \cos\phi & \sin\phi \\ -\sin\phi & \cos\phi \end{pmatrix} \begin{pmatrix} x_1 \\ x_2 \end{pmatrix} \,, \qquad \begin{pmatrix} \tilde{P} \\ \tilde{p} \end{pmatrix} = \begin{pmatrix} \cos\phi & \sin\phi \\ -\sin\phi & \cos\phi \end{pmatrix} \begin{pmatrix} p_1 \\ p_2 \end{pmatrix} \tag{2.16}$$

and choose ϕ such that the Hamiltonian decouples. Since the transformation is orthogonal, the kinetic term formally does not change, and the particular choice

$$\tan 2\phi = \frac{2k\sqrt{mM}}{kM - (k+K)m} \tag{2.17}$$

---

[1] Max Born (1882–1970) was a german physicist and one of the fathers of quantum mechanics.

[2] Julius Robert Oppenheimer (1904–1967) was a US-american physicist and director of the Manhattan project.

eventually yields

$$H = (p_1, p_2)\,\frac{1}{2}\begin{pmatrix} 1 & 0 \\ 0 & 1 \end{pmatrix}\begin{pmatrix} p_1 \\ p_2 \end{pmatrix} + (x_1, x_2)\,\frac{1}{2}\begin{pmatrix} k_- & 0 \\ 0 & k_+ \end{pmatrix}\begin{pmatrix} x_1 \\ x_2 \end{pmatrix},$$
$$k_\pm = \frac{k(m+M) + Km \pm \sqrt{k^2M^2 + m^2(k+K)^2 + 2kmM(k-K)}}{2mM}\,. \tag{2.18}$$

Here, we have assumed that $kM - (k+K)m > 0$, otherwise k_+ and k_- are just exchanged.

The energies of these coupled oscillators can accordingly be computed via

$$E_{n_1 n_2} = \sqrt{k_-}\left(n_1 + \frac{1}{2}\right) + \sqrt{k_+}\left(n_2 + \frac{1}{2}\right)\,. \tag{2.19}$$

Now, the Born-Oppenheimer approximation would simply solve the lightweight coordinate by neglecting the kinetic term of the heavy coordinate, i.e. we solve (compare Eq. (2.8))

$$H_{\rm el} = \frac{\hat{p}^2}{2m} + \frac{K}{2}X^2 + \frac{k}{2}(\hat{x} - X)^2\,. \tag{2.20}$$

where we consider X as a classical variable. Therefore, the shift $\hat{x} - X$ does not affect the eigenvalues and we can from our knowledge of the harmonic oscillator essentially read off the frequency of the oscillator via $k = m\omega^2$, which implies for the energies

$$E_n^0(X) = \sqrt{\frac{k}{m}}\left(n + \frac{1}{2}\right) + \frac{K}{2}X^2\,, \qquad n \in \{0, 1, 2, \ldots\}\,. \tag{2.21}$$

Next, we insert this into the heavy coordinate Equation, compare Eq. (2.10)

$$H_{\rm ph} = E_n^0(X) + \frac{K}{2}\hat{X}^2 - \frac{K}{2}X^2 + \frac{\hat{P}^2}{2M}\,,$$
$$= \frac{\hat{P}^2}{2M} + \frac{K}{2}\hat{X}^2 + \sqrt{\frac{k}{m}}\left(n + \frac{1}{2}\right)\,. \tag{2.22}$$

This shows that the two subsystems can for $m \ll M$ be treated independently

$$E_{n_1 n_2}^{\rm BO} = \sqrt{\frac{K}{M}}\left(n_1 + \frac{1}{2}\right) + \sqrt{\frac{k}{m}}\left(n_2 + \frac{1}{2}\right)\,. \tag{2.23}$$

Indeed, we obtain from expanding the exact solution (2.18)

$$\sqrt{k_-} = \sqrt{\frac{K}{M}}\left[1 - \frac{1}{2}\frac{m}{M} + \mathcal{O}\left\{\frac{m^2}{M^2}\right\}\right]\,, \qquad \sqrt{k_+} = \sqrt{\frac{k}{m}}\left[1 + \frac{1}{2}\frac{m}{M} + \mathcal{O}\left\{\frac{m^2}{M^2}\right\}\right]\,. \tag{2.24}$$

2.3 Phenomenologic Binding Models

Compare also Ref. [3].

In practice, it is for most systems rather impossible to calculate the effective potential $V(\boldsymbol{R})$ that stabilizes the ionic lattice. Therefore, one often uses effective parametrizations to enable fast calculations. All these share some general characteristics. First, one assumes that the total potential can be decomposed into a sum of two-body interactions depending only on the distance between the ions

$$V_{\rm eff}(\hat{\boldsymbol{R}}) = \frac{1}{2}\sum_{i \neq j} v(|\boldsymbol{R}_i - \boldsymbol{R}_j|)\,. \tag{2.25}$$

Second, the two-body interaction is repulsive for small distances, attractive for large distances and vanishes for infinite distances

$$v(d) = \begin{cases} > 0 & : \quad d < d_0 \\ < 0 & : \quad d > d_0 \\ 0 & : \quad d \to \infty \end{cases} . \tag{2.26}$$

For different elements, different effective binding models are used:

- The **van-der-Waals** [3] binding is used for noble gases. Normally, one would expect that these do not interact at all. However, due to the inner-atomic charge distribution higher order interactions such as dipole or multipole interactions are possible. This leads in the far field to an attractive r^{-6} interaction. Mainly to simplify calculations, the repulsive interaction is modeled with a r^{-12} interaction term, leading to the Lennard-Jones [4] potential

  $$v(d) = 4\epsilon \left[\left(\frac{\sigma}{d}\right)^{12} - \left(\frac{\sigma}{d}\right)^{6} \right] , \tag{2.27}$$

  where $\epsilon > 0$ and $\sigma > 0$ are phenomenological parameters. The van-der-Waals binding is present in noble gases and in crystals composed of molecules, the typical binding energy per atom is $\mathcal{O}\{.1\}$ eV.

- The **ionic** binding model is based on the assumption that by transferring one or more electrons, the atoms of a crystal form two species: positively $Q_1 > 0$ and negatively $Q_2 < 0$ charged. The interaction model becomes

  $$v(d) = \frac{Q_1 Q_2}{d} + \frac{B}{d^n} , \tag{2.28}$$

  where the parameters $B > 0$ and n are empirically determined by experiments (e.g. inter-ion distance, compressibility). Alternative choices for the repulsive part are possible. The ionic binding is present in crystals composed of elements with very different electronegativity, e.g. NaCl with a binding energy of 3.08 eV.

- The **covalent** binding can be understood with quantum-mechanical approaches only: Generally, levels hybridize when orbitals establish contact. Depending on the type of orbitals, the corresponding energy of the levels may increase compared to the isolated orbitals (anti-binding) or decrease (binding). This problem can be solved approximately for two hydrogen-like atoms but yields rather complex expressions involving an exponential decay. Therefore, one often uses in practice simplified phenomenologic expressions like the Morse [5] potential

  $$v(d) = D(e^{-2\alpha(d-d_0)} - 2e^{-\alpha(d-d_0)}) \tag{2.29}$$

  with free parameters D, α, and d_0. One prominent representative is diamond, where one has binding energies of 7.3 eV/atom. It is one hallmark of the covalent binding type that the orbitals of the element roughly determine the lattice structure.

- The **metallic binding** is similar to the ionic or covalent binding in the sense that the valence electrons are distributed over more than one atom. However, the difference is that

---

[3] Johannes Diderik van der Waals (1837–1923) was a dutch physicist.

[4] John Edward Lennard-Jones (1894–1954) was a british mathematician and theoretical physicist.

[5] Philip McCord Morse (1903–1985) was a US-american theoretical physicist.

for this binding type, the electrons are completely delocalized over the lattice (roughly homogeneously). Not surprisingly, the metallic binding ist most prominent in metals, the lattice configuration is determined by the dense packing of ions and the volume of the electron gas. It must be said though that in many materials the boundaries between the binding types are diffuse.

For just two particles, we can expand the two-body interaction around its minimum up to second order, which should be valid for small displacements. This generically leads to potentials of the form

$$v(d) = v_0 + K(d - d_0)^2 \,, \tag{2.30}$$

where v_0, $K > 0$ and $d_0 > 0$ are free parameters that can be determined by the underlying model. Below, we will learn how to perform this for many particles.

2.4 Small displacement expansion

The normal mode expansion of coupled oscillators is essentially a problem known from theoretical mechanics. We will first treat this problem classically and then perform the quantization, see also Ref. [1]. However, our example for the exact solution of the Born-Oppenheimer approximation essentially shows that we can equally start from the quantized version and then perform a canonical transformation.

So let us assume that our classical system of coupled oscillators (which in a solid state system could be the atomic positions) is described by a Lagrange function

$$L(\boldsymbol{r}, \dot{\boldsymbol{r}}) = \frac{1}{2}\dot{\boldsymbol{r}}^{\mathrm{T}}\boldsymbol{T}\dot{\boldsymbol{r}} - V(\boldsymbol{r}) \,. \tag{2.31}$$

Here, $\boldsymbol{T}$ is a quadratic matrix (which can e.g. contain the different masses) and $V(\boldsymbol{r})$ contains the sum of the two-body interactions or even many-body interactions. In addition, we assume the following: First, $\boldsymbol{T}$ is a positive definite matrix. This makes sense since if it had negative eigenvalues, one could by ever increasing the velocity decrease the energy of the kinetic term. Second, we assume that there exists an equilibrium configuration at $\boldsymbol{r}_0$, around which we can expand the potential up to second order. In a realistic system, this equilibrium configuration would be that the atoms exactly reside at the lattice points of the crystal, and for n atoms in 3d we would have $f = 3n$ degrees of freedom and therefore matrices of dimension $f \times f$. Expanding around the stationary equilibrium configuration yields new generalized coordinates

$$\boldsymbol{q} = \boldsymbol{r} - \boldsymbol{r}_0 \,, \qquad \dot{\boldsymbol{q}} = \dot{\boldsymbol{r}} \,, \tag{2.32}$$

and the Lagrange function becomes

$$L(\boldsymbol{q}, \dot{\boldsymbol{q}}) = \frac{1}{2}\dot{\boldsymbol{q}}^{\mathrm{T}}\boldsymbol{T}\dot{\boldsymbol{q}} - V(\boldsymbol{r}_0) - \frac{1}{2}\boldsymbol{q}^{\mathrm{T}}\boldsymbol{V}\boldsymbol{q} + \mathcal{O}\{\boldsymbol{q}^3\} \,. \tag{2.33}$$

Here, we have simply inserted the quadratic approximation to the many-body potential. Since we have expanded around an equilibrium configuration, the first order term (linear in $\boldsymbol{q}$) vanishes and $\boldsymbol{V}$ must be a symmetric and positive definite matrix. Since it has no effect, we can neglect the constant $V(\boldsymbol{r}_0)$. Thus, our approximate Lagrange function becomes

$$L(\boldsymbol{q}, \dot{\boldsymbol{q}}) = \frac{1}{2}\dot{\boldsymbol{q}}^{\mathrm{T}}\boldsymbol{T}\dot{\boldsymbol{q}} - \frac{1}{2}\boldsymbol{q}^{\mathrm{T}}\boldsymbol{V}\boldsymbol{q} \tag{2.34}$$

with symmetric and positive definite $f \times f$ matrices $\boldsymbol{T}$ and $\boldsymbol{V}$.

2.4.1 Normal mode decomposition

We want to transform our generalized coordinates $\boldsymbol{q}$ to new coordinates $\boldsymbol{Q}$ such that the Lagrange function decouples. To this end, we assume this transformation to be linear

$$\boldsymbol{q} = \boldsymbol{A}\boldsymbol{Q}\,, \tag{2.35}$$

with $f \times f$ matrix $\boldsymbol{A}$ for a system with f degrees of freedom. This transforms the Lagrange function into

$$L = \frac{1}{2}\dot{\boldsymbol{Q}}^{\mathrm{T}}\boldsymbol{A}^{\mathrm{T}}\boldsymbol{T}\boldsymbol{A}\dot{\boldsymbol{Q}} - \frac{1}{2}\boldsymbol{Q}^{\mathrm{T}}\boldsymbol{A}^{\mathrm{T}}\boldsymbol{V}\boldsymbol{A}\boldsymbol{Q}\,. \tag{2.36}$$

Now, decoupling the system means that both the kinetic and the potential terms become diagonal

$$\boldsymbol{A}^{\mathrm{T}}\boldsymbol{T}\boldsymbol{A} = \boldsymbol{1}\,, \qquad \boldsymbol{A}^{\mathrm{T}}\boldsymbol{V}\boldsymbol{A} = \boldsymbol{W_D}\,, \tag{2.37}$$

where $\boldsymbol{W_D}$ is a diagonal matrix. Multiplying the first equation on the second, we get

$$\boldsymbol{A}^{\mathrm{T}}\boldsymbol{V}\boldsymbol{A} = \boldsymbol{A}^{\mathrm{T}}\boldsymbol{T}\boldsymbol{A}\boldsymbol{W_D}\,. \tag{2.38}$$

Now, since the transformation is canonical, the matrix $\boldsymbol{A}$ is non-singular, i.e., we can compute its inverse and also the inverse of its transpose. Therefore, we conclude

$$\boldsymbol{V}\boldsymbol{A} = \boldsymbol{T}\boldsymbol{A}\boldsymbol{W_D}\,. \tag{2.39}$$

We can solve this equation – and thereby also the previous ones – by determining the columns $\boldsymbol{a}_i$ of the matrix $\boldsymbol{A} = (\boldsymbol{a}_1, \ldots, \boldsymbol{a}_f)$ – via solving an enlarged eigenvalue problem

$$\boldsymbol{V}\boldsymbol{a}_i = \lambda_i \boldsymbol{T}\boldsymbol{a}_i\,. \tag{2.40}$$

Now, when $\boldsymbol{T}$ is positive definite (which should be the case for a reasonable kinetic term as physically the kinetic energy should only vanish when the velocities vanish and should be positive otherwise), we can define the hermitian matrices

$$\boldsymbol{T}^{\pm 1/2} \quad : \quad \boldsymbol{T}^{+1/2}\boldsymbol{T}^{-1/2} = \boldsymbol{1}\,, \qquad \boldsymbol{T}^{-1/2}\boldsymbol{T} = \boldsymbol{T}^{+1/2}\,, \tag{2.41}$$

and thereby write the generalized eigenvalue problem as

$$(\boldsymbol{T}^{-1/2}\boldsymbol{V}\boldsymbol{T}^{-1/2})\boldsymbol{T}^{+1/2}\boldsymbol{a}_i = \lambda_i \boldsymbol{T}^{+1/2}\boldsymbol{a}_i\,, \tag{2.42}$$

which is just a conventional eigenvalue problem for $\boldsymbol{b}_i = \boldsymbol{T}^{+1/2}\boldsymbol{a}_i$ and the matrix $\boldsymbol{T}^{-1/2}\boldsymbol{V}\boldsymbol{T}^{-1/2}$. Now, given that both $\boldsymbol{V}$ and $\boldsymbol{T}$ are symmetric and positive definite, we conclude that also $\boldsymbol{T}^{-1/2}\boldsymbol{V}\boldsymbol{T}^{-1/2}$ is positive definite. We can show this by showing that for general normalized vectors $\boldsymbol{x}$ we have

$$\boldsymbol{x}^{\boldsymbol{T}}\boldsymbol{T}^{-1/2}\boldsymbol{V}\boldsymbol{T}^{-1/2}\boldsymbol{x} = \boldsymbol{x}^{\boldsymbol{T}}\boldsymbol{T}^{-1}\boldsymbol{x}\boldsymbol{y}^{\boldsymbol{T}}\boldsymbol{V}\boldsymbol{y} \geq 0\,, \qquad \boldsymbol{y} = \frac{\boldsymbol{T}^{-1/2}\boldsymbol{x}}{\boldsymbol{x}^{\boldsymbol{T}}\boldsymbol{T}^{-1}\boldsymbol{x}}\,. \tag{2.43}$$

In other words, for positive definite kinetic matrix $\boldsymbol{T}$ and positive definite potential $\boldsymbol{V}$ it follows that the eigenvalues λ_i are not only real but even positive. Inserting the solution of the generalized eigenvalue equation in the original equation above we see that decoupling of modes can be achieved with $\lambda_i > 0$

$$\boldsymbol{V}\boldsymbol{A} = \boldsymbol{V}(\boldsymbol{a}_1, \ldots, \boldsymbol{a}_f) = \boldsymbol{T}(\lambda_1\boldsymbol{a}_1, \ldots, \lambda_f\boldsymbol{a}_f) = \boldsymbol{T}\boldsymbol{A}\boldsymbol{W_D}\,, \qquad \boldsymbol{W_D} = \begin{pmatrix} \lambda_1 & & \\ & \ddots & \\ & & \lambda_f \end{pmatrix}. \tag{2.44}$$

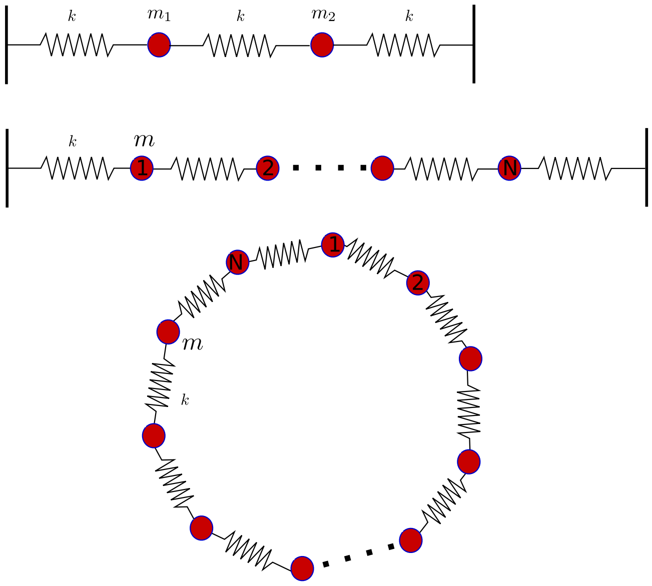

Figure 2.1: Illustration of some simple 1D models for which an analytic decomposition in terms of normal modes is possible. From top to bottom: Two coupled oscillators attached to two walls (masses and spring constants may be different). A chain of homogeneously coupled oscillators with identical masses which is attached to two walls (all normal frequencies are positive). The closed homogeneous chain: All normal frequencies are non-negative, one vanishes and corresponds to the displacement of the complete system.

Accordingly, the Lagrange function becomes

$$L = \frac{1}{2}\sum_{i=1}^{f} \dot{Q}_i^2 - \frac{1}{2}\sum_{i=1}^{f} \lambda_i Q_i^2 \,, \tag{2.45}$$

which are just the decoupled Lagrange functions of f harmonic oscillators with mass $m = 1$. Consequently, we identify

$$\omega_i = \sqrt{\lambda_i} \tag{2.46}$$

as the positive eigenfrequency of the **normal mode**.

We transform this in the usual way to a Hamilton function using a Legendre transform

$$H = \frac{1}{2}\sum_{i=1}^{f} P_i^2 + \frac{1}{2}\sum_{i=1}^{f} \omega_i^2 Q_i^2 \,. \tag{2.47}$$

2.4.2 General Examples

Normally, such computations will have to be done numerically. However, there exist some systems for which an analytic solution is possible, see Fig. 2.1.

Two coupled oscillators

For two coupled oscillators

$$L = \frac{1}{2}m_1\dot{q}_1^2 + \frac{1}{2}m_2\dot{q}_2^2 - \left[\frac{1}{2}Kq_1^2 + \frac{1}{2}Kq_2^2 + \frac{1}{2}K(q_1 - q_2)^2\right] \tag{2.48}$$

we have the matrices

$$T = \begin{pmatrix} m_1 & 0 \\ 0 & m_2 \end{pmatrix} \,, \qquad V = K\begin{pmatrix} 2 & -1 \\ -1 & 2 \end{pmatrix} \,, \tag{2.49}$$

and we see that both are positive definite. The generalized eigenvalue problem

$$V\boldsymbol{a_i} = \lambda_i T\boldsymbol{a_i} \tag{2.50}$$

can be solved in general with lengthy expressions. For the simpler case $m_1 = m_2 = m$, it becomes a normal eigenvalue problem with solutions

$$\begin{aligned}
&\boldsymbol{a}_1 = \frac{1}{\sqrt{2m}} \begin{pmatrix} 1 \\ 1 \end{pmatrix} , \qquad \boldsymbol{a}_2 = \frac{1}{\sqrt{2m}} \begin{pmatrix} 1 \\ -1 \end{pmatrix} , \\
&\lambda_1 = \frac{k}{m} , \qquad \lambda_2 = 3\frac{k}{m} .
\end{aligned} \tag{2.51}$$

As expected, we have $\lambda_i > 0$ and consequently, the frequencies of the normal modes become

$$\omega_1 = \sqrt{\frac{k}{m}} , \qquad \omega_2 = \sqrt{3\frac{k}{m}} . \tag{2.52}$$

Finite Chain

We can consider a finite-sized chain of points with the same mass m

$$L = \frac{1}{2} m \sum_{i=1}^{N} \dot{q}_i^2 - \frac{1}{2} K q_1^2 - \frac{1}{2} K \sum_{i=1}^{N-1} (q_i - q_{i+1})^2 - \frac{1}{2} K q_N^2 , \tag{2.53}$$

from which we can read off the matrices

$$T = m\mathbf{1} , \qquad V = K \begin{pmatrix} 2 & -1 & & & \\ -1 & 2 & \ddots & & \\ & \ddots & \ddots & \ddots & \\ & & \ddots & 2 & -1 \\ & & & -1 & 2 \end{pmatrix} . \tag{2.54}$$

The circle theorem by Gershgorin [6] shows that the V matrix is positive semidefinite. However, due to its simplicity, we can even calculate the eigenvalues and eigenvectors of V explicitly ($1 \le a, b \le N$)

$$V \boldsymbol{v_a} = \epsilon_a \boldsymbol{v_a} , \qquad \epsilon_a = 2K - 2K \cos \frac{\pi a}{N+1} , \qquad v_{ab} = \frac{2}{\sqrt{N+1}} \sin \frac{\pi a b}{N+1} . \tag{2.55}$$

To solve the generalized eigenvalue problem, we just need to multiply by $\frac{1}{\sqrt{m}}$, leading to the generalized eigenvectors and transformation matrix

$$\boldsymbol{a}_a = \frac{1}{\sqrt{m}} \frac{2}{\sqrt{N+1}} \begin{pmatrix} \sin \frac{\pi a 1}{N+1} \\ \vdots \\ \sin \frac{\pi a N}{N+1} \end{pmatrix} , \qquad A_{ab} = \frac{1}{\sqrt{m}} \frac{2}{\sqrt{N+1}} \sin \frac{\pi a b}{N+1} , \tag{2.56}$$

respectively. The eigenvalues of the generalized problem become

$$\lambda_a = 2\frac{K}{m} \left[1 - \cos \frac{\pi a}{N+1} \right] > 0 , \tag{2.57}$$

as $1 \le a \le N$. From this, we obtain the normal mode frequencies as $\omega_a = \sqrt{\lambda_a}$. These will be in a finite range. For $N = 2$ we reproduce the special case of the previous example. By contrast, for $N \to \infty$, the spectrum of normal mode frequencies will become continuously distributed between the extremal frequencies

$$\omega_{\min} \approx \sqrt{2\frac{K}{m}} \frac{\pi}{\sqrt{2}N} + \mathcal{O}\{N^{-2}\} , \qquad \omega_{\max} \approx 2\sqrt{\frac{K}{m}} + \mathcal{O}\{N^{-2}\} . \tag{2.58}$$

The bound obtained for the normal mode frequencies is just a manifestation of the fact that it is fully sufficient to know the frequencies within a primitive elementary cell of the reciprocal lattice.

---

[6] Semjon Aronowitsch Gerschgorin (1901–1933) was a belorussian mathematician.

Translationally invariant chain

There are two ways to end up with a translationally invariant chain. First, we could extend the chain at both ends to plus/minus infinity. Then, one will also obtain a continuum of normal modes. Any solid will however be of finite size, so another way to obtain a translationally invariant model is to use periodic boundary conditions with finite N

$$L = \frac{1}{2} m \sum_{i=1}^{N} \dot{q}_i^2 - \frac{1}{2} K \sum_{i=1}^{N} (q_i - q_{i+1})^2 \,, \qquad q_{N+1} \equiv q_1 \,. \tag{2.59}$$

The matrices for the kinetic and potential energy become

$$T = m\mathbf{1} \,, \qquad V = K \begin{pmatrix} 2 & -1 & & & -1 \\ -1 & 2 & \ddots & & \\ & \ddots & \ddots & \ddots & \\ & & \ddots & 2 & -1 \\ -1 & & & -1 & 2 \end{pmatrix} . \tag{2.60}$$

Now, we only see that the V matrix is positive semidefinite, i.e., some eigenvalues may actually vanish. However, the V matrix is circulant, and its eigenvalues and eigenvectors can also be analytically determined

$$V\boldsymbol{v_a} = \epsilon_a \boldsymbol{v_a} \,, \qquad \epsilon_a = 2K \left[1 - \cos \frac{2\pi a}{N} \right] \,, \qquad v_{ab} = \frac{1}{\sqrt{N}} \exp\left\{ \frac{2\pi \mathrm{i} ab}{N} \right\} \,. \tag{2.61}$$

We observe a few things.

First, there is now one frequency where for $a = N$ the energy vanishes $\epsilon_N = 0$. This means that when moving along the corresponding associated eigenvector

$$\boldsymbol{v_N} = \frac{1}{\sqrt{N}} \begin{pmatrix} 1 \\ \vdots \\ 1 \end{pmatrix} \tag{2.62}$$

the potential energy does not change. Physically, it means that movement along this generalized coordinate just means to move the closed chain as a whole.

Second, only for even N there is another unpaired eigenvalue at $a = N/2$ with maximal energy $\epsilon_{N/2} = 4k$

$$\boldsymbol{v_{N/2}} = \frac{1}{\sqrt{N}} \begin{pmatrix} -1 \\ +1 \\ \vdots \\ -1 \\ +1 \end{pmatrix} \tag{2.63}$$

Third, all other eigenvalues come in degenerate pairs, e.g. $a = i$ and $a = N - i$ where $1 \le i < N/2$. For each of these pairs, we can form two real superpositions of the two eigenvectors corresponding to degenerate pairs, leading to a fully real solution.

After separating off the generalized coordinate with vanishing eigenvalue we could proceed as usual and solve the generalized eigenvalue problem. Accordingly, the frequencies of the nontrivial normal modes just become

$$\omega_a = \sqrt{\frac{2K}{m} \left[1 - \cos \frac{2\pi a}{N} \right]} \,, \qquad 1 \le a \le N - 1 \,. \tag{2.64}$$

2.4.3 Examples for periodic lattices

So far, our examples above did not need to be realized on a lattice. We just demanded that the interaction strength between two lattice sites was constant along the chain, such that the actual lattice constant did not show up. Here, one generally finds it more convenient to find the frequencies not by exact diagonalization but by solving the equations of motion arising from the corresponding Lagrange function.

1D Bravais lattice

Now we explicitly state that the masses on a 1D lattice should be distributed at positions

$$x_n = na\,, \qquad n \in \mathbb{Z}\,, \tag{2.65}$$

which introduces the lattice constant a. Denoting as in Ref. [4] the local displacement of the chain at n by u_n, the potential assumes the form

$$U = \frac{1}{2}K\sum_{n=1}^{N}[u_n - u_{n+1}]^2\,, \qquad u_{N+1} \equiv u_1\,. \tag{2.66}$$

In this context, the periodic boundary conditions employed here are also often termed Born-von-Kármán [7] boundary conditions. Furthermore, we note that we have only allowed for motional degrees of freedom along the chain direction (longitudinal). Accordingly, the equations of motion (Euler Lagrange) yield the coupled system

$$m\ddot{u}_n = -K\left[2u_n - u_{n-1} - u_{n+1}\right]\,. \tag{2.67}$$

To get the energies of the normal modes, we use the ansatz

$$u_n(t) = ce^{+\mathrm{i}(nka-\omega t)} \tag{2.68}$$

with the one-dimensional wave-vector k and frequency ω and some constant c. Insertion into the equations of motion yields a relation between wave vector and frequency

$$-m\omega^2 = -K[2 - 2\cos(ka)]\,, \tag{2.69}$$

and by solving for the frequency we obtain the **dispersion relation**

$$\omega(k) = \sqrt{\frac{2K}{m}[1-\cos(ka)]} = 2\sqrt{\frac{K}{m}}|\sin(ka/2)|\,. \tag{2.70}$$

Furthermore, from the periodic boundary conditions we also get that ka is discrete

$$e^{\mathrm{i}Nka} = 1 \qquad \Longrightarrow \qquad k_n a = \frac{2\pi n}{N}\,, \qquad n \in \mathbb{Z}\,. \tag{2.71}$$

One can see that there are only N different values of k that actually correspond to different physical solutions: Adding an integer multiple of 2π to ka yields no change. It is therefore customary to constrain the considerations to the first Brillouin zone

$$-\frac{\pi}{a} \le k_n \le +\frac{\pi}{a}\,. \tag{2.72}$$

The dispersion relation (2.70) assigns a normal mode frequency $\omega_n = \omega(k_n)$ to each of the discrete values of k_n. In the limit of an infinitely large closed chain $N \to \infty$, the values of k_n

---

[7] Theodore von Kármán (1881–1963) was a hungarian physicist.

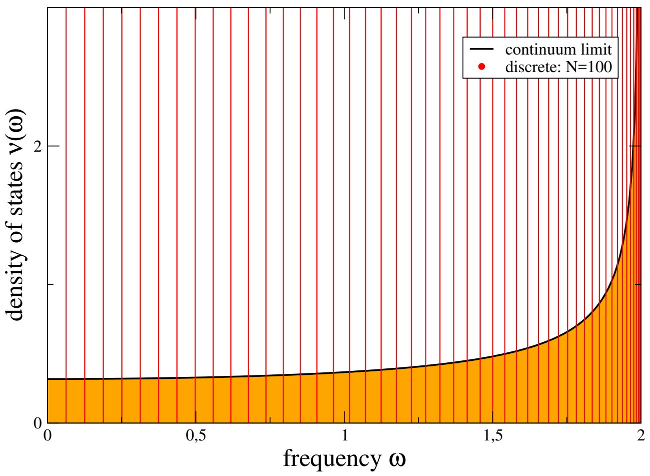

Figure 2.2: Plot of the discrete density of states (2.73) as train of δ functions (red spikes) and its continuous version (2.76) (black and orange). For each ω value there are two spikes at the same position, corresponding to $\pm k(\omega)$. The integral over both functions is the same (one).

become more and more dense, which transfers to $\omega(k)$. In this limit, it makes sense to define the density of states via

$$\nu_N(\omega) = \frac{1}{N} \sum_{j=1}^{N} \delta(\omega - \omega_j)\,, \tag{2.73}$$

where N denotes the total length of the system and ω_j its eigenfrequencies.

One way to derive the limit of the density of states for $N \to \infty$ is to perform an integration around one normal mode frequency. Apparently, we have

$$\int\limits_{(\omega_j+\omega_{j-1})/2}^{(\omega_{j+1}+\omega_j)/2} \nu_N(\omega) d\omega = \frac{2}{N} \approx \nu_N(\omega_j) \frac{\omega_{j+1} - \omega_{j-1}}{2}\,. \tag{2.74}$$

Here, the factor of 2 after the equality results from the fact that for $\pm k$ we have the same $\omega(+k) = \omega(-k)$. Now, we can insert for sufficiently dense frequencies $\omega_j = \omega(k_j)$ approximate

$$\begin{aligned}\omega_{j+1} - \omega_{j-1} &\approx \omega(k_j) + \left.\frac{d\omega(k)}{dk}\right|_{k_j} (k_{j+1} - k_j) - \omega(k_j) - \left.\frac{d\omega(k)}{dk}\right|_{k_j} (k_{j-1} - k_j) = \left.\frac{d\omega(k)}{dk}\right|_{k_j} (k_{j+1} - k_{j-1}) \\ &= \frac{d\omega(k)}{dk} \frac{4\pi}{Na}\,.\end{aligned} \tag{2.75}$$

Inserting this in the above equation and solving we obtain the density of states in the limit when $N \to \infty$

$$\begin{aligned}\nu_\infty(\omega) &\approx \frac{2}{N} \frac{Na}{2\pi} \frac{1}{\left(\frac{d\omega(k)}{dk}\right)} = \frac{2}{N} \frac{Na}{2\pi} \frac{dk(\omega)}{d\omega} = \frac{a}{\pi} \frac{2m}{a\sqrt{m(4K - m\omega^2)}} \\ &= \frac{2}{\pi} \frac{1}{\sqrt{4\frac{K}{m} - \omega^2}}\,, \qquad 0 \le \omega \le 2\sqrt{\frac{K}{m}}\,.\end{aligned} \tag{2.76}$$

In the last equality of the first line, we have first solved Eq. (2.70) for $k(\omega)$ with $k(\omega) > 0$ and then computed the derivative. This is also illustrated in Fig. 2.2.

It should be noted that in our 1D examples, we have so far only taken longitudinal vibrations into account. However, a 1d chain may also support transversal vibrations. Then, the 1d chain would also allow for transversal displacements and we would have to write $u_n(t) \to \underline{u_n}(t)$ as vectors, allowing e.g. for 3 generalized coordinates per lattice node and two additional transversal spring constants $K_\perp^1, K_\perp^2$. In this case, we would essentially increase the number of normal modes. Below, we will investigate in more detail what happens.

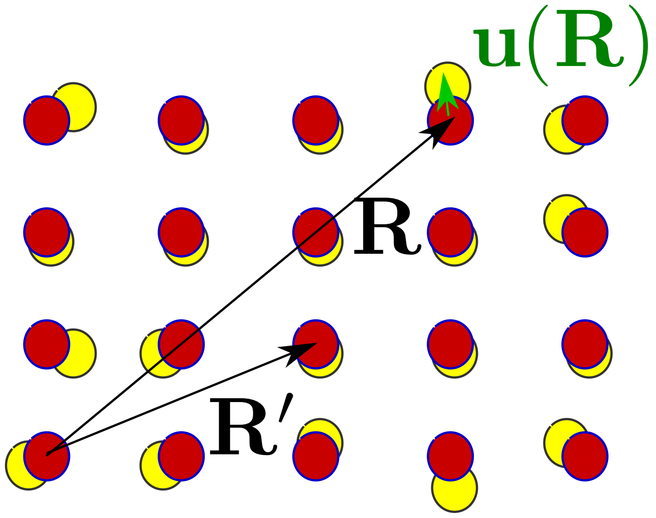

Figure 2.3: 2d illustration of a lattice with equilibrium positions $\boldsymbol{R}$ (red circles) and the displacements $\boldsymbol{u}(\boldsymbol{R})$ from them (yellow circles). The dynamical matrix $\underline{\underline{D}}(\boldsymbol{R}-\boldsymbol{R}')$ encodes the potential between sites $\boldsymbol{R}$ and $\boldsymbol{R}'$, which need not necessarily be next neighbours. Metals start to melt when the displacement reaches a few percent of the lattice constant.

Normal modes in general Bravais lattices

For a general Bravais lattice with identical atoms, we can write the potential energy as (compare Ref. [4])

$$U = \frac{1}{2}\sum_{\boldsymbol{R},\boldsymbol{R}'} \boldsymbol{u}(\boldsymbol{R})^T \underline{\underline{D}}^{\boldsymbol{R},\boldsymbol{R}'} \boldsymbol{u}(\boldsymbol{R}')\,, \qquad \underline{\underline{D}}^{\boldsymbol{R},\boldsymbol{R}'} = \underline{\underline{D}}(\boldsymbol{R}-\boldsymbol{R}')\,. \tag{2.77}$$

Now, $\boldsymbol{R}$ and $\boldsymbol{R}'$ both denote lattice nodes on the Bravais lattice. Further $\boldsymbol{u}(\boldsymbol{R})$ denotes the vector-valued local displacement of the atom that would normally be at equilibrium position $\boldsymbol{R}$, and similar for $\boldsymbol{u}(\boldsymbol{R}')$, see Fig. 2.3 for a 2D example. From translational invariance, the **dynamical matrix** $\underline{\underline{D}}$ should depend only on the difference between the two lattice vectors. In fact, for **isotropic** lattices, one would actually expect that it only depends on the modulus of the difference. However, in general we can conclude

$$\begin{aligned}\underline{\underline{D}}(\boldsymbol{R}-\boldsymbol{R}') &= \underline{\underline{D}}^T(\boldsymbol{R}'-\boldsymbol{R})\,,\\ \underline{\underline{D}}(\boldsymbol{R}) &= \underline{\underline{D}}(-\boldsymbol{R})\,,\\ \sum_{\boldsymbol{R}} \underline{\underline{D}}(\boldsymbol{R}) &= \boldsymbol{0}\,.\end{aligned} \tag{2.78}$$

The first relation follows simply from transposition of the total potential energy:

$$U = \frac{1}{2}\sum_{\boldsymbol{R},\boldsymbol{R}'} \boldsymbol{u}^T(\boldsymbol{R}')\underline{\underline{D}}^T(\boldsymbol{R}-\boldsymbol{R}')\boldsymbol{u}(\boldsymbol{R}) = \frac{1}{2}\sum_{\boldsymbol{R},\boldsymbol{R}'} \boldsymbol{u}^T(\boldsymbol{R})\underline{\underline{D}}^T(\boldsymbol{R}'-\boldsymbol{R})\boldsymbol{u}(\boldsymbol{R}')\,. \tag{2.79}$$

The second follows from the invariance of the potential energy under inversion of all positions and displacements ($\boldsymbol{R} \to -\boldsymbol{R}$ and $\boldsymbol{u}(\boldsymbol{R}) \to -\boldsymbol{u}(-\boldsymbol{R})$) or put more simply from the requirement that *actio* = *reactio*.

Finally, the third symmetry relation follows from the requirement that homogeneous shifts of all coordinates by the same constant displacement $\boldsymbol{u}(\boldsymbol{R}) = \boldsymbol{u}_0$ should not yield any potential energy (gauging)

$$0 = \boldsymbol{u}_0^T \left(\sum_{\boldsymbol{R},\boldsymbol{R}'} \underline{\underline{D}}(\boldsymbol{R}-\boldsymbol{R}')\right) \boldsymbol{u}_0 = \boldsymbol{u}_0^T \left(\sum_{\boldsymbol{R}} \underline{\underline{D}}(\boldsymbol{R})\right) \boldsymbol{u}_0\,. \tag{2.80}$$

We note that in contrast to the previous simple examples, this treatment also includes all directions of displacements, any connection topology admitted by the Bravais lattice, and also couplings between very distant neighbours of the Bravais lattice.

We will not try to write the full Lagrange function as a quadratic form involving all generalized coordinates. Rather, we will use the equations of motion to obtain the dispersion relations. These become for identical masses m

$$m\ddot{\boldsymbol{u}}(\boldsymbol{R}) = -\sum_{\boldsymbol{R}'} \underline{\underline{D}}(\boldsymbol{R}-\boldsymbol{R}')\boldsymbol{u}(\boldsymbol{R}') \,. \tag{2.81}$$

Still, the matrix $\underline{\underline{D}}$ now describes the coupling of the atom at position $\boldsymbol{R}$ to all other atoms. Since we have now a vector-valued displacement, we use an ansatz where the constant c is now replaced with the **polarization vector $\boldsymbol{\epsilon}$**

$$\boldsymbol{u}(\boldsymbol{R},t) = \boldsymbol{\epsilon} \exp\{\mathrm{i}(\boldsymbol{k}\boldsymbol{R}-\omega t)\} \,, \tag{2.82}$$

where $\boldsymbol{k}$ is a **wave vector** and ω is the normal mode frequency. The wave vector $\boldsymbol{k}$ points into the propagation direction of the wave, and $\boldsymbol{\epsilon}$ points into the direction of the displacement. If $\boldsymbol{\epsilon}$ and $\boldsymbol{k}$ are perfectly aligned (i.e., parallel or anti-parallel), one calls the vibration longitudinal, if they are perpendicular, the vibration is transversal. Inserting this ansatz into the equations of motion, we get

$$-m\omega^2\boldsymbol{\epsilon} = -\sum_{\boldsymbol{R}'} \underline{\underline{D}}(\boldsymbol{R}-\boldsymbol{R}')\boldsymbol{\epsilon} e^{-\mathrm{i}\boldsymbol{k}(\boldsymbol{R}-\boldsymbol{R}')} = -\sum_{\boldsymbol{R}} \underline{\underline{D}}(\boldsymbol{R}) e^{-\mathrm{i}\boldsymbol{k}\boldsymbol{R}}\boldsymbol{\epsilon} = -\underline{\underline{D}}(\boldsymbol{k})\boldsymbol{\epsilon} \,. \tag{2.83}$$

The Fourier-transformed matrix

$$\underline{\underline{D}}(\boldsymbol{k}) = \sum_{\boldsymbol{R}} \underline{\underline{D}}(\boldsymbol{R}) e^{-\mathrm{i}\boldsymbol{k}\boldsymbol{R}} \tag{2.84}$$

is sometimes also called dynamical matrix.

From Eq. (2.78) we can derive that the dynamical matrix is real-valued and symmetric

$$\underline{\underline{D}}(\boldsymbol{k}) = \underline{\underline{D}}(-\boldsymbol{k}) = \underline{\underline{D}}^*(\boldsymbol{k}) = \underline{\underline{D}}^T(\boldsymbol{k}) \,. \tag{2.85}$$

Consequently, it can be diagonalized with orthogonal eigenvectors $\boldsymbol{\epsilon}_\sigma(\boldsymbol{k})$ and real eigenvalues $\lambda_\sigma(\boldsymbol{k})$

$$\underline{\underline{D}}(\boldsymbol{k})\boldsymbol{\epsilon}_\sigma(\boldsymbol{k}) = \lambda_\sigma(\boldsymbol{k})\boldsymbol{\epsilon}_\sigma(\boldsymbol{k}) \,. \tag{2.86}$$

Choosing the polarization eigenvector as an eigenvector of the dynamical matrix $\boldsymbol{\epsilon}_\sigma$, we can solve the resulting equation

$$m\omega^2\boldsymbol{\epsilon}_\sigma(\boldsymbol{k}) = \underline{\underline{D}}(\boldsymbol{k})\boldsymbol{\epsilon}_\sigma(\boldsymbol{k}) = \lambda_\sigma(\boldsymbol{k})\boldsymbol{\epsilon}_\sigma(\boldsymbol{k}) \tag{2.87}$$

to get a separate dispersion relation

$$\omega_\sigma = \sqrt{\frac{\lambda_\sigma(\boldsymbol{k})}{m}} \tag{2.88}$$

for each of the polarizations σ and along the wave vector $\boldsymbol{k}$. These dispersion relations are also called **acoustic branches** of the Bravais lattice. They are called acoustic since one can show that for small $\boldsymbol{k}$, all these dispersion relations scale linearly in $\boldsymbol{k}$: Exploiting the symmetries (2.78) of the dynamical matrix, we can write

$$\begin{aligned}\underline{\underline{D}}(\boldsymbol{k}) &= \frac{1}{2}\sum_{\boldsymbol{R}} \underline{\underline{D}}(\boldsymbol{R}) \left[e^{-\mathrm{i}\boldsymbol{k}\boldsymbol{R}} + e^{+\mathrm{i}\boldsymbol{k}\boldsymbol{R}} - 2\right] = -2\sum_{\boldsymbol{R}} \underline{\underline{D}}(\boldsymbol{R}) \sin^2\frac{\boldsymbol{k}\boldsymbol{R}}{2} \approx -\frac{1}{2}\sum_{\boldsymbol{R}}(\boldsymbol{k}\boldsymbol{R})^2 \underline{\underline{D}}(\boldsymbol{R}) \\ &= -\frac{1}{2}k^2\sum_{\boldsymbol{R}}(\boldsymbol{e_k}\boldsymbol{R})^2\underline{\underline{D}}(\boldsymbol{R})\,, \qquad \boldsymbol{e_k} = \frac{\boldsymbol{k}}{k}\,.\end{aligned} \tag{2.89}$$

Accordingly, we can write for the dispersion relation

$$\omega_\sigma(\boldsymbol{e_k}) \approx c_\sigma(\boldsymbol{k})k\,, \tag{2.90}$$

where $c_\sigma(\boldsymbol{e_k})$ is the velocity of sound in direction $\boldsymbol{k}$. Given the matrix $\sum_{\boldsymbol{R}}(\boldsymbol{e_k}\boldsymbol{R})^2\underline{\underline{D}}(\boldsymbol{R})$, we can microscopically calculate these. For example, in isotropic elastic media and three dimensions one finds that the wave vector and polarization are either parallel or perpendicular, such that one has one longitudinal and two transversal modes

$$\boldsymbol{\epsilon}_1(\boldsymbol{k}) \parallel \boldsymbol{k} \qquad : \qquad 1 \text{ longitudinal mode} \tag{2.91}$$

$$\boldsymbol{\epsilon}_{2/3}(\boldsymbol{k}) \perp \boldsymbol{k} \qquad : \qquad 2 \text{ transversal modes}\,. \tag{2.92}$$

However, for non-isotropic media it may not be possible to choose the eigenvectors $\boldsymbol{\epsilon}_k$ of the dynamical matrix in this way.

However, this does not tell us anything about the allowed values of $\boldsymbol{k}$. To continue, we again demand periodic boundary conditions (Born-von-Kármán), now in terms of periodic repetitions of the basis vectors of the Bravais lattice

$$\boldsymbol{u}(\boldsymbol{R} + N_i\boldsymbol{a}_i) = \boldsymbol{u}(\boldsymbol{R})\,, \tag{2.93}$$

which simply means that the lattice is periodically continued after N_i repetitions of the basis vector $\boldsymbol{a}_i$. The total number of lattice nodes is then given by

$$N = N_1 N_2 N_3\,. \tag{2.94}$$

In particular, we can view the body spanned by

$$N_1\boldsymbol{a}_1 + N_2\boldsymbol{a}_2 + N_3\boldsymbol{a}_3 \tag{2.95}$$

as an elementary cell of an actually infinitely large lattice: Periodically repeating this elementary cell (which contains N lattice points) covers the full space. The basis vectors of the Bravais lattice can then be chosen as

$$\boldsymbol{a'}_i = N_i\boldsymbol{a}_i\,. \tag{2.96}$$

Then, when $\boldsymbol{b}_i$ denote the basis vectors of the reciprocal lattice, the $\boldsymbol{b'}_i$ are related to these via

$$\boldsymbol{b'}_i = \frac{1}{N_i}\boldsymbol{b}_i\,. \tag{2.97}$$

We can therefore write

$$\boldsymbol{k} = \sum_i k_i\boldsymbol{b'}_i = \sum_i \frac{k_i}{N_i}\boldsymbol{b}_i\,. \tag{2.98}$$

Normal modes in Bravais lattices with basis

The inversion symmetry used before in the dynamical matrix may not be respected when one has media with a basis. Therefore, one can in these systems not expect the dispersion relations for all modes to vanish linearly as ka goes to zero. In addition, so-called **optical modes** may arise, and the normal mode frequencies of these optical modes remain finite as $\boldsymbol{k}$ is small. This is simplest to illustrate with a closed chain made from a di-atomic basis in 1D. Let us denote the generalized coordinates of species A by q_i and that of species B by u_i. Then, the potential can be written as

$$U = K\frac{1}{2}\sum_i (q_i - u_i)^2 + G\frac{1}{2}\sum_i (u_i - q_{i+1})^2 \,, \qquad q_{N+1} = q_1 \,. \tag{2.99}$$

Here, the basis is modeled by introducing an alternating spring constant K and G. Now, the dispersion relation can be derived exactly from either direct diagonalization of the full Lagrange function or using the equations of motion

$$\begin{aligned} m\ddot{u}_n &= -K(u_n - q_n) - G(u_n - q_{n+1}) \,, \\ m\ddot{q}_n &= -K(q_n - u_n) - G(q_n - u_{n-1}) \,. \end{aligned} \tag{2.100}$$

We again seek for a wave solution

$$u_n = Ae^{+\mathrm{i}(nka-\omega t)} \,, \qquad q_n = Be^{+\mathrm{i}(nka-\omega t)} \,. \tag{2.101}$$

Inserting this ansatz into the equations of motion and dividing by the exponentials, we get the two coupled equations

$$(m\omega^2 - K - G)A + (K + e^{+\mathrm{i}ka}G)B = 0 \,, \qquad (K + e^{-\mathrm{i}ka}G)A + (m\omega^2 - K - G)B = 0 \,. \tag{2.102}$$

For that to have a non-trivial solution with non-vanishing A and B, the coefficient matrix determinant has to vanish

$$\begin{aligned} 0 &= (m\omega^2 - K - G)^2 - (K + e^{+\mathrm{i}ka}G)(K + e^{-\mathrm{i}ka}G) \\ &= (m\omega^2 - (K+G))^2 - (K^2 + G^2 + 2KG\cos(ka)) \,. \end{aligned} \tag{2.103}$$

Solving for the frequency now tells us that there are two positive branches of the dispersion relation

$$\omega_\pm(k) = \sqrt{\frac{K+G}{m} \pm \sqrt{\frac{K^2}{m^2} + \frac{G^2}{m^2} + 2\frac{KG}{m^2}\cos(ka)}} \,. \tag{2.104}$$

The same periodicity argument holds, and we can constrain $-\pi < ka < +\pi$, and we see that for small ka the modes behave differently

$$\omega_-(0) = 0 \,, \qquad \omega_+(0) = \sqrt{\frac{2(K+G)}{m}} \,. \tag{2.105}$$

The branch that goes to zero for small k is the usual **acoustic branch** (dispersion relations like $\omega(k) = ck$ are typical for sound waves). The other branch is called **optical branch**, as it typically interacts with light much stronger. Alternatively, we can calculate the normal mode frequencies by direct computation, see Fig. 2.4.

This qualitative picture also works in more complicated lattices, see also Fig. 2.5.

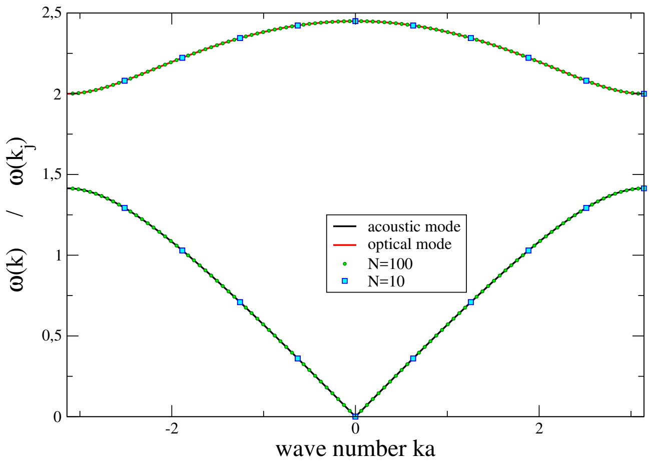

Figure 2.4: Plot of acoustic (black) and optical (red) dispersion relations for a 1d di-atomic chain (2.104) in the first Brillouin zone. The acoustic mode scales linearly for small k. Direct numerical computation of the normal mode frequencies $\omega(k_j)$ yields $2N$ modes for a lattice with N sites. Other parameters: $K/m = 1$, $G/m = 2$.

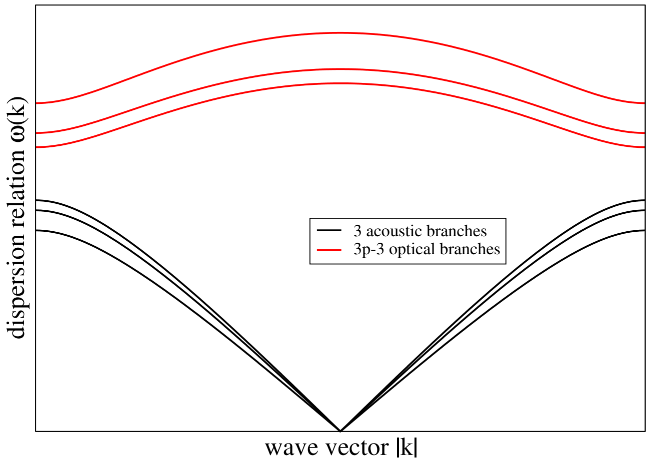

Figure 2.5: Sketch of the 3 acoustic dispersion relations (black) and the $3p-3$ optical branches (red, here for $p = 2$). Whereas acoustic modes scale linearly at the center of the Brillouin zone, the frequency of the optical branches has a finite value at $k = 0$.

Box 6 (Phonon mode classification) *For a 3d lattice with M nodes and p atoms per lattice node (and a total number of atoms $N = Mp$), one can classify the $3N = 3Mp$ vibrational modes into $3p$ branches. Of these, three are acoustic branches and $3p-3$ are optical branches. For each branch, the frequencies $\omega(k)$ are functions of k, and the three acoustic branches scale linearly in k at the center of the Brillouin zone.*

2.4.4 Quantization of lattice vibrations

Eventually, we perform the quantization by introducing position and momentum operators via the correspondence principle leading to the Hamilton operator

$$H = \frac{1}{2}\sum_{i=1}^{f} \hat{P}_i^2 + \frac{1}{2}\sum_{i=1}^{f} \omega_i^2 \hat{Q}_i^2 . \tag{2.106}$$

Here, the operators have to obey the canonical commutation relations

$$\left[\hat{Q}_k, \hat{P}_j\right] = \mathrm{i}\hbar\delta_{kj} . \tag{2.107}$$

As known from single-oscillator treatments in quantum mechanics, we can now introduce raising and lowering operators for every mode (we drop the operator hats)

$$a_j = \sqrt{\frac{\omega_j}{2\hbar}} Q_j + \frac{\mathrm{i}}{\sqrt{2\hbar\omega_j}} P_j , \qquad a_j^\dagger = \sqrt{\frac{\omega_j}{2\hbar}} Q_j - \frac{\mathrm{i}}{\sqrt{2\hbar\omega_j}} P_j , \tag{2.108}$$

and the commutation relations become

$$[a_j, a_k^\dagger] = \delta_{jk} \,. \tag{2.109}$$

In terms of these operators, the Hamiltonian becomes

$$H = \sum_{i=1}^{f} \hbar\omega_i \left[a_i^\dagger a_i + \frac{1}{2}\right] \,, \tag{2.110}$$

and since for each oscillator we can define the usual Fock [8] eigenstates

$$a_i^\dagger a_i \left|n_i\right\rangle = n_i \left|n_i\right\rangle \,, \qquad \left|n_i\right\rangle = \frac{(a_i^\dagger)^{n_i}}{\sqrt{n_i!}} \left|0\right\rangle_i \,, \tag{2.111}$$

upon which the ladder operators act as

$$a_i \left|n_i\right\rangle = \sqrt{n_i} \left|n_i - 1\right\rangle \,, \qquad a_i^\dagger \left|n_i\right\rangle = \sqrt{n_i + 1} \left|n_i + 1\right\rangle \,, \tag{2.112}$$

we obtain by the tensor product

$$\left|n_1, \ldots, n_f\right\rangle = \left|n_1\right\rangle \otimes \ldots \otimes \left|n_f\right\rangle \tag{2.113}$$

the eigenstates of the total decoupled system

$$H \left|n_1, \ldots, n_f\right\rangle = \left[\sum_{i=1}^{f} \hbar\omega_i \left(n_i + \frac{1}{2}\right)\right] \left|n_1, \ldots, n_f\right\rangle \,. \tag{2.114}$$

Since we have introduced the common classification into optical and acoustic branches, it is customary to specify the index of normal mode i in the Hamiltonian as $i = (\sigma, \boldsymbol{k})$, such that

$$H = \sum_{\sigma} \sum_{\boldsymbol{k}} \hbar\omega_\sigma(\boldsymbol{k}) \left[a_{\sigma\boldsymbol{k}}^\dagger a_{\sigma\boldsymbol{k}} + \frac{1}{2}\right] \,, \tag{2.115}$$

Here, σ labels the branch of the dispersion relation (e.g. $\sigma = 1, 2, 3$ for the acoustic modes) and $\boldsymbol{k}$ denotes the point in the Brillouin zone that labels the normal mode.

2.4.5 Specific Heat: Classical Treatment/Dulong-Petit

The thermal behaviour of solids strongly depends on the presence of phonons. In this section (compare also Ref. [4]), we will denote the internal energy of the solid by U and the total particle number by N. Dividing by the macroscopic volume V, we can introduce the corresponding internal energy density and particle density

$$u = \frac{U}{V} \,, \qquad n = \frac{N}{V} \,. \tag{2.116}$$

According to statistical mechanics, we can compute the internal energy by integrating over the Hamilton function with a Boltzmann weight function

$$U = \frac{\int H e^{-\beta H} d\Gamma}{\int e^{-\beta H} d\Gamma} \,, \qquad \beta = \frac{1}{k_B T} \,, \qquad d\Gamma = \prod_{\boldsymbol{R}} d^3u(\boldsymbol{R}) d^3p(\boldsymbol{R}) \,. \tag{2.117}$$

---

[8] Wladimir Alexandrowitsch Fock (1898–1974) was a soviet theoretical physicist.

Here, H is the total Hamilton function of the system, $\boldsymbol{R}$ denotes all N lattice nodes, $\boldsymbol{u}(\boldsymbol{R})$ denotes the displacement at position $\boldsymbol{R}$, $\boldsymbol{p}$ the momentum of the ion at position $\boldsymbol{R}$, T is the temperature, and k_B the Boltzmann constant (often, one works in units where it is set to 1). We integrate over all displacements and momenta and thereby calculate the average energy. It is a standard trick to represent such average integrals by a derivative of the logarithm

$$U = -\partial_\beta \ln \int e^{-\beta H} d\Gamma\,, \tag{2.118}$$

which can be verified by performing the derivative with respect to β.

Now, provided that the harmonic approximation holds, the Hamilton function is a quadratic function of positions and momenta, compare Eq. (2.47), and we can transform the variables

$$\begin{aligned} \boldsymbol{u}(\boldsymbol{R}) &= \beta^{-1/2}\bar{\boldsymbol{u}}(\boldsymbol{R})\,, \qquad & \boldsymbol{p}(\boldsymbol{R}) &= \beta^{-1/2}\bar{\boldsymbol{p}}(\boldsymbol{R})\,, \\ d^3u(\boldsymbol{R}) &= \beta^{-3/2}d^3\bar{u}(\boldsymbol{R})\,, \qquad & d^3p(\boldsymbol{R}) &= \beta^{-3/2}d^3\bar{p}(\boldsymbol{R})\,. \end{aligned} \tag{2.119}$$

For example, for a Hamilton function of the form

$$H(\{\boldsymbol{p}(\boldsymbol{R}), \boldsymbol{u}(\boldsymbol{R})\}) = \sum_{\boldsymbol{R}} \frac{\boldsymbol{p}^2(\boldsymbol{R})}{2M} + U^{\rm eq} + \frac{1}{2}\sum_{\boldsymbol{R},\boldsymbol{R}'} \boldsymbol{u}^T(\boldsymbol{R})\underline{\underline{D}}(\boldsymbol{R}-\boldsymbol{R}')\boldsymbol{u}(\boldsymbol{R}') \tag{2.120}$$

with constant minimum potential energy $U^{\rm eq}$ and dynamical matrix $\underline{\underline{D}}(\boldsymbol{R}-\boldsymbol{R}')$ we see that the temperature dependence of the integral for the internal energy is mapped into a simple factor

$$\begin{aligned} \int e^{-\beta H} d\Gamma &= e^{-\beta U^{\rm eq}}\beta^{-3N}\int d\bar{\Gamma} \exp\left\{-[H(\bar{\boldsymbol{p}}(\boldsymbol{R}), \bar{\boldsymbol{u}}(\boldsymbol{R})) - U^{\rm eq}]\right\} = e^{-\beta U^{\rm eq}}\beta^{-3N} I_0\,, \\ d\bar{\Gamma} &= \prod_{\boldsymbol{R}} d^3\bar{u}(\boldsymbol{R}) d^3\bar{p}(\boldsymbol{R})\,. \end{aligned} \tag{2.121}$$

Here, N is the total number of ions in the crystal (we consider no basis for the moment). The remaining integral I_0 is in principle of Gaussian type and can be calculated, but its value is not at all interesting for the internal energy: Due to the additivity of the ln function and the derivative with respect to β, the only important observation is that under the harmonic approximation, the convergent integral I_0 does not depend on β. We get for the internal energy

$$U = -\partial_\beta\left[-\beta U^{\rm eq} - 3N\ln\beta + \ln I_0\right] = U^{\rm eq} + \frac{3N}{\beta}\,. \tag{2.122}$$

Dividing by the volume, this means that the energy density scales linearly with the particle density

$$u = u^{\rm eq} + 3nk_BT\,, \tag{2.123}$$

which is known as the **law of Dulong** [9]**-Petit** [10]. At zero temperature we only have the energy resulting from the static lattice theory (which can be gauged to zero), which ignores the zero-point motion. At finite temperature, this is corrected additively, by the simple $3nk_BT$ term, which means that all degrees of freedom are equally contributing to the total internal energy.

Since the correction term for finite temperatures is the one that can be measured, one often considers instead the specific heat (capacity)

$$c_V = \left(\frac{\partial u}{\partial T}\right)_V = 3nk_B\,. \tag{2.124}$$

---

[9] Pierre Louis Dulong (1785–1838) was a french scientist.

[10] Alexis Thérŝe Petit (1791–1820) was a french physicist.

When cross-checking this law with experiments, one sees that it does not match at low temperatures, where the derivation neglected the zero-point motion which would have required a full quantum treatment. However, also at high temperatures it does not fit very well: Here, the displacements are often so large that the harmonic approximation is not well fulfilled.

2.4.6 Specific heat: Quantum treatment

We first calculate the mean energy of a single quantum harmonic oscillator of frequency ω. The Hamiltonian reads

$$H = \hbar\omega(a^\dagger a + 1/2)\,. \tag{2.125}$$

$$Z = \mathrm{Tr}\left\{e^{-\beta H}\right\} = \sum_{n=0}^{\infty} \langle n| e^{-\beta H} |n\rangle = e^{-\beta\hbar\omega/2} \sum_{n=0}^{\infty} e^{-\beta\hbar\omega n} = \frac{e^{-\beta\hbar\omega/2}}{1-e^{-\beta\hbar\omega}}\,. \tag{2.126}$$

Similar to the classical case, we can calculate the mean energy by performing a derivative of the log of the **partition function**

$$\begin{aligned} U &= \mathrm{Tr}\left\{H\frac{e^{-\beta H}}{Z}\right\} = -\partial_\beta \ln Z = -\partial_\beta\left[-\beta\hbar\omega/2 - \ln[1-e^{-\beta\hbar\omega}]\right] \\ &= \frac{\hbar\omega}{2} + \frac{\hbar\omega e^{-\beta\hbar\omega}}{1-e^{-\beta\hbar\omega}} = \frac{\hbar\omega}{2} + \frac{\hbar\omega}{e^{+\beta\hbar\omega}-1}\,. \end{aligned} \tag{2.127}$$

The first term simply yields the zero-point energy, and the second term increases monotonously with temperature, in particular we have

$$\lim_{T\to 0} U = \frac{\hbar\omega}{2}\,, \qquad \lim_{T\to\infty} U = \frac{\hbar\omega}{2} + k_B T\,. \tag{2.128}$$

Now, we reconsider the full phonon Hamilton operator (2.115)

$$H = \sum_\sigma \sum_{\boldsymbol{k}} \hbar\omega_\sigma(\boldsymbol{k}) \left[a^\dagger_{\sigma\boldsymbol{k}} a_{\sigma\boldsymbol{k}} + \frac{1}{2}\right] = \sum_{i=1}^{f} \hbar\omega_i \left[a_i^\dagger a_i + \frac{1}{2}\right]\,, \tag{2.129}$$

which decouples between different modes $\boldsymbol{k}$ and different dispersion relation branches σ that altogether generate the f degrees of freedom. The total energy can be written as

$$U = -\partial_\beta \ln Z\,, \tag{2.130}$$

where – since in the normal mode decomposition the modes do not interact – we can write the total partition function as a product of the individual partition functions

$$\begin{aligned} Z &= \mathrm{Tr}\left\{e^{-\beta H}\right\} = \sum_{\boldsymbol{n}} \langle \boldsymbol{n}| e^{-\beta H} |\boldsymbol{n}\rangle = \sum_{n_1,\ldots,n_f=0}^{\infty} \langle n_1,\ldots,n_f| e^{-\beta\sum_i \hbar\omega_i[a_i^\dagger a_i + 1/2]} |n_1,\ldots,n_f\rangle \\ &= \prod_{i=1}^{f} \sum_{n_i=0}^{\infty} \langle n_i| e^{-\beta\hbar\omega_i[n_i+1/2]} |n_i\rangle = \prod_{i=1}^{f} Z_i\,. \end{aligned} \tag{2.131}$$

Accordingly, we get as expected that the internal energy is computed from the sum of the internal energies of the individual oscillators

$$U = -\partial_\beta \sum_{i=1}^{f} \ln Z_i = \sum_i \left[\frac{\hbar\omega_i}{2} + \frac{\hbar\omega_i}{e^{+\beta\hbar\omega_i}-1}\right] = \sum_\sigma \sum_{\boldsymbol{k}} \left[\frac{\hbar\omega_\sigma(\boldsymbol{k})}{2} + \frac{\hbar\omega_\sigma(\boldsymbol{k})}{e^{+\beta\hbar\omega_\sigma(\boldsymbol{k})}-1}\right]\,. \tag{2.132}$$

Here, the zero-point motion contribution does not depend on temperature. Likewise, we have neglected the constant potential energy term U^{eq}. Now, it makes sense to divide by volume and calculate the specific heat, where the zero-point motion drops out

$$c_V = \frac{1}{V} \sum_\sigma \sum_{\boldsymbol{k}} \frac{\partial}{\partial T} \frac{\hbar\omega_\sigma(\boldsymbol{k})}{e^{+\beta\hbar\omega_\sigma(\boldsymbol{k})} - 1} \,. \tag{2.133}$$

Given the dispersion relations for all branches, we can therefore in principle calculate the specific heat for the phonons. For example, comparing with the dispersion relations for the diatomic chain in Eq. (2.104), we can directly evaluate the continuum limit by converting the sum over $\boldsymbol{k}$ to a one-dimensional integral. To do so, we just need to know how much volume of the Brillouin zone is used per $\boldsymbol{k}$ point. Given that the volume of the primitive elementary cell (e.g. the Wigner-Seitz cell) is trivially related to the macroscopic crystal volume V and the number of atoms N via

$$V_{\text{ec}} = \frac{V}{N} \tag{2.134}$$

and that the volume of the primitive reciprocal lattice cell is – compare Eq. (1.11) – given by

$$V_{\text{rec}} = \frac{(2\pi)^3}{V_{\text{ec}}} = N\frac{(2\pi)^3}{V} \,, \tag{2.135}$$

we get – as we have N different $\boldsymbol{k}$ values in the 1. Brillouin zone – for the volume element in the reciprocal lattice per $\boldsymbol{k}$ vector

$$d^3k = \frac{(2\pi)^3}{V} \,. \tag{2.136}$$

With this, we can for sufficiently large N convert sums of smooth function $f(\boldsymbol{k})$ to integrals over these functions via the recipe

$$\sum_{\boldsymbol{k}} f(\boldsymbol{k}) \to \frac{V}{(2\pi)^3} \int_{1.\text{BZ}} f(\boldsymbol{k}) d^3k \,. \tag{2.137}$$

Applied to Eq. (2.133), we get

$$c_V = \sum_\sigma \int_{1.\text{BZ}} \frac{\partial}{\partial T} \frac{\hbar\omega_\sigma(\boldsymbol{k})}{e^{+\beta\hbar\omega_\sigma(\boldsymbol{k})} - 1} \frac{d^3k}{(2\pi)^3} \,. \tag{2.138}$$

From this expression, we directly see that the dependence on the volume drops out, such that c_V only depends on the type of the material but not on the size.

In 1d, we have to use the replacement $\sum_k \to V \int_{1.\text{BZ}} \frac{dk}{2\pi}$. Revisiting our example for the 1d diatomic chain, we generate Fig. 2.6. There, one can see that for different values of spring constant G, the low temperature is linear in T and also the high-temperature behaviour of the specific heat for the phonons is essentially the same. Below, we will discuss why.

The high-temperature limit

To evaluate the high-temperature limit, we consider

$$\frac{1}{e^x - 1} = \frac{1}{x + \frac{1}{2}x^2 + \frac{1}{6}x^3 + \ldots} = \frac{1}{x}\left[1 - \frac{x}{2} + \mathcal{O}\{x^2\}\right] \tag{2.139}$$

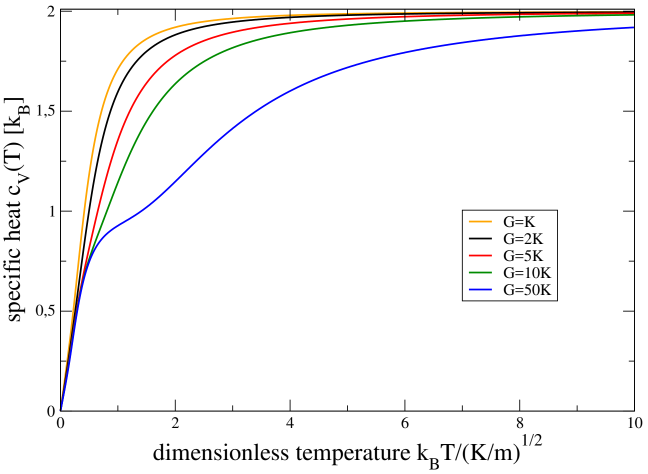

Figure 2.6: Plot of the specific heat versus temperature for the 1D diatomic chain with dispersion relations (2.104). At low temperatures, where only the acoustic mode contributes, all curves are linear in T. The curves also converge to the law of Dulong-Petit $c_V \to 2k_B$ (we have $2N$ degrees of freedom) for large temperatures. With increasing G, the optical mode is lifted higher, such that it can only be occupied for larger temperatures.

for small

$$x = \beta\hbar\omega_\sigma(\boldsymbol{k}) = \frac{\hbar\omega_\sigma(\boldsymbol{k})}{k_B T}\,, \tag{2.140}$$

which can be reached with high temperatures or small frequencies $\omega_\sigma(\boldsymbol{k})$. By keeping only the leading order term, we get for the specific heat

$$c_V = \frac{1}{V}\sum_\sigma\sum_{\boldsymbol{k}} \frac{\partial}{\partial T}\hbar\omega_\sigma(\boldsymbol{k})\frac{k_B T}{\hbar\omega_\sigma(\boldsymbol{k})} = 3\frac{N}{V}k_B = 3nk_B\,, \tag{2.141}$$

which is just the result of Dulong-Petit. However, we mention that typically at high temperatures, the anharmonic corrections (not considered here) are likely larger than the quantum corrections (higher orders in x) to this result.

The low-temperature limit

We first use that for sufficiently large crystals, the allowed values in the first Brillouin zone become dense, and we can replace the summation over $\boldsymbol{k}$ by an integral over the first Brillouin zone, such that the specific heat becomes

$$c_V = \sum_\sigma \int_{1.\mathrm{BZ}} \frac{d^3k}{(2\pi)^3}\frac{\partial}{\partial T}\frac{\hbar\omega_\sigma(\boldsymbol{k})}{e^{+\beta\hbar\omega_\sigma(\boldsymbol{k})}-1}\,. \tag{2.142}$$

Second, we see that when $\beta\hbar\omega_\sigma(\boldsymbol{k}) \gg 1$, the integrand will be exponentially suppressed, such that at low temperatures, only modes with vanishingly small frequencies have the chance to contribute. These are only the acoustic modes. Third, we can for simplicity linearize the dispersion relation of the acoustic modes over the full Brillouin zone (the higher frequencies are hardly populated anyway), and for the same reason extend the integral over the full $\boldsymbol{k}$ space. Then, we can write with $\omega_\sigma = c_\sigma(\boldsymbol{e}_{\boldsymbol{k}})k$ with sound velocity $c_\sigma(\boldsymbol{e}_{\boldsymbol{k}})$ for branch σ

$$c_V \approx \sum_{\sigma:\mathrm{ac}} \int \frac{d^3k}{(2\pi)^3}\frac{\partial}{\partial T}\frac{\hbar c_\sigma(\boldsymbol{e}_{\boldsymbol{k}})k}{e^{+\beta\hbar c_\sigma(\boldsymbol{e}_{\boldsymbol{k}})k}-1}\,. \tag{2.143}$$

Now, it is just a matter of calculating the resulting integral. Going to spherical coordinates $d^3k = k^2 dk d\Omega$ and introducing the variable

$$\beta\hbar c_\sigma(\boldsymbol{e}_{\boldsymbol{k}})k = x \tag{2.144}$$

as well as the average sound velocity of all three acoustic modes

$$\frac{1}{c^3} \equiv \frac{1}{3} \sum_{\sigma:\text{ac}} \frac{d\Omega}{4\pi} \frac{1}{c_\sigma^3(\boldsymbol{e_k})}, \tag{2.145}$$

we can write the specific heat as

$$\begin{aligned} c_V &= \frac{\partial}{\partial T} \sum_{\sigma:\text{ac}} \int \frac{k^2 dk d\Omega}{(2\pi)^3} \frac{1}{\beta} \frac{x}{e^x - 1} = \frac{\partial}{\partial T} \sum_{\sigma:\text{ac}} \int \frac{x^2 dx d\Omega}{(2\pi)^3} \frac{1}{\beta(\beta\hbar c_\sigma(\boldsymbol{e_k}))^3} \frac{x}{e^x-1} \\ &= \frac{\partial}{\partial T} \frac{3}{2\pi^2} \frac{(k_B T)^4}{(\hbar c)^3} \int_0^\infty \frac{x^3}{e^x - 1} dx = \frac{\partial}{\partial T} \frac{3}{2\pi^2} \frac{(k_B T)^4}{(\hbar c)^3} \frac{\pi^4}{15} = \frac{2\pi^2}{5} k_B \left(\frac{k_B T}{\hbar c}\right)^3 . \end{aligned} \tag{2.146}$$

This T^3 relation has been experimentally verified for many materials – the average velocity of sound c was then determined from the elastic parameters. In 1d, a very similar discussion shows that for low temperatures, the specific heat must scale linearly in T as visible in Fig. 2.6.

Finally, we mention that the failure of the Dulong-Petit model for low temperatures was quite similar to the inability of classical approaches to explain blackbody radiation. In fact, the differences are small: First, whereas for phonons one has $3p$ modes for every $\boldsymbol{k}$ and correspondingly $3p$ complicated dispersion relations $\omega_\sigma(\boldsymbol{k})$, one has for photons for a given $\boldsymbol{k}$ only the two transversal polarizations each with the dispersion relation $\omega = ck$ (with light velocity c). Second, for phonons the $\boldsymbol{k}$ is confined to the first Brillouin zone, whereas for photons $\boldsymbol{k}$ is arbitrary. Correspondingly, the equations for the thermal energy density are

$$u_{\text{pn}} = \sum_\sigma \int_{1.\text{BZ}} \frac{d^3k}{(2\pi)^3} \frac{\hbar\omega_\sigma(\boldsymbol{k})}{e^{\beta\hbar\omega_\sigma(\boldsymbol{k})} - 1}, \qquad u_{\text{pt}} = 2 \int \frac{d^3k}{(2\pi)^3} \frac{\hbar ck}{e^{\beta\hbar ck} - 1}. \tag{2.147}$$

2.4.7 Density of normal modes

We have seen that for large crystals, the energy density of normal modes is so large that sums can often be conveniently converted into integrals

$$I = \frac{1}{V} \sum_\sigma \sum_{\boldsymbol{k}} Q(\omega_\sigma(\boldsymbol{k})) = \sum_\sigma \int_{1.BZ} \frac{d^3k}{(2\pi)^3} Q(\omega_\sigma(\boldsymbol{k})). \tag{2.148}$$

For many problems, it is however more convenient to represent the integral over d^3k as a one-dimensional integral over the energies of the normal modes, leading to

$$I = \int_0^\infty \nu(\omega) Q(\omega) d\omega . \tag{2.149}$$

Comparing these expressions, we see that the density of states must be given by

$$\nu(\omega) = \sum_\sigma \int_{1.\text{BZ}} \frac{d^3k}{(2\pi)^3} \delta(\omega - \omega_\sigma(\boldsymbol{k})). \tag{2.150}$$

While this is an exact formal definition, it does not help much when one is given a dispersion relation $\omega_\sigma(\boldsymbol{k})$ but would like to have a continuous version of the density of states. Since we are now considering higher dimensions, the procedure is not as straightforward as in Eq. (2.73). We can use a property of the δ-function

$$\int_{\mathbb{R}^d} f(\boldsymbol{x}) \delta(g(\boldsymbol{x})) d^d x = \int_{g^{-1}(0)} \frac{f(\boldsymbol{x})}{|\nabla g(\boldsymbol{x})|} d\sigma(\boldsymbol{x}). \tag{2.151}$$

Here, $f(\boldsymbol{x})$ and $g(\boldsymbol{x})$ are functions $\mathbb{R}^d \to \mathbb{R}$, and $d\sigma(\boldsymbol{x})$ denotes a surface integral over the d-dimensional surface defined by $g^{-1}(0)$. Applying this to the density of states, we obtain a representation in terms of a surface integral

Box 7 (density of states) *The density of states in d dimensions can be computed via*

$$\nu(\omega) = \sum_\sigma \frac{1}{(2\pi)^d} \int_{1.\text{BZ}} d^d k \delta(\omega - \omega_\sigma(\boldsymbol{k})) = \sum_\sigma \frac{1}{(2\pi)^d} \int_{S_\sigma} \frac{1}{|\nabla_{\boldsymbol{k}} \omega_\sigma(\boldsymbol{k})|} dS\,, \tag{2.152}$$

where S_σ denotes the surface defined by $\omega = \omega_\sigma(\boldsymbol{k})$.

As a sanity check, we reconsider the 1d dispersion relation

$$\omega(k) = \sqrt{\frac{2K}{m}[1 - \cos(ka)]}\,, \tag{2.153}$$

for which we have calculated already the density of states (2.73). The surface defined by $\omega = \omega(k)$ then simply defines two points of k, and up to a factor of a (which roots in our definition) we recover Eq. (2.73)

$$\nu(\omega) = \frac{2}{\pi a} \frac{1}{\sqrt{4\frac{K}{m} - \omega^2}}\,. \tag{2.154}$$

In general, we see that for a bounded periodic function, we will expect the derivative to vanish at some points, which may lead to divergencies of the density of states. For our 1d example, such a singularity is actually observed in Fig. 2.2. In this context, they are called van-Hove [11] singularities, they were first discussed within the context of phonons [5], but they occur in a much wider context. Recently, they are still under debate as excited state quantum phase transitions.

2.5 Remarks on the Theory of Elasticity

Following Ref. [4], we can write the harmonic potential as

$$U = +\frac{1}{2} \sum_{\boldsymbol{R},\boldsymbol{R}'} \boldsymbol{u}^T(\boldsymbol{R}) \underline{\underline{D}}(\boldsymbol{R} - \boldsymbol{R}') \boldsymbol{u}(\boldsymbol{R}') = -\frac{1}{4} \sum_{\boldsymbol{R},\boldsymbol{R}'} \left[\boldsymbol{u}^T(\boldsymbol{R}') - \boldsymbol{u}^T(\boldsymbol{R})\right] \underline{\underline{D}}(\boldsymbol{R} - \boldsymbol{R}') \left[\boldsymbol{u}(\boldsymbol{R}') - \boldsymbol{u}(\boldsymbol{R})\right]\,. \tag{2.155}$$

Here, the equality follows from the symmetry properties (2.78) of the dynamical matrix $\underline{\underline{D}}$. Now, within the theory of elasticity, one does not define the displacement only at discrete lattice nodes but at all continuous positions, which we denote by the symbol $\boldsymbol{u}(\boldsymbol{r})$. Now, for any reasonable theory, the dynamical matrix $\underline{\underline{D}}(\boldsymbol{R} - \boldsymbol{R}')$ varies only over a finite range, it must decay to zero for large distances. If the displacement vector field $\boldsymbol{u}(\boldsymbol{R})$ varies little over this range (long wavelength expansion), it is permissible to use a tailor series expansion

$$\boldsymbol{u}(\boldsymbol{R}') = \boldsymbol{u}(\boldsymbol{R}) + [(\boldsymbol{R}' - \boldsymbol{R}) \cdot \nabla] \boldsymbol{u}(\boldsymbol{r})\Big|_{\boldsymbol{r}=\boldsymbol{R}} + \ldots\,, \tag{2.156}$$

or in components

$$u_\mu(\boldsymbol{R}') = u_\mu(\boldsymbol{R}) + \sum_\sigma (R'_\sigma - R_\sigma) \partial_\sigma u_\mu(\boldsymbol{R}) + \ldots \tag{2.157}$$

---

[11] Léon Charles Prudent Van Hove (1924–1990) was a belgian theoretical physicist.

Here, we have used the short-hand notation $\partial_\sigma = \frac{\partial}{\partial x_\sigma}$. Inserting this in the harmonic potential energy, we get

$$\begin{aligned} U &= -\frac{1}{4}\sum_{\mu\nu\sigma\tau}\sum_{\boldsymbol{R},\boldsymbol{R'}} \left[(R'_\sigma - R_\sigma)\partial_\sigma u_\mu(\boldsymbol{R})\right] D_{\mu\nu}(\boldsymbol{R}-\boldsymbol{R'}) \left[(R'_\tau - R_\tau)\partial_\tau u_\nu(\boldsymbol{R})\right] \\ &= \frac{1}{2}\sum_{\boldsymbol{R}}\sum_{\mu\nu\sigma\tau}[\partial_\sigma u_\mu(\boldsymbol{R})][\partial_\tau u_\nu(\boldsymbol{R})]E_{\sigma\mu\tau\nu}\,, \end{aligned} \tag{2.158}$$

where $E_{\sigma\mu\tau\nu}$ is a fourth rank tensor that contains the elastic properties of the material

$$\begin{aligned} E_{\sigma\mu\tau\nu} &= -\frac{1}{2}\sum_{\boldsymbol{R'}}(R'_\sigma - R_\sigma)D_{\mu\nu}(\boldsymbol{R}-\boldsymbol{R'})(R'_\tau - R_\tau) = -\frac{1}{2}\sum_{\boldsymbol{R'}}(R_\sigma - R'_\sigma)D_{\mu\nu}(\boldsymbol{R}-\boldsymbol{R'})(R_\tau - R'_\tau) \\ &= -\frac{1}{2}\sum_{\boldsymbol{R}} R_\sigma D_{\mu\nu}(\boldsymbol{R}) R_\tau\,. \end{aligned} \tag{2.159}$$

Since the $\boldsymbol{u}(\boldsymbol{r})$ are varying slowly, we can write the remaining summation as an integral

$$U = \frac{1}{2}\sum_{\sigma\tau\mu\nu}\int d^3r[\partial_\sigma u_\mu(\boldsymbol{r})][\partial_\tau u_\nu(\boldsymbol{r})]\bar{E}_{\sigma\mu\tau\nu}\,, \qquad \bar{E}_{\sigma\mu\tau\nu} = \frac{E_{\sigma\mu\tau\nu}}{V_{\text{ec}}}\,, \tag{2.160}$$

where V_{ec} is the volume of the primitive elementary cell. The rank 4 tensor $E_{\sigma\mu\tau\nu}$ contains all the elastic moduli.

Further, demanding that the potential energy is invariant with respect to infinitesimal rotations, one finds that the derivatives entering the energy can only enter in a certain symmetric combination

$$\epsilon_{\sigma\mu} = \frac{1}{2}[\partial_\sigma u_\mu + \partial_\mu u_\sigma]\,, \tag{2.161}$$

commonly known as **strain tensor** (Verzerrungstensor). Accordingly, the potential energy can also be written in terms of the strain tensor $U = \frac{1}{2}\sum_{\sigma\tau\mu\nu}\int d^3r\epsilon_{\sigma\mu}\epsilon_{\tau\nu}\lambda_{\sigma\mu\tau\nu}$, where from symmetry considerations one can show that the rank 4 tensor $\lambda_{\sigma\mu\tau\nu}$ contains in general 21 independent elastic parameters. This number can be further reduced when a specific crystal system is considered (obeying particular point symmetries). Also representing the kinetic term as an integral (using a constant mass density)

$$T = \rho\int d^3r\frac{1}{2}\dot{\boldsymbol{u}}^T\dot{\boldsymbol{u}}\,, \tag{2.162}$$

one can construct the Lagrange function and via Hamilton's principle derive the equations of motion. These assume the form of wave equations for sound waves, see Refs. [1, 6].

Chapter 3

Electrons

According to the Born-Oppenheimer approximation, we first need to solve the electronic Schrödinger equation for obtaining the effective potential for the ions. In the previous chapter, we have simply assumed this problem as solved and used effective descriptions. Now, we are going to make up for this. We start with neglecting the inter-electronic interaction [3].

3.1 Non-interacting electrons in periodic potentials

When the electrons do not interact, we may as well solve the single-particle Schrödinger equation with an effective background potential (according to the Born-Oppenheimer approximation, this would be the potential generated by the ions)

$$H\Psi(\boldsymbol{r}) = \left\{-\frac{\hbar^2}{2m}\nabla^2 + V(\boldsymbol{r})\right\}\Psi(\boldsymbol{r}) = \epsilon\Psi(\boldsymbol{r})\,. \tag{3.1}$$

Here, m is the electron mass and $V(\boldsymbol{r})$ is the potential felt by the electrons. In particular, we assume that it has the periodicity of the Bravais lattice

$$V(\boldsymbol{r}+\boldsymbol{R}) = V(\boldsymbol{r}) \tag{3.2}$$

for all lattice vectors $\boldsymbol{R}$. It is known that for periodically driven ordinary differential equations, Floquet's theorem applies. For periodic potentials, there exists an analogous theorem: The Bloch [1] theorem.

Box 8 (Bloch theorem) *The eigenfunctions of the single-electron Schrödinger equation (3.1) with periodic potential (3.2) can be written as*

$$\Psi_{n\boldsymbol{k}}(\boldsymbol{r}) = e^{+\mathrm{i}\boldsymbol{k}\boldsymbol{r}}u_{n\boldsymbol{k}}(\boldsymbol{r})\,, \qquad u_{n\boldsymbol{k}}(\boldsymbol{r}+\boldsymbol{R}) = u_{n\boldsymbol{k}}(\boldsymbol{r})\,. \tag{3.3}$$

Here, n is called **band index** and $\boldsymbol{k}$ is the wave vector. For the eigenfunctions of H, this means that although they are not periodic, they only acquire a trivial phase factor when translated by a lattice vector

$$\Psi_{n\boldsymbol{k}}(\boldsymbol{r}+\boldsymbol{R}) = e^{+\mathrm{i}\boldsymbol{k}\boldsymbol{R}}\Psi_{n\boldsymbol{k}}(\boldsymbol{r})\,. \tag{3.4}$$

---

[1] Felix Bloch (1905–1983) was an austrian-swiss physicist who earned the Nobel prize for his contributions to nuclear spin resonance spectroscopy.

This is actually an alternative statement of Bloch's theorem. Clearly, the probability density of finding the electron at position $\boldsymbol{r}$ is therefore fully periodic over the lattice, as the phase factor cancels

$$\left|\Psi_{n\boldsymbol{k}}(\boldsymbol{r}+\boldsymbol{R})\right|^2 = \left|\Psi_{n\boldsymbol{k}}(\boldsymbol{r})\right|^2 . \tag{3.5}$$

Proof of Bloch's theorem

One proof goes as follows: The translation operator for a Bravais lattice vector $\boldsymbol{R}$ acts on an arbitrary function $f(\boldsymbol{r})$ as

$$T_{\boldsymbol{R}} f(\boldsymbol{r}) \equiv f(\boldsymbol{r}+\boldsymbol{R}) . \tag{3.6}$$

It must commute with the systems Hamiltonian: As the system Hamiltonian is periodic, one has for any function $\Psi(\boldsymbol{r})$ the identity

$$T_{\boldsymbol{R}} H(\boldsymbol{r})\Psi(\boldsymbol{r}) = H(\boldsymbol{r}+\boldsymbol{R})\Psi(\boldsymbol{r}+\boldsymbol{R}) = H(\boldsymbol{r})\Psi(\boldsymbol{r}+\boldsymbol{R}) = H(\boldsymbol{r}) T_{\boldsymbol{R}}\Psi(\boldsymbol{r}) , \tag{3.7}$$

which can only be true if

$$T_{\boldsymbol{R}} H(\boldsymbol{r}) = H(\boldsymbol{r}) T_{\boldsymbol{R}} . \tag{3.8}$$

Furthermore, two different translation operators must also commute

$$T_{\boldsymbol{R}} T_{\boldsymbol{R'}} = T_{\boldsymbol{R'}} T_{\boldsymbol{R}} . \tag{3.9}$$

Thus, the operators H and $T_{\boldsymbol{R}}$ are a mutually commuting set of operators whenever $\boldsymbol{R}$ is a Bravais lattice vector. Such operators have a common set of eigenfunctions

$$H\Psi(\boldsymbol{r}) = \epsilon\Psi(\boldsymbol{r}) , \qquad T_{\boldsymbol{R}}\Psi(\boldsymbol{r}) = c(\boldsymbol{R})\Psi(\boldsymbol{r}) , \tag{3.10}$$

with energy eigenvalues ϵ and eigenvalues of the translation operators $c(\boldsymbol{R})$. In general, eigenfunctions and eigenvalues will depend on some generalized quantum number, which we have omitted for brevity. From the properties of the translation operator it further follows that its eigenvalues must satisfy

$$c(\boldsymbol{R}+\boldsymbol{R'}) = c(\boldsymbol{R})c(\boldsymbol{R'}) , \tag{3.11}$$

which is only satisfied by the exponential function. Without loss of generality we can write the eigenvalues of translations by the basis vectors of the Bravais lattice as

$$c(\boldsymbol{a_i}) = e^{+2\pi \mathrm{i} x_i} \tag{3.12}$$

with suitably chosen x_i (for now, we can interpret them as complex numbers). Since by construction

$$\boldsymbol{R} = \sum_i n_i \boldsymbol{a_i} , \tag{3.13}$$

it follows that the eigenvalues of general Bravais lattice translations must obey

$$\begin{aligned} c(\boldsymbol{R}) &= c^{n_1}(\boldsymbol{a_1}) c^{n_2}(\boldsymbol{a_2}) c^{n_3}(\boldsymbol{a_3}) = e^{2\pi \mathrm{i} x_1 n_1 + 2\pi \mathrm{i} x_2 n_2 + 2\pi \mathrm{i} x_3 n_3} = e^{\mathrm{i}[x_1\boldsymbol{b_1}+x_2\boldsymbol{b_2}+x_3\boldsymbol{b_3}][n_1\boldsymbol{a_1}+n_2\boldsymbol{a_2}+n_3\boldsymbol{a_3}]} \\ &= e^{\mathrm{i}\boldsymbol{k}\boldsymbol{R}} , \qquad \text{with} \qquad \boldsymbol{k} = x_1\boldsymbol{b_1} + x_2\boldsymbol{b_2} + x_3\boldsymbol{b_3} . \end{aligned} \tag{3.14}$$

Here, we have used the relation for the basis vectors of the reciprocal lattice $\boldsymbol{a_i}\boldsymbol{b_j} = 2\pi\delta_{ij}$. Consequently, we have

$$T_{\boldsymbol{R}}\Psi(\boldsymbol{r}) = \Psi(\boldsymbol{r}+\boldsymbol{R}) = c(\boldsymbol{R})\Psi(\boldsymbol{r}) = e^{+\mathrm{i}\boldsymbol{k}\boldsymbol{R}}\Psi(\boldsymbol{r}) , \tag{3.15}$$

which concludes the proof.

Remarks on the electronic wave vector

So far, the wave vector $\boldsymbol{k}$ in our discussion was quite arbitrary, but we can imagine that the same restrictions as for the phonons must apply. Let us assume that we consider a crystal of $N = N_1 N_2 N_3$ atoms where $N_i \gg 1$. By imposing periodic boundary conditions on the wave function

$$\Psi(\boldsymbol{r} + N_i \boldsymbol{a_i}) = \Psi(\boldsymbol{r}) \tag{3.16}$$

one can show that the wave vector $\boldsymbol{k}$ can only assume discrete and real values. First, we note that the above periodicity assumption (also called Born-von-Kármán boundary conditions here) does not render general phase factors in the Bloch theorem to one, since we only demand it to equal the identity for three different lattice vectors of the Bravais lattice. The periodicity assumption yields the conditions

$$e^{\mathrm{i}N_i \boldsymbol{k}\boldsymbol{a_i}} = 1\,, \qquad i \in \{1,2,3\}\,, \tag{3.17}$$

which implies for $\boldsymbol{k} = x_1 \boldsymbol{b_1} + x_2 \boldsymbol{b_2} + x_3 \boldsymbol{b_3}$ that

$$x_i = \frac{m_i}{N_i}\,, \qquad m_i \in \mathbb{Z}\,. \tag{3.18}$$

This shows that the wave vector $\boldsymbol{k}$ must be real and that it can only assume discrete values. For example, it would suffice to consider $1 \le m_i \le N_i$ as the other values do not yield any new physics. It is conventional to choose the allowed values of m_i such that the wave vector lies in the first Brillouin zone as we did with the phonons. Now, we see that by increasing the number of atoms N_i, the allowed k values get closer and closer as e.g. visible for the phonon example in Fig. 2.4, such that the same recipe as Eq. (2.137) applies.

Solutions to Schrödingers equation

In our formulation of the Bloch theorem, we have already used that one will in general have multiple solutions n for each $\boldsymbol{k}$. As the k becomes continuous, these become bands, and accordingly n is called band index. Using the Bloch theorem in the Schrödinger equation

$$\begin{aligned} H e^{+\mathrm{i}\boldsymbol{k}\boldsymbol{r}} u_{n\boldsymbol{k}}(\boldsymbol{r}) &= \left[-\frac{\hbar^2}{2m}\nabla^2 + V(\boldsymbol{r})\right] e^{+\mathrm{i}\boldsymbol{k}\boldsymbol{r}} u_{n\boldsymbol{k}}(\boldsymbol{r}) \\ &= e^{+\mathrm{i}\boldsymbol{k}\boldsymbol{r}} \left[-\frac{\hbar^2}{2m}\nabla^2 - 2\frac{\hbar^2}{2m}\mathrm{i}\boldsymbol{k}\nabla + \frac{\hbar^2}{2m}\boldsymbol{k}^2 + V(\boldsymbol{r})\right] u_{n\boldsymbol{k}}(\boldsymbol{r}) \\ &= e^{+\mathrm{i}\boldsymbol{k}\boldsymbol{r}} \left[+\frac{\hbar^2}{2m}\left(-\mathrm{i}\nabla + \boldsymbol{k}\right)^2 + V(\boldsymbol{r})\right] u_{n\boldsymbol{k}}(\boldsymbol{r})\,, \end{aligned} \tag{3.19}$$

we get an equation for the periodic function $u_{n\boldsymbol{k}}(\boldsymbol{r})$ only

$$\left[+\frac{\hbar^2}{2m}\left(-\mathrm{i}\nabla + \boldsymbol{k}\right)^2 + V(\boldsymbol{r})\right] u_{n\boldsymbol{k}}(\boldsymbol{r}) = E_n(\boldsymbol{k}) u_{n\boldsymbol{k}}(\boldsymbol{r})\,. \tag{3.20}$$

Since according to Bloch's theorem $u_{n\boldsymbol{k}}(\boldsymbol{r})$ must be periodic, we can solve this by constraining ourselves to an arbitrary elementary cell. Since it is a hermitian eigenvalue problem constrained to a finite volume, we will accordingly for each $\boldsymbol{k}$ get an infinite number of discrete eigenvalues $E_n(\boldsymbol{k})$. Accordingly, the eigenvalues are discretely spaced in n and continuous in $\boldsymbol{k}$. In particular, one can choose the $E_n(\boldsymbol{k})$ to have the periodicity of the reciprocal lattice, and they are then denoted as the **electronic band structure** of the solid.

For an arbitrary $\boldsymbol{k}$ vector, we can normalize the solutions over the volume of a primitive elementary cell

$$\frac{1}{V_{ec}} \int_{\text{ec}} d^3 r u^*_{n\boldsymbol{k}}(\boldsymbol{r}) u_{m\boldsymbol{k}}(\boldsymbol{r}) = \delta_{nm} \,. \tag{3.21}$$

Furthermore, we note that the completeness relation

$$\sum_n u^*_{n\boldsymbol{k}}(\boldsymbol{r}) u_{n\boldsymbol{k}}(\boldsymbol{r'}) = V_{\text{ec}} \delta(\boldsymbol{r} - \boldsymbol{r'}) \tag{3.22}$$

has to hold. Then, we find that the full **Bloch functions**

$$\Psi_{n\boldsymbol{k}}(\boldsymbol{r}) = \frac{1}{\sqrt{V}} e^{+\mathrm{i}\boldsymbol{k}\boldsymbol{r}} u_{n\boldsymbol{k}}(\boldsymbol{r}) \,, \tag{3.23}$$

where V denotes the macroscopic volume of the crystal, are also orthonormal

$$\begin{aligned}
\int_V d^3 r \Psi^*_{n\boldsymbol{k}}(\boldsymbol{r}) \Psi_{m\boldsymbol{q}}(\boldsymbol{r}) &= \frac{1}{V} \int d^3 r e^{-\mathrm{i}\boldsymbol{k}\boldsymbol{r}} u^*_{n\boldsymbol{k}}(\boldsymbol{r}) e^{+\mathrm{i}\boldsymbol{q}\boldsymbol{r}} u_{m\boldsymbol{q}}(\boldsymbol{r}) \\
&= \frac{1}{V} \sum_{\boldsymbol{R}} \int_{ec(\boldsymbol{R})} d^3 r e^{-\mathrm{i}\boldsymbol{k}(\boldsymbol{R}+\boldsymbol{r})} u^*_{n\boldsymbol{k}}(\boldsymbol{R}+\boldsymbol{r}) e^{+\mathrm{i}\boldsymbol{q}(\boldsymbol{R}+\boldsymbol{r})} u_{m\boldsymbol{q}}(\boldsymbol{R}+\boldsymbol{r}) \\
&= \frac{1}{V_{\text{ec}}} \left[\frac{1}{N} \sum_{\boldsymbol{R}} e^{+\mathrm{i}(\boldsymbol{q}-\boldsymbol{k})\boldsymbol{R}} \right] \int_{ec(\boldsymbol{R})} d^3 r e^{\mathrm{i}(\boldsymbol{q}-\boldsymbol{k})\boldsymbol{r}} u^*_{n\boldsymbol{k}}(\boldsymbol{r}) u_{m\boldsymbol{q}}(\boldsymbol{r}) \\
&= \delta_{\boldsymbol{k},\boldsymbol{q}} \frac{1}{V_{\text{ec}}} \int_{ec(\boldsymbol{R})} d^3 r u^*_{n\boldsymbol{k}}(\boldsymbol{r}) u_{m\boldsymbol{q}}(\boldsymbol{r}) = \delta_{\boldsymbol{k},\boldsymbol{q}} \delta_{nm} \,.
\end{aligned} \tag{3.24}$$

This simply means that the eigenfunctions and eigenvalues for single (non-interacting) electrons in a periodic potential can be classified by the two quantum numbers n and $\boldsymbol{k}$, and by solving Eq. (3.20) we can obtain an orthonormal set of solutions for the full Schrödinger equation.

But how can one solve the periodic Schrödinger equation in general? Since we can presuppose that the $u_{n\boldsymbol{k}}$ are periodic functions, we can use the Fourier decomposition of both the periodic potential and the $u_{n\boldsymbol{k}}$

$$\begin{aligned}
V(\boldsymbol{r}) &= \sum_{\boldsymbol{G}} V_{\boldsymbol{G}} e^{+\mathrm{i}\boldsymbol{G}\boldsymbol{r}} \,, \qquad & V_{\boldsymbol{G}} &= \frac{1}{V_{\text{ec}}} \int_{V_{\text{ec}}} V(\boldsymbol{r}) e^{-\mathrm{i}\boldsymbol{G}\boldsymbol{r}} d^3 r \,, \\
u_{n\boldsymbol{k}}(\boldsymbol{r}) &= \sum_{\boldsymbol{G}} u^{n\boldsymbol{k}}_{\boldsymbol{G}} e^{+\mathrm{i}\boldsymbol{G}\boldsymbol{r}} \,, \qquad & u^{n\boldsymbol{k}}_{\boldsymbol{G}} &= \frac{1}{V_{\text{ec}}} \int_{V_{\text{ec}}} u_{n\boldsymbol{k}}(\boldsymbol{r}) e^{-\mathrm{i}\boldsymbol{G}\boldsymbol{r}} d^3 r \,.
\end{aligned} \tag{3.25}$$

Here, $\boldsymbol{G}$ runs over all nodes of the reciprocal lattice and $V_{\boldsymbol{G}}$ as well as $u^{n\boldsymbol{k}}_{\boldsymbol{G}}$ are the corresponding Fourier coefficients. Inserting these decompositions into Eq. (3.20) we get

$$\begin{aligned}
E_n(\boldsymbol{k}) u_{n\boldsymbol{k}}(\boldsymbol{r}) &= \sum_{\boldsymbol{G}} e^{+\mathrm{i}\boldsymbol{G}\boldsymbol{r}} E_n(\boldsymbol{k}) u^{n\boldsymbol{k}}_{\boldsymbol{G}} \\
&= \left[+ \frac{\hbar^2}{2m} \left(-\mathrm{i}\nabla + \boldsymbol{k}\right)^2 + \sum_{\boldsymbol{G'}} V_{\boldsymbol{G'}} e^{+\mathrm{i}\boldsymbol{G'}\boldsymbol{r}} \right] \sum_{\boldsymbol{G}} u^{n\boldsymbol{k}}_{\boldsymbol{G}} e^{+\mathrm{i}\boldsymbol{G}\boldsymbol{r}} \\
&= \sum_{\boldsymbol{G}} e^{+\mathrm{i}\boldsymbol{G}\boldsymbol{r}} \left[+ \frac{\hbar^2}{2m} \left(\boldsymbol{G} + \boldsymbol{k}\right)^2 u^{n\boldsymbol{k}}_{\boldsymbol{G}} + \sum_{\boldsymbol{G'}} V_{\boldsymbol{G'}} u^{n\boldsymbol{k}}_{\boldsymbol{G}-\boldsymbol{G'}} \right] \,.
\end{aligned} \tag{3.26}$$

This leads to an algebraic eigenvalue problem for the unknown functions $u^{n\boldsymbol{k}}_{\boldsymbol{G}}$

$$\left[+\frac{\hbar^2}{2m}\left(\boldsymbol{G}+\boldsymbol{k}\right)^2 u^{n\boldsymbol{k}}_{\boldsymbol{G}} - E_n(\boldsymbol{k}) u^{n\boldsymbol{k}}_{\boldsymbol{G}} + \sum_{\boldsymbol{K}} V_{\boldsymbol{G}-\boldsymbol{K}} u^{n\boldsymbol{k}}_{\boldsymbol{K}}\right] = 0\,, \tag{3.27}$$

which in principle couples all Fourier coefficients that are connected by a reciprocal lattice vector. In principle, this could be an all-to-all coupling, but one has the hope that the Fourier coefficients of the potential $V_{\boldsymbol{G}-\boldsymbol{K}}$ will be small when $|\boldsymbol{G}-\boldsymbol{K}|$ is large. Now, we recall the dispersion relation for free nonrelativistic electrons

$$E^{(0)}(\boldsymbol{k}) = \frac{\hbar^2 \boldsymbol{k}^2}{2m}\,, \tag{3.28}$$

such that we can write

$$u^{n\boldsymbol{k}}_{\boldsymbol{G}} = -\sum_{\boldsymbol{K}} \frac{V_{\boldsymbol{G}-\boldsymbol{K}}}{E^{(0)}(\boldsymbol{G}+\boldsymbol{k}) - E_n(\boldsymbol{k})} u^{n\boldsymbol{k}}_{\boldsymbol{K}}\,. \tag{3.29}$$

This expression is still exact.

Perturbation theory

For more clarity we write in the following

$$u_{n\boldsymbol{k}}(\boldsymbol{G}) = -\sum_{\boldsymbol{K}} \frac{V(\boldsymbol{G}-\boldsymbol{K})}{E^{(0)}(\boldsymbol{G}+\boldsymbol{k}) - E_n(\boldsymbol{k})} u_{n\boldsymbol{k}}(\boldsymbol{K})\,. \tag{3.30}$$

We can perform a perturbative treatment by using the free expressions in the r.h.s. of the above equation. Since it is already of order V, the correction we neglect with this is of even higher order in the potential V. The free solutions are plane waves which do not depend on the band index n

$$E_n^{(0)}(\boldsymbol{k}) = E^{(0)}(\boldsymbol{k}) = \frac{\hbar^2 \boldsymbol{k}^2}{2m}\,, \qquad u^{(0)}_{n\boldsymbol{k}} = \delta_{\boldsymbol{K},0}\,. \tag{3.31}$$

The second condition would imply that $u_{n\boldsymbol{k}} = 1$ as one would expect for plane waves. Inserting the free solution on the r.h.s., we get the first order correction on the l.h.s., i.e.,

$$u^{(1)}_{n\boldsymbol{k}}(\boldsymbol{G}) = -\frac{V(\boldsymbol{G})}{E^{(0)}(\boldsymbol{G}+\boldsymbol{k}) - E^{(0)}(\boldsymbol{k})}\,. \tag{3.32}$$

This yields the first correction to the plane wave ansatz, but the **perturbation theory fails when**

$$(\boldsymbol{G}+\boldsymbol{k})^2 = \boldsymbol{k}^2\,. \tag{3.33}$$

This condition is identical to what we had for Bragg reflection in Eq. (1.27). This means that as far as we are far from the Bragg reflection points, we can use this naive perturbation theory. However, when we are close to the Bragg reflections, we need to be more careful.

In the delicate case, we rewrite the exact equation without any denominator

$$\left[E^{(0)}(\boldsymbol{G}+\boldsymbol{k}) - E_n(\boldsymbol{k})\right] u_{n\boldsymbol{k}}(\boldsymbol{G}) + \sum_{\boldsymbol{K}} V(\boldsymbol{G}-\boldsymbol{K}) u_{n\boldsymbol{k}}(\boldsymbol{K}) = 0\,. \tag{3.34}$$

Now, when one gets close to a Bragg point, e.g. $\boldsymbol{k} = -\boldsymbol{G}/2$, the Fourier components for $u_{n\boldsymbol{k}}(\boldsymbol{K}=0)$ and for $u_{n\boldsymbol{k}}(\boldsymbol{K}=\boldsymbol{G})$ are most important, as they diverge to lowest order. We therefore only keep these in the sum, neglecting the coupling of the potential to other modes. This yields

$$\left[E^{(0)}(\boldsymbol{G}+\boldsymbol{k}) - E_n(\boldsymbol{k})\right] u_{n\boldsymbol{k}}(\boldsymbol{G}) + V(\boldsymbol{G})u_{n\boldsymbol{k}}(\boldsymbol{0}) + V(\boldsymbol{0})u_{n\boldsymbol{k}}(\boldsymbol{G}) = 0\,. \tag{3.35}$$

When we consider the same equation at $\boldsymbol{G} = 0$, we get

$$\left[E^{(0)}(\boldsymbol{k}) - E_n(\boldsymbol{k})\right] u_{n\boldsymbol{k}}(0) + V(\boldsymbol{0}-\boldsymbol{G})u_{n\boldsymbol{k}}(\boldsymbol{G}) + V(\boldsymbol{0}-\boldsymbol{0})u_{n\boldsymbol{k}}(\boldsymbol{0}) = 0\,. \tag{3.36}$$

We can always shift the periodic potential by a constant, such that $V(\boldsymbol{0}) = 0$. Accordingly, we get the coupled two by two system

$$\begin{aligned}\left[E^{(0)}(\boldsymbol{G}+\boldsymbol{k}) - E_n(\boldsymbol{k})\right] u_{n\boldsymbol{k}}(\boldsymbol{G}) + V(\boldsymbol{G})u_{n\boldsymbol{k}}(\boldsymbol{0}) &= 0\,,\\ V(-\boldsymbol{G})u_{n\boldsymbol{k}}(\boldsymbol{G}) + \left[E^{(0)}(\boldsymbol{k}) - E_n(\boldsymbol{k})\right] u_{n\boldsymbol{k}}(0) &= 0\,.\end{aligned} \tag{3.37}$$

To get a nontrivial solution, the coefficient matrix determinant must vanish

$$\left[E^{(0)}(\boldsymbol{G}+\boldsymbol{k}) - E_n(\boldsymbol{k})\right]\left[E^{(0)}(\boldsymbol{k}) - E_n(\boldsymbol{k})\right] - V(-\boldsymbol{G})V(+\boldsymbol{G}) = 0\,. \tag{3.38}$$

Now, inserting that at the Bragg reflection point we have $(\boldsymbol{G}+\boldsymbol{k})^2 = \boldsymbol{k}^2$, we can solve the above condition for the true energy at a Bragg reflection point

$$E_n(\boldsymbol{k}) = \frac{\hbar^2\boldsymbol{k}^2}{2m} \pm \sqrt{V(+\boldsymbol{G})V(-\boldsymbol{G})} = \frac{\boldsymbol{k}^2}{2m} \pm |V(\boldsymbol{G})|\,, \tag{3.39}$$

where we have used $V(-\boldsymbol{G}) = V^*(+\boldsymbol{G})$. This tells us that at the Bragg reflection points, the energy bands will split up! When we are not exactly at the Bragg reflection point, we have to solve Eq. (3.38) for $E_n(\boldsymbol{k})$ to get an approximate dispersion relation. Note however, as we have considered only the closest $\boldsymbol{K}$ modes, this yields only the splitting at the first avoided crossing. To get the full spectrum, all Fourier components need to be involved.

Things become really complicated in higher dimensions, so we will consider only a one-dimensional example here. Think e.g. of considering the full problem only along a preferred direction. In 1d, the reciprocal lattice vector runs over

$$G \in \{0, \pm\frac{2\pi}{a}, \pm\frac{4\pi}{a}, \ldots\} \tag{3.40}$$

and the Bragg reflection condition is given by $k = -G/2 \in \{0, \pm\frac{\pi}{a}, \pm\frac{2\pi}{a}, \ldots\}$. Correspondingly, the reflection condition is fulfilled when $k = \frac{n\pi}{a}$ with $n \in \mathbb{Z}$. At these points, free dispersion relations $E_n^{(0)}(\boldsymbol{k})$ and $E_n^{(0)}(\boldsymbol{k}+\boldsymbol{G})$ cross. However, at the Bragg points, the exact eigenvalues split with leading order splitting value $2|V(\boldsymbol{G})|$, and in the vicinity of the splitting point, we have the shape of an avoided crossing, see Fig. 3.1.

Example: Full band structure calculation

Clearly, the two-mode approximation fails when we consider also other values of $\boldsymbol{K}$ in the exact band structure problem (3.34). For illustration, we consider a cosine potential in a 1d problem

$$V(x) = V_0 \cos\left(2\pi\frac{x}{a}\right)\,, \tag{3.41}$$

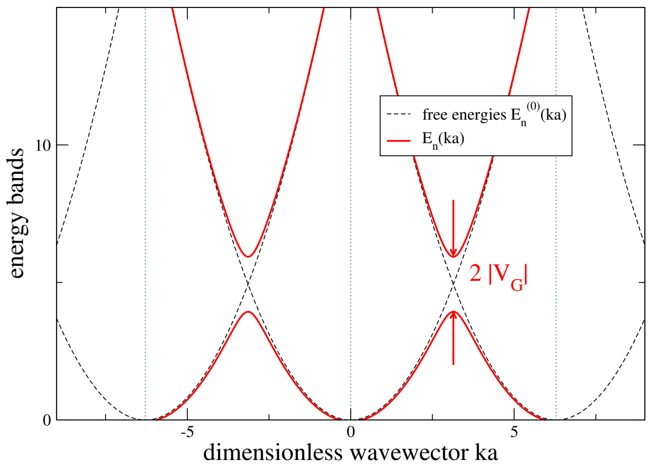

Figure 3.1: Plot of the free electronic dispersion relations and their displaced copies (dashed curves) at reciprocal lattice vectors G (vertical dotted lines). Adding a weak periodic potential with just two Fourier components (e.g. of cos shape) leads to a splitting into energy bands, where under the two-mode approximation the exact crossings become avoided ones (red curves). Parameters $V(\pm\boldsymbol{G}) = 1$, $m = 1$, $Ga = \pm 2\pi$.

where $2V_0$ is the depth of the potential and a is the lattice constant. In 1D, the Fourier coefficients are just given by

$$V_G = \frac{1}{a}\int_0^a V(x) e^{-\mathrm{i}Gx} dx\,, \qquad G \in \{0, \pm\frac{2\pi}{a}, \pm\frac{4\pi}{a}, \ldots\}\,. \tag{3.42}$$

We just have two non-vanishing Fourier coefficients

$$V_{+1} \equiv V_{+2\pi/a} = \frac{V_0}{2}\,, \qquad V_{-1} \equiv V_{-2\pi/a} = \frac{V_0}{2}\,. \tag{3.43}$$

This simplifies the summation over $\boldsymbol{K}$ a lot, but nevertheless it remains an infinitely large coupled system. For clarity, we also introduce some abbreviations for the nth Fourier coefficient of the u_{mk} mode and the free energy dispersion relation

$$u_{mk}^n = u_{mk}\left(n\frac{2\pi}{a}\right)\,, \qquad E_n^{(0)}(k) = E^{(0)}\left(k + n\frac{2\pi}{a}\right)\,. \tag{3.44}$$

Now, since the potential only has two Fourier components, Eq. (3.34) becomes

$$\left[E_n^{(0)}(k) - E_m(k)\right] u_{mk}^n + V_{-1} u_{mk}^{n+1} + V_{+1} u_{mk}^{n-1} = 0\,. \tag{3.45}$$

For given mk, this defines an infinitely large coupled set of equations, which we will have to truncate at some point. The coefficient matrix reads

$$\begin{pmatrix} \ddots & V_0/2 & & & \\ V_0/2 & E_{-1}^{(0)}(k) - E_n(k) & V_0/2 & & \\ & V_0/2 & E_0^{(0)}(k) - E_n(k) & V_0/2 & \\ & & V_0/2 & E_{+1}^{(0)}(k) - E_n(k) & V_0/2 \\ & & & V_0/2 & \ddots \end{pmatrix}\,. \tag{3.46}$$

By setting its determinant to zero we obtain a number of solutions for the electronic energies. One will have to truncate the matrix dimension and check for convergence. It turns out that for moderate potential depts V_0, it suffices to keep only a few modes. For example, when we just keep five modes, the dispersion relations are obtained from

$$\left|\begin{pmatrix} E_{-2}^{(0)}(k) - E_n(k) & V_0/2 & & & \\ V_0/2 & E_{-1}^{(0)}(k) - E_n(k) & V_0/2 & & \\ & V_0/2 & E_0^{(0)}(k) - E_n(k) & V_0/2 & \\ & & V_0/2 & E_{+1}^{(0)}(k) - E_n(k) & V_0/2 \\ & & & V_0/2 & E_{+2}^{(0)}(k) - E_n(k) \end{pmatrix}\right| = 0\,, \tag{3.47}$$

which yields five solutions for the energy bands $E_n(k)$. These form **energy bands**. The result is depicted in Fig. 3.2. There, we observe that depending on the value of V_0 band gaps will change. In particular, with increasing V_0, an increased number of bands will clearly separate from the rest of the spectrum.

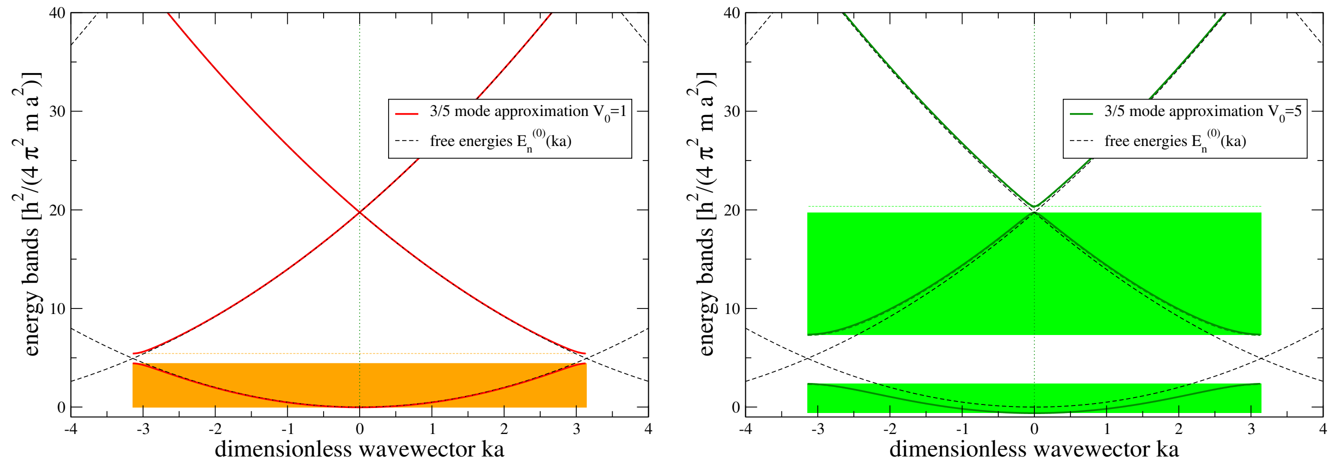

Figure 3.2: Plots of the arising band structure in the first Brillouin zone when three modes or five modes (solid and dashed, identical results) are taken into account, for different potential depths V_0. For weak potential depth (red and orange, left), one separate band (orange box) is clearly visible. In fact, there is also an avoided crossing at $k = 0$, but it is at weak potential depth very small (quasi-continuous). For stronger potential (dark and light green, right), two bands (marked boxes) are clearly separated from the rest of the spectrum. Above the horizontal dashed lines, one still has tiny avoided crossings with hardly visible band gaps.

As mentioned, in higher dimensions, things become difficult. As k becomes a vector, the energy bands become sheets in two dimensions and in three dimensions they become volumes difficult to visualize. The takehome message is that in analogy to a single potential well, which may support a finite number of bound states with sharp energies depending on its depth and width, periodic potentials support bound states only with energies distributed within bands which with increasing potential depth become more separate.

3.1.1 Kramer theorem

Finally, we would like to comment on the visible symmetry of the dispersion relation which we calculated so far.

Box 9 (Kramers theorem) *The dispersion relations obey*

$$E_n(\boldsymbol{k}) = E_n(-\boldsymbol{k})\,. \tag{3.48}$$

More generally, one could even say that

$$E_n(\underline{\underline{S}}\boldsymbol{k}) = E_n(\boldsymbol{k})\,, \tag{3.49}$$

whenever $\underline{\underline{S}}$ is a symmetry operation of the underlying lattice.

For now, we just consider the inversion symmetry

$$S\Psi_{nk}(\boldsymbol{r}) \equiv \Psi_{nk}(-\boldsymbol{r})\,. \tag{3.50}$$

By construction, it commutes then with the Hamiltonian

$$SH(\boldsymbol{r})\Psi_{nk}(\boldsymbol{r}) = H(-\boldsymbol{r})\Psi_{nk}(-\boldsymbol{r}) = H(\boldsymbol{r})S\Psi_{nk}(\boldsymbol{r}) = E_n(\boldsymbol{k})S\Psi_{nk}(\boldsymbol{r})\,. \tag{3.51}$$

From this we conclude that if $\Psi_{nk}(\boldsymbol{r})$ is an eigenfunction of $H(\boldsymbol{r})$, then also $\underline{\underline{S}}\Psi_{nk}(\boldsymbol{r})$ is an eigenfunction with the same eigenvalue. Further, we have for the translation operator

$$\begin{aligned} T_{\boldsymbol{R}}S\Psi_{n\boldsymbol{k}}(\boldsymbol{r}) &= T_{\boldsymbol{R}}e^{-\mathrm{i}\boldsymbol{k}\boldsymbol{r}}u_{n\boldsymbol{k}}(-\boldsymbol{r}) = e^{-\mathrm{i}\boldsymbol{k}(\boldsymbol{r}+\boldsymbol{R})}u_{n\boldsymbol{k}}(-\boldsymbol{r}-\boldsymbol{R}) \\ &= e^{-\mathrm{i}\boldsymbol{k}\boldsymbol{R}}e^{-\mathrm{i}\boldsymbol{k}\boldsymbol{r}}u_{n\boldsymbol{k}}(-\boldsymbol{r}) = e^{-\mathrm{i}\boldsymbol{k}\boldsymbol{R}}S\Psi_{n\boldsymbol{k}}(\boldsymbol{r})\,. \end{aligned} \tag{3.52}$$

From this we conclude that $S\Psi_{n\boldsymbol{k}}(\boldsymbol{r})$ is an eigenstate to the translation operator with eigenvalue $e^{-\mathrm{i}\boldsymbol{k}\boldsymbol{R}}$. However, we had already used in our proof of Bloch's theorem, compare Eq. (3.15), that the corresponding eigenvalue must actually be $e^{+\mathrm{i}\boldsymbol{k}\boldsymbol{R}}$. Therefore, they must be equal $S\Psi_{n,+\boldsymbol{k}}(\boldsymbol{r}) = \Psi_{n,-\boldsymbol{k}}(\boldsymbol{r})$. The symmetry operation for Kramers theorem is just the inversion. The proof for general point symmetries is analogous.

3.1.2 Tight-binding method with single-atom orbitals

The basic idea of perturbation theory in periodic potentials was fine to observe the qualitative appearance of energy bands. However, we have started from a perturbation of the free limit, and in practice we will typically not go beyond a few orders. For typical experimental setups however, this limit is not realistic. Rather, the potential is strong, and most electrons are tightly bound to their nuclei. Therefore, the tight-binding method does the perturbation from exactly the opposite perspective (compare Ref. [3]): The unperturbed problem is the interaction of an electron with a single atom at position $\boldsymbol{R}$

$$H_{\boldsymbol{R}}\phi_n(\boldsymbol{r}-\boldsymbol{R}) = \left[\frac{\boldsymbol{p}^2}{2m} + V(\boldsymbol{r}-\boldsymbol{R})\right]\phi_n(\boldsymbol{r}-\boldsymbol{R}) = E_n\phi_n(\boldsymbol{r}-\boldsymbol{R})\,. \tag{3.53}$$

Here, $\boldsymbol{r}$ is the position of the electron and $\boldsymbol{R}$ is the position of the atom, $V(\boldsymbol{r}-\boldsymbol{R})$ is their (at least in some region attractive) interaction potential, and $\boldsymbol{p}$ is the electronic momentum operator. So for example, the quantum number n is in general a multi-index with $n\hat{=}(\tilde{n},\ell,m,\sigma)$ with main quantum number $\tilde{n}$, total angular momentum ℓ, z-component of angular momentum m and spin σ.

The full problem for non-interacting electrons is now given by adding the potentials of the other atoms

$$H = \frac{\boldsymbol{p}^2}{2m} + \sum_{\boldsymbol{R}'} V(\boldsymbol{r}-\boldsymbol{R}') = \frac{\boldsymbol{p}^2}{2m} + V(\boldsymbol{r}-\boldsymbol{R}) + \Delta H\,, \qquad \Delta H = \sum_{\boldsymbol{R}'\neq\boldsymbol{R}} V(\boldsymbol{r}-\boldsymbol{R}')\,. \tag{3.54}$$

Within tight-binding, we assume that the single-atom-single-electron problem (3.53) has been solved for $\phi_n(\boldsymbol{r}-\boldsymbol{R})$. Assuming that these functions do hardly overlap, i.e., that they are localized close to the respective atom $\boldsymbol{R}$, it follows that

$$\sum_{\boldsymbol{R}'\neq\boldsymbol{R}} V(\boldsymbol{r}-\boldsymbol{R}')\phi_n(\boldsymbol{r}-\boldsymbol{R}) \approx 0\,, \tag{3.55}$$

and these wave functions are also approximate solutions to the full problem with the same eigenvalue

$$H\phi_n(\boldsymbol{r}-\boldsymbol{R}) \approx E_n\phi_n(\boldsymbol{r}-\boldsymbol{R})\,. \tag{3.56}$$

We can use them as a basis to construct Bloch functions (N is the number of atoms)

$$\Psi_{n\boldsymbol{k}}(\boldsymbol{r}) = \frac{1}{\sqrt{N}} \sum_{\boldsymbol{R}} e^{+\mathrm{i}\boldsymbol{k}\boldsymbol{R}} \phi_n(\boldsymbol{r}-\boldsymbol{R})\,. \tag{3.57}$$

By construction, these wave functions exactly obey the Bloch condition

$$\begin{aligned}\Psi_{n\boldsymbol{k}}(\boldsymbol{r}+\boldsymbol{R}) &= \frac{1}{\sqrt{N}} \sum_{\boldsymbol{R}'} e^{+\mathrm{i}\boldsymbol{k}(\boldsymbol{R}'-\boldsymbol{R}+\boldsymbol{R})} \phi_n(\boldsymbol{r}+\boldsymbol{R}-\boldsymbol{R}') = e^{+\mathrm{i}\boldsymbol{k}\boldsymbol{R}} \frac{1}{\sqrt{N}} \sum_{\boldsymbol{R}''} e^{+\mathrm{i}\boldsymbol{k}\boldsymbol{R}''} \phi_n(\boldsymbol{r}-\boldsymbol{R}'') \\ &= e^{+\mathrm{i}\boldsymbol{k}\boldsymbol{R}} \Psi_{n\boldsymbol{k}}(\boldsymbol{r})\,,\end{aligned} \tag{3.58}$$

and they are also approximate eigenfunctions of the full problem

$$\begin{aligned}H\Psi_{n\boldsymbol{k}}(\boldsymbol{r}) &= \frac{1}{\sqrt{N}} \sum_{\boldsymbol{R}} \left[-\frac{\hbar^2}{2m}\nabla^2 + V(\boldsymbol{r}-\boldsymbol{R}) + \sum_{\boldsymbol{R}'\neq\boldsymbol{R}} V(\boldsymbol{r}-\boldsymbol{R}') \right] e^{+\mathrm{i}\boldsymbol{k}\boldsymbol{R}} \phi_n(\boldsymbol{r}-\boldsymbol{R}) \\ &\approx \frac{1}{\sqrt{N}} \sum_{\boldsymbol{R}} E_n(\boldsymbol{k}) e^{+\mathrm{i}\boldsymbol{k}\boldsymbol{R}} \phi_n(\boldsymbol{r}-\boldsymbol{R}) = E_n(\boldsymbol{k}) \Psi_{n\boldsymbol{k}}(\boldsymbol{r})\,.\end{aligned} \tag{3.59}$$

However, the underlying approximation (3.56) can be assumed to hold for the inner electrons only. Nevertheless, it can be used to obtain a first approximation to the true eigenvalues and eigenfunctions of the problem. Since the wave functions $\phi_n(\boldsymbol{r}-\boldsymbol{R})$ are not fully localized to the respective atom at $\boldsymbol{R}$, the Bloch functions constructed from them are not orthonormal

$$\begin{aligned}\left\langle \Psi_{n\boldsymbol{k}} | \Psi_{m\boldsymbol{k}} \right\rangle &= \frac{1}{N} \sum_{\boldsymbol{R},\boldsymbol{R}'} e^{\mathrm{i}\boldsymbol{k}(\boldsymbol{R}-\boldsymbol{R}')} \int d^3r \phi_n^*(\boldsymbol{r}-\boldsymbol{R}') \phi_m(\boldsymbol{r}-\boldsymbol{R}) \\ &= \frac{1}{N} \sum_{\boldsymbol{R},\boldsymbol{R}'} e^{-\mathrm{i}\boldsymbol{k}(\boldsymbol{R}'-\boldsymbol{R})} \int d^3r' \phi_n^*(\boldsymbol{r}'-(\boldsymbol{R}'-\boldsymbol{R})) \phi_m(\boldsymbol{r}') \\ &= \frac{1}{N} \sum_{\boldsymbol{R}} \sum_{\boldsymbol{R}''} e^{-\mathrm{i}\boldsymbol{k}\boldsymbol{R}''} \int d^3r' \phi_n^*(\boldsymbol{r}'-\boldsymbol{R}'') \phi_m(\boldsymbol{r}') \\ &= \delta_{nm} + \sum_{\boldsymbol{R}\neq\boldsymbol{0}} e^{-\mathrm{i}\boldsymbol{k}\boldsymbol{R}} \int d^3r \phi_n^*(\boldsymbol{r}-\boldsymbol{R}) \phi_m(\boldsymbol{r}) \\ &= \delta_{nm} + \sum_{\boldsymbol{R}\neq\boldsymbol{0}} e^{-\mathrm{i}\boldsymbol{k}\boldsymbol{R}} \alpha_{nm}(\boldsymbol{R})\,.\end{aligned} \tag{3.60}$$

Here, we have introduced the **overlap** between wave-functions at the origin and different atoms as

$$\alpha_{nm}(\boldsymbol{R}) = \int d^3r \phi_n^*(\boldsymbol{r}-\boldsymbol{R}) \phi_m(\boldsymbol{r})\,. \tag{3.61}$$

An estimate for the true eigenvalue $\epsilon_n(\boldsymbol{k})$ is then obtained from computing the expectation value of the Hamiltonian with the (normalized) wave function ansatz

$$\epsilon_n(\boldsymbol{k}) \approx \frac{\langle \Psi_n(\boldsymbol{k}) | H | \Psi_n(\boldsymbol{k}) \rangle}{\langle \Psi_n(\boldsymbol{k}) | \Psi_n(\boldsymbol{k}) \rangle}\,. \tag{3.62}$$

The denominator follows from the normalization

$$\langle \Psi_n(\boldsymbol{k}) | \Psi_n(\boldsymbol{k}) \rangle = 1 + \sum_{\boldsymbol{R}\neq 0} e^{-\mathrm{i}\boldsymbol{k}\boldsymbol{R}} \alpha_{nn}(\boldsymbol{R})\,. \tag{3.63}$$

However, for the numerator we get

$$\begin{aligned}\left\langle\Psi_n(\boldsymbol{k})\right| H \left|\Psi_n(\boldsymbol{k})\right\rangle &= E_n \left\langle\Psi_n(\boldsymbol{k})|\Psi_n(\boldsymbol{k})\right\rangle \\ &\quad + \frac{1}{N}\sum_{\boldsymbol{R}\boldsymbol{R}'} e^{+\mathrm{i}\boldsymbol{k}(\boldsymbol{R}-\boldsymbol{R}')}\int d^3r\phi_n^*(\boldsymbol{r}-\boldsymbol{R}')\sum_{\boldsymbol{R}''\neq\boldsymbol{R}} V(\boldsymbol{r}-\boldsymbol{R}'')\phi_n(\boldsymbol{r}-\boldsymbol{R})\,. \end{aligned} \tag{3.64}$$

Depending on the configurations of $\boldsymbol{R}$, $\boldsymbol{R}'$, and $\boldsymbol{R}''$, the integral may or may not yield significant contributions.

First, we see that when all positions are different, we have at any point of the integral always a product of two small terms, and in tight-binding approximation we neglect these terms

$$\boldsymbol{R}\neq\boldsymbol{R}'\neq\boldsymbol{R}''\neq\boldsymbol{R} \qquad : \qquad \int d^3r\phi_n^*(\boldsymbol{r}-\boldsymbol{R}')V(\boldsymbol{r}-\boldsymbol{R}'')\phi_n(\boldsymbol{r}-\boldsymbol{R})\approx 0\,. \tag{3.65}$$

Second, we can consider the case $\boldsymbol{R}=\boldsymbol{R}'\neq\boldsymbol{R}''$. For this regime, we define

$$\beta_n \equiv \frac{1}{N}\sum_{\boldsymbol{R}}\int d^3r\phi_n^*(\boldsymbol{r}-\boldsymbol{R})\sum_{\boldsymbol{R}''\neq\boldsymbol{R}} V(\boldsymbol{r}-\boldsymbol{R}'')\phi_n(\boldsymbol{r}-\boldsymbol{R})\,. \tag{3.66}$$

This is just the expectation value of all background atoms with respect to the wavefunctions localized at $\boldsymbol{R}$ and corresponds to a constant shift of the energies.

Third, we can choose $\boldsymbol{R}'=\boldsymbol{R}''\neq\boldsymbol{R}$. Then, we have

$$\begin{aligned}&\frac{1}{N}\sum_{\boldsymbol{R}\neq\boldsymbol{R}'} e^{+\mathrm{i}\boldsymbol{k}(\boldsymbol{R}-\boldsymbol{R}')}\int d^3r\phi_n^*(\boldsymbol{r}-\boldsymbol{R}')V(\boldsymbol{r}-\boldsymbol{R}')\phi_n(\boldsymbol{r}-\boldsymbol{R}) \\ &= \sum_{\boldsymbol{R}\neq 0} e^{-\mathrm{i}\boldsymbol{k}\boldsymbol{R}}\int d^3r\phi_n^*(\boldsymbol{r}-\boldsymbol{R})V(\boldsymbol{r}-\boldsymbol{R})\phi_n(\boldsymbol{r}) \equiv \sum_{\boldsymbol{R}\neq 0} e^{-\mathrm{i}\boldsymbol{k}\boldsymbol{R}}\lambda_n(\boldsymbol{R})\,.\end{aligned} \tag{3.67}$$

This integral does now lead to a nontrivial transformation of all eigenvalues.

Putting these ingredients together, we find the eigenvalues in the tight-binding approximation.

Box 10 (tight-binding-approximation) *Given single-atom electronic functions $\phi_n(\boldsymbol{r})$ with single-atom electronic energies E_n, in tight-binding approximation the full eigenfunction and its eigenvalue are given by*

$$\Psi_{n\boldsymbol{k}}(\boldsymbol{r}) \approx \frac{\frac{1}{\sqrt{N}}\sum_{\boldsymbol{R}} e^{+\mathrm{i}\boldsymbol{k}\boldsymbol{R}}\phi_n(\boldsymbol{r}-\boldsymbol{R})}{\sqrt{1+\sum_{\boldsymbol{R}\neq 0} e^{-\mathrm{i}\boldsymbol{k}\boldsymbol{R}}\alpha_n(\boldsymbol{R})}}\,, \qquad \epsilon_n(\boldsymbol{k}) \approx E_n + \frac{\beta_n+\sum_{\boldsymbol{R}\neq 0} e^{-\mathrm{i}\boldsymbol{k}\boldsymbol{R}}\lambda_n(\boldsymbol{R})}{1+\sum_{\boldsymbol{R}\neq 0} e^{-\mathrm{i}\boldsymbol{k}\boldsymbol{R}}\alpha_n(\boldsymbol{R})}\,. \tag{3.68}$$

The auxiliary quantities can be computed from the overlap integrals

$$\begin{aligned}\alpha_n(\boldsymbol{R}) &= \int d^3r\phi_n^*(\boldsymbol{r}-\boldsymbol{R})\phi_n(\boldsymbol{r})\,, \qquad \beta_n = \int d^3r\phi_n^*(\boldsymbol{r})\sum_{\boldsymbol{R}\neq 0} V(\boldsymbol{r}-\boldsymbol{R})\phi_n(\boldsymbol{r})\,, \\ \lambda_n(\boldsymbol{R}) &= \int d^3r\phi_n^*(\boldsymbol{r}-\boldsymbol{R})V(\boldsymbol{r}-\boldsymbol{R})\phi_n(\boldsymbol{r})\,.\end{aligned} \tag{3.69}$$

Very often, one additionally restricts the summations over next or next-to-next neighbours, as the overlap integrals become extremely small for distant neighbours.

3.1.3 Improvements on the tight-binding method

In the discussion above, we have used the localized single-atom wave functions although they do not pose an orthogonal basis – except perhaps in the limit where the atoms do not interact. However, there exists an orthonormal basis based on the Bloch functions. These are called **Wannier** [2] states. Given the full exact solutions $\Psi_{n\boldsymbol{k}}(\boldsymbol{r})$ with N atoms, the Wannier states are formally defined by

$$w_n(\boldsymbol{r}-\boldsymbol{R}) = \frac{1}{\sqrt{N}} \sum_{\boldsymbol{k}} e^{-\mathrm{i}\boldsymbol{k}\boldsymbol{R}} \Psi_{n\boldsymbol{k}}(\boldsymbol{r}) \,. \tag{3.70}$$

Of course, this formula only demonstrates the existence of the Wannier states, and the summation over $\boldsymbol{k}$ involves all allowed values in the first Brillouin zone. However, from this definition it follows that they form an orthonormal set

$$\begin{aligned}\int d^3r w_n^*(\boldsymbol{r}-\boldsymbol{R}) w_m(\boldsymbol{r}-\boldsymbol{R}') &= \frac{1}{N}\sum_{\boldsymbol{k}\boldsymbol{k}'} e^{\mathrm{i}\boldsymbol{k}\boldsymbol{R}-\mathrm{i}\boldsymbol{k}'\boldsymbol{R}'} \int d^3r \Psi_{n\boldsymbol{k}}^*(\boldsymbol{r})\Psi_{m\boldsymbol{k}'}(\boldsymbol{r}) \\ &= \frac{1}{N}\sum_{\boldsymbol{k}\boldsymbol{k}'} e^{\mathrm{i}\boldsymbol{k}\boldsymbol{R}-\mathrm{i}\boldsymbol{k}'\boldsymbol{R}'} \delta_{nm}\delta_{\boldsymbol{k}\boldsymbol{k}'} = \delta_{nm}\frac{1}{N}\sum_{\boldsymbol{k}} e^{\mathrm{i}\boldsymbol{k}(\boldsymbol{R}-\boldsymbol{R}')} = \delta_{nm}\delta_{\boldsymbol{R},\boldsymbol{R}'} \,.\end{aligned} \tag{3.71}$$

Instead of using the local atomic orbitals $\phi_n(\boldsymbol{r}-\boldsymbol{R})$ in the Bloch functions, we could redo the derivation with the Wannier functions instead

$$\Psi_{n\boldsymbol{k}}(\boldsymbol{r}) = \frac{1}{\sqrt{N}} \sum_{\boldsymbol{R}} e^{+\mathrm{i}\boldsymbol{k}\boldsymbol{R}} w_n(\boldsymbol{r}-\boldsymbol{R}) \,. \tag{3.72}$$

Then, we would have

$$\begin{aligned}\epsilon_{n\boldsymbol{k}} &= \left\langle \Psi_{n\boldsymbol{k}} \right| H \left| \Psi_{n\boldsymbol{k}} \right\rangle \\ &= \frac{1}{N}\sum_{\boldsymbol{R}\boldsymbol{R}'} e^{-\mathrm{i}\boldsymbol{k}(\boldsymbol{R}-\boldsymbol{R}')} \int d^3r w_n^*(\boldsymbol{r}-\boldsymbol{R}) \left[\frac{p^2}{2m} + \sum_{\boldsymbol{R}''} V(\boldsymbol{r}-\boldsymbol{R}'')\right] w_n(\boldsymbol{r}-\boldsymbol{R}') \\ &= \frac{1}{N}\sum_{\boldsymbol{R}\boldsymbol{R}'} e^{-\mathrm{i}\boldsymbol{k}(\boldsymbol{R}-\boldsymbol{R}')} \int d^3r w_n^*(\boldsymbol{r}-(\boldsymbol{R}-\boldsymbol{R}')) \left[\frac{p^2}{2m} + \sum_{\boldsymbol{R}''} V(\boldsymbol{r}-(\boldsymbol{R}''-\boldsymbol{R}'))\right] w_n(\boldsymbol{r}) \\ &= \int d^3r w_n^*(\boldsymbol{r}) \left[\frac{p^2}{2m} + \sum_{\boldsymbol{R}''} V(\boldsymbol{r}-\boldsymbol{R}'')\right] w_n(\boldsymbol{r}) \\ &\quad + \frac{1}{N}\sum_{\boldsymbol{R}\neq\boldsymbol{R}'} e^{-\mathrm{i}\boldsymbol{k}(\boldsymbol{R}-\boldsymbol{R}')} \int d^3r w_n^*(\boldsymbol{r}-(\boldsymbol{R}-\boldsymbol{R}')) \left[\frac{p^2}{2m} + \sum_{\boldsymbol{R}''} V(\boldsymbol{r}-\boldsymbol{R}'')\right] w_n(\boldsymbol{r}) \,.\end{aligned} \tag{3.73}$$

In the last line, we have only separated the sum into two contributions $\boldsymbol{R}' = \boldsymbol{R}$ and $\boldsymbol{R}' \neq \boldsymbol{R}$ and simplified the diagonal contribution, which yields N identical terms. In the last term, we do now again neglect the three-center contributions, i.e., terms where $\boldsymbol{R}'' \neq \boldsymbol{R}-\boldsymbol{R}'$ and also

---

[2] Gregory Hugh Wannier (1911–1983) was a swiss solid state physicist.

the kinetic overlap term. Altogether, we do then have for the full energies

$$\begin{aligned}
\epsilon_{n\boldsymbol{k}} &\approx \tilde{E}_n + \frac{1}{N}\sum_{\boldsymbol{R}\neq\boldsymbol{0}} e^{-\mathrm{i}\boldsymbol{k}\boldsymbol{R}}\tilde{\lambda}_n(\boldsymbol{R})\,,\\
\tilde{E}_n &= \int d^3r w_n^*(\boldsymbol{r})\left[\frac{p^2}{2m}+\sum_{\boldsymbol{R}} V(\boldsymbol{r}-\boldsymbol{R})\right] w_n(\boldsymbol{r})\,,\\
\tilde{\lambda}_n(\boldsymbol{R}) &= \int d^3r w_n^*(\boldsymbol{r}-\boldsymbol{R})V(\boldsymbol{r}-\boldsymbol{R})w_n(\boldsymbol{r})\,. \qquad (3.74)
\end{aligned}$$

Unfortunately, we usually do not know the Wannier functions $w_n(\boldsymbol{r}-\boldsymbol{R})$ as they are defined to be exact.

Therefore, one often determines their parameters experimentally and starts from representing the Hamiltonian in the Wannier basis. When $|n\boldsymbol{R}\rangle$ denotes the nth Wannier state for an electron localized at site $\boldsymbol{R}$, this is formally achieved via

$$\begin{aligned}
H &= \sum_{n\boldsymbol{R},n'\boldsymbol{R'}} \langle n\boldsymbol{R}| H |n'\boldsymbol{R'}\rangle |n\boldsymbol{R}\rangle \langle n'\boldsymbol{R'}|\\
&= \sum_{n\boldsymbol{R},n'\boldsymbol{R'}} \left[\int w_n^*(\boldsymbol{r}-\boldsymbol{R})Hw_{n'}(\boldsymbol{r}-\boldsymbol{R'})d^3r\right] |n\boldsymbol{R}\rangle \langle n'\boldsymbol{R'}|\,, \qquad (3.75)
\end{aligned}$$

where H is given by Eq. (3.54). Calculating the matrix elements can actually often not be performed in practice, but the generic resulting form of the Hamiltonian is (neglecting transitions between different bands)

$$H = \sum_{n\boldsymbol{R}} \tilde{E}_n |n\boldsymbol{R}\rangle \langle n\boldsymbol{R}| + \sum_n \sum_{\boldsymbol{R}\neq\boldsymbol{R'}} t^n_{\boldsymbol{R}\boldsymbol{R'}} |n\boldsymbol{R}\rangle \langle n\boldsymbol{R'}|\,. \qquad (3.76)$$

The matrix element $t_{\boldsymbol{R}\boldsymbol{R'}}$ is called **hopping amplitude** as it describes a transition of an electron from state n localized at $\boldsymbol{R'}$ to state n localized at $\boldsymbol{R}$. This Hamiltonian is the starting point of many calculations – where the hopping amplitudes $t_{\boldsymbol{R}\boldsymbol{R'}}$ and on-site energies $\tilde{E}_n$ are to be determined experimentally. In many models, this is even further approximated to include next neighbour processes only

$$t^n_{\boldsymbol{R}\boldsymbol{R'}} = \begin{cases} t & : \quad \boldsymbol{R} \text{ and } \boldsymbol{R'} \text{ are next neighbours}\\ 0 & : \quad \text{else}\end{cases}\,. \qquad (3.77)$$

We just mention here that another way to obtain good approximations to the full Hamiltonian is to approximate the Wannier functions by not just one atomic orbital (as we did in the previous section) but a linear combination of them

$$w(\boldsymbol{r}-\boldsymbol{R}) = \sum_n a_n\phi_n(\boldsymbol{r}-\boldsymbol{R})\,. \qquad (3.78)$$

Here, the a_n are variational parameters, upon which one has to optimize to improve the method. This method is called **linear combinations of atomic orbitals (LCAO)**.

3.1.4 Tight-Binding Example: Single Electron

As a simple example to the tight-binding model, we revisit the chain Hamiltonian

$$H_1 = E\sum_{n=1}^N |n\rangle\langle n| + t\sum_{n=1}^N \left[|n\rangle\langle n+1| + |n+1\rangle\langle n|\right]\,, \qquad |N+1\rangle = |1\rangle\,, \qquad (3.79)$$

where $E_n = E$ is the homogeneous single-orbital energy and $t \in \mathbb{C}$ is a hopping matrix element. We only consider jumps to the next neighbors and neglect jumps to neighbours farther away in the structure. The state $|n\rangle$ denotes a single(!) localized electron residing at site n – all other sites are empty (so far, we only discuss single-electron physics). The states are defined orthogonal $\langle n|m\rangle = \delta_{nm}$, and therefore we define the $|n\rangle$ states as the Wannier basis. Further, the term $|n\rangle \langle n+1|$ describes the tunneling from site $n+1$ to site n. This Hamiltonian has a Hilbert space dimension corresponding to the number of sites N. The index n denotes where the electron is localized, and consequently the position operator would be given by

$$x = a \sum_n n \left|n\right\rangle \left\langle n\right| \,, \tag{3.80}$$

where a is the lattice constant. It is not possible to represent the momentum operator with the $|n\rangle$ state basis alone.

Coming back to our tight-binding problem, the atomic orbitals and energies are given by

$$\phi_n(\boldsymbol{r} - n\boldsymbol{R}) = \langle r - na|n\rangle \,, \qquad E_n = E \,. \tag{3.81}$$

By construction, these already form an orthogonal basis and they are therefore a Wannier basis for our problem. By defining the $|n\rangle$ states to represent a localized electron at site n, it follows that some approximations performed (neglect of many-center contributions) are valid exactly. The Bloch states become

$$|k\rangle = \frac{1}{\sqrt{N}} \sum_{n=1}^{N} e^{+\mathrm{i}kna} |n\rangle \,, \tag{3.82}$$

and they are orthogonal as well

$$\langle k|k'\rangle = \frac{1}{N} \sum_{n=1}^{N} e^{-\mathrm{i}(k-k')na} = \delta_{kk'} \,. \tag{3.83}$$

In the continuum limit, we would have $\delta(k - k')$. The Bloch states are exact eigenstates of our Hamiltonian

$$\begin{aligned} H|k\rangle &= E|k\rangle + t\frac{1}{\sqrt{N}} \sum_{n=1}^{N} e^{+\mathrm{i}\boldsymbol{kna}} |n-1\rangle + t\frac{1}{\sqrt{N}} \sum_{n=1}^{N} e^{+\mathrm{i}\boldsymbol{kna}} |n+1\rangle \\ &= E|k\rangle + t(e^{+\mathrm{i}ka} + e^{-\mathrm{i}ka})|k\rangle = [E + 2t\cos(ka)]|k\rangle \,. \end{aligned} \tag{3.84}$$

Indeed, we can read off the full energies, and they correspond to Eq. (3.74)

$$\begin{aligned} \epsilon_{n\boldsymbol{k}} &= \langle n| H |n\rangle + \sum_{n' \neq n} e^{-\mathrm{i}kna} \langle n'| V_{nn'} |n\rangle \\ &= E + 2t\cos(ka) \,. \end{aligned} \tag{3.85}$$

The energies in this example are only distributed along a single band, ranging from $E - 2t$ to $E + 2t$.

3.1.5 Tight-Binding Example: Noninteracting Electrons

If we would now add an additional non-interacting electron (so far, our electrons are assumed spinless), we cannot simply consider the sum of two such Hamiltonians. This would, for example, allow for the double occupation of the same site by two (spinless) electrons. This should be forbidden by the exclusion principle, and therefore, we rather use fermionic creation and annihilation operators for an electron on site n

$$\{c_n, c_m^\dagger\} = \delta_{nm}\,, \qquad \{c_n, c_m\} = 0 \tag{3.86}$$

to define the state of an electron at site n via the action of a creation operator on the vacuum state. The anticommutation relations then automatically enforce the Pauli exclusion principle. take into account that we cannot create more than one electron on a single site. The Hamiltonian is then written as

$$H_N = E \sum_n c_n^\dagger c_n + t \sum_n \left[c_n^\dagger c_{n+1} + c_{n+1}^\dagger c_n \right]\,, \qquad c_{N+1} = c_1\,. \tag{3.87}$$

Here, we can put at most N electrons into the system, leading in total to a Hilbert space dimension of $d = 2^N$ – much bigger than the single-electron example used before. An electron on site n is created by $c_n^\dagger$ acting on the vacuum state, and the term $c_{n+1}^\dagger c_n$ represents a tunneling process from site n to site $n+1$. In contrast to bosons, the fermionic creation and annihilation operators act on multi-particle Fock states by creating a phase factor [2], which can be chosen as

$$\begin{aligned}
c_i \left|n_1, n_2, \ldots, 1_i, \ldots, n_N\right\rangle &= (-1)^{n_1+\ldots+n_{i-1}} \left|n_1, n_2, \ldots, 0_i, \ldots, n_N\right\rangle\,,\\
c_i \left|n_1, n_2, \ldots, 0_i, \ldots, n_N\right\rangle &= 0\,,\\
c_i^\dagger \left|n_1, n_2, \ldots, 1_i, \ldots, n_N\right\rangle &= 0\,,\\
c_i^\dagger \left|n_1, n_2, \ldots, 0_i, \ldots, n_N\right\rangle &= (-1)^{n_1+\ldots+n_{i-1}} \left|n_1, n_2, \ldots, 1_i, \ldots, n_N\right\rangle\,.
\end{aligned} \tag{3.88}$$

When two operators act on the same site, the phase factor always cancels

$$c_i^\dagger c_i \left|n_1, \ldots, n_N\right\rangle = n_i \left|n_1, \ldots, n_N\right\rangle\,, \tag{3.89}$$

and the particle number operator is given by

$$\hat{N} = \sum_i c_i^\dagger c_i\,. \tag{3.90}$$

The relation to the single-particle sector is obtained by sandwhiching the Hamiltonian with many-particle Fock states. For example, we can recover the single-particle sector by computing the matrix elements

$$\begin{aligned}
\left\langle n_1 n_2 \ldots n_{N-1} n_N\right| H \left|n_1 n_2 \ldots n_{N-1} n_N\right\rangle &= E \sum_{i=1}^N n_i\,,\\
\left\langle n_1 \ldots 10 \ldots n_N\right| H \left|n_1 \ldots 01 \ldots n_N\right\rangle &= t\,.
\end{aligned} \tag{3.91}$$

in the single-particle subspace where $\sum_i n_i = 1$. However, we are now free to put up to N electrons on the chain, as becomes visible by decoupling the Hamiltonian

$$H_N = (c_1^\dagger \ldots c_N^\dagger) \begin{pmatrix} E & t & & & t \\ t & \ddots & \ddots & & \\ & \ddots & \ddots & \ddots & \\ & & \ddots & \ddots & t \\ t & & & t & E \end{pmatrix} \begin{pmatrix} c_1 \\ \vdots \\ c_N \end{pmatrix}\,. \tag{3.92}$$

We can perform a unitary rotation of both the creation and annihilation operators

$$c_i = \sum_k u_{ik} d_k \,, \qquad c_i^\dagger = \sum_k u_{ik}^* d_k^\dagger \,, \tag{3.93}$$

to new fermionic operators that also obey the fermionic anticommutation relations. Since the u_{ik} are the matrix elements of a unitary matrix, we get from presupposing fermionic anticommutation relations for the transformed modes

$$\{c_i, c_j^\dagger\} = \sum_{kq} u_{ik} u_{jq}^* \{d_k, d_q^\dagger\} = \sum_k u_{ik} u_{jk}^* = \delta_{ij} \,. \tag{3.94}$$

However, since the transformation is unitary, its inverse is unitary as well, such that the argument also works in the opposite direction. In fact, this unitary transform is a special case of a transformation known as Bogoliubov transform – we will encounter it again later. For now, we just need that any unitary transformation preserves the fermionic anticommutation relations. Particularly, we choose the one that decouples the Hamiltonian

$$\begin{aligned} H_N &= \left(d_1^\dagger \dots d_N^\dagger\right) U^\dagger \begin{pmatrix} E & t & & & t \\ t & \ddots & \ddots & & \\ & \ddots & \ddots & \ddots & \\ & & \ddots & \ddots & t \\ t & & & t & E \end{pmatrix} U \begin{pmatrix} d_1 \\ \vdots \\ d_N \end{pmatrix} = \left(d_1^\dagger \dots d_N^\dagger\right) \begin{pmatrix} \epsilon_1 & & \\ & \ddots & \\ & & \epsilon_N \end{pmatrix} \begin{pmatrix} d_1 \\ \vdots \\ d_N \end{pmatrix} \\ &= \sum_i \epsilon_i d_i^\dagger d_i \,. \end{aligned} \tag{3.95}$$

This is the same matrix as is present in the single-particle Hamiltonian, and we have already computed its spectrum in Eq. (3.85). In addition, we also encountered such a structure when analyzing normal mode transformations in rings, compare Sec. 2.4.2. The single-particle energies therefore lie in the energy band $[E-2t, E+2t]$, and the energy band of the single-electron subspace is identical to the one computed in the previous section. When we now consider two different electrons, we have to take two different modes due to the Pauli exclusion principle. For sufficiently long chains however, all energy eigenvalues become quasi-continuous, and the two-electron subspace will cover the values $[2E-4t, 2E+4t]$.

3.1.6 Electronic Band Structure Classification

Coming from both sides – the free electrons and the Wannier states – we have seen that in periodic potentials, band structures will develop. These band structures are very important for the material properties.

To begin, we postulate that we have a class of electronic eigenstates to the Hamiltonian $\left|\{n_{\ell \boldsymbol{k}\sigma}\}\right\rangle$, where ℓ denotes the band index, $\boldsymbol{k}$ the wave vector, and $\sigma \in \{-1/2, +1/2\}$ the electronic spin (we have neglected it so far). The number $n_{\ell \boldsymbol{k}_\sigma} \in \{0, 1\}$ then just tells us whether the corresponding single-particle eigenstate is occupied ($n_{\ell \boldsymbol{k}_\sigma} = 1$) or not ($n_{\ell \boldsymbol{k}_\sigma} = 0$). In the absence of any interaction, the many-electron states can be constructed from the single particle eigenstates $\left|n_{\ell \boldsymbol{k}_\sigma}\right\rangle$ via

$$\left|\{n_{\ell \boldsymbol{k}\sigma}\}\right\rangle = \bigotimes_{\ell \boldsymbol{k}\sigma} \left|n_{\ell \boldsymbol{k}\sigma}\right\rangle \,, \tag{3.96}$$

and their energies follow directly from summing up the single-particle energies of the occupied states

$$H \left|\{n_{\ell\boldsymbol{k}\sigma}\}\right\rangle = \sum_{\ell\boldsymbol{k}\sigma} n_{\ell\boldsymbol{k}\sigma}\epsilon_\ell(\boldsymbol{k}) \left|\{n_{\ell\boldsymbol{k}\sigma}\}\right\rangle , \tag{3.97}$$

which is automatically implemented by $n_{\ell\boldsymbol{k}_\sigma} \in \{0, 1\}$. Here, $\epsilon_\ell(\boldsymbol{k})$ is the energy for wave vector $\boldsymbol{k}$ in band ℓ and it has been assumed that the two spin degrees of freedom have the same energy. For a system with N atoms, each of the bands has exactly N different $\boldsymbol{k}$ values, which corresponds to $2N$ single particle electronic states per band if we include the spin. In general, the total number of bound states will exceed the total number of electrons N_e. Therefore, at very low temperatures, we can construct the many-particle ground state by successively filling the bands with electrons until the total number of occupied states equals the total number of electrons. The energy above the highest occupied and below the lowest empty state is then called the **Fermi energy** E_F

$$2 \sum_{\ell\boldsymbol{k}:\epsilon_\ell(\boldsymbol{k})<E_F} 1 = N_e . \tag{3.98}$$

Depending on the band configuration and the ratio of the total number of atoms N and the total number of electrons N_e, there are two different possibilities

- All lower bands are completely filled and all higher bands are completely empty. The Fermi energy is then actually not well defined and lies somewhere in the **band gap** between the highest filled band and the lowest empty band. To excite an electron, it is necessary to provide at least the band gap energy in the order of a few eV. Consequently, current is hardly supported and these materials are semiconductors or even insulators. The highest completely filled band is then called **valence band**.
- One band is only partially filled even at zero temperature. Then – keeping in mind that the k-values are continuous – one can excite an electron with arbitrarily little energy, which allows conduction. Correspondingly, this is the case in metals, and the corresponding partially filled band is called a **conduction band**.

Provided the bands do not overlap, this allows a vague classification from the crystal structure and the number of electrons per primitive elementary cell Z_e. Clearly, we have

$$N_e = N Z_e . \tag{3.99}$$

Since we have $2N$ states per band, we can – if Z_e is odd – fill $\frac{Z_e-1}{2}$ bands fully and one band half. The total number of electrons is then $2N(Z_e - 1)/2 + 2N/2 = NZ_e = N_e$. Thus, one would expect a metal and the $(Z_e + 1)/2$-th band to be the conduction band – and indeed, this is often the case.

Now, for even Z_e, we can fully fill $\frac{Z_e}{2}$ bands, and one would expect a semiconductor or an insulator. This second rule does not always work since the underlying assumption of non-overlapping bands is often violated.

The classification is summarized in Fig. 3.3.

3.1.7 Electronic Density of States

As with phonons (compare Sec. 2.4.7), one often encounters summations over functions that actually only depend on the electronic dispersion relation

$$S = \frac{1}{V}\sum_{n\boldsymbol{k}\sigma} f(\epsilon_{n\boldsymbol{k}}) = \sum_{n\sigma}\int_{1.BZ} \frac{d^3k}{(2\pi)^3} f(\epsilon_n(\boldsymbol{k})) = \int dE f(E)\rho(E) , \tag{3.100}$$

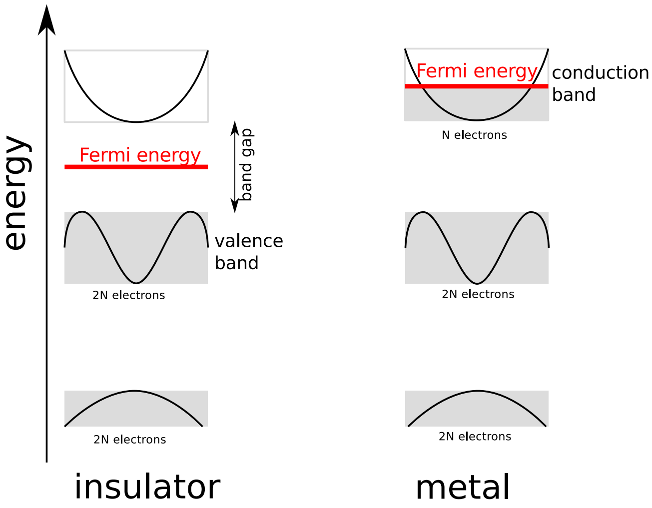

Figure 3.3: Sketch of the band filling for semiconductors and insulators (left) or metals (right), together with the corresponding position of the Fermi energy. Due to the electronic spin, each filled band hosts $2N$ electrons.

which defines the **electronic density of states**

$$\rho(E)=\frac{1}{V}\sum_{n\boldsymbol{k}\sigma}\delta(E-\epsilon_n(\boldsymbol{k}))=\sum_{n\sigma}\int\frac{d^3k}{(2\pi)^3}\delta(E-\epsilon_n(\boldsymbol{k}))\,. \tag{3.101}$$

Sometimes, one also defines these densities of states specific to individual bands. Here, V denotes the macroscopic volume and E has units of energy (sometimes we also write $\rho(\omega)$).

The Fermi energy (3.98) is now defined by (the lower energy bound is handled by the electronic density of states $\rho(E)$)

$$\int_{-\infty}^{E_F}\rho(E)dE=\frac{N_e}{V}\,. \tag{3.102}$$

Here, N_e is the total number of electrons and V the macroscopic volume. Similar to the phonon case we can express the electronic density of states in terms of a surface integral

$$\rho(E)=\frac{1}{4\pi^3}\sum_n\int_{S(E)}\frac{d^2k}{\left|\nabla_{\boldsymbol{k}}\epsilon_n(\boldsymbol{k})\right|}\,, \tag{3.103}$$

where $S(E)$ is the surface in $\boldsymbol{k}$ space that is defined by the solution of $E=\epsilon_n(\boldsymbol{k})$ with respect to $\boldsymbol{k}$. The **Fermi surface** is then defined by $S_F=S(E_F)$. Its physical interpretation is that this surface separates at zero temperature the occupied parts of $\boldsymbol{k}$-space from the unoccupied ones. It has characteristic shapes for each solid.

Example: Density of states for free electrons

A particularly simple example is of course the dispersion relation of free electrons $\epsilon_n(\boldsymbol{k})=E(k)=\frac{\hbar^2k^2}{2m}$. We have $\nabla_{\boldsymbol{k}}\epsilon_n(\boldsymbol{k})=\frac{\hbar^2}{m}\boldsymbol{k}$, such that the density of states becomes for the single "band"

$$\rho(E)=\frac{1}{4\pi^3}\frac{m}{\hbar^2}\int_{S(E)}\frac{d^2k}{k}=\frac{1}{4\pi^3}\frac{m}{\hbar^2}\frac{4\pi k^2}{k}=\frac{\sqrt{2m^3}}{\pi^2\hbar^3}\sqrt{E}\,,\qquad E\geq 0\,. \tag{3.104}$$

Here, the surface integral is just over the sphere defined by $E=\hbar^2k^2/(2m)$. At the band edge the density of states becomes non-analytic with a root scaling. In general, a scaling of $\rho(E)\propto\sqrt{E-E_c}$ is characteristic at band edges of 3d systems, compare the discussion of van-Hove singularities in case of phonons. The Fermi energy E_F is then defined by

$$\frac{\sqrt{2m^3}}{\pi^2\hbar^3}\int_0^{E_F}E^{1/2}dE=\frac{\sqrt{2m^3}}{\pi^2\hbar^3}\frac{2}{3}E_F^{3/2}=\frac{N_e}{V}\,. \tag{3.105}$$

Example: Higher dimensions

Let $|i,j,k\rangle$ denote the Wannier state of a single electron localized at site $i,j,k \in \mathbb{Z}$ on a simple cubic lattice. Then, the single-particle Hamiltonian in tight-binding approximation can be written as

$$\begin{aligned} H = E_0 \sum_{ijk} |i,j,k\rangle \langle i,j,k| \\ &+ t\Big[|i,j,k\rangle \langle i+1,j,k| + |i+1,j,k\rangle \langle i,j,k| + |i,j,k\rangle \langle i,j+1,k| + |i,j+1,k\rangle \langle i,j,k| \\ &+ |i,j,k\rangle \langle i,j,k+1| + |i,j,k+1\rangle \langle i,j,k| \Big] . \end{aligned} \tag{3.106}$$

As before, we define these Wannier states to be fully localized, such that the overlap integrals vanish. Assuming a simple cubic lattice with lattice constant a, the Bloch states become

$$|\boldsymbol{k}\rangle = \frac{1}{\sqrt{N_x N_y N_z}} \sum_{i=1}^{N_x} \sum_{j=1}^{N_y} \sum_{k=1}^{N_z} e^{\mathrm{i}\boldsymbol{k}a(i\boldsymbol{e_x}+j\boldsymbol{e_y}+k\boldsymbol{e_z})} |i,j,k\rangle = \frac{1}{\sqrt{N}} \sum_{i=1}^{N_x} \sum_{j=1}^{N_y} \sum_{k=1}^{N_z} e^{\mathrm{i}a(ik_x+jk_y+kk_z)} |i,j,k\rangle , \tag{3.107}$$

where the $\boldsymbol{k}$ vectors are distributed over the 1. BZ of the reciprocal lattice (also simple cubic). More specifically, the periodicity condition demands that they are discrete

$$k_\alpha = \frac{2\pi}{a} \frac{n_\alpha}{N_\alpha} , \qquad n_\alpha \in \mathbb{Z} , \qquad -\frac{N_\alpha}{2} \le n_\alpha < +\frac{N_\alpha}{2} . \tag{3.108}$$

The Bloch states are eigenstates of the Hamiltonian

$$\begin{aligned} H|\boldsymbol{k}\rangle &= E_0 |\boldsymbol{k}\rangle + \frac{t}{\sqrt{N}} \sum_{i,j,k} [2\cos(k_x a) + 2\cos(k_y a) + 2\cos(k_z a)]\, e^{\mathrm{i}a(ik_x+jk_y+kk_z)} |i,j,k\rangle \\ &= [E_0 + 2t(\cos(k_x a) + \cos(k_y a) + \cos(k_z a))] |\boldsymbol{k}\rangle , \end{aligned} \tag{3.109}$$

and we can read off the 3d dispersion relation

$$\epsilon_n(\boldsymbol{k}) = E_0 + 2t\,[\cos(k_x a) + \cos(k_y a) + \cos(k_z a)] . \tag{3.110}$$

We can easily compute the gradient of this with respect to $\boldsymbol{k}$, but the surface defined by $E = \epsilon_n(\boldsymbol{k})$ is highly complicated, such that even within tight-binding, the density of states should be computed numerically.

3.1.8 Specific Heat of metals at low temperatures

Let us assume that we are given the full electronic Hamiltonian and that we know the single-particle energies for band index ℓ, wave vector $\boldsymbol{k}$, electron spin σ and their corresponding eigenstates $|\ell\boldsymbol{k}\sigma\rangle$. With the dispersion relation $\epsilon_\ell(\boldsymbol{k})$, and occupation number $n_{\ell\boldsymbol{k}\sigma} \in \{0,1\}$, we can express the total eigenvalue equation as

$$H|\{n_{\ell\boldsymbol{k}\sigma}\}\rangle = \sum_{\ell\boldsymbol{k}\sigma} \epsilon_\ell(\boldsymbol{k}) c^\dagger_{\ell\boldsymbol{k}\sigma} c_{\ell\boldsymbol{k}\sigma} |\{n_{\ell\boldsymbol{k}\sigma}\}\rangle = \sum_{\ell\boldsymbol{k}\sigma} n_{\ell\boldsymbol{k}\sigma} \epsilon_\ell(\boldsymbol{k}) |\{n_{\ell\boldsymbol{k}\sigma}\}\rangle . \tag{3.111}$$

Now, we follow essentially the same calculations as for the phonons. However, there are two fundamental differences. First, the statistics of the involved operators is evidently fermionic and not bosonic. Second, we do now have to take a chemical potential into account, since the macroscopic many-body state is not only determined by temperature but also by the number of electrons. Therefore, we consider the grand-canonical equilibrium state.

For a single fermion, we consider the grand-canonical density matrix

$$\rho = \frac{e^{-\beta(\hat{H}-\mu\hat{N})}}{\mathrm{Tr}\left\{e^{-\beta(\hat{H}-\mu\hat{N})}\right\}} \tag{3.112}$$

with $\hat{H} = \epsilon c^\dagger c$ and $\hat{N} = c^\dagger c$. The mean energy cannot be simply determined with a derivative with respect to β. Instead, it can be calculated directly

$$\begin{aligned} U &= \mathrm{Tr}\left\{\epsilon c^\dagger c \frac{e^{-\beta(\epsilon-\mu)c^\dagger c}}{\mathrm{Tr}\left\{e^{-\beta(\epsilon-\mu)c^\dagger c}\right\}}\right\} \\ &= \epsilon \left\langle 0\right| c^\dagger c \frac{e^{-\beta(\epsilon-\mu)c^\dagger c}}{\mathrm{Tr}\left\{e^{-\beta(\epsilon-\mu)c^\dagger c}\right\}} \left|0\right\rangle + \epsilon \left\langle 1\right| c^\dagger c \frac{e^{-\beta(\epsilon-\mu)c^\dagger c}}{\mathrm{Tr}\left\{e^{-\beta(\epsilon-\mu)c^\dagger c}\right\}} \left|1\right\rangle \\ &= \epsilon \frac{e^{-\beta(\epsilon-\mu)}}{1+e^{-\beta(\epsilon-\mu)}} = \epsilon \frac{1}{e^{\beta(\epsilon-\mu)}+1} \,. \end{aligned} \tag{3.113}$$

This defines the Fermi function

$$f(\omega) = \frac{1}{e^{\beta(\omega-\mu)}+1} \,, \tag{3.114}$$

which depends on inverse temperature β and chemical potential μ. For low temperatures, the Fermi function behaves similar to an inverted step function, but generally it is a function that decays from a value $+1 = \lim_{\omega\to-\infty} f(\omega)$ at the position of the chemical potential $1/2 = f(\mu)$ down to the value $0 = \lim_{\omega\to+\infty} f(\omega)$ over a region with a width corresponding to β^{-1}. The chemical potential is typically fixed such that the total electron number N_e is given by $N_e = f(\epsilon)$. For a single mode, this simply fixes the Fermi function to N_e and the internal energy to $N_e\epsilon$.

For many non-interacting electrons, we take the same grand-canonical equilibrium state as before, but now with the total Hamiltonian and total particle number

$$\hat{H} = \sum_i \epsilon_i c_i^\dagger c_i \,, \qquad \hat{N} = \sum_i c_i^\dagger c_i \,. \tag{3.115}$$

As the Hamiltonian is non-interacting, its exponential factorizes. More formally, we note that

$$\left[c_i^\dagger c_i, c_j^\dagger c_j\right] = 0 \,, \tag{3.116}$$

which allows us to separate the exponential of these terms into individual ones. Accordingly, the internal energy just becomes a sum of the internal energies

$$U = \sum_i \epsilon_i f(\epsilon_i) = \sum_i \epsilon_i \left\langle c_i^\dagger c_i \right\rangle \,. \tag{3.117}$$

Fixing the chemical potential now becomes non-trivial

$$N_e = \sum_i f(\epsilon_i) \,. \tag{3.118}$$

Specifically for our problem, $i = (\ell, \boldsymbol{k}, \sigma)$, and we would like to compute internal energy and electronic particle number

$$U = \sum_{\ell \boldsymbol{k} \sigma} f(\epsilon_\ell(\boldsymbol{k}))\epsilon_\ell(\boldsymbol{k}) = \sum_{\ell\sigma} \frac{V}{(2\pi)^3} \int_{1.\text{BZ}} d^3k f(\epsilon_\ell(\boldsymbol{k}))\epsilon_\ell(\boldsymbol{k}) = V \int f(\omega)\omega\rho(\omega)d\omega\,,$$
$$N_e = \sum_{\ell \boldsymbol{k} \sigma} f(\epsilon_\ell(\boldsymbol{k})) = \sum_{\ell\sigma} \frac{V}{(2\pi)^3} \int_{1.\text{BZ}} d^3k f(\epsilon_\ell(\boldsymbol{k})) = V \int f(\omega)\rho(\omega)d\omega\,. \tag{3.119}$$

Here, $\rho(\omega)$ denotes the electronic density of states. To compute the heat capacity, we want to compute the derivative of U with respect to T. The computation of the particle number is required to fix the chemical potential μ.

Integrals over a product of a well-behaved function $H(\omega)$ and the Fermi function can be computed with the **Sommerfeld expansion**

$$\lim_{\omega\to-\infty} H(\omega) < \infty\,, \qquad K(\omega) = \int_{-\infty}^{\omega} H(\omega')d\omega'\,,$$
$$I = \int H(\omega)f(\omega)d\omega = \left[K(\omega)f(\omega)\right]_{\omega=-\infty}^{+\infty} - \int K(\omega)f'(\omega)d\omega$$
$$= \int K(\omega)[-f'(\omega)]d\omega\,. \tag{3.120}$$

Here, we have used that $f(+\infty) = 0$ and by construction $K(-\infty) = 0$. The derivative of the Fermi function is actually non-negligible only in a region $[\mu - \mathcal{O}\{k_BT\}, \mu + \mathcal{O}\{k_BT\}$.

$$-f'(\omega) = \frac{1}{e^{\beta(\omega-\mu)}+1}\frac{\beta e^{\beta(\omega-\mu)}}{e^{\beta(\omega-\mu)}+1} = \beta f(\omega)[1-f(\omega)]\,, \tag{3.121}$$

and decays exponentially fast farther away from it. This means that for numerical solutions, one actually only needs a small interval around μ. This can be exploited by expanding the function $K(\omega)$ in a Taylor series around μ

$$K(\omega) = K(\mu) + \sum_{n=1}^{\infty} \frac{(\omega-\mu)^n}{n!} K^{(n)}(\omega)|_{\omega=\mu}\,. \tag{3.122}$$

This implies for the full integral

$$I = \int \left[K(\mu) + \sum_{n=1}^{\infty} \frac{(\omega-\mu)^n}{n!} K^{(n)}(\omega)|_{\omega=\mu}\right] [-f'(\omega)]d\omega$$
$$= -K(\mu)f(\omega)|_{-\infty}^{+\infty} + \sum_{n=1}^{\infty} H^{(n-1)}(\mu) \int \frac{(\omega-\mu)^n}{n!}[-f'(\omega)]d\omega$$
$$= +K(\mu) + \sum_{n=1}^{\infty} H^{(2n-1)}(\mu) \int \frac{(\omega-\mu)^{2n}}{(2n)!}[-f'(\omega)]d\omega$$
$$= \int_{-\infty}^{\mu} H(\omega)d\omega + \sum_{n=1}^{\infty} a_n (k_BT)^{2n} H^{(2n-1)}(\mu)\,,$$
$$a_n = \int \frac{x^{2n}}{(2n)!}\frac{1}{(e^x+1)(e^{-x}+1)}dx\,, \tag{3.123}$$

where we have used that $f'(\omega)$ is an even function around μ (this lets all odd powers vanish), and where we also introduced $x = \beta(\omega-\mu)$. One can calculate the coefficients a_n analytically, specifically

$$a_1 = \frac{\pi^2}{6} \,. \tag{3.124}$$

Eventually, this implies for the electronic particle number and internal energy

$$\begin{aligned} N_e &= V \left[\int_{-\infty}^{\mu} \rho(\omega) d\omega + \frac{\pi^2}{6} (k_B T)^2 \rho'(\mu) + \mathcal{O}\{T^4\} \right] \,, \\ U &= V \left[\int_{-\infty}^{\mu} \omega\rho(\omega) d\omega + \frac{\pi^2}{6} (k_B T)^2 \left(\mu\rho'(\mu) + \rho(\mu)\right) + \mathcal{O}\{T^4\} \right] \,. \end{aligned} \tag{3.125}$$

If the chemical potential was constant, we could now directly compute the specific heat. However, the chemical potential depends on temperature, since it is fixed by the first equation. Therefore, we consider now the first equation to establish a relation between chemical potential and particle number at low temperatures. At zero temperature, the chemical potential must be exactly at the Fermi energy $\mu(T=0) = E_F$, such that at low temperatures we can assume it to be close to this value and therefore approximate the upper bound as

$$\begin{aligned} N_e &\approx V \left[\int_{-\infty}^{E_F} \rho(\omega) d\omega + \int_{E_F}^{\mu} \rho(\omega) d\omega + \frac{\pi^2}{6} (k_B T)^2 \rho'(\mu) \right] \\ &\approx V \left[\int_{-\infty}^{E_F} \rho(\omega) d\omega + (\mu - E_F)\rho(E_F) + \frac{\pi^2}{6} (k_B T)^2 \rho'(\mu) \right] \\ &= N_e + V(\mu - E_F)\rho(E_F) + V\frac{\pi^2}{6} (k_B T)^2 \rho'(E_F) \,, \end{aligned} \tag{3.126}$$

where we have used Eq. (3.102). Accordingly, we get that at low temperatures, the chemical potential must scale quadratically with temperature

$$\mu = E_F - \frac{\pi^2}{6} \frac{\rho'(E_F)}{\rho(E_F)} (k_B T)^2 \,. \tag{3.127}$$

We can insert this into the second equation for the energy density, using a similar expansion of the upper integral bound and keeping only terms to quadratic order in temperature

$$\begin{aligned} u = \frac{U}{V} &\approx \int_{-\infty}^{E_F} \omega\rho(\omega) d\omega + (\mu - E_F)E_F\rho(E_F) + \frac{\pi^2}{6} (k_B T)^2 (E_F\rho'(E_F) + \rho(E_F)) \\ &= u_0 - \frac{\pi^2}{6} \rho'(E_F) E_F (k_B T)^2 + \frac{\pi^2}{6} (k_B T)^2 (E_F\rho'(E_F) + \rho(E_F)) \\ &= u_0 + \frac{\pi^2}{6} \rho(E_F) (k_B T)^2 \,. \end{aligned} \tag{3.128}$$

Accordingly, we get for the electronic specific heat at low temperatures

$$c_V^{\text{el}} = \frac{\pi^2}{3} \rho(E_F) k_B^2 T \,. \tag{3.129}$$

This has to be seen in combination with our result for the phonons at low temperatures from Eq. (2.146). By adding both contributions, we get

$$\lim_{T\to 0} c_V = \left[\frac{\pi^2}{3} \rho(E_F) k_B \right] k_B T + \left[\frac{2\pi^2}{5} k_B \left(\frac{1}{\hbar c} \right)^3 \right] (k_B T)^3 \,. \tag{3.130}$$

Accordingly, both $\rho(E_F)$ and the average sound velocity c can be determined from measuring the heat capacity scaling at low temperatures.

This derivation only holds for metals, since we used that the density of states is a smooth function at the Fermi energy. For semiconductors and insulators, we always have by construction $\rho(E_F) = 0$, such that the calculated contribution to the specific heat would vanish.

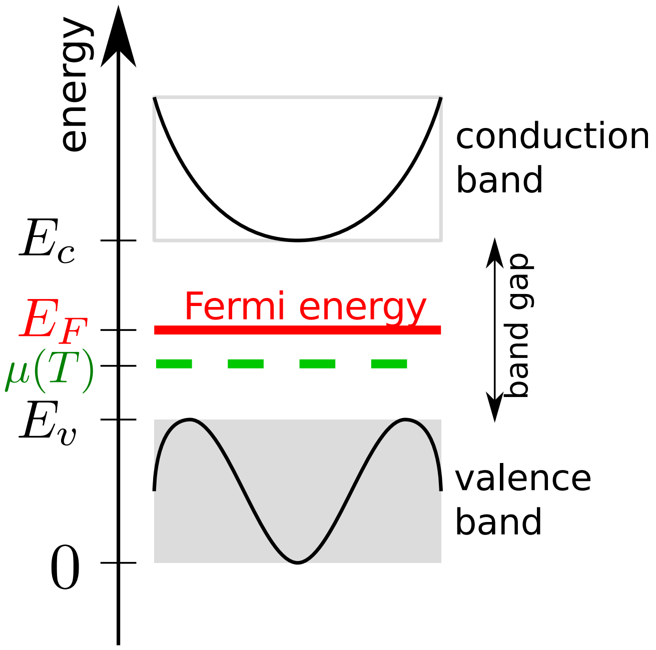

Figure 3.4: Sketch of the semiconductor band structure in two-mode approximation with relevant parameters. At zero temperature, the lower valence band is completely filled, whereas at finite temperatures, electrons will occasionally be excited into the conduction band, leaving holes in the valence band. The sought-after chemical potential will lie somewhere in the band gap.

3.1.9 Specific Heat of semiconductors at low temperatures

Clearly, when the Fermi energy lies within the band gap, we have $\rho(E_F) = 0$, as there are no states available. Therefore, we have to treat this configuration differently.

For a feasible analysis, we first postulate some assumptions

- We only consider a two-band approximation by only taking the valence band and the conduction band into account. At low temperatures, only these bands will contribute to the specific heat.
- We will furthermore assume that the bands do not overlap and that the temperatures are low.
- At the band edges, we will assume that the density of states for electrons and holes will scale like the electronic density of states for free electrons.

The total density of states is then given by the sum over two bands

$$\rho(\omega) = \rho_v(\omega) + \rho_c(\omega)\,, \tag{3.131}$$

where $\rho_v(\omega)$ denotes the valence band density of states and $\rho_c(\omega)$ the conduction band density of states. Let $E_v > 0$ denote the upper edge of the valence band and $E_c < \infty$ the lower edge of the conduction band. The Fermi energy lies between them, see Fig. 3.4. Then, at zero temperatures, where only the valence band is occupied, the total number of electrons is given by

$$N_e = V \int_0^{E_F} \rho(\omega) d\omega = V \int_0^{E_v} \rho_v(\omega) d\omega\,, \qquad T = 0\,. \tag{3.132}$$

At the same time, at finite temperatures we will have some states occupied in the valence band, such that then, the total number of electrons is given by

$$N_e = V \int_0^{\infty} \rho(\omega) d\omega = V \left[\int_0^{E_v} \rho_v(\omega) f(\omega) d\omega + \int_{E_c}^{\infty} \rho_c(\omega) f(\omega) d\omega\right]\,, \qquad T > 0\,, \tag{3.133}$$

where $f(\omega)$ denotes the Fermi function. Equating the last two expressions, we obtain the relation

$$n_h(\beta) \equiv \int_0^{E_v} \rho_v(\omega)[1-f(\omega)]d\omega = \int_{E_c}^{\infty} \rho_c(\omega) f(\omega) d\omega \equiv n_e(\beta)\,. \tag{3.134}$$

The l.h.s. represents the (volume) **density of holes in the valence band**, and the r.h.s. is the (volume) **density of electrons in the conduction band**, i.e., the density of holes equals the density of electrons. Due to the exclusion principle, each electron excited from the valence band into the conduction band leaves a hole, which also obeys the same Fermi-Dirac statistics as the electrons. We can think of the holes just as particles with an effective mass.

Our first goal will now be to find the temperature-dependence of the chemical potential. From the constraint of the total particle number we can already conclude that it must lie within the band gap $E_v \le \mu \le E_c$, but its exact value at low temperatures must be obtained from the above equation. Now, at low temperatures

$$\beta(E_c-\mu) \gg 1\,, \qquad \beta(\mu-E_v) \gg 1\,. \tag{3.135}$$

With this, we can approximate the Fermi functions in the respective energy regions as

$$\begin{aligned} \omega > E_c \qquad &: \qquad f(\omega) = \frac{1}{e^{\beta(\omega-\mu)}+1} \approx e^{-\beta(\omega-\mu)}\,, \\ \omega < E_v \qquad &: \qquad 1-f(\omega) = \frac{1}{e^{\beta(\mu-\omega)}+1} \approx e^{-\beta(\mu-\omega)}\,, \end{aligned} \tag{3.136}$$

i.e., the volume density of electrons above the band gap and the density of holes below the band gap will be exponentially suppressed at low temperatures. Now, we further specify our assumption of the density of states for electrons in the conduction $\rho_c(\omega)$ and valence band $\rho_v(\omega)$ near the band gaps

$$\begin{aligned} \rho_c(\omega) &\approx \frac{(2m_e)^{3/2}}{2\pi^2\hbar^3}(\omega-E_c)^{1/2} \qquad : \qquad \omega > E_c\,, \\ \rho_v(\omega) &\approx \frac{(2m_h)^{3/2}}{2\pi^2\hbar^3}(E_v-\omega)^{1/2} \qquad : \qquad \omega < E_v\,. \end{aligned} \tag{3.137}$$

For the conduction band electrons, this just corresponds to Eq. (3.104), and for the holes we have assumed the same distribution, just with an effective mass m_h instead. The electron density in the conduction band therefore becomes

$$\begin{aligned} n_e(\beta) &\approx \int_{E_c}^{\infty} \rho_c(\omega) e^{-\beta(\omega-\mu)} d\omega = e^{-\beta(E_c-\mu)} \int_{E_c}^{\infty} \rho_c(\omega) e^{-\beta(\omega-E_c)} d\omega \\ &= \frac{(2m_e)^{3/2}}{2\pi^2\hbar^3} e^{-\beta(E_c-\mu)} \int_{E_c}^{\infty} (\omega-E_c)^{1/2} e^{-\beta(\omega-E_c)} d\omega \\ &= \frac{(2m_e)^{3/2}}{2\pi^2\hbar^3} e^{-\beta(E_c-\mu)} \beta^{-3/2} 2 \int_0^{\infty} x^2 e^{-x^2} dx = \frac{(2m_e)^{3/2}}{2\pi^2\hbar^3} \frac{\sqrt{\pi}}{2} e^{-\beta(E_c-\mu)} \beta^{-3/2}\,. \end{aligned} \tag{3.138}$$

Here, we have used that due to the exponential suppression at low temperatures, it is permissible to extend the upper integration bound to $+\infty$ and furthermore used the substitution $x =$

$\beta(\omega - E_c)$. The calculation for the hole volume density in the valence band is similar

$$\begin{aligned} n_h(\beta) &\approx e^{-\beta(\mu-E_v)}\frac{(2m_h)^{3/2}}{2\pi^2\hbar^3}\int_0^{E_v}(E_v-\omega)^{1/2}e^{-\beta(E_v-\omega)}d\omega \\ &= \frac{(2m_h)^{3/2}}{2\pi^2\hbar^3}e^{-\beta(\mu-E_v)}\beta^{-3/2}2\int_0^{\sqrt{\beta E_v}}y^2e^{-y^2}dy \\ &\approx \frac{(2m_h)^{3/2}}{2\pi^2\hbar^3}e^{-\beta(\mu-E_v)}\beta^{-3/2}2\int_0^{\infty}y^2e^{-y^2}dy \\ &= \frac{(2m_h)^{3/2}}{2\pi^2\hbar^3}\frac{\sqrt{\pi}}{2}e^{-\beta(\mu-E_v)}\beta^{-3/2}\,. \end{aligned} \tag{3.139}$$

From equating the last two equations, compare Eq. (3.134), we obtain a relation for the chemical potential

$$m_e^{3/2}e^{-\beta(E_c-\mu)} = m_h^{3/2}e^{-\beta(\mu-E_v)}\,, \tag{3.140}$$

from which it follows that the ratio of effective hole mass and electron masses determines whether the chemical potential lies above or below the Fermi energy

$$\mu(T) = \frac{E_c+E_v}{2} + \frac{3}{4}k_BT\ln\left(\frac{m_h}{m_e}\right)\,. \tag{3.141}$$

Experimentally, this mass ratio can be tuned by doping the semiconductor with other atoms. In contrast to metals we see that the chemical potential scales linearly with temperature. At zero temperature, it is by construction equal to the Fermi energy $\mu(0) = E_F = \frac{E_c+E_v}{2}$.

The calculation of the specific heat now proceeds along similar lines

$$\begin{aligned} c_V &= \int \omega\rho(\omega)\frac{\partial f(\omega)}{\partial T}d\omega \\ &= \int_0^{E_v}\omega\rho_v(\omega)\left[\underline{\frac{\omega-\mu}{k_BT^2}} + \beta\frac{\partial\mu}{\partial T}\right]\frac{e^{\beta(\omega-\mu)}}{\left(e^{\beta(\omega-\mu)}+1\right)^2}d\omega + \int_{E_c}^{\infty}\omega\rho_c(\omega)\left[\underline{\frac{\omega-\mu}{k_BT^2}} + \beta\frac{\partial\mu}{\partial T}\right]\frac{e^{\beta(\omega-\mu)}}{\left(e^{\beta(\omega-\mu)}+1\right)^2}d\omega \\ &\approx \int_0^{E_v}\omega\rho_v(\omega)\frac{\omega-E_F}{k_BT^2}e^{\beta(\omega-\mu)}d\omega + \int_{E_c}^{\infty}\omega\rho_c(\omega)\frac{\omega-E_F}{k_BT^2}e^{-\beta(\omega-\mu)}d\omega \\ &= \frac{e^{-\beta(E_c-E_v)/2}}{k_BT^2}\left[\int_0^{E_v}\omega(\omega-E_F)\rho_v(\omega)e^{-\beta(E_v-\omega)}d\omega + \int_{E_c}^{\infty}\omega(\omega-E_F)\rho_c(\omega)e^{-\beta(\omega-E_c)}d\omega\right]\,. \end{aligned} \tag{3.142}$$

Here, we have only kept the leading order terms for small temperatures (underlined) and neglected the temperature dependence of the chemical potential, as that would lead to higher-order corrections.

Eventually, we do now insert the densities of states of the individual bands (3.137), which allows to evaluate these integrals as before. For example, we get for the first integral

$$\begin{aligned} I_v &= \int_0^{E_v}\omega(\omega-E_F)\rho_v(\omega)e^{-\beta(E_v-\omega)}d\omega \\ &= \frac{(2m_h)^{3/2}}{2\pi^2\hbar^3}\int_0^{E_v}\left[(E_v-\omega)-\underline{E_v}\right]\left[(E_v-\omega)+\underline{(E_F-E_v)}\right](E_v-\omega)^{1/2}e^{-\beta(E_v-\omega)}d\omega \\ &\approx -\frac{(2m_h)^{3/2}}{2\pi^2\hbar^3}E_v(E_F-E_v)\beta^{-3/2}\frac{\sqrt{\pi}}{2} + \ldots\,, \end{aligned} \tag{3.143}$$

where we have only kept the leading order terms for small temperatures (underlined). The same calculation is performed for the conductance band

$$\begin{aligned}
I_c &= \int_{E_c}^{\infty} \omega(\omega - E_F)\rho_c(\omega) e^{-\beta(\omega - E_c)} d\omega \\
&= \frac{(2m_e)^{3/2}}{2\pi^2\hbar^3} \int_{E_c}^{\infty} \left[(\omega - E_c) + \underline{E_c}\right] \left[(\omega - E_c) + \underline{(E_c - E_F)}\right] (\omega - E_c)^{1/2} e^{-\beta(\omega - E_c)} d\omega \\
&\approx + \frac{(2m_e)^{3/2}}{2\pi^2\hbar^3} E_c(E_c - E_F)\beta^{-3/2}\frac{\sqrt{\pi}}{2} + \ldots\,,
\end{aligned} \tag{3.144}$$

where we have only kept the leading order terms for small temperatures (underlined). Putting it all together, we eventually obtain

$$\begin{aligned}
c_V &= \frac{2k_B}{2^{3/2}\pi^{3/2}\hbar^3} \frac{e^{-\beta(E_c - E_v)/2}}{k_B T} \left[m_e^{3/2} E_c(E_c - E_F) - m_h^{3/2} E_v(E_F - E_v)\right] \\
&= \frac{2k_B}{(2\pi\hbar^2)^{3/2}} \frac{E_c - E_v}{2} \left[m_e^{3/2} E_c - m_h^{3/2} E_v\right] \frac{e^{-\beta(E_c - E_v)/2}}{k_B T}\,.
\end{aligned} \tag{3.145}$$

For temperatures small in comparison with the band gap $k_B T \ll (E_c - E_v) \equiv \Delta$, this is exponentially suppressed. Of course, these results depend on the specific assumptions on the density of states (3.137), but the exponential suppression is characteristic for all systems with a gapped spectrum.

3.2 Interacting Electrons

In addition to the previous section, we will now examine the effects of electron-electron interactions, i.e., the total Hamiltonian is given by

$$H = \sum_{i=1}^{N_e} \frac{\boldsymbol{p_i}^2}{2m} + \sum_{i=1}^{N_e} V(\boldsymbol{r_i}) + \sum_{i<j} u(\boldsymbol{r_i} - \boldsymbol{r_j})\,, \tag{3.146}$$

where N_e is the total number of electrons, $\boldsymbol{p_i}$ is the momentum operator of the i-th electron, $V(\boldsymbol{r_i})$ is the lattice-periodic ion-potential felt by the i-th electron at position $\boldsymbol{r_i}$, and $u(\boldsymbol{r_i} - \boldsymbol{r_j})$ denotes the electronic interaction potential. Microscopically, the last term should be given by the Coulomb repulsion

$$u(\boldsymbol{r} - \boldsymbol{r'}) = \frac{e^2}{|\boldsymbol{r} - \boldsymbol{r'}|}\,. \tag{3.147}$$

However, very often, parts of the effective electron-electron interaction can be treated by effective single particle potentials $V(\boldsymbol{r_i})$, such that a full microscopic description of all electron-electron interactions is hardly ever performed. For example, the inner electrons of an ion can be considered as tightly bound, such that it is well justified to treat the interaction between a conduction band electron and such an inner shell electron effectively as an interaction between the conduction band electron and the screened ion potential.

3.2.1 Operator representations

We have already discussed the fundamental properties of creation and annihilation operators in Sec. 3.1.5, where we saw how one could represent a tight-binding Hamiltonian for many non-interacting electrons by comparing with the single-particle case. In this section, we will dominantly work with creation and annihilatin operators, such that it is useful to step back for a moment and to define the field operators more formally, compare Ref. [3]. Let $|\alpha\rangle$ denote an (electronic) single-particle state with quantum number α. That means, $\alpha \hat{=} (\ell \boldsymbol{k} \sigma)$ is in general some multi-index containing the band index ℓ, wavevector $\boldsymbol{k}$ and electron spin σ. Then, the corresponding wave function at position $\boldsymbol{r}$ is defined by

$$\phi_\alpha(\boldsymbol{r}) = \langle \boldsymbol{r} | \alpha \rangle \,. \tag{3.148}$$

We would like to find representations of single-particle operators

$$A = \sum_{i=1}^{N_e} a(\boldsymbol{r_i})\,, \tag{3.149}$$

which are additively composed from electronic single-particle contributions $a(\boldsymbol{r_i})$. For example, the single-particle contribution of our Hamiltonian (3.146) would be given by $a(\boldsymbol{r_i}) = \frac{\boldsymbol{p_i}^2}{2m} + V(\boldsymbol{r_i})$. Although single-particle operators contain no direct interaction between the electrons, the dimension of the Hilbert space is different. To represent general single particle operators, we label the single-particle basis for the i-th electron at position $\boldsymbol{r_i}$ by the state $|\alpha^i\rangle$. Then, we can insert identities $\sum_\alpha |\alpha^i\rangle \langle\alpha^i| = \mathbf{1}$ (on the remaining Hilbert space, the operators $|\alpha^i\rangle\langle\alpha^i|$ act like the identity) to obtain

$$\begin{aligned} A &= \sum_{i=1}^{N_e} \sum_{\alpha\beta} \langle\alpha^i| \, a(\boldsymbol{r_i}) \, |\beta^i\rangle \, |\alpha^i\rangle \langle\beta^i| \\ &= \sum_{\alpha\beta} a_{\alpha\beta} c_\alpha^\dagger c_\beta \,, \qquad c_\alpha^\dagger c_\beta = \sum_{i=1}^{N_e} |\alpha^i\rangle \langle\beta^i| \,. \end{aligned} \tag{3.150}$$

Here, we have used that the matrix element does not depend on the index i,

$$\begin{aligned} a_{\alpha\beta} &= \langle\alpha^i| \, a(\boldsymbol{r_i}) \, |\beta^i\rangle = \int d^3r_i d^3r_i' \, \langle\alpha^i|\boldsymbol{r_i}\rangle \langle\boldsymbol{r_i}| \, a(\boldsymbol{r_i}) \, |\boldsymbol{r_i'}\rangle \langle\boldsymbol{r_i'}|\beta^i\rangle \\ &= \int d^3r_i \phi_\alpha^*(\boldsymbol{r_i}) a(\boldsymbol{r_i}) \phi_\beta(\boldsymbol{r_i}) = \int d^3r \phi_\alpha^*(\boldsymbol{r}) a(\boldsymbol{r}) \phi_\beta(\boldsymbol{r})\,, \end{aligned} \tag{3.151}$$

since the electrons are indistinguishable. This shows that the most general particle-number-preserving electronic single-particle operators will be given by quadratic fermionic operators, where the numbers of creation and annihilation operators is balanced.

The same argument can be applied to two-particle operators, which can be decomposed into terms acting only on pairs of particles

$$B = \frac{1}{2} \sum_{i \neq j}^{N_e} b(\boldsymbol{r_i}, \boldsymbol{r_j})\,. \tag{3.152}$$

One example of such a two-particle operator is the Coulomb interaction term $b(\boldsymbol{r_i}, \boldsymbol{r_j}) = u(\boldsymbol{r_i} - \boldsymbol{r_j})$ in Eq. (3.146). Now, we insert on both sides identities $\mathbf{1} = \sum_\alpha |\alpha^i\rangle\langle\alpha^i|$ and $\mathbf{1} = \sum_\beta |\beta^j\rangle\langle\beta^j|$ to obtain

$$B = \frac{1}{2} \sum_{i \neq j}^{N_e} \sum_{\alpha\beta\gamma\delta} \langle\alpha^i| \langle\beta^j| \, b(\boldsymbol{r_i}, \boldsymbol{r_j}) \, |\gamma^j\rangle |\delta^i\rangle \, |\alpha^i\rangle |\beta^j\rangle \langle\gamma^j| \langle\delta^i| \,. \tag{3.153}$$

Here, we just note that expressions like $\langle\alpha^i|\,|\beta^j\rangle$ must not be further simplified as $i \neq j$ and the operators act on different Hilbert spaces. Again, the matrix element does not depend on the indices i and j

$$\begin{aligned} b_{\alpha\beta\gamma\delta} &= \langle\alpha^i|\,\langle\beta^j|\, b(\boldsymbol{r_i},\boldsymbol{r_j})\,|\gamma^j\rangle\,|\delta^i\rangle = \int d^3r_i \int d^3r_j \phi^*_\alpha(\boldsymbol{r_i})\phi_\delta(\boldsymbol{r_i})\phi^*_\beta(\boldsymbol{r_j})\phi_\gamma(\boldsymbol{r_j}) b(\boldsymbol{r_i},\boldsymbol{r_j}) \\ &= \int d^3r \int d^3r' \phi^*_\alpha(\boldsymbol{r})\phi_\delta(\boldsymbol{r})\phi^*_\beta(\boldsymbol{r'})\phi_\gamma(\boldsymbol{r'}) b(\boldsymbol{r},\boldsymbol{r'})\,. \end{aligned} \tag{3.154}$$

This allows us to represent general particle-number conserving two-body interactions with quartic fermionic operators

$$B = \frac{1}{2}\sum_{\alpha\beta\gamma\delta} b_{\alpha\beta\gamma\delta} c^\dagger_\alpha c^\dagger_\beta c_\gamma c_\delta\,, \qquad c^\dagger_\alpha c^\dagger_\beta c_\gamma c_\delta = \sum_{i\neq j}^{N_e} |\alpha^i\rangle\,|\beta^j\rangle\,\langle\gamma^j|\,\langle\delta^i|\;, \tag{3.155}$$

where the constraint is that the number of creation and annihilation operators must be balanced.

A perhaps more compact way to derive these relations uses the wave functions $\phi_\alpha(\boldsymbol{r})$ and the fermionic operators c_α to define **field operators** for particles at position $\boldsymbol{r}$

$$\Phi(\boldsymbol{r}) = \sum_\alpha \phi_\alpha(\boldsymbol{r}) c_\alpha\,, \qquad \Phi^\dagger(\boldsymbol{r}) = \sum_\alpha \phi^*_\alpha(\boldsymbol{r}) c^\dagger_\alpha\,. \tag{3.156}$$

Since the c_α and $c^\dagger_\alpha$ are fermionic annihilation and creation operators, the field operators obey the anticommutation relations

$$\{\Phi(\boldsymbol{r}),\Phi(\boldsymbol{r'})\} = 0\,, \qquad \left\{\Phi(\boldsymbol{r}),\Phi^\dagger(\boldsymbol{r'})\right\} = \delta(\boldsymbol{r}-\boldsymbol{r'})\,, \tag{3.157}$$

which follows from the completeness relation of the wave functions $\sum_\alpha \phi^*_\alpha(\boldsymbol{r})\phi_\alpha(\boldsymbol{r'}) = \delta(\boldsymbol{r}-\boldsymbol{r'})$. These field operators allow for the convenient representation of single-particle and two-particle operators via

$$\begin{aligned} A &= \int d^3r \Phi^\dagger(\boldsymbol{r}) a(\boldsymbol{r}) \Phi(\boldsymbol{r})\,, \\ B &= \frac{1}{2}\int d^3r \int d^3r' \Phi^\dagger(\boldsymbol{r})\Phi^\dagger(\boldsymbol{r'}) b(\boldsymbol{r},\boldsymbol{r'}) \Phi(\boldsymbol{r'})\Phi(\boldsymbol{r})\,. \end{aligned} \tag{3.158}$$

Inserting the definition of the field operators, we recover our previous representations.

3.2.2 Important interacting models

The most general Hamiltonian (3.146) can therefore be written with balanced quadratic and quartic fermionic operators. However, we still have the freedom e.g. to diagonalize the free single-particle part of the Hamiltonian as we did for non-interacting electrons. Furthermore, the normal Coulomb interactions will generally not flip the electronic spin, such that not all matrix elements need to be considered.

Homogeneous electron gas

In this model, we just consider interacting electrons, i.e., we neglect the potential of the ions completely $V(\boldsymbol{r}) = 0$ and just consider the Coulomb interaction between the electrons. With a plane-wave ansatz for the wave function

$$\phi_{\boldsymbol{k}\sigma}(\boldsymbol{r})\,|\sigma\rangle = \frac{e^{+\mathrm{i}\boldsymbol{kr}}}{\sqrt{V}}\,|\sigma\rangle\;, \tag{3.159}$$

where V denotes the volume, the free Hamiltonian just yields the well-known quadratic dispersion relation. The free Hamiltonian becomes

$$\begin{aligned} H_0 &= \int d^3r \Phi^\dagger(\boldsymbol{r}) \left(-\frac{\hbar^2\nabla^2}{2m}\right) \Phi(\boldsymbol{r}) \\ &= \sum_{\boldsymbol{k}\boldsymbol{q},\sigma} \int d^3r \frac{1}{V} e^{-\mathrm{i}\boldsymbol{k}\boldsymbol{r}} \left(\frac{\hbar^2\boldsymbol{q}^2}{2m}\right) e^{+\mathrm{i}\boldsymbol{q}\boldsymbol{r}} c^\dagger_{\boldsymbol{k}\sigma} c_{\boldsymbol{q}\sigma} = \sum_{\boldsymbol{k}} \sum_{\sigma} \frac{\hbar^2\boldsymbol{k}^2}{2m} c^\dagger_{\boldsymbol{k}\sigma} c_{\boldsymbol{k}\sigma} \,. \end{aligned} \tag{3.160}$$

Furthermore, we can also compute the matrix element of the interaction via

$$\begin{aligned} H_1 &= \frac{1}{2} \int d^3r \int d^3r' \Phi^\dagger(\boldsymbol{r}) \Phi^\dagger(\boldsymbol{r'}) \frac{e^2}{|\boldsymbol{r}-\boldsymbol{r'}|} \Phi(\boldsymbol{r'}) \Phi(\boldsymbol{r}) \\ &= \frac{1}{2} \sum_{\sigma\sigma'} \sum_{\boldsymbol{k}\boldsymbol{q}\boldsymbol{k'}\boldsymbol{q'}} \int d^3r \int d^3r' \phi^*_{\boldsymbol{k}\sigma}(\boldsymbol{r}) \phi^*_{\boldsymbol{q}\sigma'}(\boldsymbol{r'}) \frac{e^2}{|\boldsymbol{r}-\boldsymbol{r'}|} \phi_{\boldsymbol{q'}\sigma'}(\boldsymbol{r'}) \phi_{\boldsymbol{k'}\sigma}(\boldsymbol{r}) c^\dagger_{\boldsymbol{k}\sigma} c^\dagger_{\boldsymbol{q}\sigma'} c_{\boldsymbol{q'}\sigma'} c_{\boldsymbol{k'}\sigma} \\ &= \frac{1}{2} \sum_{\sigma\sigma'} \sum_{\boldsymbol{k}\boldsymbol{q}\boldsymbol{k'}\boldsymbol{q'}} I_{\boldsymbol{k}\boldsymbol{q}\boldsymbol{k'}\boldsymbol{q'}} c^\dagger_{\boldsymbol{k}\sigma} c^\dagger_{\boldsymbol{q}\sigma'} c_{\boldsymbol{q'}\sigma'} c_{\boldsymbol{k'}\sigma} \end{aligned} \tag{3.161}$$

Here, we have already used that the interaction does not induce spin flips. The remaining integral can now be explicitly computed as

$$\begin{aligned} I_{\boldsymbol{k}\boldsymbol{q}\boldsymbol{k'}\boldsymbol{q'}} &= \frac{1}{V^2} \int d^3r \int d^3r' e^{-\mathrm{i}\boldsymbol{k}\boldsymbol{r}} e^{-\mathrm{i}\boldsymbol{q}\boldsymbol{r'}} \frac{e^2}{|\boldsymbol{r}-\boldsymbol{r'}|} e^{+\mathrm{i}\boldsymbol{q'}\boldsymbol{r'}} e^{+\mathrm{i}\boldsymbol{k'}\boldsymbol{r}} \\ &= \frac{1}{V^2} \int d^3r \int d^3r'' e^{-\mathrm{i}\boldsymbol{k}\boldsymbol{r}} e^{-\mathrm{i}\boldsymbol{q}(\boldsymbol{r}-\boldsymbol{r''})} \frac{e^2}{|\boldsymbol{r''}|} e^{+\mathrm{i}\boldsymbol{q'}(\boldsymbol{r}-\boldsymbol{r''})} e^{+\mathrm{i}\boldsymbol{k'}\boldsymbol{r}} \\ &= \left[\frac{1}{V} \int d^3r e^{+\mathrm{i}\left(\boldsymbol{k'}+\boldsymbol{q'}-\boldsymbol{k}-\boldsymbol{q}\right)\boldsymbol{r}}\right] \left[\frac{1}{V} \int d^3r'' \frac{e^2}{|\boldsymbol{r''}|} e^{+\mathrm{i}(\boldsymbol{q}-\boldsymbol{q'})\boldsymbol{r''}}\right] . \end{aligned} \tag{3.162}$$

While the first factor just yields a δ-function that conserves the total momentum (the Coulomb interaction only implies elastic scattering events), the second term can also be calculated exactly in spherical coordinates

$$\begin{aligned} \int d^3r \frac{1}{|\boldsymbol{r}|} e^{+\mathrm{i}\boldsymbol{q}\boldsymbol{r}} &= 2\pi \int_0^\infty dr \int_{-1}^{+1} dx e^{+\mathrm{i}qrx} r = \lim_{\delta\to0} 2\pi \int_0^\infty dr \int_{-1}^{+1} dx e^{+\mathrm{i}qrx-\delta r} r \\ &= \lim_{\delta\to0} 2\pi \int_0^\infty dr \frac{\mathrm{i}}{q} e^{-\delta r} \left[e^{-\mathrm{i}qr} - e^{+\mathrm{i}qr}\right] \\ &= \lim_{\delta\to0} \frac{2\pi\mathrm{i}}{q} \left(-\frac{2\mathrm{i}q}{q^2+\delta^2}\right) = \frac{4\pi}{q^2} \,. \end{aligned} \tag{3.163}$$

Here, we have used the usual substitution $x = \cos(\theta)$ and chose the angle θ between $\boldsymbol{r}$ and $\boldsymbol{q}$ via $\boldsymbol{r}\boldsymbol{q} = rq\cos(\theta)$. Accordingly, the integral becomes

$$I_{\boldsymbol{k}\boldsymbol{q}\boldsymbol{k'}\boldsymbol{q'}} = \delta_{\boldsymbol{k}+\boldsymbol{q},\boldsymbol{k'}+\boldsymbol{q'}} \frac{4\pi e^2}{V|\boldsymbol{q}-\boldsymbol{q'}|^2} \,, \tag{3.164}$$

which eventually yields for the total Hamiltonian of the homogeneous electron gas

$$\begin{aligned} H &= \sum_{\boldsymbol{k}} \sum_{\sigma} \frac{\hbar^2\boldsymbol{k}^2}{2m} c^\dagger_{\boldsymbol{k}\sigma} c_{\boldsymbol{k}\sigma} + \frac{1}{2} \sum_{\sigma\sigma'} \sum_{\boldsymbol{k}\boldsymbol{q}\boldsymbol{k'}\boldsymbol{q'}} \delta_{\boldsymbol{k}+\boldsymbol{q},\boldsymbol{k'}+\boldsymbol{q'}} \frac{4\pi e^2}{V|\boldsymbol{q}-\boldsymbol{q'}|^2} c^\dagger_{\boldsymbol{k}\sigma} c^\dagger_{\boldsymbol{q}\sigma'} c_{\boldsymbol{q'}\sigma'} c_{\boldsymbol{k'}\sigma} \\ &= \sum_{\boldsymbol{k}} \sum_{\sigma} \frac{\hbar^2\boldsymbol{k}^2}{2m} c^\dagger_{\boldsymbol{k}\sigma} c_{\boldsymbol{k}\sigma} + \frac{1}{2} \sum_{\sigma\sigma'} \sum_{\bar{\boldsymbol{k}}\bar{\boldsymbol{k}}'\bar{\boldsymbol{q}}} \frac{4\pi e^2}{V\bar{q}^2} c^\dagger_{\bar{\boldsymbol{k}}-\bar{\boldsymbol{q}},\sigma} c^\dagger_{\bar{\boldsymbol{k}}'+\bar{\boldsymbol{q}},\sigma'} c_{\bar{\boldsymbol{k}}',\sigma'} c_{\bar{\boldsymbol{k}},\sigma} \,. \end{aligned} \tag{3.165}$$

In the last line, we have only renamed some terms. The conventional interpretation of the last term are two incoming electrons at momenta $\bar{\boldsymbol{k}}$ and $\bar{\boldsymbol{k}}'$ that exchange momentum $2\bar{\boldsymbol{q}}$, such that after the scattering event, they have momenta $\bar{\boldsymbol{k}} + \bar{\boldsymbol{q}}$ and $\bar{\boldsymbol{k}}' - \bar{\boldsymbol{q}}$. Since we assumed a bare Coulomb potential, the contribution without momentum transfer $\bar{\boldsymbol{q}} = 0$ actually diverges. This artifact can be cured by considering a screened electron-electron interaction. If instead we used a screened potential – for a Yukawa type potential this would correspond to keeping finite δ in the calculation of the above two-body integral – all matrix elements would remain finite.

The Hubbard model

We are not forced to diagonalize the free Hamiltonian. If we do not do this, the free Hamiltonian has hopping terms and on-site energies. The simplest model taking some interactions and tunneling of electrons into account is the Hubbard [3] model, originally suggested to explain band magnetism. It has a hopping term and an on-site Coulomb interaction

$$H = t \sum_{\sigma} \sum_{<\boldsymbol{R},\boldsymbol{R}'>} c^{\dagger}_{\boldsymbol{R},\sigma} c_{\boldsymbol{R}',\sigma} + U \sum_{\sigma\sigma'} \sum_{\boldsymbol{R}} c^{\dagger}_{\boldsymbol{R},\sigma} c^{\dagger}_{\boldsymbol{R},\sigma'} c_{\boldsymbol{R},\sigma'} c_{\boldsymbol{R},\sigma} \,. \tag{3.166}$$

The notation $< \boldsymbol{R}, \boldsymbol{R}' >$ denotes next neighbours on a lattice. With just two parameters t and U, the model exhibits rich physics. Depending on the parameters and the filling ratio of the model (number of electrons versus number of sites), it can model metal and insulator behaviour and the corresponding transition between them. The Hubbard model has the exactly solvable limits $U = 0$ (non-interacting electrons, hopping phase) and $t = 0$ (insulating phase). For small and finite number of lattice sites N, it can be diagonalized exactly with exponential effort: The dimension of the Hilbert space is $2 \cdot 2^N$ if the number of electrons is not specified, and still as $2\frac{N!}{N_e!(N-N_e)!}$ for N_e electrons distributed over N sites. This shows that exact numerical diagonalizations of the model are numerically demanding and will be restricted to small systems. One very important feature of the Hubbard model is that can model band magnetism just from the ingredients of electronic spin and strong Coulomb interaction, which we will revisit later.

3.2.3 Hartree-Fock approximation

The basis of all our considerations is the grand-canonical thermal equilibrium state

$$\rho_{gc} = \frac{e^{-\beta(H-\mu N)}}{\mathrm{Tr}\left\{e^{-\beta(H-\mu N)}\right\}} \,, \tag{3.167}$$

where H and N are Hamiltonian and particle number operator, and β and μ are inverse temperature and chemical potential. From statistical physics we know that to compute mean values of operators, it is helpful to compute only the normalization factor, i.e., the grand-canonical partition function

$$Z_{gc} = \mathrm{Tr}\left\{e^{-\beta(H-\mu N)}\right\} \,. \tag{3.168}$$

For example, we can compute the mean particle number from derivatives with respect to the chemical potential

$$\langle N \rangle = \mathrm{Tr}\left\{N\rho_{gc}\right\} = \beta^{-1}\partial_{\mu} \ln Z_{gc} \,. \tag{3.169}$$

From this, we can also compute the mean energy

$$\langle H \rangle = \mathrm{Tr}\left\{H\rho_{gc}\right\} = \left[\mu\beta^{-1}\partial_{\mu} - \partial_{\beta}\right] \ln Z_{gc} \,, \tag{3.170}$$

---

[3] J. Hubbard (1931–1980) was a british physicist.

where we already used this formula for $\mu = 0$ in the calculation of the specific heat of phonons, compare Sec. 2.4.6. However, such relations are even more powerful. For example, when the Hamiltonian depends on a parameter λ via $H = H_0 + \lambda H_1$, where both H_0 and H_1 are operators, this parameter dependence will transfer to the partition function. Then, we get

$$\begin{aligned}
-\beta^{-1}\partial_\lambda \ln Z_{gc} &= \frac{-\beta^{-1}}{Z_{gc}} \mathrm{Tr}\left\{\partial_\lambda e^{-\beta(H_0+\lambda H_1-\mu N)}\right\} = \frac{1}{Z_{gc}} \sum_{n=0}^\infty \frac{(-\beta)^{n-1}}{n!} \mathrm{Tr}\left\{\partial_\lambda \left[H_0+\lambda H_1-\mu N\right]^n\right\} \\
&= \frac{1}{Z_{gc}} \sum_{n=0}^\infty \frac{(-\beta)^{n-1}}{n!} \mathrm{Tr}\left\{\sum_{i=1}^n \left[H_0+\lambda H_1-\mu N\right]^{i-1} H_1 \left[H_0+\lambda H_1-\mu N\right]^{n-i}\right\} \\
&= \frac{1}{Z_{gc}} \sum_{n=1}^\infty \frac{(-\beta)^{n-1}}{(n-1)!} \mathrm{Tr}\left\{\left[H_0+\lambda H_1-\mu N\right]^{n-1} H_1\right\} = \frac{1}{Z_{gc}} \mathrm{Tr}\left\{e^{-\beta(H-\mu N)} H_1\right\} \\
&= \left\langle H_1 \right\rangle \,, \qquad (3.171)
\end{aligned}$$

where we have used that the trace is invariant under cyclic permutations of its arguments. In summary, the partition function, or derived quantities such as the grand-canonical potential are very useful to determine mean values of operators.

Box 11 (grand-canonical potential) *The grand-canonical potential is given from the logarithm of the grand-canonical partition function via*

$$\Phi_{gc} = -k_B T \ln Z_{gc} = -k_B T \ln \mathrm{Tr}\left\{e^{-\beta(H-\mu N)}\right\} \,. \qquad (3.172)$$

The problem is that the partition function can be easily calculated for non-interacting models – where the Hamiltonian can be brought in the form of independent modes. For interacting models it is in general a difficult problem, which in reality means impossible. The basic idea is now to find an approximate non-interacting Hamiltonian

$$H_{\text{eff}} = \sum_k \chi_k c_k^\dagger c_k \,, \qquad (3.173)$$

where the parameters $\chi_k \in \mathbb{R}$ have to be determined such that the resulting grand-canonical potential with respect to the effective Hamiltonian is close to the exact grand-canonical potential (and therefore all derived quantities should also be close to the true values). In order to quantify what is meant by the term "close to", we introduce the quantum relative entropy.

Box 12 (quantum relative entropy) *The quantum relative entropy between two density matrices ρ and σ is given by*

$$D(\rho||\sigma) = \mathrm{Tr}\left\{\rho\left[\ln\rho - \ln\sigma\right]\right\} \geq 0 \,. \qquad (3.174)$$

Obviously, the relative entropy vanishes when the two density matrices are equal $D(\rho||\rho) = 0$. However, it is not symmetric, such that it cannot be considered a distance. We can also see that it is positive by using the spectral decompositions of both density matrices

$$\begin{aligned}
\rho &= \sum_\ell \rho_\ell \left|\ell\right\rangle \left\langle\ell\right| \,, \qquad 0 \leq \rho_\ell \leq 1 \,, \qquad \sum_\ell \rho_\ell = 1 \,, \\
\sigma &= \sum_\alpha \sigma_\alpha \left|\alpha\right\rangle \left\langle\alpha\right| \,, \qquad 0 \leq \sigma_\alpha \leq 1 \,, \qquad \sum_\alpha \sigma_\alpha = 1 \,, \qquad (3.175)
\end{aligned}$$

which yields

$$\begin{aligned}
-D(\rho||\sigma) &= \sum_\ell \rho_\ell \left[\langle\ell| \ln\sigma |\ell\rangle - \ln\rho_\ell\right] = \sum_\ell \rho_\ell \left[\sum_\alpha \ln(\sigma_\alpha) |\langle\ell|\alpha\rangle|^2 - \ln\rho_\ell\right] \\
&= \sum_\ell \rho_\ell \left[\sum_\alpha \ln(\sigma_\alpha) |\langle\ell|\alpha\rangle|^2 - \ln(\rho_\ell) \sum_\alpha |\langle\ell|\alpha\rangle|^2\right] = \sum_\ell \sum_\alpha \rho_\ell |\langle\ell|\alpha\rangle|^2 \ln\frac{\sigma_\alpha}{\rho_\ell} \\
&\le \sum_\ell \sum_\alpha \rho_\ell |\langle\ell|\alpha\rangle|^2 \left[\frac{\sigma_\alpha}{\rho_\ell} - 1\right] = \sum_\alpha \sigma_\alpha - \sum_\ell \rho_\ell = 0\,, \qquad (3.176)
\end{aligned}$$

where we have used $\ln(x) \le x - 1$, such that accordingly $D(\rho||\sigma) \ge 0$. Specifically, the relative entropy between an arbitrary density matrix ρ and the grand-canonical one ρ_{gc} becomes

$$D(\rho||\rho_{gc}) = \text{Tr}\left\{\rho\ln\rho\right\} - \text{Tr}\left\{\rho \ln\frac{e^{-\beta(H-\mu N)}}{Z_{gc}}\right\} = \text{Tr}\left\{\rho\ln\rho\right\} + \text{Tr}\left\{\rho\beta(H-\mu N)\right\} + \ln Z_{gc}\,. \qquad (3.177)$$

We now define the functional on an arbitrary density matrix ρ

$$\Phi[\rho] \equiv \text{Tr}\left\{\rho(H-\mu N) + k_B T \rho\ln\rho\right\}\;. \qquad (3.178)$$

From Eq. (3.172) and Eq. (3.177) we see that we can express this functional by a relative entropy to the thermal state

$$\Phi[\rho] = \Phi[\rho_{gc}] + k_B T D(\rho||\rho_{gc}) \ge \Phi[\rho_{gc}]\,, \qquad (3.179)$$

and accordingly, it assumes its minimal value when ρ is the grand-canonical equilibrium state.

Specifically applied to our effective Hamiltonian, we can define an effective density matrix and effective grand canonical potential (simple to compute)

$$\rho_{\text{eff}} = \frac{e^{-\beta(H_{\text{eff}}-\mu N)}}{Z_{\text{eff}}}\,, \qquad \Phi_{\text{eff}} = -k_B T \ln Z_{\text{eff}} = -k_B T \ln \text{Tr}\left\{e^{-\beta(H_{\text{eff}}-\mu N)}\right\}\;. \qquad (3.180)$$

Inserting this in the functional, we get the relation

$$\begin{aligned}
\Phi[\rho_{\text{eff}}] &= \text{Tr}\left\{\rho_{\text{eff}}\left[(H-\mu N) + k_B T\left(-\beta(H_{\text{eff}}-\mu N) - \ln Z_{\text{eff}}\right)\right]\right\} \\
&= \text{Tr}\left\{(H - H_{\text{eff}})\rho_{\text{eff}}\right\} - k_B T \ln Z_{\text{eff}} \ge \Phi[\rho_{gc}]\,. \qquad (3.181)
\end{aligned}$$

This relation now tells us that by minimizing $\text{Tr}\left\{(H-H_{\text{eff}})\rho_{\text{eff}}\right\} - k_B T \ln Z_{\text{eff}}$ with respect to the free parameters in the effective Hamiltonian (3.173), we get that the effective grand potential is close to the true one (at least with respect to single-particle operator representations of the Hamiltonian). The advantage is now that we can explicitly minimize the grand-canonical potential as all parameters are directly computable.

As an example, we can consider the Hamiltonian

$$H = \sum_k \epsilon_k c_k^\dagger c_k + \frac{1}{2}\sum_{kk'qq'} u_{kk'qq'} c_k^\dagger c_{k'}^\dagger c_{q'} c_q\,, \qquad (3.182)$$

with simply describes electronic modes with energies ϵ_k and interaction term coefficients $u_{kk'qq'}$ (we neglect the spin for the moment). We note that this may also include tunneling, since by diagonalizing the tunneling Hamiltonian we would obtain a diagonal representaion of the quadratic part of the Hamiltonian. Furthermore, the interaction must be invariant when incoming and outgoing particles are exchanged

$$u_{kk'qq'} = u_{k'kq'q} \,. \tag{3.183}$$

The effective density matrix becomes

$$\rho_{\text{eff}} = \frac{e^{-\beta \sum_k (\chi_k - \mu) c_k^\dagger c_k}}{Z_{\text{eff}}} \,. \tag{3.184}$$

Insertion into the functional, which should be minimized, yields

$$\begin{aligned}\Phi[\rho_{\text{eff}}] &= \operatorname{Tr}\left\{(H - H_{\text{eff}})\rho_{\text{eff}}\right\} - k_B T \ln Z_{\text{eff}} \\ &= -k_B T \ln Z_{\text{eff}} + \sum_k (\epsilon_k - \chi_k) \left\langle c_k^\dagger c_k \right\rangle_{\text{eff}} + \frac{1}{2} \sum_{kk'qq'} u_{kk'qq'} \left\langle c_k^\dagger c_{k'}^\dagger c_{q'} c_q \right\rangle_{\text{eff}} \,.\end{aligned} \tag{3.185}$$

For a non-interacting model, we can explicitly determine the expectation values

$$\left\langle c_k^\dagger c_k \right\rangle_{\text{eff}} = \frac{e^{-\beta(\chi_k - \mu)}}{1 + e^{-\beta(\chi_k - \mu)}} = \frac{1}{e^{\beta(\chi_k - \mu)} + 1} = f(\chi_k) \tag{3.186}$$

in terms of the Fermi function $f(\omega)$. In general contexts, we can think of $f(\chi_k)$ as a general function describing the expectation value above. To treat the quartic term, we use

$$\begin{aligned}\left\langle c_k^\dagger c_{k'}^\dagger c_{q'} c_q \right\rangle_{\text{eff}} &= (1 - \delta_{qq'})(1 - \delta_{kk'}) \left[\delta_{kq}\delta_{k'q'} \left\langle c_k^\dagger c_q \right\rangle_{\text{eff}} \left\langle c_{k'}^\dagger c_{q'} \right\rangle_{\text{eff}} - \delta_{kq'}\delta_{k'q} \left\langle c_k^\dagger c_{q'} \right\rangle_{\text{eff}} \left\langle c_{k'}^\dagger c_q \right\rangle_{\text{eff}}\right] \\ &= \left[\delta_{kq}\delta_{k'q'} \left\langle c_k^\dagger c_q \right\rangle_{\text{eff}} \left\langle c_{k'}^\dagger c_{q'} \right\rangle_{\text{eff}} - \delta_{kq'}\delta_{k'q} \left\langle c_k^\dagger c_{q'} \right\rangle_{\text{eff}} \left\langle c_{k'}^\dagger c_q \right\rangle_{\text{eff}}\right] \\ &= \delta_{kq}\delta_{k'q'} f(\chi_k) f(\chi_{k'}) - \delta_{kq'}\delta_{k'q} f(\chi_k) f(\chi_{k'}) \,.\end{aligned} \tag{3.187}$$

We insert this in the grand-canonical functional

$$\Phi[\rho_{\text{eff}}] = -k_B T \ln Z_{\text{eff}} + \sum_k (\epsilon_k - \chi_k) f(\chi_k) + \frac{1}{2} \sum_{kk'} \left[u_{kk'kk'} - u_{kk'k'k}\right] f(\chi_k) f(\chi_{k'}) \,. \tag{3.188}$$

We still want to find the minimum of this functional with respect to the unknown parameters χ_k. For this, we note that

$$-k_B T \partial_{\chi_q} \ln Z_{\text{eff}} = \left\langle c_q^\dagger c_q \right\rangle_{\text{eff}} = f(\chi_q) \,, \tag{3.189}$$

which follows from Eq. (3.171) or can be checked directly. Accordingly, the minimization equations become

$$\begin{aligned}0 &= f(\chi_q) - f(\chi_q) + (\epsilon_q - \chi_q) f'(\chi_q) \\ &\quad + \frac{1}{2} \sum_{k'} \left[u_{qk'qk'} - u_{qk'k'q}\right] f'(\chi_q) f(\chi_{k'}) + \frac{1}{2} \sum_k \left[u_{kqkq} - u_{kqqk}\right] f(\chi_k) f'(\chi_q) \\ &= f'(\chi_q) \left[\epsilon_q - \chi_q + \frac{1}{2} \sum_k \left(u_{qkqk} - u_{qkkq} + u_{kqkq} - u_{kqqk}\right) f(\chi_k)\right] \\ &= f'(\chi_q) \left[\epsilon_q - \chi_q + \sum_k \left(u_{qkqk} - u_{qkkq}\right) f(\chi_k)\right]\end{aligned} \tag{3.190}$$

Here, we have used the symmetry constraints on the interaction to simplify the last term. The term in square brackets should vanish, which yields a self-consistent solution for the best possible parameters

$$\chi_q^* = \epsilon_q + \sum_k \left(u_{qkqk} - u_{qkkq}\right) f(\chi_k^*) \,. \tag{3.191}$$

Clearly, for a non-interacting model, we recover $\chi_q^* = \epsilon_q$, but for finite interactions, this non-linear coupled system will in general have to be solved numerically. However, for very high temperatures we could e.g. approximate the Fermi functions by $f(\chi_k) = 1/2 - \beta/4(\chi_k - \mu) + \ldots$ to linearize the system. In general, the effective Hamiltonian becomes

$$H_{\text{eff}} = \sum_k \left[\epsilon_k + \sum_q \left(u_{kqkq} - u_{kqqk}\right) f(\chi_q^*)\right] c_k^\dagger c_k \,. \tag{3.192}$$

This corresponds to the Hamiltonian in Hartree [4]-Fock approximation. Traditional derivations use a Slater determinant as an ansatz for the full wave function and then derive an effective Schrödinger equation for interacting systems. The two terms u_{kqkq} and u_{kqqk} correspond to the Hartree-contribution and the Fock- (or exchange) contribution, respectively.

A shortcut recipe to obtain the general form of the Hamiltonian in Hartree-Fock approximation is the replacement

$$\begin{aligned} c_k^\dagger c_{k'}^\dagger c_{q'} c_q \approx & - \left\langle c_k^\dagger c_{q'} \right\rangle_{\text{eff}} c_{k'}^\dagger c_q + \left\langle c_k^\dagger c_q \right\rangle_{\text{eff}} c_{k'}^\dagger c_{q'} \\ & + \left\langle c_{k'}^\dagger c_{q'} \right\rangle_{\text{eff}} c_k^\dagger c_q - \left\langle c_{k'}^\dagger c_q \right\rangle_{\text{eff}} c_k^\dagger c_{q'} \,, \end{aligned} \tag{3.193}$$

where we consider the expectation value of one creation and one annihilation operator, and where the sign in front is determined by the fermionic anticommutation relations. Inserting this into the original Hamiltonian (3.182), and demanding the resulting effective Hamiltonian to be diagonal, i.e., of the form $H_{\text{eff}} = \sum_k \chi_k c_k^\dagger c_k$ (which yields an additional Kronecker-delta), we recover the mean-field Hamiltonian (3.192)(exercise). In general, such approximations where higher-order operators are replaced by expectation values of few-body operators are called **mean-field** approximations (”Molekularfeldnäherung”).

3.2.4 Example: Double Quantum Dot

As an extremely small-scale example, we consider a double quantum dot under the assumption that only one spin species is present. The total Hamiltonian reads

$$H = \epsilon(d_L^\dagger d_L + d_R^\dagger d_R) + T(d_L^\dagger d_R + d_R^\dagger d_L) + U d_L^\dagger d_L d_R^\dagger d_R \,, \tag{3.194}$$

where ϵ is the on-site energy of the dots and T is a next-neighbor hopping amplitude and $U > 0$ is a Coulomb interaction. We have chosen T as real (a possible phase can be absorbed in the operators). Note also that the on-site energies can be chosen different for both dots, which makes all transformations technically more complex.

To bring it into the form that we used to derive the Hartree-Fock approximation, we have to diagonalize the free (quadratic) part of the Hamiltonian first

$$\begin{aligned} H_0 &= (d_L^\dagger, d_R^\dagger) \begin{pmatrix} \epsilon & T \\ T & \epsilon \end{pmatrix} \begin{pmatrix} d_L \\ d_R \end{pmatrix} \\ &= (d_L^\dagger, d_R^\dagger) V^\dagger V \begin{pmatrix} \epsilon & T \\ T & \epsilon \end{pmatrix} V^\dagger V \begin{pmatrix} d_L \\ d_R \end{pmatrix} \,. \end{aligned} \tag{3.195}$$

---

[4] D. R. Hartree (1897–1958) was a british mathematician and physicist.

Here, the special choice

$$V = \frac{1}{\sqrt{2}} \begin{pmatrix} 1 & -1 \\ 1 & 1 \end{pmatrix} \tag{3.196}$$

Diagonalizes the free Hamiltonian

$$H_0 = (c_1^\dagger, c_2^\dagger) \begin{pmatrix} \epsilon - T & 0 \\ 0 & \epsilon + T \end{pmatrix} \begin{pmatrix} c_1 \\ c_2 \end{pmatrix} = (\epsilon - T) c_1^\dagger c_1 + (\epsilon + T) c_2^\dagger c_2 \,. \tag{3.197}$$

New and old operators are connected via

$$\begin{pmatrix} c_1 \\ c_2 \end{pmatrix} = \frac{1}{\sqrt{2}} \begin{pmatrix} 1 & -1 \\ 1 & 1 \end{pmatrix} \begin{pmatrix} d_L \\ d_R \end{pmatrix} , \qquad \begin{pmatrix} d_L \\ d_R \end{pmatrix} = \frac{1}{\sqrt{2}} \begin{pmatrix} 1 & 1 \\ -1 & 1 \end{pmatrix} \begin{pmatrix} c_1 \\ c_2 \end{pmatrix} . \tag{3.198}$$

To represent the interaction in terms of the new operators, we compute (exercise)

$$H_1 = \frac{U}{4} (c_1^\dagger + c_2^\dagger)(c_1 + c_2)(c_1^\dagger - c_2^\dagger)(c_1 - c_2) = \ldots = U c_1^\dagger c_1 c_2^\dagger c_2 \,. \tag{3.199}$$

To arrive at this result, one has to use the fermionic anticommutation relations a few times, which implies relations like

$$c_i c_i^\dagger = 1 - c_i^\dagger c_i \,, \qquad c_i^2 = (c_i^\dagger)^2 = 0 \,, \qquad c_i c_i^\dagger c_i = c_i \,, \qquad c_i^\dagger c_i c_i^\dagger = c_i^\dagger \,. \tag{3.200}$$

Accordingly, expressed with the new operators the Hamiltonian reads

$$H = (\epsilon - T) c_1^\dagger c_1 + (\epsilon + T) c_2^\dagger c_2 + U c_1^\dagger c_1 c_2^\dagger c_2 \,, \tag{3.201}$$

which can be solved exactly. Generically, we get for transformations that do not mix between creation and annihilation operators, that the operator for the total particle number remains the same

$$N = d_L^\dagger d_L + d_R^\dagger d_R = c_1^\dagger c_1 + c_2^\dagger c_2 \,. \tag{3.202}$$

First, we note that the system is small enough such that we can treat it exactly. In the basis $|n_1, n_2\rangle$ ordered with increasing eigenvalues $|0,0\rangle$,$|1,0\rangle$,$|0,1\rangle$, and $|1,1\rangle$, Hamiltonian and particle number operator have the matrix representations

$$H = \begin{pmatrix} 0 & & & \\ & \epsilon - T & & \\ & & \epsilon + T & \\ & & & 2\epsilon + U \end{pmatrix} , \qquad N = \begin{pmatrix} 0 & & & \\ & 1 & & \\ & & 1 & \\ & & & 2 \end{pmatrix} . \tag{3.203}$$

Since they are both diagonal, we can straightforwardly compute the grand-canonical equilibrium state

$$\rho_{gc} = \frac{e^{-\beta(H - \mu N)}}{\operatorname{Tr}\left\{e^{-\beta(H-\mu N)}\right\}} \tag{3.204}$$

and the corresponding partition function

$$Z_{gc} = 1 + e^{-\beta(\epsilon - T - \mu)} + e^{-\beta(\epsilon + T - \mu)} + e^{-\beta(2\epsilon + U - 2\mu)} \,. \tag{3.205}$$

Since we have seen that the particle number can be obtained via $\langle N\rangle = \beta^{-1}\partial_\mu \ln Z_{gc}$, this yields a nonlinear equation linking the chemical potential and the expectation value of the particle number

$$\langle N\rangle = \frac{e^{-\beta(\epsilon-T-\mu)} + e^{-\beta(\epsilon+T-\mu)} + 2e^{-\beta(2\epsilon+U-2\mu)}}{Z_{gc}}\,, \tag{3.206}$$

which can be solved for the chemical potential due to the small dimension of the system (not shown). In particular, one can check that at half-filling, the temperature-independent choice $\mu_1 = \epsilon + \frac{U}{2}$ fixes the particle number to $\langle N\rangle = 1$. For other values of $\langle N\rangle$, the chemical potential μ_N will be temperature-dependent. From the grand-canonical equilibrium state with fixed chemical potential, we can now compute arbitrary observables of the double quantum dot system.

Second, to obtain the Hartree-Fock (mean-field) approximation, we represent the Hamiltonian in our standard form

$$H = (\epsilon - T)c_1^\dagger c_1 + (\epsilon + T)c_2^\dagger c_2 + \frac{U}{2}\left[c_1^\dagger c_2^\dagger c_2 c_1 + c_2^\dagger c_1^\dagger c_1 c_2\right]\,, \tag{3.207}$$

where by comparison with (3.182) we can read off the non-vanishing coefficients $\epsilon_1 = \epsilon - T$, $\epsilon_2 = \epsilon + T$, $u_{1212} = u_{2121} = U$. The single-particle chemical potential is again fixed by the expectation value of the total particle number

$$\langle N\rangle = f(\chi_1^*) + f(\chi_2^*)\,, \tag{3.208}$$

which for $\langle N\rangle = 1$ simply becomes $\mu_1 = 1/2(\chi_1^* + \chi_2^*)$.

From this, we see that we need to solve the equations

$$\begin{aligned}
\chi_1^* &= \epsilon - T + Uf(\chi_2^*) = \epsilon - T + \frac{U}{e^{\beta(\chi_2^*-\mu^*)}+1}\,,\\
\chi_2^* &= \epsilon + T + Uf(\chi_1^*) = \epsilon + T + \frac{U}{e^{\beta(\chi_1^*-\mu^*)}+1}\,,\\
\langle N\rangle &= f(\chi_1^*) + f(\chi_2^*) = \frac{1}{e^{\beta(\chi_1^*-\mu^*)}+1} + \frac{1}{e^{\beta(\chi_2^*-\mu^*)}+1}
\end{aligned} \tag{3.209}$$

self-consistently for the single-particle energies χ_i^* and the chemical potential μ^*. If we instead applied our recipe (3.193), the effective Hamiltonian would read

$$H_{\text{eff}} = (\epsilon - T)c_1^\dagger c_1 + (\epsilon + T)c_2^\dagger c_2 + U\left\langle c_1^\dagger c_1\right\rangle_{\text{eff}} c_2^\dagger c_2 + U\left\langle c_2^\dagger c_2\right\rangle_{\text{eff}} c_1^\dagger c_1\,, \tag{3.210}$$

which leads to precisely the same single-particle equations – provided the self-consistency is respected. The approximation to the grand-canonical density matrix is then given by

$$\rho_{gc} \approx \frac{e^{-\beta[(\chi_1^*-\mu^*)c_1^\dagger c_1 + (\chi_2^*-\mu^*)c_2^\dagger c_2]}}{\operatorname{Tr}\left\{e^{-\beta[(\chi_1^*-\mu^*)c_1^\dagger c_1 + (\chi_2^*-\mu^*)c_2^\dagger c_2]}\right\}}\,. \tag{3.211}$$

It is truly necessary to solve these equations self-consistently, which yields a satisfactory agreement with the exact solution for small values of U and also for extremely large values of U, see Fig. 3.5. For example, inserting just the interaction-free values of the single-particle energies $\epsilon \pm T$ in the Fermi functions, the exact solution is hardly reproduced (dashed orange).

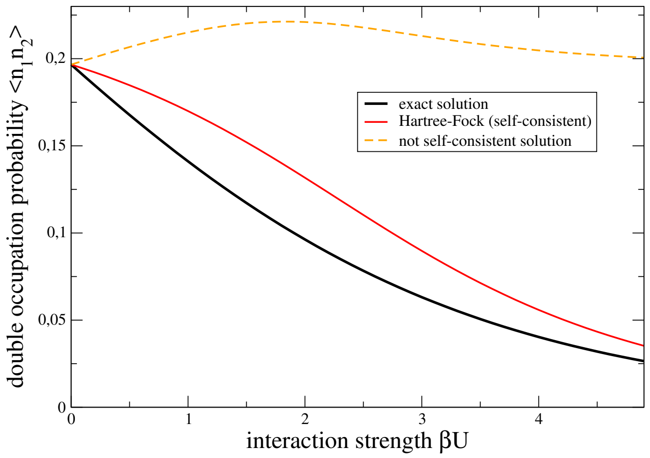

Figure 3.5: Plot of the two-electron-occupation probability $\left\langle c_1^\dagger c_1 c_2^\dagger c_2 \right\rangle$ for the exact solution (solid black, Eq. (3.204)), for the Hartree-Fock approximation (solid red, Eq. (3.211)), and for an inconsistent application of the Hartree-Fock approximation (dashed orange), where in the arguments of the Fermi functions the single-particle energies are replaced by the values at vanishing interaction. Other parameters: $\beta\epsilon = 1$, $\beta T = 2$, $\langle N \rangle = 1$.

3.2.5 Example: Jellium model

To treat the homogeneous electron gas within Hartree-Fock approximation, we add a positive background density $\rho(\boldsymbol{r})$, which in the most idealized limit could be a homogeneous background density $e\rho_0 = \frac{eN_e}{V}$, where e is the electron charge, N_e is the number of electrons and V is the total physical volume. More realistically, this should be a summation of point charges distributed at the ion positions. In first quantization, the Hamiltonian reads

$$H = \sum_{i=1}^{N_e} \frac{\boldsymbol{p_i}^2}{2m} - \sum_{i=1}^{N_e} \int d^3r \frac{e^2 \rho(\boldsymbol{r})}{|\boldsymbol{r_i} - \boldsymbol{r}|} + \frac{1}{2} \sum_{i \neq j = 1}^{N_e} \frac{e^2}{|\boldsymbol{r_i} - \boldsymbol{r_j}|} \,. \tag{3.212}$$

We have already computed the representations of the first (momentum) and the last (electronic repulsion) term in Eq. (3.165). The additional term is a single-particle operator, and we can find its representation in second quantization by using the field operators

$$\begin{aligned}
\Delta H &= -e^2 \int d^3r d^3r' \Phi^\dagger(\boldsymbol{r}) \frac{\rho(\boldsymbol{r'})}{|\boldsymbol{r} - \boldsymbol{r'}|} \Phi(\boldsymbol{r}) \\
&= -e^2 \sum_\sigma \sum_{\boldsymbol{kk'}} \int d^3r d^3r' \frac{1}{V} e^{-\mathrm{i}\boldsymbol{kr}} \frac{\rho(\boldsymbol{r'})}{|\boldsymbol{r} - \boldsymbol{r'}|} e^{+\mathrm{i}\boldsymbol{k'r}} c^\dagger_{\boldsymbol{k}\sigma} c_{\boldsymbol{k'}\sigma} \\
&= -e^2 \sum_\sigma \sum_{\boldsymbol{kk'q}} \int d^3r d^3r'' \frac{1}{V} e^{-\mathrm{i}\boldsymbol{kr}} e^{+\mathrm{i}\boldsymbol{k'r}} \frac{\rho(-\boldsymbol{q})}{q^2} e^{+\mathrm{i}\boldsymbol{q}(\boldsymbol{r}-\boldsymbol{r''})} c^\dagger_{\boldsymbol{k}\sigma} c_{\boldsymbol{k'}\sigma} \\
&= -e^2 \sum_\sigma \sum_{\boldsymbol{kq}} \frac{4\pi\rho(-\boldsymbol{q})}{q^2} c^\dagger_{\boldsymbol{k}\sigma} c_{\boldsymbol{k}-\boldsymbol{q},\sigma} = -4\pi e^2 \sum_\sigma \sum_{\boldsymbol{kq}} \frac{\rho(\boldsymbol{q})}{q^2} c^\dagger_{\boldsymbol{k}-\boldsymbol{q},\sigma} c_{\boldsymbol{k},\sigma} \,.
\end{aligned} \tag{3.213}$$

Here, we have introduced the Fourier transform of the charge density (for a truly homogeneous background charge density, the contribution $\boldsymbol{q} = 0$ to the sum would diverge) via the decomposition

$$\rho(\boldsymbol{r}) = \sum_{\boldsymbol{q}} \rho(-\boldsymbol{q}) e^{+\mathrm{i}\boldsymbol{rq}} \,. \tag{3.214}$$

Altogether, the full Hamilton operator in second quantization reads

$$H = \sum_{\boldsymbol{k}\sigma} \frac{\hbar^2 \boldsymbol{k}^2}{2m} c^\dagger_{\boldsymbol{k}\sigma} c_{\boldsymbol{k}\sigma} - 4\pi e^2 \sum_\sigma \sum_{\boldsymbol{kq}} \frac{\rho(\boldsymbol{q})}{q^2} c^\dagger_{\boldsymbol{k}-\boldsymbol{q},\sigma} c_{\boldsymbol{k},\sigma} + \frac{1}{2} \sum_{\sigma\sigma'} \sum_{\boldsymbol{kk'q}} \frac{4\pi e^2}{Vq^2} c^\dagger_{\boldsymbol{k}-\boldsymbol{q},\sigma} c^\dagger_{\boldsymbol{k'}+\boldsymbol{q},\sigma'} c_{\boldsymbol{k'},\sigma'} c_{\boldsymbol{k},\sigma} \,. \tag{3.215}$$

To this example, we can now apply the single-particle aproximation

$$H_{\text{eff}} = \sum_k \sum_\sigma \chi_{k\sigma} c_{k\sigma}^\dagger c_{k\sigma} \tag{3.216}$$

and determine the single-particle energies $\chi_{k\sigma}$ self-consistently.

To avoid the lengthy minimization procedure, we directly follow the recipe (3.193) and obtain for the effective Hamiltonian

$$\begin{aligned}
H_{\text{eff}} &= \sum_{\boldsymbol{k}\sigma} \frac{\hbar^2 \boldsymbol{k}^2}{2m} c_{\boldsymbol{k}\sigma}^\dagger c_{\boldsymbol{k}\sigma} - 4\pi e^2 \sum_\sigma \sum_{\boldsymbol{kq}} \frac{\rho(\boldsymbol{q})}{q^2} c_{\boldsymbol{k}-\boldsymbol{q},\sigma}^\dagger c_{\boldsymbol{k},\sigma} \\
&\quad + \frac{1}{2} \sum_{\sigma\sigma'} \sum_{\boldsymbol{kk'q}} \frac{4\pi e^2}{V q^2} \Big[\left\langle c_{\boldsymbol{k}-\boldsymbol{q},\sigma}^\dagger c_{\boldsymbol{k},\sigma} \right\rangle_{\text{eff}} c_{\boldsymbol{k'}+\boldsymbol{q},\sigma'}^\dagger c_{\boldsymbol{k'},\sigma'} + \left\langle c_{\boldsymbol{k'}+\boldsymbol{q},\sigma'}^\dagger c_{\boldsymbol{k'},\sigma'} \right\rangle_{\text{eff}} c_{\boldsymbol{k}-\boldsymbol{q},\sigma}^\dagger c_{\boldsymbol{k},\sigma} \\
&\quad - \left\langle c_{\boldsymbol{k}-\boldsymbol{q},\sigma}^\dagger c_{\boldsymbol{k'},\sigma'} \right\rangle_{\text{eff}} c_{\boldsymbol{k'}+\boldsymbol{q},\sigma'}^\dagger c_{\boldsymbol{k},\sigma} - \left\langle c_{\boldsymbol{k'}+\boldsymbol{q},\sigma'}^\dagger c_{\boldsymbol{k},\sigma} \right\rangle_{\text{eff}} c_{\boldsymbol{k}-\boldsymbol{q},\sigma}^\dagger c_{\boldsymbol{k'},\sigma'} \Big] \\
&= \sum_{\boldsymbol{k}\sigma} \frac{\hbar^2 \boldsymbol{k}^2}{2m} c_{\boldsymbol{k}\sigma}^\dagger c_{\boldsymbol{k}\sigma} - 4\pi e^2 \sum_\sigma \sum_{\boldsymbol{kq}} \frac{\rho(\boldsymbol{q})}{q^2} c_{\boldsymbol{k}-\boldsymbol{q},\sigma}^\dagger c_{\boldsymbol{k},\sigma} \\
&\quad + \sum_\sigma \sum_{\boldsymbol{kq}} \left[\frac{4\pi e^2}{V q^2} \sum_{\sigma'\boldsymbol{k'}} \left\langle c_{\boldsymbol{k'}+\boldsymbol{q},\sigma'}^\dagger c_{\boldsymbol{k'},\sigma'} \right\rangle_{\text{eff}} \right] c_{\boldsymbol{k}-\boldsymbol{q},\sigma}^\dagger c_{\boldsymbol{k},\sigma} \\
&\quad - \sum_\sigma \sum_{\boldsymbol{kk'}} \frac{4\pi e^2}{V(\boldsymbol{k}-\boldsymbol{k'})^2} \left\langle c_{\boldsymbol{k'}\sigma}^\dagger c_{\boldsymbol{k'}\sigma} \right\rangle_{\text{eff}} c_{\boldsymbol{k}\sigma}^\dagger c_{\boldsymbol{k}\sigma} \,.
\end{aligned} \tag{3.217}$$

Now, we use that the FT of the charge density can be written as

$$\begin{aligned}
\rho(\boldsymbol{q}) &= \frac{1}{V} \int \langle \rho(\boldsymbol{r}) \rangle e^{+\mathrm{i}\boldsymbol{qr}} d^3r = \frac{1}{V} \int d^3r \left\langle \sum_i \delta(\boldsymbol{r}-\boldsymbol{r_i}) \right\rangle e^{+\mathrm{i}\boldsymbol{qr}} d^3r = \frac{1}{V} \sum_i \left\langle e^{\mathrm{i}\boldsymbol{qr_i}} \right\rangle \\
&= \frac{1}{V} \int d^3r \left\langle \Phi^\dagger(\boldsymbol{r}) e^{\mathrm{i}\boldsymbol{qr}} \Phi(\boldsymbol{r}) \right\rangle = \frac{1}{V} \sum_{\boldsymbol{kk'},\sigma} \frac{1}{V} \int e^{-\mathrm{i}\boldsymbol{kr}} e^{+\mathrm{i}\boldsymbol{k'r}} e^{+\mathrm{i}\boldsymbol{qr}} d^3r \left\langle c_{\boldsymbol{k}\sigma}^\dagger c_{\boldsymbol{k'}\sigma} \right\rangle_{\text{eff}} \\
&= \frac{1}{V} \sum_{\boldsymbol{kk'},\sigma'} \delta(\boldsymbol{k}-\boldsymbol{k'}-\boldsymbol{q}) \left\langle c_{\boldsymbol{k}\sigma'}^\dagger c_{\boldsymbol{k'}\sigma'} \right\rangle_{\text{eff}} = \frac{1}{V} \sum_{k'\sigma'} \left\langle c_{\boldsymbol{k'}+\boldsymbol{q},\sigma'}^\dagger c_{\boldsymbol{k'},\sigma'} \right\rangle_{\text{eff}} \,.
\end{aligned} \tag{3.218}$$

This means that the two summations with $\boldsymbol{q}$ in the previous equation cancel and we are left with

$$H_{\text{eff}} = \sum_{\boldsymbol{k}\sigma} \left[\frac{\hbar^2 \boldsymbol{k}^2}{2m} - \frac{1}{V} \sum_{\boldsymbol{k'}} \frac{4\pi e^2}{V(\boldsymbol{k}-\boldsymbol{k'})^2} \left\langle c_{\boldsymbol{k'}\sigma}^\dagger c_{\boldsymbol{k'}\sigma} \right\rangle_{\text{eff}} \right] c_{\boldsymbol{k}\sigma}^\dagger c_{\boldsymbol{k}\sigma} \,, \tag{3.219}$$

which is the effective single-particle Hamiltonian in Hartree-Fock approximation. The effective single-particle energies have to be determined self-consistently

$$\epsilon_{k\sigma} = \frac{\hbar^2 \boldsymbol{k}^2}{2m} - \sum_{\boldsymbol{k'}} \frac{4\pi e^2}{V(\boldsymbol{k}-\boldsymbol{k'})^2} \left\langle c_{\boldsymbol{k'}\sigma}^\dagger c_{\boldsymbol{k'}\sigma} \right\rangle_{\text{eff}} = \frac{\hbar^2 \boldsymbol{k}^2}{2m} - \frac{1}{V} \sum_{\boldsymbol{k'}} \frac{4\pi e^2}{(\boldsymbol{k}-\boldsymbol{k'})^2} \frac{1}{e^{\beta(\epsilon_{k'\sigma}-\mu)}+1} \,. \tag{3.220}$$

Still, we see that in the summation over k', the case $k' = k$ leads to a divergent contribution, and the reason for this is the long-range Coulomb interaction. Within the Hartree-Fock approximation with bare Coulomb interaction, it is not possible to overcome this artifact. Using a screened Yukawa potential $\Phi(\boldsymbol{r}) = \frac{Q}{r} e^{-\delta r}$ would correspond to the replacement $(\boldsymbol{k}-\boldsymbol{k'})^2 \to (\boldsymbol{k}-\boldsymbol{k'})^2 + \delta^2$. Therefore, we discuss below how screened potentials may arise.

3.2.6 Thomas-Fermi theory of screening

From electrodynamics we know that an external field applied to a medium with charges that can move will lead to a polarization of these charges. This in turn will lead to a change of the external field, which acts on the charges, and so on. Here, we will discuss that this self-consistent solution may explain the screening effect.

From electrostatics we recall that polarization effects are effectively described by a dielectric tensor $\underline{\underline{\epsilon}}$ [7, 8], which relates displacement field $\boldsymbol{D}$ and electric field $\boldsymbol{E}$ typically linearly $\boldsymbol{D}(\boldsymbol{r}) = \underline{\underline{\epsilon}}(\boldsymbol{r})\epsilon_0 \boldsymbol{E}(\boldsymbol{r}) = \left[1 + \underline{\underline{\chi}}(\boldsymbol{r})\right] \epsilon_0 \boldsymbol{E}(\boldsymbol{r}) = \epsilon_0 \boldsymbol{E}(\boldsymbol{r}) + \boldsymbol{P}(\boldsymbol{r})$. Here, the tensor $\underline{\underline{\chi}}$ is the dielectric susceptibility, it describes how the polarization $\boldsymbol{P}$ of the medium is related to the external field. However, it should be noted that this already involves some approximations: For example, for large fields the polarization will in general not scale linearly with the external field. Furthermore, the polarization at position $\boldsymbol{r}$ will depend on the field also at different positions $\boldsymbol{r'}$, such that in reality the relations between external electric field and polarization are more difficult. Following Ref. [4], we consider the potential $\Phi^0(\boldsymbol{r})$ due to an unscreened charge density $\rho^0(\boldsymbol{r})$, which obeys the Poisson equation

$$\Delta\Phi^0(\boldsymbol{r}) = -4\pi\rho^0(\boldsymbol{r})\,. \tag{3.221}$$

The full potential does of course also fulfill a Poisson equation

$$\Delta\Phi(\boldsymbol{r}) = -4\pi\rho(\boldsymbol{r}) = -4\pi\left[\rho^0(\boldsymbol{r}) + \rho^{\rm ind}(\boldsymbol{r})\right]\,, \tag{3.222}$$

where $\rho^{\rm ind}(\boldsymbol{r})$ is the induced charge density due to the polarizability of the medium. One assumes that the bare potential and the full potential are related via a convolution

$$\Phi^0(\boldsymbol{r}) = \int d^3r' \epsilon(\boldsymbol{r}, \boldsymbol{r'})\Phi(\boldsymbol{r'}) = \int d^3r' \epsilon(\boldsymbol{r} - \boldsymbol{r'})\Phi(\boldsymbol{r'})\,, \tag{3.223}$$

where we assumed an isotropic medium, where the dielectric tensor is just a scalar, which should in addition only depend on the difference between the positions but not on their absolute values. To relate with simpler results, we can consider the corresponding equation for the displacement fields and take the limit where the fields vary rather slowly over the range on which $\epsilon(\boldsymbol{r})$ changes

$$\boldsymbol{D}(\boldsymbol{r}) \equiv \int d^3r' \epsilon(\boldsymbol{r} - \boldsymbol{r'})\boldsymbol{E}(\boldsymbol{r'}) \approx \left[\int d^3r' \epsilon(\boldsymbol{r'})\right] \boldsymbol{E}(\boldsymbol{r}) = \epsilon \boldsymbol{E}(\boldsymbol{r})\,. \tag{3.224}$$

Performing a 3d Fourier transform of all quantities in the convolution equation, we obtain that the Fourier transforms of the bare and full potentials are related linearly

$$\Phi^0(\boldsymbol{q}) = \epsilon(\boldsymbol{q})\Phi(\boldsymbol{q})\,. \tag{3.225}$$

Here, $\epsilon(\boldsymbol{q})$ is the FT of $\epsilon(\boldsymbol{r})$. In addition, we can compute the FT of the two Poisson equations for the bare and the full potential

$$q^2\Phi^0(\boldsymbol{q}) = 4\pi\rho^0(\boldsymbol{q})\,, \qquad q^2\Phi(\boldsymbol{q}) = 4\pi\rho(\boldsymbol{q})\,, \tag{3.226}$$

which yields

$$\frac{q^2}{4\pi}[\Phi(\boldsymbol{q}) - \Phi^0(\boldsymbol{q})] = \rho^{\rm ind}(\boldsymbol{q}) = \chi(\boldsymbol{q})\Phi(\boldsymbol{q})\,. \tag{3.227}$$

Here, $\boldsymbol{\chi}(\boldsymbol{q})$ is the FT of the dielectric susceptibility. Solving for the potential, we get the relation

$$\Phi(\boldsymbol{q}) = \frac{\Phi^0(\boldsymbol{q})}{1 - \frac{4\pi\chi(\boldsymbol{q})}{q^2}} . \tag{3.228}$$

With Eq. (3.225), this links the FT of $\epsilon(\boldsymbol{r})$ to the FT of the electric susceptibility

$$\epsilon(\boldsymbol{q}) = 1 - \frac{4\pi}{q^2}\chi(\boldsymbol{q}) = 1 - \frac{4\pi}{q^2}\frac{\rho^{\text{ind}}(\boldsymbol{q})}{\Phi(\boldsymbol{q})} . \tag{3.229}$$

Now, the Thomas [5]-Fermi approach starts from the single-electron Schrödinger equation in presence of the full potential

$$\frac{-\hbar^2\nabla^2}{2m}\Psi_i(\boldsymbol{r}) - e\Phi(\boldsymbol{r})\Psi_i(\boldsymbol{r}) = \epsilon_i\Psi_i(\boldsymbol{r}) , \tag{3.230}$$

where i is a quantum number, ϵ_i are the eigenenergies and $\Psi_i(\boldsymbol{r})$ are the corresponding eigenfunctions. When we assume that the total potential varies very slowly, we can discretize space in many volume elements, and for each volume element approximate the potential by a constant. The dispersion relation in each volume element is then just the plane-wave dispersion relation – shifted by the constant, i.e.,

$$\epsilon_{\boldsymbol{r}}(\boldsymbol{k}) = \frac{\hbar^2\boldsymbol{k}^2}{2m} - e\Phi(\boldsymbol{r}) . \tag{3.231}$$

For each volume element, we can compute the density of electrons via

$$n_{\boldsymbol{r}} = \frac{1}{V}\sum_{\boldsymbol{k}}\left\langle c_{\boldsymbol{k}}^\dagger c_{\boldsymbol{k}}\right\rangle = \frac{1}{(2\pi)^3}\int d^3k \frac{1}{\exp[\beta(\epsilon_{\boldsymbol{r}}(\boldsymbol{k}) - \mu)] + 1} . \tag{3.232}$$

Now, in absence of any potential, this equation would read

$$n_0(\mu) = \int \frac{d^3k}{(2\pi)^3}\frac{1}{\exp[\beta(\frac{\hbar^2k^2}{2m} - \mu)] + 1} , \tag{3.233}$$

and the induced charge density is given by the difference of the particle density in presence of a potential and the particle density in absence of a potential – multiplied by the electron charge

$$\rho^{\text{ind}}(\boldsymbol{r}) = -e[n_0(\mu + e\Phi(\boldsymbol{r})) - n_0(\mu)] \approx -e^2\frac{\partial n_0(\mu)}{\partial\mu}\Phi(\boldsymbol{r}) , \tag{3.234}$$

where we have used that the shift due to the electric field potential can be equally well described as a shift of the chemical potential and performed a Taylor series for small Φ. Fourier-transforming and comparing this with Eq. (3.227), we conclude that the susceptibility and derived dielectric constant do both not depend on $\boldsymbol{q}$

$$\chi(\boldsymbol{q}) = -e^2\frac{\partial n_0(\mu)}{\partial\mu} , \qquad \epsilon(\boldsymbol{q}) = 1 + \frac{4\pi e^2}{q^2}\frac{\partial n_0(\mu)}{\partial\mu} . \tag{3.235}$$

Now, let us finally consider the bare potential of a point charge and its FT

$$\Phi^0(\boldsymbol{r}) = \frac{Q}{r} , \qquad \Phi^0(\boldsymbol{q}) = \frac{4\pi Q}{q^2} , \tag{3.236}$$

---

[5] Llewellyn Hilleth Thomas (1903–1992) was a british-american physicist.

where we had computed the 3d FT of a $1/r$ term before. From Eq. (3.225), we get the FT of the full potential

$$\Phi(\boldsymbol{q}) = \frac{\Phi^0(\boldsymbol{q})}{\epsilon(\boldsymbol{q})} = \frac{4\pi Q}{q^2 + 4\pi e^2 \frac{\partial n_0(\mu)}{\partial \mu}} \equiv \frac{4\pi Q}{q^2 + k_{TF}^2}\,, \tag{3.237}$$

where k_{TF} is also known as **Thomas-Fermi wavevector**. Inverting the FT, we get the screened Coulomb potential (we have effectively computed this before in Sec. 3.2.2 when discussing the regularization of an integral)

$$\Phi(\boldsymbol{r}) = \frac{Q}{r} e^{-k_{TF} r}\,. \tag{3.238}$$

In the theory of mesons, an analogous form had been derived, such that such a potential is also known as **Yukawa potential** [6]

3.2.7 Lindhard theory of screening

In the previous chapter, we used that the external potential is weak and that it varied slowly, such that we could assume an equilibrium distribution in the small volume elements. Since on top of this, we used the assumption that the field potential was small, we may directly obtain the induced charge density from applying perturbation theory in the strength of the field potential to the Schrödinger equation

$$\frac{-\hbar^2\nabla^2}{2m}\Psi_k(\boldsymbol{r}) - e\Phi(\boldsymbol{r})\Psi_k(\boldsymbol{r}) = \epsilon_k \Psi_k(\boldsymbol{r})\,. \tag{3.239}$$

In general, for a splitting $H = H_0 + H_1$ and free (non-degenerate) eigenvalues $H_0 \left|\Psi_k^{(0)}\right\rangle = E_k^{(0)} \left|\Psi_k^{(0)}\right\rangle$, the correction to first order on the eigenvectors is given by

$$\left|\Psi_k\right\rangle = \left|\Psi_k^{(0)}\right\rangle + \sum_{q\neq k} \frac{\left\langle \Psi_q^{(0)} \right| H_1 \left| \Psi_k^{(0)} \right\rangle}{\epsilon_k^{(0)} - \epsilon_q^{(0)}} \left|\Psi_q^{(0)}\right\rangle + \ldots = \left|\Psi_k^{(0)}\right\rangle + \left|\Psi_k^{(1)}\right\rangle + \ldots\,. \tag{3.240}$$

Specifically, the free problem solutions are just plane waves with $\epsilon_k = \frac{\hbar^2 k^2}{2m}$ and

$$\left\langle r \middle| \Psi_k^{(0)} \right\rangle = \frac{1}{\sqrt{V}} e^{+\mathrm{i}\boldsymbol{k}\boldsymbol{r}}\,, \qquad \left\langle r \middle| \Psi_k^{(1)} \right\rangle = \sum_{q\neq k} \frac{\left\langle \Psi_q^{(0)} \right| H_1 \left| \Psi_k^{(0)} \right\rangle}{\epsilon_k^{(0)} - \epsilon_q^{(0)}} \frac{1}{\sqrt{V}} e^{+\mathrm{i}\boldsymbol{q}\boldsymbol{r}}\,, \tag{3.241}$$

and we use for the perturbation

$$H_1 = -e\Phi(\boldsymbol{r})\,. \tag{3.242}$$

Then, we get that the matrix element in the correction is just given by the FT of the full potential

$$\left\langle \Psi_q^{(0)} \right| H_1 \left| \Psi_k^{(0)} \right\rangle = -\frac{e}{V} \int d^3 r e^{+\mathrm{i}(\boldsymbol{k}-\boldsymbol{q})\boldsymbol{r}} \Phi(\boldsymbol{r}) = -e\Phi(\boldsymbol{k}-\boldsymbol{q})\,. \tag{3.243}$$

---

[6] Yukawa Hideki (1907–1981) was a japanese physicist and Nobel laureate.

When one inserts this in the particle density at position $\boldsymbol{r}$ (the factor of two results from the spin)

$$n(\boldsymbol{r}) = 2\sum_{\boldsymbol{k}} f(\epsilon_{\boldsymbol{k}}) \left|\Psi_{\boldsymbol{k}}(\boldsymbol{r})\right|^2 , \qquad f(\epsilon_{\boldsymbol{k}}) = \frac{1}{e^{\beta(\epsilon_{\boldsymbol{k}}-\mu)}+1} , \tag{3.244}$$

we would get to first order

$$\begin{aligned} n(\boldsymbol{r}) &= 2\sum_{\boldsymbol{k}} f(\epsilon_{\boldsymbol{k}}) \left\langle \boldsymbol{r}|\Psi_{\boldsymbol{k}}\right\rangle \left\langle \Psi_{\boldsymbol{k}}|\boldsymbol{r}\right\rangle \\ &= 2\sum_{\boldsymbol{k}} f(\epsilon_{\boldsymbol{k}}) \left\langle \boldsymbol{r}|\Psi_{\boldsymbol{k}}^{(0)}\right\rangle \left\langle \Psi_{\boldsymbol{k}}^{(0)}|\boldsymbol{r}\right\rangle + 2\sum_{\boldsymbol{k}} f(\epsilon_{\boldsymbol{k}}) \left[\left\langle \boldsymbol{r}|\Psi_{\boldsymbol{k}}^{(0)}\right\rangle \left\langle \Psi_{\boldsymbol{k}}^{(1)}|\boldsymbol{r}\right\rangle + \left\langle \boldsymbol{r}|\Psi_{\boldsymbol{k}}^{(1)}\right\rangle \left\langle \Psi_{\boldsymbol{k}}^{(0)}|\boldsymbol{r}\right\rangle\right] + \ldots \end{aligned} \tag{3.245}$$

The second term (and higher corrections) is identified as the <u>induced</u> particle density, such that we get for the induced charge density

$$\begin{aligned} \rho^{\text{ind}}(\boldsymbol{r}) &= -2e\sum_{\boldsymbol{k}} f(\epsilon_{\boldsymbol{k}}) \left[\left\langle \boldsymbol{r}|\Psi_{\boldsymbol{k}}^{(1)}\right\rangle \left\langle \Psi_{\boldsymbol{k}}^{(0)}|\boldsymbol{r}\right\rangle + \text{h.c.}\right] \\ &= +\frac{2e^2}{V}\sum_{\boldsymbol{k}\neq\boldsymbol{q}} f(\epsilon_{\boldsymbol{k}}) \left[e^{-\mathrm{i}\boldsymbol{k}\boldsymbol{r}} \frac{\Phi(\boldsymbol{k}-\boldsymbol{q})}{\epsilon_{\boldsymbol{k}}-\epsilon_{\boldsymbol{q}}} e^{+\mathrm{i}\boldsymbol{q}\boldsymbol{r}} + \text{h.c.}\right] \\ &= +\frac{2e^2}{V}\sum_{\boldsymbol{k}}\sum_{\boldsymbol{q}\neq 0} f(\epsilon_{\boldsymbol{k}}) \frac{e^{-\mathrm{i}\boldsymbol{q}\boldsymbol{r}}\Phi(\boldsymbol{q}) + e^{+\mathrm{i}\boldsymbol{q}\boldsymbol{r}}\Phi(-\boldsymbol{q})}{\frac{\hbar^2}{m}\boldsymbol{k}\boldsymbol{q} - \frac{\hbar^2 q^2}{2m}} \\ &= +\sum_{\boldsymbol{q}\neq 0} e^{-\mathrm{i}\boldsymbol{q}\boldsymbol{r}} \left[\frac{2e^2}{V}\sum_{\boldsymbol{k}} f(\epsilon_{\boldsymbol{k}}) \left(\frac{1}{\frac{\hbar^2}{m}\left(\boldsymbol{k}-\frac{\boldsymbol{q}}{2}\right)\boldsymbol{q}} - \frac{1}{\frac{\hbar^2}{m}\left(\boldsymbol{k}+\frac{\boldsymbol{q}}{2}\right)\boldsymbol{q}}\right)\Phi(\boldsymbol{q})\right] \\ &= +\sum_{\boldsymbol{q}\neq 0} e^{-\mathrm{i}\boldsymbol{q}\boldsymbol{r}} \left[\frac{2e^2}{V}\sum_{\boldsymbol{k}} \frac{f(\epsilon_{\boldsymbol{k}+\boldsymbol{q}/2}) - f(\epsilon_{\boldsymbol{k}-\boldsymbol{q}/2})}{\hbar^2\boldsymbol{k}\boldsymbol{q}/m}\Phi(\boldsymbol{q})\right] . \end{aligned} \tag{3.246}$$

The term in square brackets must now apparently be the FT of the induced charge density (the exclusion of the $\boldsymbol{q}=0$ term is not problematic in the continuum limit). Therefore, we conclude

$$\rho^{\text{ind}}(\boldsymbol{q}) = \frac{2e^2}{V}\sum_{\boldsymbol{k}} \frac{f(\epsilon_{\boldsymbol{k}+\boldsymbol{q}/2}) - f(\epsilon_{\boldsymbol{k}-\boldsymbol{q}/2})}{\hbar^2\boldsymbol{k}\boldsymbol{q}/m}\Phi(\boldsymbol{q}) = \chi(\boldsymbol{q})\Phi(\boldsymbol{q}) , \tag{3.247}$$

and the FT of the susceptibility becomes

$$\chi(\boldsymbol{q}) = \frac{2e^2}{V}\sum_{\boldsymbol{k}} \frac{f(\epsilon_{\boldsymbol{k}+\boldsymbol{q}/2}) - f(\epsilon_{\boldsymbol{k}-\boldsymbol{q}/2})}{\hbar^2\boldsymbol{k}\boldsymbol{q}/m} \to e^2\int\frac{d^3k}{4\pi^3}\frac{f(\epsilon_{\boldsymbol{k}+\boldsymbol{q}/2}) - f(\epsilon_{\boldsymbol{k}-\boldsymbol{q}/2})}{\hbar^2\boldsymbol{k}\boldsymbol{q}/m} . \tag{3.248}$$

This is known as the Lindhard [7] susceptibility [9]. As a consistency check, we consider the limit of small $\boldsymbol{q}$, where we can expand the Fermi functions to get

$$\chi(\boldsymbol{q}\to 0) \to -e^2\int\frac{d^3k}{4\pi^3}\frac{\partial f(\epsilon_{\boldsymbol{k}})}{\partial\mu} = -e^2\frac{\partial n_0(\mu)}{\partial\mu} , \tag{3.249}$$

---

[7] J. Lindhard (1922–1997) was a danish theoretical physicist.

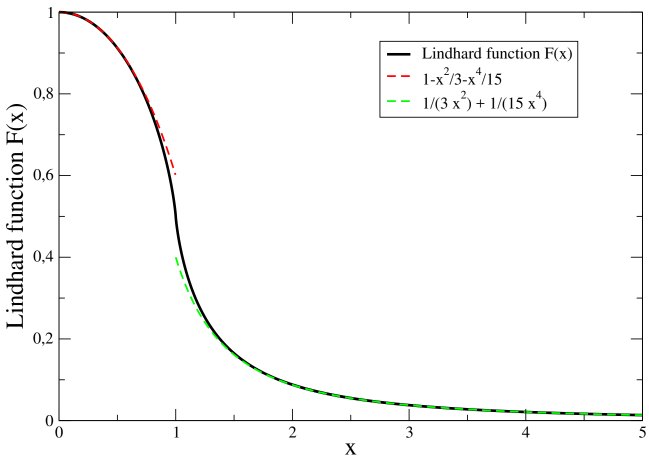

Figure 3.6: Plot of the Lindhard function (3.252) with asymptotic behaviour. At $x = 1$, the first derivative diverges, while $F(1) = 1/2$.

which is just the Thomas-Fermi susceptibility from Eq. (3.235). Inserting the general Lindhard susceptibility into the FT of the dielectric constant one arrives at

$$\epsilon(\boldsymbol{q}) = 1 - \frac{4\pi}{q^2}\chi(\boldsymbol{q}) = 1 - \frac{e^2 m}{\hbar^2 \pi^2 q^2} \int d^3k \frac{f(\epsilon_{\boldsymbol{k}+\boldsymbol{q}/2}) - f(\epsilon_{\boldsymbol{k}-\boldsymbol{q}/2})}{\boldsymbol{k}\boldsymbol{q}} \,. \tag{3.250}$$

At zero temperature $T = 0$, this integral can be simplified by constraining the integration over $\boldsymbol{k}$ by the Fermi surface, and one obtains (lengthy exercise [10, 3])

$$\lim_{T\to 0} \epsilon(\boldsymbol{q}) = 1 + \frac{4mk_F e^2}{\pi\hbar^2 q^2} F\left(\frac{q}{2k_F}\right) \,, \tag{3.251}$$

with Fermi wavenumber k_F (related to $E_F = \hbar^2 k_F^2/(2m)$) and with the Lindhard function

$$F(x) = \frac{1}{2} + \frac{1-x^2}{4x} \ln\left|\frac{1+x}{1-x}\right| \,. \tag{3.252}$$

The Lindhard function is non-analytic at $x = 1$ (mapping to $q = 2k_F$), where its first derivative diverges, see Fig. 3.6. Eventually, this results in an oscillatory behaviour of the reverse FT.

We can compute the screened Coulomb potential of a point charge from the reverse FT

$$\Phi(\boldsymbol{r}) = \int \frac{d^3q}{(2\pi)^3} \Phi(\boldsymbol{q}) e^{-\mathrm{i}\boldsymbol{q}\boldsymbol{r}} = \int \frac{d^3q}{(2\pi)^3} \frac{4\pi Q}{q^2 - 4\pi\chi(\boldsymbol{q})} e^{-\mathrm{i}\boldsymbol{q}\boldsymbol{r}} \,. \tag{3.253}$$

At zero temperature, an analytic calculation of the screening is possible

$$\begin{aligned} \Phi(\boldsymbol{r}) &= \int \frac{d^3q}{(2\pi)^3} \frac{4\pi Q}{q^2 + \frac{4mk_F e^2}{\pi\hbar^2} F\left(\frac{q}{2k_F}\right)} \\ &= \ldots = \left(\frac{k_{TF}}{4k_F \epsilon(2k_F)}\right)^2 \frac{\cos(2k_F r)}{r^3} \,. \end{aligned} \tag{3.254}$$

Here, we recall the definition of the Thomas-Fermi wavenumber $k_{TF}^2 = 4\pi e^2 \frac{\partial n_0(\mu)}{\partial\mu}$. This means that the screening does not only affect the farfield behaviour, but also the near-field behaviour of a screened potential is different. Furthermore, the screening behaviour is in general temperature-dependent. To obtain the Lindhard approximation, we performed a perturbative expansion in the field strength, such that one should treat the small $\boldsymbol{r}$ behaviour – where already the bare potential $\Phi^0(\boldsymbol{r})$ is large – with caution. Nevertheless, what is also observed is that the screened potential exhibits oscillations (so-called Friedel [8] oscillations), see Fig. 3.7. These

---

[8] Jacques Friedel (1921 – 2014) was a French physicist and material scientist.

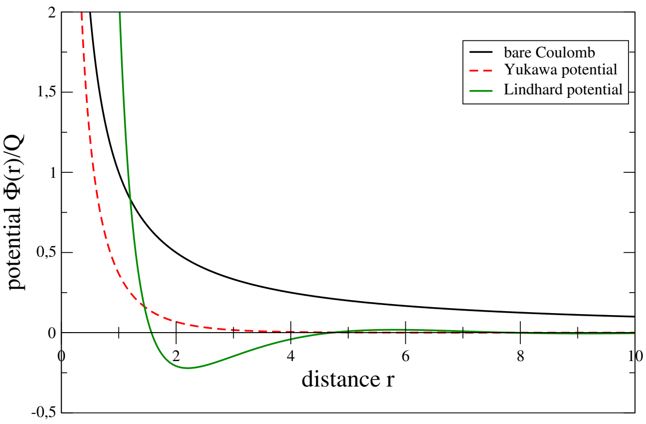

Figure 3.7: Plot of bare (solid black), Yukawa (dashed red), and Lindhard (solid green) potentials versus distance r. Parameters $k_{TF} = 1$, $\left(\frac{k_{TF}}{4k_F\epsilon(2k_F)}\right)^2 = 4$, $2k_F = 1$. The screened Lindhard potential exhibits weak oscillations.

oscillations of the potential eventually map to oscillations of the observed electronic particle density, and similar effects can be observed also for other charged particles.

The Lindhard screening model fits well for metals, where the free electron model does apply aproximately. Further modifications are necessary for insulators and semiconductors [3].

3.2.8 Basics of the density functional theory

The fact that interacting models are notoriously difficult to treat, has given rise to the development of many different methods. In recent years, the density functional theory has become quite important, and we will briefly discuss its main ideas. The Hamiltonian considered is still given by

$$H = \sum_i \frac{\boldsymbol{p}_i^2}{2m} + \sum_i V(\boldsymbol{r_i}) + \sum_{i<j} \frac{e^2}{|\boldsymbol{r_i} - \boldsymbol{r_j}|}\,, \tag{3.255}$$

where $\boldsymbol{p_i}$ and $\boldsymbol{r_i}$ are position and momentum operators for the i-th electron, and $V(\boldsymbol{r_i})$ is the background potential of the ions felt by the i-th electron.

The probability density to find the first electron at $\boldsymbol{r_1}$, the second at $\boldsymbol{r_2}$, and so on is given by the square of the many-particle wave function, which at zero temperatures is just the ground state of the system

$$P(\boldsymbol{r_1}, \ldots, \boldsymbol{r_N}) = |\Psi_0(\boldsymbol{r_1}, \ldots, \boldsymbol{r_N})|^2\,. \tag{3.256}$$

However, since the electrons are indistinguishable, we have to consider the particle density in the ground state instead

$$n_0(\boldsymbol{r}) = \int d^3r_1 \ldots \int d^3r_N \Psi_0^*(\boldsymbol{r_1}, \ldots, \boldsymbol{r_N}) \left[\sum_{i=1}^N \delta(\boldsymbol{r} - \boldsymbol{r_i})\right] \Psi_0(\boldsymbol{r_1}, \ldots, \boldsymbol{r_N})\,. \tag{3.257}$$

The theorem of Hohenberg [9] and Kohn [10] tells us that the ground state energy can be found from the particle density.

Box 13 (Hohenberg-Kohn theorem) *The ground state energy is a unique functional of the ground state particle density* $n_0(\boldsymbol{r})$.

---

[9] P.C. Hohenberg (1934–2017) was a US-american theoretical physicist.

[10] W. Kohn (1923–2016) was a US-american physicist and Nobel laureate.

This statement is not trivial. Clearly, we can uniquely assign an energy to any wave function via $E = \langle\Psi| H |\Psi\rangle$, i.e., the ground state energy is clearly a functional of the ground state wave function. However, for the particle density we still have to show that. Let us assume that we have two different normalized and non-degenerate ground states $|\Psi_0\rangle$ and $|\Psi_0'\rangle$ that result from different Hamiltonians $H|\Psi_0\rangle = E_0|\Psi_0\rangle$ and $H'|\Psi_0'\rangle = E_0'|\Psi_0'\rangle$. We furthermore use that the difference in the Hamiltonians can only come from the single-particle potential, since for a given number of electrons, the kinetic and electron-electron interactions are fixed $H = H' + V - V'$. The Rayleigh-Ritz theorem tells us that when these states are different, we must have

$$\begin{aligned}
E_0 &= \langle\Psi_0| H |\Psi_0\rangle < \langle\Psi_0'| H |\Psi_0'\rangle = \langle\Psi_0'| (H' + V - V') |\Psi_0'\rangle \\
&= E_0' + \int d^3r_1 \ldots \int d^3r_N \Psi_0^{*'}(\boldsymbol{r_1}, \ldots, \boldsymbol{r_N}) \left[\sum_i V(\boldsymbol{r_i}) - V'(\boldsymbol{r_i})\right] \Psi_0'(\boldsymbol{r_1}, \ldots, \boldsymbol{r_N}) \\
&= E_0' + \int d^3r \int d^3r_1 \ldots \int d^3r_N \Psi_0^{*'}(\boldsymbol{r_1}, \ldots, \boldsymbol{r_N}) \left[\sum_i \delta(\boldsymbol{r} - \boldsymbol{r_i})\right] [V(\boldsymbol{r}) - V'(\boldsymbol{r})] \Psi_0'(\boldsymbol{r_1}, \ldots, \boldsymbol{r_N}) \\
&= E_0' + \int d^3r [V(\boldsymbol{r}) - V'(\boldsymbol{r})] n'(\boldsymbol{r}) \,. \qquad (3.258)
\end{aligned}$$

Analogously, we get

$$E_0' < E_0 + \int d^3r [V'(\boldsymbol{r}) - V(\boldsymbol{r})] n(\boldsymbol{r}) \,. \qquad (3.259)$$

Adding these inequalities leads – as we assumed $n(\boldsymbol{r}) = n'(\boldsymbol{r})$ – to a contradiction, and hence we conclude that the initial assumption (different Hamiltonians with different ground states) was wrong, such that for equal particle densities we must have $|\Psi_0'\rangle = |\Psi_0\rangle$ (up to a global phase of course).

Together with the Rayleigh-Ritz minimization principle, this allows to obtain the ground state energy from a minimization of the energy functional $E[n(\boldsymbol{r})]$ of the particle density and not of the wave function, i.e.,

$$E_0 = E[n_0(\boldsymbol{r})] \leq E[n(\boldsymbol{r})] \,. \qquad (3.260)$$

In particular, the density, for which the energy functional assumes its global minimum, is then the ground state density. Formally, we have a minimization problem under side constraints

$$\delta \left[E[n(\boldsymbol{r})] - \mu \left(\int d^3r n(\boldsymbol{r}) - N_e\right)\right] \,, \qquad (3.261)$$

where the chemical potential μ acts as a Lagrange multiplier and N_e is the total electron number, and we have to vary over all possible particle densities that are formally written as $\langle\Psi| (\sum_i \delta(\boldsymbol{r} - \boldsymbol{r_i})) |\Psi\rangle$. The problem is, we do not know the functional that should be minimized. Assuming that the energy functional is additively composed from kinetic, background potential and interaction potential contributions

$$E[n(\boldsymbol{r})] = T[n(\boldsymbol{r})] + V[n(\boldsymbol{r})] + U[n(\boldsymbol{r})] \,, \qquad (3.262)$$

we only know the functional dependence of the potential energy (compare the proof of the Hohenberg-Kohn theorem above):

$$V[n(\boldsymbol{r})] = \int d^3r V(\boldsymbol{r}) n(\boldsymbol{r}) \,. \qquad (3.263)$$

Instead, the functional for the kinetic energy is not known – we can only calculate its value when we know the wave function

$$T[n(\boldsymbol{r})] \hat{=} \langle\Psi| \sum_i \frac{\boldsymbol{p_i}^2}{2m} |\Psi\rangle \,. \tag{3.264}$$

Also, the functional for the interaction is not known – here it is customary to approximate it by a classical ansatz

$$U[n(\boldsymbol{r})] = \frac{e^2}{2} \int d^3r \int d^3r' \frac{n(\boldsymbol{r})n(\boldsymbol{r'})}{|\boldsymbol{r}-\boldsymbol{r'}|} + E_x[n(\boldsymbol{r})] \,. \tag{3.265}$$

Here, the first term corresponds to the classical interaction energy of a charge distribution $\rho(\boldsymbol{r}) = -en(\boldsymbol{r})$, and the second term (called exchange-correlation-energy) is unknown. Therefore, to proceed, one needs the functionals of kinetic and interaction terms. These can be guessed from exactly solvable cases such as the homogeneous electron gas. However, it should be stressed that even if the density functional theory applies, we can only use it to determine the ground state energy and the corresponding ground state particle density, for the finite-temperature behaviour other methods need to be applied.

Chapter 4

Electron-Phonon Interaction

So far, we understood solids as a complicated problem of electrons and nuclei, where we want to take the electron-electron as well as the electron-nucleus interactions into account. In the discussion of the Born-Oppenheimer approximation in Sec. 2.2, we learned that due to the large asymmetry between nucleus and electron masses, we could treat the electrons and nuclei at least partially independently: First, the electronic Schrödinger equation had to be solved, by inserting the positions of the nuclei as classical variables. The resulting electronic wave function then had to be taken to generate a background potential for the nuclei.

Swapping the order, we discussed in section 2.4 how an effective electronic potential with postulated equilibrium positions for the nuclei at the lattice nodes would – upon expansion – lead to a harmonic potential for the nuclei, which could be quantized with bosonic annihilation and creation operators. This led to the concept of a phonon, and we learned how the structure of a crystal (dimension, type and basis) would upon application of a normal mode decomposition give rise to different phonon modes (acoustic and optical modes), we arrived in Eq. (2.115) at a phonon Hamiltonian of the form

$$H_{\mathrm{ph}} = \sum_{\boldsymbol{q}j} \hbar\omega_j(\boldsymbol{q}) \left(b^\dagger_{\boldsymbol{q}j} b_{\boldsymbol{q}j} + \frac{1}{2} \right) , \tag{4.1}$$

with bosonic annihilation operators $b_{\boldsymbol{q}j}$ of normal mode $\boldsymbol{q}, j$ in the first Brillouin zone and phonon branch index j denoting the optical or acoustic branch. Here, $\omega_j(\boldsymbol{q})$ was the phonon dispersion relation, with different behaviour depending on optical or acoustic modes.

In the previous chapter, specifically Sec. 3.1, we discussed how the electronic Schrödinger equation could be solved for **periodic** background potentials of the nuclei. This means, we assumed that the nuclei were fixed at their lattice positions, neglecting both the presence of phonons and also the zero-point motion of the nuclei. When in addition we neglected the electron-electron interaction, this led to electronic Hamiltonians (3.111) of the form

$$H_{\mathrm{el}} = \sum_{\boldsymbol{k}\nu\sigma} \epsilon_{\boldsymbol{k}\nu} c^\dagger_{\boldsymbol{k}\nu\sigma} c_{\boldsymbol{k}\nu\sigma} , \tag{4.2}$$

with fermionic annihilation operators $c_{\boldsymbol{k}\nu\sigma}$ for an electron in band ν, wave number $\boldsymbol{k}$ in the first Brillouin zone and spin σ. With taking electron-electron interactions into account in Sec. 3.2, we arrived at representations with additional quartic terms (e.g. in the homogeneous electron gas or the Hubbard model)

$$H_{ee} = \frac{1}{2} \sum_{\boldsymbol{k_1},\boldsymbol{k_2}\boldsymbol{q}} \sum_{\sigma\sigma'} \sum_{\nu\nu'} u_{\boldsymbol{k_1}+\boldsymbol{q},\nu,\boldsymbol{k_2}-\boldsymbol{q},\nu';\boldsymbol{k_2},\nu',\boldsymbol{k_1},\nu} c^\dagger_{\boldsymbol{k_1}+\boldsymbol{q},\nu,\sigma} c^\dagger_{\boldsymbol{k_2}-\boldsymbol{q},\nu',\sigma'} c_{\boldsymbol{k_2}\nu'\sigma'} c_{\boldsymbol{k_1}\nu\sigma} , \tag{4.3}$$

which could be intuitively interpreted as an elastic scattering event of two electrons, entering at momenta $\boldsymbol{k_1}$ and $\boldsymbol{k_2}$, exchanging momentum $2\boldsymbol{q}$, and leaving the scattering region with momenta $\boldsymbol{k_1}+\boldsymbol{q}$ and $\boldsymbol{k_2}-\boldsymbol{q}$, while keeping their spin (exact) and their band index (approximate).

So what is left in this picture is now to take deviations of the nuclei positions from their lattice position into account, but now in the equations for the electrons.

4.1 The Fröhlich model of electron-phonon interaction

The position of the n-th nucleus is then given by

$$\boldsymbol{R}_n = \boldsymbol{R}_n^0 + \boldsymbol{u}_n\,, \tag{4.4}$$

where the $\boldsymbol{u}_n$ is the displacement of the n-th ion from its equilibrium position, see also Fig. 2.3. Typically, these displacements are below 10 percent of the lattice constant, since for larger displacements the solid will start to melt. This means that we are allowed to expand the potential around the equilibrium position of the nuclei. However, there is one important difference: For the nuclei, we expanded the potential felt by the nuclei around the equilibrium position of the nuclei, and therefore the first order vanished. Here, the equilibrium position of the nuclei is not the equilibrium position of the potential felt by the electrons, therefore, the first order term does not vanish but mediates the electron-phonon interaction.

Specifically, we can write the background potential felt by the ith electron as

$$V(\boldsymbol{r_i}) = \sum_{n=1}^{N} v(\boldsymbol{r_i}-\boldsymbol{R}_n^0) - \sum_{n=1}^{N}\left[\nabla v(\boldsymbol{r_i}-\boldsymbol{R}_n^0)\right]\cdot\boldsymbol{u}_n + \ldots\,. \tag{4.5}$$

Here, N is the total number of nuclei (ions) and $\boldsymbol{r_i}$ is the position of the i-th electron. We note that only the lowest order contribution is periodic with respect to lattice vector shifts $\boldsymbol{R}$

$$V_{\rm per}(\boldsymbol{r}) = \sum_{n=1}^{N} v(\boldsymbol{r_i}-\boldsymbol{R}_n^0) = V_{\rm per}(\boldsymbol{r}+\boldsymbol{R})\,, \tag{4.6}$$

and consequently all the properties such as Bloch theorem etc. only hold when neglecting the influence of the phonons completely.

We will sketch how to compute the representation of the electron-phonon interaction in second quantization

$$H_{\rm el-ph} = -\sum_{n=1}^{N}\sum_{\boldsymbol{k}\boldsymbol{k'}\sigma} \langle\boldsymbol{k'}|\, V_{\rm el-ph}(\boldsymbol{r})\,|\boldsymbol{k}\rangle\, c^\dagger_{\boldsymbol{k'}\sigma} c_{\boldsymbol{k}\sigma}\,. \tag{4.7}$$

Here, we have already used that the spin is not flipped. Accordingly, we need to evaluate the matrix element of the single-particle operator

$$\langle\boldsymbol{k'}|\, V_{\rm el-ph}(\boldsymbol{r})\,|\boldsymbol{k}\rangle = \sum_{\ell=1}^{N}\int d^3r\,\Psi^*_{\boldsymbol{k'}}(\boldsymbol{r})\left[\nabla v(\boldsymbol{r}-\boldsymbol{R}_\ell^0)\right]\cdot\boldsymbol{u}_\ell\Psi_{\boldsymbol{k}}(\boldsymbol{r})\,. \tag{4.8}$$

The most important ingredient is now that we can map the displacement of the ℓ-th ion to bosonic operators [3]

$$\boldsymbol{u}_\ell = \frac{1}{\sqrt{N}}\sum_{\boldsymbol{q}j}\sqrt{\frac{\hbar}{2M\omega_j(\boldsymbol{q})}}\left(b_{\boldsymbol{q}j}+b^\dagger_{-\boldsymbol{q},j}\right)\boldsymbol{e}_j(\boldsymbol{q})e^{+\mathrm{i}\boldsymbol{q}\boldsymbol{R}_\ell^0}\,. \tag{4.9}$$

Here, M is the ion mass and $\boldsymbol{e}_j$ describes the polarization vector of branch j. Inserting all this, we arrive at the Fröhlich [1]-Model for the electron-phonon interaction

$$H_{\text{el-ph}} = \sum_{\boldsymbol{kq}} \sum_{\boldsymbol{G}} \sum_{j} \sum_{\nu} \sum_{\sigma} M^j_{\boldsymbol{k},\boldsymbol{q}+\boldsymbol{G}} \left(b_{\boldsymbol{q},j} + b^\dagger_{-\boldsymbol{q},j} \right) c^\dagger_{\boldsymbol{k}+\boldsymbol{q}+\boldsymbol{G},\nu,\sigma} c_{\boldsymbol{k},\nu,\sigma} \tag{4.10}$$

with matrix elements $M^j_{\boldsymbol{k},\boldsymbol{q}+\boldsymbol{G}}$. Here, the sums over $\boldsymbol{k}$ and $\boldsymbol{q}$ run over the first Brillouin zone and become continuous in the large N limit. The sum over $\boldsymbol{G}$ runs over all reciprocal lattice vectors and remains discrete. The sum over j denotes the phonon branch index, and the sum over ν the electronic band index. The Hamiltonian has a simple interpretation. In particular, the term $b_{\boldsymbol{q},j} c^\dagger_{\boldsymbol{k}+\boldsymbol{q}+\boldsymbol{G},\nu,\sigma} c_{\boldsymbol{k},\nu,\sigma}$ is interpreted as an incoming electron with wavenumber $\boldsymbol{k}$, band index ν, and spin σ absorbing a phonon from branch j and with wavenumber $\boldsymbol{q}$, leaving the interaction region as an electron with wavenumber $\boldsymbol{k}+\boldsymbol{q}+\boldsymbol{G}$ but unchanged band index and spin. Likewise, the other term $b^\dagger_{-\boldsymbol{q},j} c^\dagger_{\boldsymbol{k}+\boldsymbol{q}+\boldsymbol{G},\nu,\sigma} c_{\boldsymbol{k},\nu,\sigma}$ describes the emission of a phonon with wavenumber $-\boldsymbol{q}$ and branch j by an incoming electron of band index ν and spin σ.

Importantly, we see that the full quasi-momentum is not conserved in this process, this holds true only up to a lattice vector $\boldsymbol{G}$ of the reciprocal lattice. As $\boldsymbol{k}+\boldsymbol{q}$ may lie outside the first Brillouin zone, we have to add a reciprocal lattice vector, such that $\boldsymbol{k}+\boldsymbol{q}+\boldsymbol{G}$ lies in the first Brillouin zone again. Since adding a reciprocal lattice vector may nearly completely change the wavenumber, such processes (where $\boldsymbol{G} \neq 0$) are called **Umklapp processes**. In principle, it would be possible that phonons also change the band index etc.

We can combine these things in the complete electron-phonon Hamiltonian.

Box 14 (Electron-Phonon Hamiltonian) *Denoting the electron band index by ν, the electron spin by σ, the phonon branches by j, the Hamiltonian is given by*

$$\begin{aligned} H = &\sum_{\boldsymbol{k}\nu\sigma} \epsilon_\nu(\boldsymbol{k}) c^\dagger_{\boldsymbol{k}\nu\sigma} c_{\boldsymbol{k}\nu\sigma} + \sum_{\boldsymbol{q}j} \hbar\omega_j(\boldsymbol{q}) \left(b^\dagger_{\boldsymbol{q},j} b_{\boldsymbol{q},j} + \frac{1}{2} \right) \\ &+ \frac{1}{2} \sum_{\boldsymbol{k_1}\boldsymbol{k_2}\boldsymbol{q}} \sum_{\sigma\sigma'} \sum_{\nu\nu'} u_{\boldsymbol{k_1}+\boldsymbol{q},\nu,\boldsymbol{k_2}-\boldsymbol{q},\nu';\boldsymbol{k_2},\nu',\boldsymbol{k_1},\nu} c^\dagger_{\boldsymbol{k_1}+\boldsymbol{q},\nu,\sigma} c^\dagger_{\boldsymbol{k_2}-\boldsymbol{q},\nu',\sigma'} c_{\boldsymbol{k_2},\nu',\sigma'} c_{\boldsymbol{k_1},\nu,\sigma} \\ &+ \sum_{\boldsymbol{kq}} \sum_{\boldsymbol{G}} \sum_{\nu} \sum_{j} \sum_{\sigma} M^j_{\boldsymbol{k},\boldsymbol{q}+\boldsymbol{G}} \left(b_{\boldsymbol{q},j} + b^\dagger_{-\boldsymbol{q},j} \right) c^\dagger_{\boldsymbol{k}+\boldsymbol{q}+\boldsymbol{G},\nu,\sigma} c_{\boldsymbol{k},\nu,\sigma} \,. \end{aligned} \tag{4.11}$$

Here, the first two lines are the free electron and phonon Hamiltonians, respectively, the second line denotes the electron-electron interaction, and the last line encodes the electron-phonon interaction with matrix element $M^j_{\boldsymbol{k},\boldsymbol{q}+\boldsymbol{G}}$.

To memorize this Hamiltonian, it is useful to represent the interaction processes by diagrams, where it is conventional to use wave lines for the phonons and solid lines for the electrons, see Fig. 4.1. From these elementary processes we already learn that both the electronic and phononic wavenumbers $\boldsymbol{k}$ and $\boldsymbol{q}$ are no good quantum numbers, as the electrons may be scattered into different $\boldsymbol{k}$ modes, and new phonons with wave numbers $\boldsymbol{q}$ may be created. In particular, these scattering processes are the main reason for electric resistance, with phonon contributions dominating at high temperature. The remaining contribution is generated by

---

[1] H. Fröhlich (1905–1991) was a german physicist who published a famous work on the elctron phonon interaction in 1950.

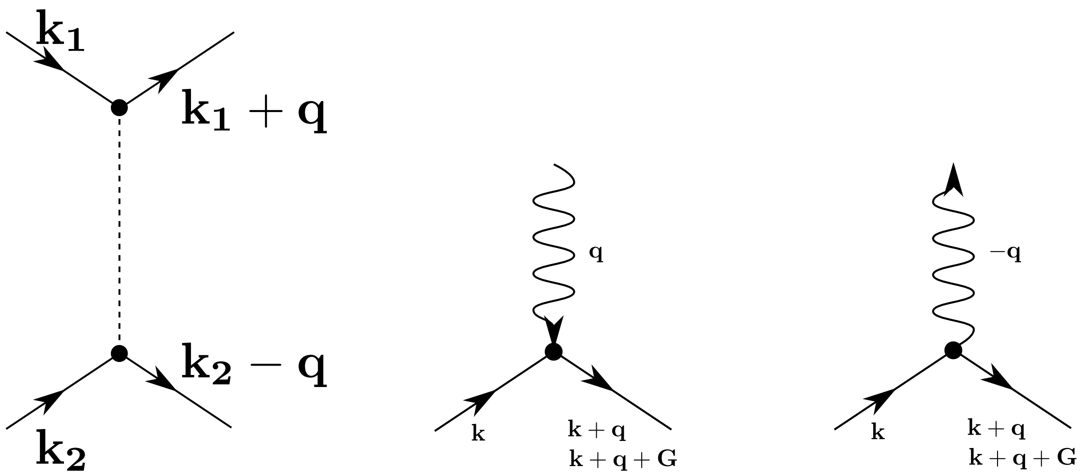

Figure 4.1: Diagrams for the electron-electron Coulomb interaction (solid and dashed line, left) and elementary electron-phonon processes for he absorbtion and emission of a phonon by an electron (solid and wavy lines, right). The electron spin is not changed, and usually also the band index is invariant.

Figure 4.2: Classically, the emission and re-absorbtion of a phonon by a moving electron can be interpreted as a localized lattice polarization, that is attached to the electron – called a polaron.

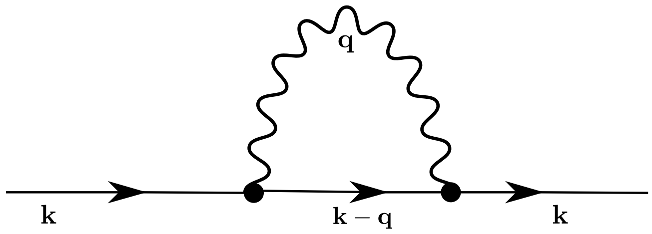

deviations from the ideal lattice structure. Further, the phonon particle number is obviously not conserved, while the electronic particle number (and spin) is.

Such elementary processes can be combined in larger diagrams (with multiple vertices), which can mediate effective interactions. For example, an electron may emit phonon(s) and re-absorb them later-on, see Fig. 4.2. Such a localized lattice polarization that is attached to an electron is called **polaron**. It is a **quasi-particle** which consists of a real-particle (the electron) and another quasi-particle (the phonons).

Alternatively, the emitted phonon(s) can be absorbed by another electron, leading to an effective scattering process between two electrons, see Fig. 4.3.

Further processes are conceivable. For example, the diagrams can be understood as effective, with lines representing e.g. only the creation of free electrons in the conduction band. Then,

Figure 4.3: Emitted phonons may be absorbed by other electrons. Unlike shown in the figure, the mediated effective interaction may be attractive.

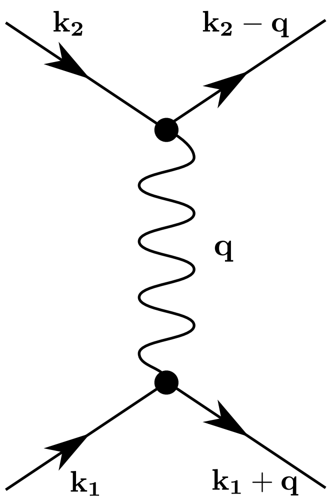

phonons can even create an electron-hole pair by exciting an electron from the valence band into the conduction band. Altogether, there are some analogies between diagrams of electron-phonon interactions and those in quantum field theory, where the effective interaction between electrons is mediated by photons.

4.2 Method: The polaron transform and Hamiltonian of mean force

The polaron transfom is a useful method for a unitary mapping of Hamiltonians with a linear coupling to a non-interacting bosonic reservoir.

Box 15 (electronic polaron transform) *The small polaron transform (also: Lang-Firsov transform) is a unitary transform defined by*

$$U = e^{A(\alpha b - \alpha^* b^\dagger)}\,, \tag{4.12}$$

where $A = A^\dagger$ is an operator acting on a different Hilbert space than the bosonic operators b and $b^\dagger$, and where the coefficients $\alpha \in \mathbb{C}$ can be chosen conveniently.

In the electronic context, we will see that we will often choose A as the particle number operator of electrons, e.g.

$$A = \sum_k c_k^\dagger c_k\,. \tag{4.13}$$

Below, we will practice its application at some simple models. In the evaluation of the polaron transform, it will be helpful to use that

$$e^{+S} A e^{-S} = A + [S, A] + \frac{1}{2!}[S, [S, A]] + \ldots = \sum_{n=0}^{\infty} \frac{1}{n!}[S, A]_n\,, \tag{4.14}$$

where the generalized commutator is defined recursively as

$$[S, A]_{n+1} = [S, [S, A]_n]\,, \qquad [S, A]_0 = A\,. \tag{4.15}$$

Another useful concept for bipartite systems is the Hamiltonian of mean force.

Box 16 (Hamiltonian of mean force) *For a bipartite system with parts A and B, which is described by the full Hamiltonian $H = H_A + H_B + H_{AB}$ with $[H_A, H_B] = 0$ the Hamiltonian of mean force is implicitly defined by the reduced density matrix of the global canonical equilibrium state*

$$\frac{e^{-\beta H_A^*}}{\mathrm{Tr}_A\left\{e^{-\beta H_A^*}\right\}} = \mathrm{Tr}_B \left\{ \frac{e^{-\beta(H_A + H_B + H_{AB})}}{\mathrm{Tr}_{\mathrm{AB}}\left\{e^{-\beta(H_A + H_B + H_{AB})}\right\}} \right\}\,. \tag{4.16}$$

The r.h.s. is just the reduced density matrix of a global Gibbs state. It can always be written as the exponential of a different Hamiltonian as the reduced density matrix is positive semidefinite. For consistency, we note that it will be equal to H_A when $H_{AB} = 0$. The Hamiltonian of mean force can be seen as the effective Hamiltonian that acts on a system in presence of some environment, but in general it is very hard to compute and will obviously depend on the temperature.

4.2.1 Example: A single phonon-coupled quantum dot

Reducing the complexity of the Fröhlich Hamiltonian, we can consider just one electronic mode (i.e., no spin, no bands, no wave numbers) and just one phonon mode (no branches, no wave numbers). Then, there cannot be any electron-electron interaction and only the terms with $\boldsymbol{q} = 0$ and $\boldsymbol{G} = 0$ in the complete Hamiltonian remain. We can therefore suppress all indices and the system is given by

$$H = \epsilon c^\dagger c + \lambda(b + b^\dagger)c^\dagger c + \Omega b^\dagger b \,. \tag{4.17}$$

Here, λ describes the coupling between the electrons (c) and the phonons (b). The model could be realized in a quantum dot that is hosted on a small molecule, where the phonons represent just one particular vibrational mode of the molecule. It would be trivial if the electron number were not allowed to change: We would either have an electron on the molecule or not for all times, and we could eliminate the electronic operators from the Hamiltonian by replacing them with their eigenvalue $c^\dagger c \to \{0, 1\}$, leaving it either a normal oscillator

$$H_0 = \Omega b^\dagger b \tag{4.18}$$

with spectrum

$$E_n^0 = \Omega n \,, \tag{4.19}$$

or a displaced oscillator

$$H_1 = \epsilon + \lambda(b + b^\dagger) + \Omega b^\dagger b = \epsilon + \Omega\left(b^\dagger + \frac{\lambda}{\Omega}\right)\left(b + \frac{\lambda}{\Omega}\right) - \frac{\lambda^2}{\Omega} \,. \tag{4.20}$$

Since $\tilde{b} = b + \frac{\lambda}{\Omega}\mathbf{1}$ is also a valid bosonic annihilation operator, we can immediately conclude the spectrum of the displaced oscillator

$$E_n^1 = \epsilon - \frac{\lambda^2}{\Omega} + \Omega n \,. \tag{4.21}$$

Some interesting dynamics can be introduced into the model by coupling it to electronic leads [12], which allow for electrons entering the quantum dot and leaving it. In particular, an electron jumping into the system will not just create an electron, but it will be dressed by a whole cloud of phonons. Formally, this can be seen by the polaron transform. For example, one can show that the polaron transform acts on the bosonic and fermionic operators as

$$\begin{aligned} UbU^\dagger &= b + [c^\dagger c(\alpha b - \alpha^* b^\dagger), b] + \ldots = b + \alpha^* c^\dagger c \,, \\ Ub^\dagger U^\dagger &= b^\dagger + \alpha c^\dagger c \,, \\ UcU^\dagger &= c e^{-(\alpha b - \alpha^* b^\dagger)} = d(\alpha) \,, \\ Uc^\dagger U^\dagger &= c^\dagger e^{+(\alpha b - \alpha^* b^\dagger)} = d^\dagger(\alpha) \,. \end{aligned} \tag{4.22}$$

Here, the new operators $d(\alpha)$ and $d^\dagger(\alpha)$ obey fermionic statistics. To diagonalize our Hamiltonian, we can therefore choose α such that all couplings vanish

$$UHU^\dagger = \epsilon c^\dagger c + \lambda(b + \alpha^* c^\dagger c + b^\dagger + \alpha c^\dagger c)c^\dagger c + \Omega(b^\dagger + \alpha c^\dagger c)(b + \alpha^* c^\dagger c) \,, \tag{4.23}$$

which decouples when

$$\alpha = -\frac{\lambda}{\Omega} \,, \tag{4.24}$$

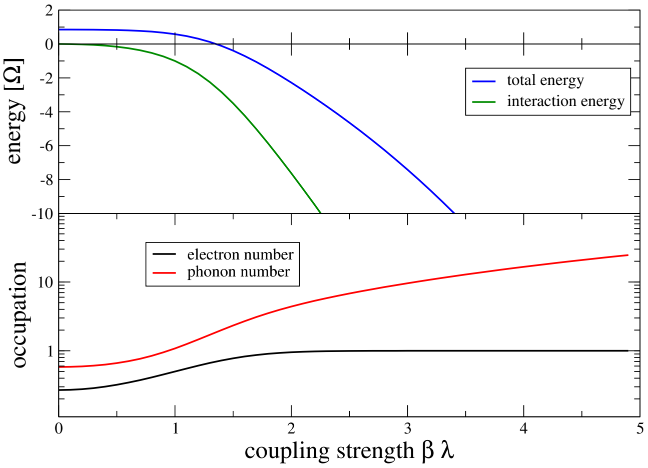

Figure 4.4: Bottom: Plot of electronic expectation values $\left\langle c^\dagger c\right\rangle$ (black), phonon expectation values $\left\langle b^\dagger b\right\rangle$ (red) versus coupling strength. Top: Plot of the total energy $\langle H\rangle$ and the interaction energy $\left\langle \lambda c^\dagger c(b+b^\dagger)\right\rangle$. Other parameters: $\beta\epsilon = 1 = \beta\Omega$. The total energy is dominated by the interaction Hamiltonian at stronger couplings and is negative despite an increase in the phonon number (with a positive contribution).

and yields the Hamiltonian

$$UHU^\dagger = \left[\epsilon - \frac{\lambda^2}{\Omega}\right] c^\dagger c + \Omega b^\dagger b = \left[\epsilon - \frac{\lambda^2}{\Omega}\right] d^\dagger\left(-\frac{\lambda}{\Omega}\right) d\left(-\frac{\lambda}{\Omega}\right) + \Omega b^\dagger b\,. \tag{4.25}$$

Effectively, the energy of the dressed fermionic quasiparticle – a mini-polaron – described by the $d(\alpha)$ on the dot is reduced in comparison to the single electron energy ϵ – for free electrons with dispersion relation $E = \hbar^2\boldsymbol{k}^2/(2m)$ this could be interpreted as a larger mass. When we add a coupling Hamiltonian to some fermionic lead

$$H_I = \sum_k t_k c c_k^\dagger + \text{h.c.}\,, \tag{4.26}$$

we see that an electron jumping into the system creates a mini-polaron instead

$$UH_IU^\dagger = \sum_k \left[t_k d(\alpha) c_k^\dagger + t_k^* c_k d^\dagger(\alpha)\right]\,. \tag{4.27}$$

We learn from this example that the polaron has a renormalized electronic energy.

To calculate mean expectation values, it is useful to compute the partition function, for which it is helpful to employ the polaron transform (we do not fix the mean particle number and do not use a chemical potential)

$$\begin{aligned} Z_{can} &= \text{Tr}\left\{e^{-\beta H}\right\} = \text{Tr}\left\{Ue^{-\beta H}U^\dagger\right\} \\ &= \text{Tr}\left\{\exp\left\{-\beta\left[\left(\epsilon - \frac{\lambda^2}{\Omega}\right)c^\dagger c + \Omega b^\dagger b\right]\right\}\right\} \\ &= \frac{\left[1+\exp\left\{-\beta\left(\epsilon-\frac{\lambda^2}{\Omega}\right)\right\}\right]}{1-e^{-\beta\Omega}} = \bar{Z}_{el} Z_{ph}\,. \end{aligned} \tag{4.28}$$

This shows that for these types of models the polaron transform leads to a factorization of the partition function.

Computing derivatives of the partition function with respect to all parameters in the Hamiltonian, we can e.g. compute mean electron and phonon occupations, see Fig. 4.4.

Let us compute the Hamiltonian of mean force. We first note that the unitary of the polaron transform can also be written as

$$U = e^{-\frac{\lambda}{\Omega}c^\dagger c(b-b^\dagger)} = \mathbf{1} + c^\dagger c\left(e^{\frac{\lambda}{\Omega}(b^\dagger - b)} - \mathbf{1}\right) = cc^\dagger + c^\dagger c e^{\frac{\lambda}{\Omega}(b^\dagger-b)} = cc^\dagger + c^\dagger c U_{\rm ph}\,. \tag{4.29}$$

This decomposition can be helpful to evaluate the reduced density matrix of the electronic part only. Defining $\bar{H}_{el} = (\epsilon - \lambda^2/\Omega)c^\dagger c$, we get

$$\begin{aligned}
\rho_{\rm el} &= \frac{1}{Z_{gc}} {\rm Tr}_{ph} \left\{ U^\dagger U e^{-\beta H} U^\dagger U \right\} = \frac{1}{Z_{gc}} {\rm Tr}_{ph} \left\{ U^\dagger e^{-\beta \bar{H}_{\rm el}} e^{-\beta\Omega b^\dagger b} U \right\} \\
&= \frac{1}{Z_{gc}} {\rm Tr}_{ph} \left\{ \left[c c^\dagger + c^\dagger c U_{\rm ph}^\dagger \right] e^{-\beta \bar{H}_{\rm el}} e^{-\beta\Omega b^\dagger b} \left[c c^\dagger + c^\dagger c U_{\rm ph} \right] \right\} \\
&= \frac{1}{Z_{gc}} \left[e^{-\beta \bar{H}_{\rm el}} c c^\dagger {\rm Tr}_{ph} \left\{ e^{-\beta\Omega b^\dagger b} \right\} + e^{-\beta \bar{H}_{\rm el}} c^\dagger c {\rm Tr}_{ph} \left\{ U_{\rm ph}^\dagger e^{-\beta\Omega b^\dagger b} U_{\rm ph} \right\} \right] \\
&= e^{-\beta \bar{H}_{\rm el}} \frac{Z_{ph}}{\bar{Z}_{el} Z_{ph}} = \frac{e^{-\beta \bar{H}_{\rm el}}}{\bar{Z}_{\rm el}} \, .
\end{aligned} \tag{4.30}$$

Here, we have used that $[c^\dagger c, \bar{H}_{\rm el}] = 0 = [c c^\dagger, \bar{H}_{\rm el}]$ and also the fermionic properties. From this we conclude that in this case, the Hamiltonian of mean force is actually independent of the temperature

$$H_{\rm el}^* = \bar{H}_{\rm el} = \left[\epsilon - \frac{\lambda^2}{\Omega} \right] c^\dagger c \, . \tag{4.31}$$

4.2.2 Example: Phonon-coupled double quantum dot

We can revisit our example of the Hartree-Fock treatment of a double quantum dot from Sec. 3.2.4, now augmented by an electron-phonon interaction with a single phonon mode

$$\begin{aligned}
H &= \epsilon(d_L^\dagger d_L + d_R^\dagger d_R) + U_c d_L^\dagger d_L d_R^\dagger d_R + T(d_L^\dagger d_R + d_R^\dagger d_L) \\
&\quad + \lambda(d_L^\dagger d_L + d_R^\dagger d_R)(b + b^\dagger) + \Omega b^\dagger b \\
&= (\epsilon - T) c_1^\dagger c_1 + (\epsilon + T) c_2^\dagger c_2 + U_c c_1^\dagger c_1 c_2^\dagger c_2 \\
&\quad + \lambda(c_1^\dagger c_1 + c_2^\dagger c_2)(b + b^\dagger) + \Omega b^\dagger b \, .
\end{aligned} \tag{4.32}$$

Here, we have used the Bogoliubov transform from Sec. 3.2.4, such that $c_1 = (d_L - d_R)/\sqrt{2}$ and $c_2 = (d_L + d_R)/\sqrt{2}$ and correspondingly for $c_i^\dagger$. Now, the required polaron transform becomes

$$U = \exp\left\{ \frac{\lambda}{\Omega}(c_1^\dagger c_1 + c_2^\dagger c_2)(b^\dagger - b) \right\} , \tag{4.33}$$

which acts on the operators as

$$\begin{aligned}
U b U^\dagger &= b - \frac{\lambda}{\Omega}[c_1^\dagger c_1 + c_2^\dagger c_2] \, , \qquad U b^\dagger U^\dagger = b^\dagger - \frac{\lambda}{\Omega}[c_1^\dagger c_1 + c_2^\dagger c_2] \, , \\
U c_i U^\dagger &= c_i \exp\left\{ -\frac{\lambda}{\Omega}(b^\dagger - b) \right\} = d_i \, , \qquad U c_i^\dagger U^\dagger = c_i^\dagger \exp\left\{ +\frac{\lambda}{\Omega}(b^\dagger - b) \right\} = d_i^\dagger \, .
\end{aligned} \tag{4.34}$$

Inserting this in the full Hamiltonian, we get

$$\begin{aligned}
U H U^\dagger &= (\epsilon - T) c_1^\dagger c_1 + (\epsilon + T) c_2^\dagger c_2 + U_c c_1^\dagger c_1 c_2^\dagger c_2 + \Omega \left(b^\dagger - \frac{\lambda}{\Omega}(c_1^\dagger c_1 + c_2^\dagger c_2) \right) \left(b - \frac{\lambda}{\Omega}(c_1^\dagger c_1 + c_2^\dagger c_2) \right) \\
&\quad + \lambda(c_1^\dagger c_1 + c_2^\dagger c_2) \left[b + b^\dagger - 2\frac{\lambda}{\Omega}(c_1^\dagger c_1 + c_2^\dagger c_2) \right] \\
&= (\epsilon - T) c_1^\dagger c_1 + (\epsilon + T) c_2^\dagger c_2 + U_c c_1^\dagger c_1 c_2^\dagger c_2 + \Omega b^\dagger b - \frac{\lambda^2}{\Omega} \left[c_1^\dagger c_1 + c_2^\dagger c_2 \right]^2 \\
&= \left(\epsilon - T - \frac{\lambda^2}{\Omega} \right) c_1^\dagger c_1 + \left(\epsilon + T - \frac{\lambda^2}{\Omega} \right) c_2^\dagger c_2 + \left(U_c - 2\frac{\lambda^2}{\Omega} \right) c_1^\dagger c_1 c_2^\dagger c_2 + \Omega b^\dagger b \, .
\end{aligned} \tag{4.35}$$

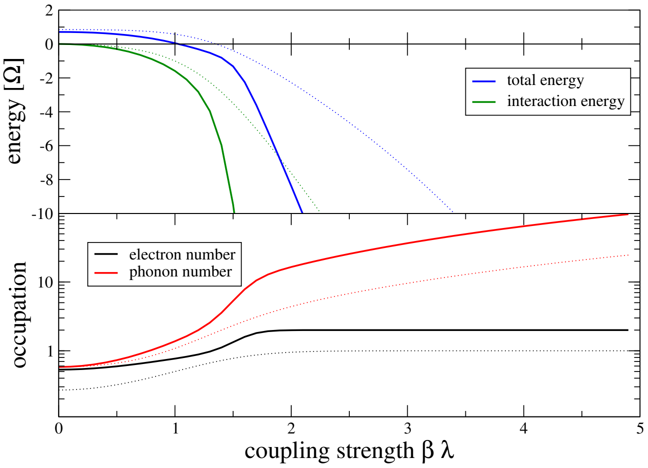

Figure 4.5: Same as Fig. 4.4(thin dotted curves) but for the double quantum dot with a single phonon mode. Other parameters: $\beta\epsilon = 1 = \beta\Omega$, $\beta U_c = 5$, $\beta T = 1$. At strong couplings, the electronic occupation reaches 2 indicating that the phonons mediate an attractive electron-electron interaction.

Since after the transformation – which due to its unitarity leaves the eigenvalues invariant – the Hamiltonian can be written as a sum of decoupled modes, we can directly compute the spectrum

$$E_{-,n} = \epsilon - T - \frac{\lambda^2}{\Omega} + n\Omega\,, \qquad E_{+,n} = \epsilon + T - \frac{\lambda^2}{\Omega} + n\Omega\,,$$
$$E_{0,n} = +n\Omega\,, \qquad E_{2,n} = 2\epsilon + U_c - 4\frac{\lambda^2}{\Omega} + n\Omega\,. \tag{4.36}$$

This now tells us that since the effective Coulomb interaction energy between the modes can become negative, i.e., attractive $U_{\rm eff} = E_{2,0} - E_{+,0} - E_{-,0} = U_c - 2\frac{\lambda^2}{\Omega}$, the doubly occupied state need not be the energetically highest one in particular for large couplings λ. We learn from this example that the phonons may mediate an attractive interaction between electrons that can overcome the Coulomb repulsion at strong electron-phonon couplings.

In a similar fashion as before we can compute the partition function and derive from suitable derivatives the expectation values of desired quantities in thermal equilibrium, see Fig. 4.5

However, one can also understand this using the Hamiltonian of mean force. Representing the polaron transform as

$$U = \left[c_1 c_1^\dagger + c_1^\dagger c_1 U_{\rm ph}\right]\left[c_2 c_2^\dagger + c_2^\dagger c_2 U_{\rm ph}\right]\,, \qquad U_{\rm ph} = e^{\frac{\lambda}{\Omega}(b^\dagger - b)}\,, \tag{4.37}$$

and defining furthermore $\bar{H}_{el} = \left(\epsilon - T - \frac{\lambda^2}{\Omega}\right) c_1^\dagger c_1 + \left(\epsilon + T - \frac{\lambda^2}{\Omega}\right) c_2^\dagger c_2 + \left(U_c - 2\frac{\lambda^2}{\Omega}\right) c_1^\dagger c_1 c_2^\dagger c_2\,,$ we can follow the same lines of calculation as in the previous section to arrive at (exercise)

$$\rho_{el} = \frac{e^{-\beta \bar{H}_{el}}}{{\rm Tr}_{el}\left\{e^{-\beta \bar{H}_{el}}\right\}}\,, \tag{4.38}$$

such that we conclude again that the Hamiltonian of mean force is temperature-independent and has an effective possibly attractive Coulomb interaction in the strong coupling limit

$$H_{el}^* = \left(\epsilon - T - \frac{\lambda^2}{\Omega}\right) c_1^\dagger c_1 + \left(\epsilon + T - \frac{\lambda^2}{\Omega}\right) c_2^\dagger c_2 + \left(U_c - 2\frac{\lambda^2}{\Omega}\right) c_1^\dagger c_1 c_2^\dagger c_2\,. \tag{4.39}$$

4.2.3 Example: Chain of electrons

Let us consider a chain of N sites, with each of the sites coupling to the same phonon mode

$$H = \epsilon \sum_{i=1}^N d_i^\dagger d_i + T \sum_{i=1}^{N-1}\left[d_i^\dagger d_{i+1} + d_{i+1}^\dagger d_i\right] + \lambda \sum_{i=1}^N d_i^\dagger d_i (b + b^\dagger) + \Omega b^\dagger b\,. \tag{4.40}$$

Here, ϵ is the on-site energy, T the next-neighbour hopping amplitude, λ represents the coupling to the phonons, and Ω is the phonon frequency. We neglected the Coulomb interaction completely (e.g. due to screening effects).

The transform that diagonalizes the free (quadratic) part of the system is now given by (compare the open chain example in Sec. 2.4.2)

$$d_i = \sqrt{\frac{2}{N+1}} \sum_{k=1}^{N} \sin \frac{\pi i k}{N+1} c_k \,, \qquad d_i^\dagger = \sqrt{\frac{2}{N+1}} \sum_{k=1}^{N} \sin \frac{\pi i k}{N+1} c_k^\dagger \,. \tag{4.41}$$

We can use that for integer $1 \le k, q \le N$ one has

$$\begin{aligned} \delta_{kq} &= \frac{2}{N+1} \sum_{i=1}^{N} \sin\left(\frac{\pi i k}{N+1}\right) \sin\left(\frac{\pi i q}{N+1}\right) \,, \\ \delta_{kq} 2\cos\left(\frac{\pi k}{N+1}\right) &= \frac{2}{N+1} \sum_{i=1}^{N-1} \left[\sin\left(\frac{\pi (i+1) k}{N+1}\right) \sin\left(\frac{\pi i q}{N+1}\right) + \sin\left(\frac{\pi i k}{N+1}\right) \sin\left(\frac{\pi (i+1) q}{N+1}\right)\right] \,. \end{aligned} \tag{4.42}$$

This means that the Hamiltonian reads in terms of the new operators

$$H = \sum_{k=1}^{N} \left[\epsilon - 2T \cos \frac{\pi k}{N+1}\right] c_k^\dagger c_k + \lambda \sum_{k=1}^{N} c_k^\dagger c_k (b + b^\dagger) + \Omega b^\dagger b \,. \tag{4.43}$$

Now, we again invoke the polaron transform

$$U = \exp\left\{\frac{\lambda}{\Omega} \sum_{k=1}^{N} c_k^\dagger c_k (b^\dagger - b)\right\} \,, \tag{4.44}$$

which acts on the operators as

$$\begin{aligned} U b U^\dagger &= b - \frac{\lambda}{\Omega} \sum_{k=1}^{N} c_k^\dagger c_k \,, \qquad & U b^\dagger U^\dagger &= b^\dagger - \frac{\lambda}{\Omega} \sum_{k=1}^{N} c_k^\dagger c_k \,, \\ U c_k U^\dagger &= c_k \exp\left\{-\frac{\lambda}{\Omega}(b^\dagger - b)\right\} \,, \qquad & U c_k^\dagger U^\dagger &= c_k^\dagger \exp\left\{+\frac{\lambda}{\Omega}(b^\dagger - b)\right\} \,. \end{aligned} \tag{4.45}$$

Alltogether, we see that the the Hamiltonian becomes

$$\begin{aligned} U H U^\dagger &= \sum_{k=1}^{N} \left[\epsilon - 2T \cos \frac{\pi k}{N+1}\right] c_k^\dagger c_k + \Omega b^\dagger b - \frac{\lambda^2}{\Omega} \left(\sum_{k=1}^{N} c_k^\dagger c_k\right)^2 \\ &= \epsilon \sum_{i=1}^{N} d_i^\dagger d_i + T \sum_{i=1}^{N-1} \left[d_i^\dagger d_{i+1} + d_{i+1}^\dagger d_i\right] + \Omega b^\dagger b - \frac{\lambda^2}{\Omega} \left(\sum_{i=1}^{N} d_i^\dagger d_i\right)^2 \,. \end{aligned} \tag{4.46}$$

This Hamiltonian again exhibits an effective negative (attractive) Coulomb interaction between the electrons. From this example, we learn that the electron-phonon interaction need not necessarily be strong to generate an effective attractive inter-electronic interaction: By increasing the number of electrons N, the attractive term scales as N^2, whereas the Coulomb repulsion will scale more mildly (e.g. only as N if we considered next-neighbour interactions). However, these examples only consider a single phonon mode and also the electron-phonon interaction does not change the electronic nor phononic wave numbers (conserves the quasi-momentum). Therefore, it is not very representative for the realistic situation in solids.

4.3 Attractive electron-electron interaction

It is possible to discuss the effective attraction between electrons in the same way as we did for the Thomas-Fermi screening theory, i.e., by treating the ions classically and computing their polarization. The only difference [1] is that the retardation of the response needs to be taken into account. One then obtains further corrections to the Yukawa-screening potential. By analyzing them, one can see that the effective interaction may become attractive under certain conditions.

We will rather follow the polaron approach here. We recall the part of the full Hamiltonian (4.11) and neglect phonon branches j, electron bands ν, Umklapp processes ($\boldsymbol{G} = 0$), electron-electron interaction as well as electron spin σ

$$H = \sum_{\boldsymbol{k}} \epsilon_{\boldsymbol{k}} c_{\boldsymbol{k}}^\dagger c_{\boldsymbol{k}} + \sum_{\boldsymbol{q}} \hbar\omega(\boldsymbol{q}) \left(b_{\boldsymbol{q}}^\dagger b_{\boldsymbol{q}} + \frac{1}{2}\right) + \sum_{\boldsymbol{k}\boldsymbol{q}} M_{\boldsymbol{k},\boldsymbol{q}} \left(b_{\boldsymbol{q}} + b_{-\boldsymbol{q}}^\dagger\right) c_{\boldsymbol{k}+\boldsymbol{q}}^\dagger c_{\boldsymbol{k}} \,. \tag{4.47}$$

Therefore, the difference to the previous treatments is that we now take the wave numbers of the phonons into account. For this case, it is not possible to come up with a simple polaron transform that completely decouples phonons and electrons at all values of the coupling strength.

However, we may proceed perturbatively [13, 3, 1]. Recalling the formula

$$e^{+S} H e^{-S} = \sum_{m=0} \frac{1}{m!} [S, H]_m = H + [S, H] + \frac{1}{2!}[S, [S, H]] + \frac{1}{3!}[S, [S, [S, H]]] + \ldots \,, \tag{4.48}$$

we see that upon the splitting $H = H_0 + H_1$ we can find a particular transform $S = \mathcal{O}\{H_1\}$ that approximately decouples the subsystems

$$e^{+S}(H_0 + H_1)e^{-S} = H_0 + H_1 + [S, H_0] + [S, H_1] + \frac{1}{2}[S, [S, H_0]] + \mathcal{O}\{H_1^3\} \,. \tag{4.49}$$

The trick is now to choose the particular transform S such that

$$[S, H_0] = -H_1 \tag{4.50}$$

is fulfilled. Obviously, this requires $S = \mathcal{O}\{H_1\}$, and then, we have

$$\begin{aligned} e^{+S}(H_0 + H_1)e^{-S} &= H_0 + \underbrace{[S, H_1] + \frac{1}{2}[S, [S, H_0]]}_{\mathcal{O}\{H_1^2\}} + \mathcal{O}\{H_1^3\} \\ &= H_0 + \underbrace{\frac{1}{2}[S, H_1]}_{\mathcal{O}\{H_1^2\}} + \mathcal{O}\{H_1^3\} \,. \end{aligned} \tag{4.51}$$

Specifically, we use the partition

$$\begin{aligned} H_0 &= \sum_{\boldsymbol{k}} \epsilon_{\boldsymbol{k}} c_{\boldsymbol{k}}^\dagger c_{\boldsymbol{k}} + \sum_{\boldsymbol{q}} \hbar\omega(\boldsymbol{q}) \left(b_{\boldsymbol{q}}^\dagger b_{\boldsymbol{q}} + \frac{1}{2}\right) \,, \\ H_1 &= \sum_{\boldsymbol{k}\boldsymbol{q}} \left(M_{\boldsymbol{k},\boldsymbol{q}} c_{\boldsymbol{k}+\boldsymbol{q}}^\dagger c_{\boldsymbol{k}} b_{\boldsymbol{q}} + M_{\boldsymbol{k},-\boldsymbol{q}} b_{\boldsymbol{q}}^\dagger c_{\boldsymbol{k}-\boldsymbol{q}}^\dagger c_{\boldsymbol{k}}\right) \,. \end{aligned} \tag{4.52}$$

Still, it is not straightforward to obtain the transformation that obeys $[S, H_0] = -H_1$. However, as H_0 is decoupled, it is convenient to compute it via its matrix elements. With the eigenstates of $H_0 \left|n\right> = E_n \left|n\right>$, we formally obtain from Eq. (4.50) for the matrix elements of S in the unperturbed eigenbasis

$$\left<n\right| S \left|m\right> = \frac{\left<n\right| H_1 \left|m\right>}{E_n - E_m}\,, \tag{4.53}$$

which yields for our expansion

$$\begin{aligned} H' = e^{+S} H e^{-S} &\approx H_0 + \frac{1}{2} \sum_\ell \left|\ell\right> \left<\ell\right| S \sum_m \left|m\right> \left<m\right| H_1 \sum_n \left|n\right> \left<n\right| \\ &\qquad - \frac{1}{2} \sum_\ell \left|\ell\right> \left<\ell\right| H_1 \sum_m \left|m\right> \left<m\right| S \sum_n \left|n\right> \left<n\right| \\ &= H_0 + \frac{1}{2} \sum_{\ell m n} \left[\frac{\left<\ell\right| H_1 \left|m\right>}{E_\ell - E_m} \left<m\right| H_1 \left|n\right> - \left<\ell\right| H_1 \left|m\right> \frac{\left<m\right| H_1 \left|n\right>}{E_m - E_n} \right] \left|\ell\right> \left<n\right| \\ &= H_0 - \frac{1}{2} \sum_{\ell m n} \left<\ell\right| H_1 \left|m\right> \left<m\right| H_1 \left|n\right> \left[\frac{1}{E_m - E_n} - \frac{1}{E_\ell - E_m} \right] \left|\ell\right> \left<n\right| \,. \end{aligned} \tag{4.54}$$

Now, specifically for our problem the eigenstates of H_0 are many-particle Fock states $\left|n\right> = \left|\{n_{\boldsymbol{k}}\}, \{n_{\boldsymbol{q}}\}\right>$ with $n_{\boldsymbol{k}} \in \{0,1\}$ and $n_{\boldsymbol{q}} \in \{0,1,2,3,\ldots\}$. This leads to an effective interaction Hamiltonian transforming the state $\left|n\right>$ into the state $\left|\ell\right>$. To obtain an effective Hamiltonian for the electrons only, we have to trace over the phonons. This requires that the incoming states $\left|n\right>$ and the outgoing states $\left|\ell\right>$ must have the same phonon configurations. Therefore, when the first process $\left<m\right| H_1 \left|n\right>$ describes the absorbtion of a particular phonon, the second $\left<\ell\right| H_1 \left|m\right>$ must include an emission process of a phonon with the same wavenumber and vice versa.

For example, when the incoming state $\left|n\right>$ has two electrons with $\boldsymbol{k}$ and $\boldsymbol{k'}$, and the first process describes the absorbtion of a phonon of wavenumber $\boldsymbol{q}$, the intermediate state $\left|m\right>$ has two electrons with $\boldsymbol{k}+\boldsymbol{q}$ and $\boldsymbol{k'}$. The second process is then the emission of a phonon with the same wavenumber $\boldsymbol{q}$, such that in the outgoing state $\left|\ell\right>$ one now has two electrons with wavenumbers $\boldsymbol{k}+\boldsymbol{q}$ and $\boldsymbol{k'}-\boldsymbol{q}$. For this process, the energy differences are given by

$$\begin{aligned} &\left|n\right> \hat{=} \left|\boldsymbol{k}, \boldsymbol{k'}\right> \otimes \left|n_{\boldsymbol{q}}\right> \to \left|m\right> \hat{=} \left|\boldsymbol{k}+\boldsymbol{q}, \boldsymbol{k'}\right> \otimes \left|n_{\boldsymbol{q}} - 1\right> \to \left|\ell\right> \hat{=} \left|\boldsymbol{k}+\boldsymbol{q}, \boldsymbol{k'}-\boldsymbol{q}\right> \otimes \left|n_{\boldsymbol{q}}\right> \quad : \\ &E_m - E_n = \epsilon_{\boldsymbol{k}+\boldsymbol{q}} - \epsilon_{\boldsymbol{k}} - \omega_{\boldsymbol{q}}\,, \qquad E_\ell - E_m = \epsilon_{\boldsymbol{k'}-\boldsymbol{q}} - \epsilon_{\boldsymbol{k'}} + \omega_{\boldsymbol{q}}\,. \end{aligned} \tag{4.55}$$

Likewise, the first process could describe the emission of a phonon with wavenumber $\boldsymbol{q}$ by the incoming electron with wavenumber $\boldsymbol{k}$, leading to an intermediate state with an electron at $\boldsymbol{k}-\boldsymbol{q}$ and an additional phonon. This must then be absorbed by the second incoming electron at $\boldsymbol{k'}$, leading to electrons at $\boldsymbol{k}-\boldsymbol{q}$ and $\boldsymbol{k'}+\boldsymbol{q}$ in the outgoing state

$$\begin{aligned} &\left|n\right> \hat{=} \left|\boldsymbol{k}, \boldsymbol{k'}\right> \otimes \left|n_{\boldsymbol{q}}\right> \to \left|m\right> \hat{=} \left|\boldsymbol{k}-\boldsymbol{q}, \boldsymbol{k'}\right> \otimes \left|n_{\boldsymbol{q}} + 1\right> \to \left|\ell\right> \hat{=} \left|\boldsymbol{k}-\boldsymbol{q}, \boldsymbol{k'}+\boldsymbol{q}\right> \otimes \left|n_{\boldsymbol{q}}\right> \quad : \\ &E_m - E_n = \omega_{\boldsymbol{q}} + \epsilon_{\boldsymbol{k}-\boldsymbol{q}} - \epsilon_{\boldsymbol{k}}\,, \qquad E_\ell - E_m = \epsilon_{\boldsymbol{k'}+\boldsymbol{q}} - \epsilon_{\boldsymbol{k'}} - \omega_{\boldsymbol{q}}\,. \end{aligned} \tag{4.56}$$

Now, depending on the number of phonons already present in mode $\boldsymbol{q}$, we will get factors of $n_{\boldsymbol{q}}$ (for phonon absorbtion followed by emission) and $1 + n_{\boldsymbol{q}}$ (for phonon emission followed by absorbtion), respectively. Altogether, the Hamiltonian reads

$$\begin{aligned} H' = H_0 - \frac{1}{2} \sum_{\boldsymbol{k}\boldsymbol{k'}\boldsymbol{q}} \Bigg[& M_{\boldsymbol{k},\boldsymbol{q}} M_{\boldsymbol{k'},-\boldsymbol{q}} n_{\boldsymbol{q}} \left(\frac{1}{\epsilon_{\boldsymbol{k}+\boldsymbol{q}} - \epsilon_{\boldsymbol{k}} - \omega_{\boldsymbol{q}}} - \frac{1}{\epsilon_{\boldsymbol{k'}-\boldsymbol{q}} - \epsilon_{\boldsymbol{k'}} + \omega_{\boldsymbol{q}}} \right) c^\dagger_{\boldsymbol{k}+\boldsymbol{q}} c_{\boldsymbol{k}} c^\dagger_{\boldsymbol{k'}-\boldsymbol{q}} c_{\boldsymbol{k'}} \\ & + M_{\boldsymbol{k},-\boldsymbol{q}} M_{\boldsymbol{k'},+\boldsymbol{q}} (1 + n_{\boldsymbol{q}}) \left(\frac{1}{\epsilon_{\boldsymbol{k}-\boldsymbol{q}} - \epsilon_{\boldsymbol{k}} + \omega_{\boldsymbol{q}}} - \frac{1}{\epsilon_{\boldsymbol{k'}+\boldsymbol{q}} - \epsilon_{\boldsymbol{k'}} - \omega_{\boldsymbol{q}}} \right) c^\dagger_{\boldsymbol{k}-\boldsymbol{q}} c_{\boldsymbol{k}} c^\dagger_{\boldsymbol{k'}+\boldsymbol{q}} c_{\boldsymbol{k'}} \Bigg] \,. \end{aligned} \tag{4.57}$$

Imposing energy conservation

$$\epsilon_{\boldsymbol{k}'\pm\boldsymbol{q}} - \epsilon_{\boldsymbol{k}'} = \epsilon_{\boldsymbol{k}\mp\boldsymbol{q}} - \epsilon_{\boldsymbol{k}}\,, \tag{4.58}$$

we can join the fractions and upon renaming $\boldsymbol{q} \to -\boldsymbol{q}$ we eventually get the effective electron-electron interaction in presence of phonons (the occupation number $n_{\boldsymbol{q}}$ cancels)

$$H' = H_0 + \sum_{\boldsymbol{k}\boldsymbol{k}'\boldsymbol{q}} M_{\boldsymbol{k},\boldsymbol{q}} M_{\boldsymbol{k}',-\boldsymbol{q}} \frac{\omega_{\boldsymbol{q}}}{(\epsilon_{\boldsymbol{k}+\boldsymbol{q}} - \epsilon_{\boldsymbol{k}})^2 - \omega_{\boldsymbol{q}}^2} c^\dagger_{\boldsymbol{k}+\boldsymbol{q}} c_{\boldsymbol{k}} c^\dagger_{\boldsymbol{k}'-\boldsymbol{q}} c_{\boldsymbol{k}'}\,, \tag{4.59}$$

which is the final result for effective phonon-mediated electron-electron interaction. Typically, one approximates that the matrix element in front only depends on $\boldsymbol{q}$, such that $M_{\boldsymbol{k},\boldsymbol{q}} M_{\boldsymbol{k}',-\boldsymbol{q}} \to |M(\boldsymbol{q})|^2 \geq 0$. The spectrum of H' is the same as the spectrum of the original Hamiltonian, and we see that the electron-electron interaction may become attractive when

$$\left|\epsilon_{\boldsymbol{k}+\boldsymbol{q}} - \epsilon_{\boldsymbol{k}}\right| < \omega_{\boldsymbol{q}}\,. \tag{4.60}$$

This affects a small region near the Fermi surface, and one often strongly simplifies by approximating the complicated $\boldsymbol{q}\boldsymbol{k}\boldsymbol{k}'$ dependence with a single constant $V > 0$

$$H' = H_0 - \frac{V}{2} \sum_{\boldsymbol{k}\boldsymbol{k}'\boldsymbol{q}} c^\dagger_{\boldsymbol{k}+\boldsymbol{q}} c_{\boldsymbol{k}} c^\dagger_{\boldsymbol{k}'-\boldsymbol{q}} c_{\boldsymbol{k}'} \delta(\epsilon_{\boldsymbol{k}+\boldsymbol{q}} - \epsilon_{\boldsymbol{k}}, \epsilon_{\boldsymbol{k}'-\boldsymbol{q}} - \epsilon_{\boldsymbol{k}'}) \Theta\left(\omega_{\boldsymbol{q}} - \left|\epsilon_{\boldsymbol{k}+\boldsymbol{q}} - \epsilon_{\boldsymbol{k}}\right|\right)\,. \tag{4.61}$$

To have a net attractive effect, this contribution must overcome the intrinsic electronic Coulomb repulsion (which we neglected in our treatment so far).

4.4 Scaling of electric Resistance

To get an idea on the temperature dependence of the electric conductivity of metals, the simplest models just analyze single electron-phonon scattering events [4]. For example, when a single phonon of crystal momentum $\boldsymbol{q} = \boldsymbol{k} - \boldsymbol{k}'$ is absorbed, or emitted, energy conservation and crystal momentum conservation require that

$$\epsilon_{\boldsymbol{k}} = \epsilon_{\boldsymbol{k}'} \pm \hbar\omega_{\boldsymbol{k}-\boldsymbol{k}'}\,. \tag{4.62}$$

Here, we have neglected Umklapp processes. Compared to the electronic energy scales $\epsilon_{\boldsymbol{k}}$, the phonon contribution – which is bounded by $\hbar\omega_D$ – is minute. To obey the conservation of both energy and total crystal momentum with the constraint that the allowed phonon energies are bound by the Debye frequency, it follows that the energies of the incoming and outgoing electron are approximately equal. Further, one has to take the dependence of the electron-phonon matrix element on the phonon energy into account and also that scattering processes perpendicular to the original momentum are most effective in reducing the current.

First, we can address the high-temperature regime (defined by $k_B T \gg \hbar\omega_D$) by directly expanding the Bose-Einstein distribution for the phonons

$$n_{\boldsymbol{q}} = \frac{1}{e^{\beta\hbar\omega_{\boldsymbol{q}}} - 1} \approx \frac{k_B T}{\hbar\omega_{\boldsymbol{q}}}\,. \tag{4.63}$$

Accordingly, the number of phonons scales linearly with temperature, and so does the resistance, as the number of scattering events is directly proportional to the number of phonons

$$R \propto T\,, \qquad k_B T \gg \hbar\omega_D\,. \tag{4.64}$$

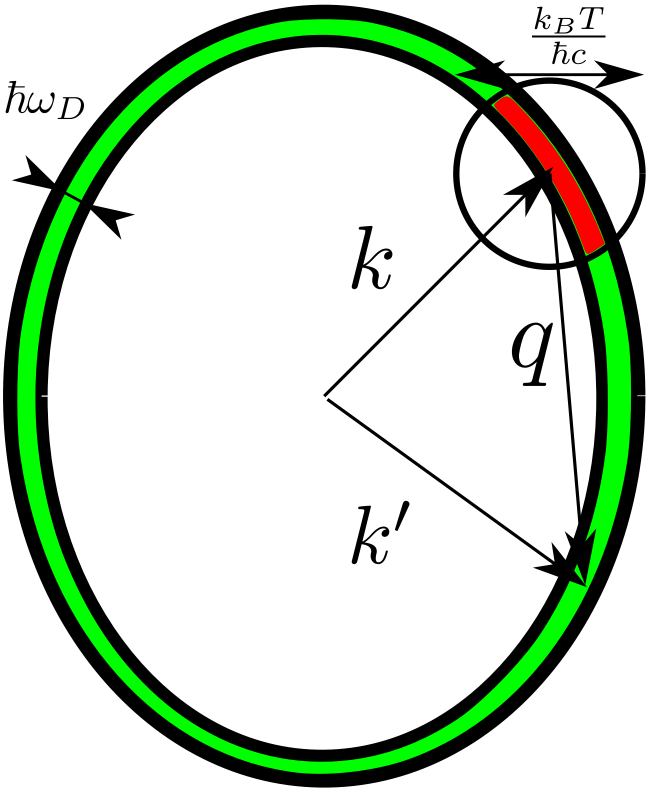

Figure 4.6: Sketch of the constraints on electron-phonon scattering in k space. The wave vectors of incoming and outgoing electrons $\boldsymbol{k}$ and $\boldsymbol{k'}$ must have very similar energies close to the Fermi energy, since the phonon energies are bounded by $\hbar\omega_D$ (ring). At low temperatures, only acoustic phonons are occupied with $\omega_{\boldsymbol{q}} = cq$ (smaller black circle), and in three dimensions the area of the resulting region scales as $q^2 \propto T^2$ (red).

When the temperature is significantly below the so-called Debye temperature $k_B T \ll \hbar\omega_D = k_B T_D$, one will actually only occupy the low-energy phonon modes. Therefore, only these phonon modes can be absorbed. The same actually holds true for emission, since we assume that the electrons and phonons are in thermal equilibrium, such that electrons emitting a phonon can only relax by small amounts of energy as all sites below the Fermi surface are practically blocked. We discussed before that these are just the acoustic modes obeying

$$\omega_{\boldsymbol{q}} = cq \,, \tag{4.65}$$

where c was the velocity of sound. Therefore, in this limit, only phonon modes with

$$q \approx \frac{k_B T}{\hbar c} \tag{4.66}$$

will participate in these scattering events. Compared to the full Fermi surface, the area in q-space that provides suitable phonons scales quadratically in q and hence quadratically in T, see Fig. 4.6. A further factor of q (and hence T) comes in as the square of the effective electron-phonon coupling matrix element scales linearly in the phonon frequency for small phonon frequencies, such that the inverse electron-phonon scattering rate scales as

$$\frac{1}{\tau_{\text{el-ph}}} \propto T^3 \,, \qquad k_B T \ll \hbar\omega_D \,. \tag{4.67}$$

However, we are still not done. The effective scattering rate will sensitively depend on the angle between incoming and outgoing electrons. For example, when electrons were scattered only in forward and backward directions, on average these effects would cancel and the net effect of phonon scattering would not reduce the electronic current. Therefore, the effective scattering rate is given by

$$1/\tau_{\text{eff}} = (1 - \cos(\theta))/\tau_{\text{el-ph}} \,, \tag{4.68}$$

where we further compute

$$(1-\cos(\theta)) = 2\sin^2(\theta/2) \approx 2\left(\frac{q/2}{k_F}\right)^2 = \frac{1}{2}\frac{q^2}{k_F^2} \propto T^2\,. \tag{4.69}$$

From these simple power-counting arguments, we conclude the Bloch T^5 law at low temperatures

$$R \propto T^5\,, \qquad k_B T \ll \hbar\omega_D\,. \tag{4.70}$$

4.5 Superconductivity

The electric resistance in metals is controlled by impurities, electron-electron, and electron-phonon scattering. Normally, one would expect a resistance to scale with temperature as

$$R(T) = R_0 + aT^2 + bT^5\,. \tag{4.71}$$

Here, R_0 depends on the concentration of impurities, a describes the electron-electron interaction, and b the electron-phonon scattering.

In 1908, Heike Kamerlingh-Onnes [2] succeeded in putting helium in its fluid state and further cooling it down to 1K. In 1911, his lab reported to complete vanishing of electric resistance in mercury at a temperature of $T_c = 4.15K$, whereas it followed the empirical curve for temperatures above T_c pretty well

$$R_{Hg}(T < 4.15K) = 0\,, \tag{4.72}$$

see Fig. 4.7.

This discovery, which led to many investigations later-on, had tremendous impact, since without resistance, one can transport electric currents without losses. Soon many other metals were investigated for superconductivity, but up until 1986 he highest critical temperature was at $T_c \approx 23K$. This was a hurdle for technological application, since liquid helium had to be used for cooling, which was expensive. In 1986, high-temperature superconductivity has been reported by Bednorz and Müller, which with a critical temperature of $T_c \approx 35K$ allowed to cool with liquid hydrogen (which was cheaper). Shortly after, other materials were found, and today the critical temperature is around $T_c \approx 135K$ for high-temperature ceramic superconductors, which allows cooling these materials with liquid nitrogen.

Beyond the breakdown of electric resistance, superconductors also exhibit the **Meißner-Ochsenfeld** effect: Superconductors exhibit perfect diamagnetism. An applied external magnetic field induces ring currents in a superconductor, which can – due to the missing electric resistance – in principle be arbitrarily strong and thus is able to completely compensate the external field H

$$\boldsymbol{B} = \boldsymbol{H} + 4\pi\boldsymbol{M} = 0\,. \tag{4.73}$$

This will only work up to a critical field strength, which can be phenomenologically related to the critical temperature in absence of a magnetic field via

$$H_c(T) = H_c(0)\left[1 - \frac{T^2}{T_c^2}\right]\,. \tag{4.74}$$

The qualitative understanding of this formula is that the magnetic field provides the energy to split Cooper pairs, leading to the breakdown of superconductivity, as we shall see later.

---

[2] H. Kamerling-Onnes (1853–1926) was a dutch physicist.

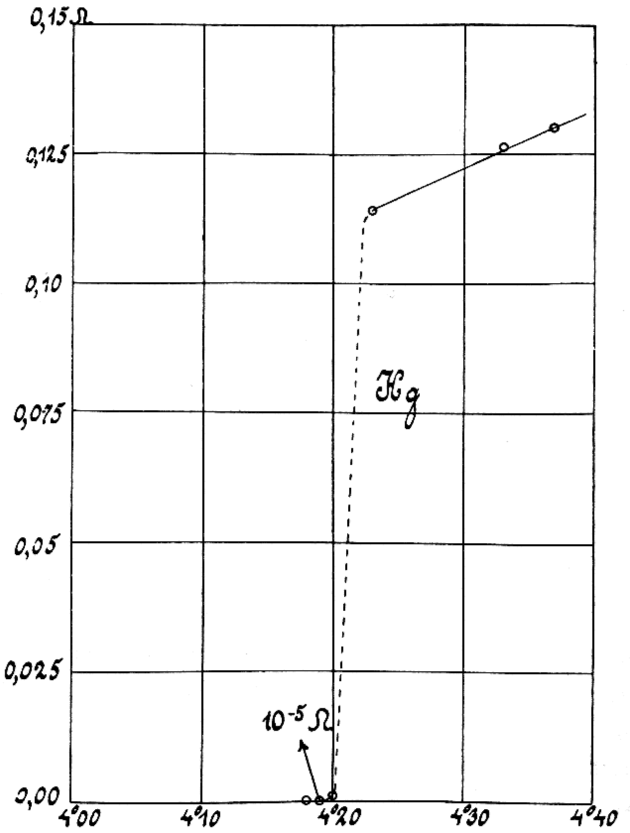

Figure 4.7: Electric resistance of mercury versus temperature, original publication of Kamerlingh-Onnes (1911), KAWA, December 30, 1911; scanned from Boston Studies in the Philosophy of Science volume 124 (page 269). Secondary source: Wikipedia.

Depending on the dependence of the magnetic field, one generally distinguishes between type I and type II superconductors. In Type I superconductors, superconductivity breaks down completely (i.e., both magnetic field behaviour and resistance return to their normal value) when the critical field strength is exceeded. In type II superconductors, the electric resistance still vanishes beyond a first critical field strength, but the magnetic field becomes finite within the superconductor. In this phase, the material is split: Within small flux tubes, the material is pierced by regions of finite magnetic field, and superconductivity breaks down completely when the flux tubes cover the whole material, which defines a second critical field strength.

4.5.1 Formation of Cooper pairs

In the previous discussions, we learned that the effective interaction of electrons may be attractive. It has also become plausible that the interaction is attractive only between a fraction of electrons, particularly those with wavenumbers obeying both

$$\left|\epsilon_{\boldsymbol{k}+\boldsymbol{q}} - \epsilon_{\boldsymbol{k}}\right|, \left|\epsilon_{\boldsymbol{k}'-\boldsymbol{q}} - \epsilon_{\boldsymbol{k}'}\right| < \hbar\omega_D\,, \tag{4.75}$$

while conserving the total momentum $\boldsymbol{K}$

$$\boldsymbol{K} = \boldsymbol{k} + \boldsymbol{k}' = \boldsymbol{k} + \boldsymbol{q} + \boldsymbol{k}' - \boldsymbol{q}\,. \tag{4.76}$$

The first condition constrains the energy of the participating electrons onto a thin shell around the Fermi surface

$$E_F \le \epsilon_{\boldsymbol{k}}, \epsilon_{\boldsymbol{k}'} \le E_F + \hbar\omega_D\,. \tag{4.77}$$

The thickness of this shell is constrained by the participating phonon branches and the matrix element of the electron-phonon interaction. The second (momentum-conserving) condition

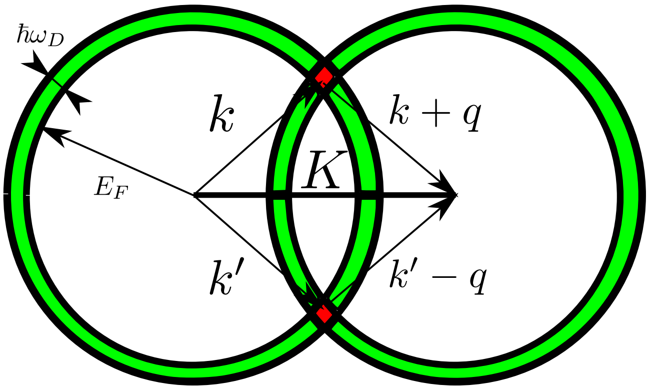

Figure 4.8: Visualization of the energy conservation condition (4.75) – green shells – and the momentum conservation condition (4.76) – black arrows. The inner circles denote the Fermi surface, and the shell thickness the maximum phonon energy. For general total momenta $\boldsymbol{K}$, only a small fraction of all electrons will participate in the attractive interaction (red regions), only for $\boldsymbol{K}=0$ the complete shells will contribute.

shows that if $\boldsymbol{K}$ is chosen arbitrary, only a small fraction of all electrons in $\boldsymbol{k}$-space are obeying some attractive interaction, see Fig. 4.8. There, it is visible that processes with $\boldsymbol{K}=0$ will yield the dominant contribution to the attractive interaction. We can therefore eliminate the variable $\boldsymbol{k'}$ by considering only the dominant contribution with $\boldsymbol{k'}=-\boldsymbol{k}$. Equipping Eq. (4.61) with spin degrees of freedom, we get

$$\begin{aligned} H' &= H_0 - \frac{V}{2}\sum_{\boldsymbol{kq}}\sum_{\sigma\sigma'} c^\dagger_{+\boldsymbol{k}+\boldsymbol{q},\sigma} c_{\boldsymbol{k},\sigma} c^\dagger_{-\boldsymbol{k}-\boldsymbol{q},\sigma'} c_{-\boldsymbol{k},\sigma'} \delta(\epsilon_{\boldsymbol{k}+\boldsymbol{q}} - \epsilon_{\boldsymbol{k}}, \epsilon_{-\boldsymbol{k}-\boldsymbol{q}} - \epsilon_{-\boldsymbol{k}}) \Theta(\hbar\omega_{\boldsymbol{q}} - \left|\epsilon_{\boldsymbol{k}+\boldsymbol{q}} - \epsilon_{\boldsymbol{k}}\right|) \\ &= H_0 - \frac{V}{2}\sum_{\boldsymbol{kq}}\sum_{\sigma\sigma'} c^\dagger_{+\boldsymbol{k}+\boldsymbol{q},\sigma} c^\dagger_{-\boldsymbol{k}-\boldsymbol{q},\sigma'} c_{-\boldsymbol{k},\sigma'} c_{\boldsymbol{k},\sigma} \Theta(\hbar\omega_{\boldsymbol{q}} - \left|\epsilon_{\boldsymbol{k}+\boldsymbol{q}} - \epsilon_{\boldsymbol{k}}\right|)\,. \end{aligned} \tag{4.78}$$

Here, $H_0 = \sum_{\boldsymbol{k}}\sum_\sigma \epsilon(\boldsymbol{k}) c^\dagger_{\boldsymbol{k}\sigma} c_{\boldsymbol{k}\sigma}$ contains the free Hamiltonian of the considered electronic band and $V>0$ is a simplified interaction constant. We would like to find the ground state energy of this interacting Hamiltonian. To obtain it, we use an ansatz for the ground state wave function and minimize the expectation value of the energies with respect to the free parameters. Our ansatz for the ground state is that all states up to the Fermi surface are filled, and in addition we allow for two additional electrons (the Cooper [3] pair)

$$|\Psi_{\sigma\sigma'}\rangle = \sum_{\boldsymbol{k}} a_{\sigma\sigma'}(\boldsymbol{k}) c^\dagger_{+\boldsymbol{k}\sigma} c^\dagger_{-\boldsymbol{k},\sigma'} |\Psi_0\rangle\,, \qquad |\Psi_0\rangle = \left[\prod_{\sigma''}\prod_{k'\le k_F} c^\dagger_{\boldsymbol{k'},\sigma''} |0\rangle\right]\,. \tag{4.79}$$

In this ansatz, summation over $\boldsymbol{k}$ only runs over the states of the shell around the Fermi surface. Further, the coefficients $a_{\sigma\sigma'}(\boldsymbol{k}) \in \mathbb{C}$ are a priori unknown, but by minimizing the energy functional

$$E = \langle\Psi_{\sigma\sigma'}| H' |\Psi_{\sigma\sigma'}\rangle \tag{4.80}$$

under the side-constraint of unit normalization $\langle\Psi_{\sigma\sigma'}|\Psi_{\sigma\sigma'}\rangle = 1$, which leads to

$$\sum_{\boldsymbol{k}} \left|a_{\sigma\sigma'}(\boldsymbol{k})\right|^2 = 1\,, \tag{4.81}$$

we obtain a reasonable estimate of the ground state energy. In particular, we have (we set the energy scale such that the filled states up to the Fermi energy have energy zero)

$$\begin{aligned} \langle\Psi_{\sigma\sigma'}| H' |\Psi_{\sigma\sigma'}\rangle &= \sum_{\boldsymbol{k}} (\epsilon_{\boldsymbol{k}} + \epsilon_{-\boldsymbol{k}}) |a_{\sigma\sigma'}(\boldsymbol{k})|^2 - \frac{V}{2}\sum_{\bar\sigma\bar\sigma'}\sum_{\boldsymbol{kq}} \langle\Psi_{\sigma\sigma'}| c^\dagger_{\boldsymbol{k}+\boldsymbol{q},\bar\sigma} c^\dagger_{-\boldsymbol{k}-\boldsymbol{q},\bar\sigma'} c_{-\boldsymbol{k},\bar\sigma'} c_{+\boldsymbol{k},\bar\sigma} |\Psi_{\sigma\sigma'}\rangle \\ &= +\sum_{\boldsymbol{k}} 2\epsilon_{\boldsymbol{k}} |a_{\sigma\sigma'}(\boldsymbol{k})|^2 - V\sum_{\boldsymbol{kq}} a^*_{\sigma\sigma'}(\boldsymbol{k}+\boldsymbol{q}) a_{\sigma\sigma'}(\boldsymbol{k})\,. \end{aligned} \tag{4.82}$$

---

[3] Leon N. Cooper (1930–) is an American physicist and Nobel Prize laureate.

Here, the first term denotes the energy from the two additional electrons created with opposite momenta, and the last term comes from the expectation value of the interaction with our ansatz wave function. The factor of 2 has cancelled in the evaluation of the last line, since we have the two pairing possibilities of $\boldsymbol{k}+\boldsymbol{q}=\boldsymbol{k'}$ and $\bar{\sigma}=\sigma$ and $\bar{\sigma}'=\sigma'$ or $-\boldsymbol{k}-\boldsymbol{q}=\boldsymbol{k'}$ and $\bar{\sigma}'=\sigma$ and $\bar{\sigma}=\sigma'$, where $\boldsymbol{k'}$ is the summation index in our wave function ansatz and σ and σ' are its spin indices.

Adding the normalization condition with a Lagrange multiplier, we eventually have to minimize

$$\begin{aligned} E = &+\sum_{\boldsymbol{k}} 2\epsilon_{\boldsymbol{k}} a^*_{\sigma\sigma'}(\boldsymbol{k}) a_{\sigma\sigma'}(\boldsymbol{k}) - V \sum_{\boldsymbol{kq}} a^*_{\sigma\sigma'}(\boldsymbol{k}+\boldsymbol{q}) a_{\sigma\sigma'}(\boldsymbol{k}) \\ &+ \lambda \left(1 - \sum_{\boldsymbol{k}} a^*_{\sigma\sigma'}(\boldsymbol{k}) a_{\sigma\sigma'}(\boldsymbol{k})\right) \end{aligned} \tag{4.83}$$

with respect to the parameters λ and $a_{\sigma\sigma'}(\boldsymbol{k})$. Now, a derivative with respect to λ does of course just reproduce the normalization condition. In contrast, derivatives with respect to $a^*_{\sigma\sigma'}(\boldsymbol{k})$ yield

$$0 = (2\epsilon_{\boldsymbol{k}} - \lambda) a_{\sigma\sigma'}(\boldsymbol{k}) - V \sum_{\boldsymbol{k'}} a_{\sigma\sigma'}(\boldsymbol{k'})\,. \tag{4.84}$$

Defining $c_{\sigma\sigma'} = \sum_{\boldsymbol{k}} a_{\sigma\sigma'}(\boldsymbol{k})$, we can write

$$a_{\sigma\sigma'}(\boldsymbol{k}) = \frac{V c_{\sigma\sigma'}}{2\epsilon_{\boldsymbol{k}} - \lambda}\,, \tag{4.85}$$

and by simply summing over $\boldsymbol{k}$ we get

$$c_{\sigma\sigma'} = c_{\sigma\sigma'} \sum_{\boldsymbol{k}} \frac{V}{2\epsilon_{\boldsymbol{k}} - \lambda}\,. \tag{4.86}$$

When $c_{\sigma\sigma'} \neq 0$ – we will discuss later hat this implies $\sigma \neq \sigma'$, we can divide by this quantity, which eventually results into the constraint

$$1 = \sum_{\boldsymbol{k}} \frac{V}{2\epsilon_{\boldsymbol{k}} - \lambda}\,. \tag{4.87}$$

We still have to determine the Lagrange parameter. From multiplying the equation (4.84) with $a^*_{\sigma\sigma'}(\boldsymbol{k})$ and performing a subsequent summation over $\boldsymbol{k}$, we obtain (compare Eq. (4.82))

$$\begin{aligned} 0 &= \sum_{\boldsymbol{k}} (2\epsilon_{\boldsymbol{k}} - \lambda) \left|a_{\sigma\sigma'}(\boldsymbol{k})\right|^2 - V \sum_{\boldsymbol{kk'}} a^*_{\sigma\sigma'}(\boldsymbol{k}) a_{\sigma\sigma'}(\boldsymbol{k'}) \\ &= E - \lambda \sum_{\boldsymbol{k}} \left|a_{\sigma\sigma'}(\boldsymbol{k})\right|^2 = E - \lambda\,, \end{aligned} \tag{4.88}$$

which means that the Lagrange multiplier is just the energy. This implies that the energy is implicitly determined by the equation

$$1 = \sum_{\boldsymbol{k}} \frac{V}{2\epsilon_{\boldsymbol{k}} - E} = V \int_{E_F}^{E_F + \hbar\omega_D} \frac{\rho(\epsilon)}{2\epsilon - E} d\epsilon \approx V \rho(E_F) \frac{1}{2} \ln \frac{2E_F + 2\hbar\omega_D - E}{2E_F - E}\,, \tag{4.89}$$

where we have used that the electronic density of states hardly changes over the small energy interval defined by $\hbar\omega_D$. The Debye freqency ω_D represents some characteristic energy cutoff for the maximum frequency of the participating phonons. Exponentiating the equation yields

$$e^{2/(V\rho(E_F))} = \frac{2E_F + 2\hbar\omega_D - E}{2E_F - E}\,, \tag{4.90}$$

which yields for the energy

$$E = 2E_F + \frac{2\hbar\omega_D}{1 - e^{2/(V\rho(E_F))}} \approx 2E_F - e^{-\frac{2}{V\rho(E_F)}} 2\hbar\omega_D\,. \tag{4.91}$$

Here, we have used that the electron-phonon interaction is typically small and approximated the fraction accordingly. Since the first term corresponds to the energy that the free electron pair would have in absence of any attractive interaction, we get that the energy of the ground state is reduced in comparison to the free electron case. The **energy decrease of the Cooper pair** becomes [14]

$$\Delta E = -2\hbar\omega_D \exp\left\{-\frac{2}{V\rho(E_F)}\right\}\,. \tag{4.92}$$

This depends on the characteristic energy of the mediating phonon $\hbar\omega_D$, the electronic density of states at the Fermi surface $\rho(E_F)$, and the coupling constant V. In particular, we find that the dependence on V is non-analytic at $V = 0$, such that this phenomenon cannot be understood perturbatively.

In principle, a Cooper pair mechanism would work for arbitrary spin configuration $\sigma\sigma'$. However, in the course of the derivation we used that $c_{\sigma\sigma'} \neq 0$. The total wave function must be anti-symmmetric under exchange of both electrons (i.e., $\boldsymbol{r}_1 \leftrightarrow \boldsymbol{r}_2$ and $\sigma \leftrightarrow \sigma'$). For equal spins, the spin contribution is obviously symmetric under exchange, such that the spatial component of the wavefunction must be antisymmetric. Specifically, it must vanish when the two electrons are at the same place. Since one generally has

$$\Psi_{\sigma\sigma'}(\boldsymbol{r}_1 - \boldsymbol{r}_2) = \langle \boldsymbol{r}_1\boldsymbol{r_2}|\Psi_{\sigma\sigma'}\rangle \propto \sum_{\boldsymbol{k}} a_{\sigma\sigma'}(\boldsymbol{k}) e^{+\mathrm{i}\boldsymbol{k}\boldsymbol{r_1}} e^{-\mathrm{i}\boldsymbol{k}\boldsymbol{r_2}}\,, \tag{4.93}$$

we would get for equal spins from $\Psi_{\sigma\sigma}(0) = 0$ that $c_{\sigma\sigma} = \sum_{\boldsymbol{k}} a_{\sigma\sigma}(\boldsymbol{k}) = 0$, which is a contradiction with the assumption used in the derivation. Therefore, the **spins in a standard Cooper pair are different**

$$|\Psi_{\uparrow\downarrow}\rangle = \sum_{\boldsymbol{k}} a_{\uparrow\downarrow}(\boldsymbol{k}) c^\dagger_{+\boldsymbol{k}\uparrow} c^\dagger_{-\boldsymbol{k}\downarrow} |\Psi_0\rangle\,, \tag{4.94}$$

which in general describes an entangled superposition of states with single electron pairs above the Fermi sea with opposite momenta and different spin. Note though that more sophisticated pairing mechanisms are conceivable, allowing in principle also for pairing of electrons with equal spins.

4.5.2 BCS theory

Shortly after the pioneering work of Cooper, in 1957 Bardeen [4], Cooper and Schrieffer [5] (BCS) published a paper [15] which shaped our understanding of superconductivity in metals and

---

[4] J. Bardeen (1908–1991) was an american physicist and Nobel laureate.

[5] J. R. Schrieffer (1931–) is an americal physicist and Nobel laureate.

which earned them the Nobel price in 1972. Superconductivity in high-temperature (ceramic) superconductors is still not satisfactorily understood.

The Hamiltonian for BCS theory is given by

$$H = \sum_{\boldsymbol{k}} \sum_{\sigma} \epsilon_{\boldsymbol{k}} c^\dagger_{\boldsymbol{k}\sigma} c_{\boldsymbol{k}\sigma} - V \sum_{\boldsymbol{k}\boldsymbol{k'}} c^\dagger_{+\boldsymbol{k'}\uparrow} c^\dagger_{-\boldsymbol{k'}\downarrow} c_{-\boldsymbol{k}\downarrow} c_{+\boldsymbol{k}\uparrow} \,. \tag{4.95}$$

It shall include electron-electron as well as electron-phonon interaction to the extent that $V > 0$ is an effective attractive interaction. Here, the energy of the Fermi surface is set to zero $E_F = 0$, and the summations in this section will always include only modes fulfilling the constraints $\epsilon_{\boldsymbol{k}} \le \hbar\omega_D$ and $\epsilon_{\boldsymbol{k'}} \le \hbar\omega_D$, with ω_D denoting the **Debye frequency**. The Debye [6] frequency is a characteristic phonon frequency (e.g. cutoff due to a narrow phonon branch that couples via the Fröhlich interaction). We could try to treat this BCS Hamiltonian using the Hartree-Fock theory presented in Sec. 3.2.3. However, superconductivity is no single-particle effect, and we will thus from the beginning expect that a single-particle Hamiltonian will not be suitable to treat the phenomenon of superconductivity. Formally, the interaction is not of the simple type of products of particle number operators that we encountered before (unless $\boldsymbol{k} = \boldsymbol{k'}$). Instead, we still like to follow a mean-field approach. We can always write the product of any two operators as

$$AB = \langle A \rangle B + \langle B \rangle A - \langle A \rangle \langle B \rangle + (A - \langle A \rangle)(B - \langle B \rangle) \,. \tag{4.96}$$

Here, the last term describes the fluctuations, and it is neglected within the mean-field approximation

$$(A - \langle A \rangle)(B - \langle B \rangle) \approx 0 \,. \tag{4.97}$$

The art is to identify the correct splitting into operators A and B correctly: Whereas in the conventional Hartree-Fock treatment in Sec. 3.2.3, these were both hermitian operators, here this is no longer the case. Thus, we factorize the BCS Hamiltonian in a different way, expressed by the effective Hamiltonian

$$\begin{aligned}
H_{\text{eff}} &= \sum_{\boldsymbol{k}} \sum_{\sigma} \epsilon_{\boldsymbol{k}} c^\dagger_{\boldsymbol{k}\sigma} c_{\boldsymbol{k}\sigma} \\
&\quad - V \sum_{\boldsymbol{k}\boldsymbol{k'}} \left\langle c^\dagger_{+\boldsymbol{k'}\uparrow} c^\dagger_{-\boldsymbol{k'}\downarrow} \right\rangle_{\text{eff}} c_{-\boldsymbol{k}\downarrow} c_{+\boldsymbol{k}\uparrow} - V \sum_{\boldsymbol{k}\boldsymbol{k'}} \left\langle c_{-\boldsymbol{k}\downarrow} c_{+\boldsymbol{k}\uparrow} \right\rangle_{\text{eff}} c^\dagger_{+\boldsymbol{k'}\uparrow} c^\dagger_{-\boldsymbol{k'}\downarrow} \\
&\quad + V \sum_{\boldsymbol{k}\boldsymbol{k'}} \left\langle c^\dagger_{+\boldsymbol{k'}\uparrow} c^\dagger_{-\boldsymbol{k'}\downarrow} \right\rangle_{\text{eff}} \left\langle c_{-\boldsymbol{k}\downarrow} c_{+\boldsymbol{k}\uparrow} \right\rangle_{\text{eff}} \\
&= \sum_{\boldsymbol{k}} \sum_{\sigma} \epsilon_{\boldsymbol{k}} c^\dagger_{\boldsymbol{k}\sigma} c_{\boldsymbol{k}\sigma} - \Delta^* \sum_{\boldsymbol{k}} c_{-\boldsymbol{k}\downarrow} c_{+\boldsymbol{k}\uparrow} - \Delta \sum_{\boldsymbol{k}} c^\dagger_{+\boldsymbol{k}\uparrow} c^\dagger_{-\boldsymbol{k}\downarrow} + \frac{|\Delta|^2}{V} \,, \\
\Delta &= V \sum_{\boldsymbol{k}} \left\langle c_{-\boldsymbol{k}\downarrow} c_{+\boldsymbol{k}\uparrow} \right\rangle_{\text{eff}} \,,
\end{aligned} \tag{4.98}$$

where Δ^* is the complex conjugate of Δ. The last term expresses a shift of the Hamiltonian and is necessary to avoid overcounting. The only difference to the conventional Hartree-Fock procedure is that we allow now for anomalous expectation values that apparently do not conserve the total particle number. The expectation value Δ will later-on turn out to be the order parameter for the superconductivity. To compute the energy eigenvalues of this effective

---

[6] Peter Joseph William Debye (1884–1966) was a Dutch-American physicist and Nobel laureate.

Hamiltonian, we can bring it into the conventional form by using a Bogoliubov [7] transform, i.e., we perform a symplectic transform to new fermionic creation $\alpha_{\boldsymbol{k}}^\dagger$ and $\beta_{\boldsymbol{k}}^\dagger$ and annihilation operators $\alpha_{\boldsymbol{k}}$ and $\beta_{\boldsymbol{k}}$ that also obey fermionic anticommutation relations. With (in general complex-valued) expansion coefficients $u_{\boldsymbol{k}}$ and $v_{\boldsymbol{k}}$, the transformation reads

$$\begin{aligned} \alpha_{\boldsymbol{k}} &= u_{\boldsymbol{k}} c_{+\boldsymbol{k}\uparrow} - v_{\boldsymbol{k}} c_{-\boldsymbol{k}\downarrow}^\dagger \,, & \alpha_{\boldsymbol{k}}^\dagger &= u_{\boldsymbol{k}}^* c_{+\boldsymbol{k}\uparrow}^\dagger - v_{\boldsymbol{k}}^* c_{-\boldsymbol{k}\downarrow} \,, \\ \beta_{\boldsymbol{k}} &= u_{\boldsymbol{k}} c_{-\boldsymbol{k}\downarrow} + v_{\boldsymbol{k}} c_{+\boldsymbol{k}\uparrow}^\dagger \,, & \beta_{\boldsymbol{k}}^\dagger &= u_{\boldsymbol{k}}^* c_{-\boldsymbol{k}\downarrow}^\dagger + v_{\boldsymbol{k}}^* c_{+\boldsymbol{k}\uparrow} \,. \end{aligned} \tag{4.99}$$

It should be kept in mind that Bogoliubov transforms need to preserve the fermionic anticommutation relations, which imposes further constraints on the coefficients. Fermionic and bosonic Bogoliubov transforms can be generalized to transformations between an arbitrary number of modes, but here we see that it suffices to couple only two modes of positive and negative momenta. With the above transform, one can now check that

$$\{\alpha_{\boldsymbol{k}}, \beta_{\boldsymbol{k'}}\} = 0 \,, \qquad \{\alpha_{\boldsymbol{k}}, \beta_{\boldsymbol{k'}}^\dagger\} = 0 \,, \qquad \{\alpha_{\boldsymbol{k}}, \alpha_{\boldsymbol{k'}}^\dagger\} = \{\beta_{\boldsymbol{k}}, \beta_{\boldsymbol{k'}}^\dagger\} = (|u_k|^2 + |v_k|^2)\delta_{\boldsymbol{k}\boldsymbol{k'}} \,, \tag{4.100}$$

where we see that we need to demand

$$|u_k|^2 + |v_k|^2 = 1 \tag{4.101}$$

to preserve the anticommutation relations. Furthermore, one can actually see that although the effective Hamiltonian does not commute with the total particle number operator, the expectation value of the commutator vanishes, which means that the expectation value of the particle number is indeed conserved also under the evolution of the effective Hamiltonian

$$\left\langle \left[H_{\text{eff}}, \sum_{\boldsymbol{q}} \left(c_{\boldsymbol{q}\uparrow}^\dagger c_{\boldsymbol{q}\uparrow} + c_{\boldsymbol{q}\downarrow}^\dagger c_{\boldsymbol{q}\downarrow} \right) \right] \right\rangle = \left\langle -2\Delta^* \sum_{\boldsymbol{k}} c_{-\boldsymbol{k}\uparrow} c_{+\boldsymbol{k}\downarrow} + 2\Delta \sum_{\boldsymbol{k}} c_{+\boldsymbol{k}\downarrow}^\dagger c_{-\boldsymbol{k}\uparrow}^\dagger \right\rangle = 0 \,. \tag{4.102}$$

The general strategy is now to invert the transformation (4.99), we just state the results for two annihilation operators (the rest follows from general symmetry arguments)

$$c_{\boldsymbol{k}\uparrow} = u_{\boldsymbol{k}}^* \alpha_{\boldsymbol{k}} + v_{\boldsymbol{k}} \beta_{\boldsymbol{k}}^\dagger \,, \qquad c_{-\boldsymbol{k}\downarrow} = -v_{\boldsymbol{k}} \alpha_{\boldsymbol{k}}^\dagger + u_{\boldsymbol{k}}^* \beta_{\boldsymbol{k}} \,. \tag{4.103}$$

Not having any idea on the mean-field Hamiltonian, we would have started from such a mapping with a priori unknown coefficients and would then that the Hamiltonian assumes the form

$$H_{\text{eff}} = \sum_{\boldsymbol{k}} \left[\lambda_{\boldsymbol{k}\alpha} \alpha_{\boldsymbol{k}}^\dagger \alpha_{\boldsymbol{k}} + \lambda_{\boldsymbol{k}\beta} \beta_{\boldsymbol{k}}^\dagger \beta_{\boldsymbol{k}} \right] + \sigma \,. \tag{4.104}$$

The additional requirement that there are not terms proportional to quasi-particle non-conserving terms such as $\alpha_{\boldsymbol{k}}\beta_{\boldsymbol{k}}$ eventually fixes the transform and determines the $u_{\boldsymbol{k}}$ and $v_{\boldsymbol{k}}$ parameters. We just state the result here. In fact, it is possible to choose the Bogoliubov coefficients real and positive

$$u_k^2 = \frac{1}{2}\left(1 + \frac{\epsilon_k}{\sqrt{\epsilon_k^2 + |\Delta|^2}}\right) \,, \qquad v_k^2 = \frac{1}{2}\left(1 - \frac{\epsilon_k}{\sqrt{\epsilon_k^2 + |\Delta|^2}}\right) \,. \tag{4.105}$$

---

[7] Nikolai Nikolajewitsch Bogoljubow (1909–1992) was a soviet theoretical physicist and mathematician.

With these parameters, the effective Hamiltonian becomes diagonal

$$H_{\text{eff}} = \sum_{\boldsymbol{k}} \sqrt{\epsilon_{\boldsymbol{k}}^2 + |\Delta|^2} \left(\alpha_{\boldsymbol{k}}^\dagger \alpha_{\boldsymbol{k}} + \beta_{\boldsymbol{k}}^\dagger \beta_{\boldsymbol{k}} \right) + \sum_{\boldsymbol{k}} \left(\epsilon_{\boldsymbol{k}} - \sqrt{\epsilon_{\boldsymbol{k}}^2 + |\Delta|^2} \right) + \frac{|\Delta|^2}{V} . \tag{4.106}$$

This means that we can approximately describe the effective dynamics under the full BCS Hamiltonian (4.95) just with an effective single-particle Hamiltonian, just within a rotated particle basis. If $\Delta \neq 0$ can be found, this means that all effective electron-electron interactions will be gone, from which we can intuitively understand that such scattering processes will no longer hinder electronic transport. Formally, non-vanishing Δ means that the quasiparticle excitation energy is always bounded by value $|\Delta|$ from below.

However, the single-particle excitation energies $\sqrt{\epsilon_{\boldsymbol{k}}^2 + |\Delta|^2}$ (which depend on the order parameter Δ), still have to be determined self-consistently. This is most easily calculated by inserting the corresponding Bogoliubov transform in the order parameter

$$\begin{aligned}
\Delta &= V \sum_{\boldsymbol{k}} \left\langle c_{-\boldsymbol{k}\downarrow} c_{+\boldsymbol{k}\uparrow} \right\rangle_{\text{eff}} = V \sum_{\boldsymbol{k}} \left\langle \left(-v_{\boldsymbol{k}} \alpha_{\boldsymbol{k}}^\dagger + u_{\boldsymbol{k}}^* \beta_{\boldsymbol{k}} \right) \left(u_{\boldsymbol{k}}^* \alpha_{\boldsymbol{k}} + v_{\boldsymbol{k}} \beta_{\boldsymbol{k}}^\dagger \right) \right\rangle_{\text{eff}} \\
&= V \sum_{\boldsymbol{k}} \left[-u_k^* v_k \left\langle \alpha_{\boldsymbol{k}}^\dagger \alpha_{\boldsymbol{k}} \right\rangle_{\text{eff}} + u_k^* v_k \left\langle 1 - \beta_{\boldsymbol{k}}^\dagger \beta_{\boldsymbol{k}} \right\rangle_{\text{eff}} \right] \\
&= V \sum_{\boldsymbol{k}} \frac{\Delta}{\sqrt{\epsilon_{\boldsymbol{k}}^2 + |\Delta|^2}} \left(\frac{1}{2} - f(\sqrt{\epsilon_{\boldsymbol{k}}^2 + |\Delta|^2}) \right) = \frac{V\Delta}{2} \sum_{\boldsymbol{k}} \frac{1}{\sqrt{\epsilon_{\boldsymbol{k}}^2 + |\Delta|^2}} \tanh \frac{\beta \sqrt{\epsilon_{\boldsymbol{k}}^2 + |\Delta|^2}}{2} .
\end{aligned} \tag{4.107}$$

In the last step, we have inserted the Fermi function with $\mu = 0$ (also all energies are counted with respect to the Fermi energy). This equation is always trivially solved by $\Delta = 0$. Inserting $\Delta = 0$ in the coefficients of the Bogoliubov transform (4.105), we see that $u_k \to 1$ and $v_k \to 0$, such that the trivial quasi-particles described by $\alpha_{\boldsymbol{k}} \to c_{+\boldsymbol{k}\uparrow}$ and $\beta_{\boldsymbol{k}} \to c_{-\boldsymbol{k}\downarrow}$ are just the usual electrons with spin up and spin down, respectively. To find a non-trivial solution, we divide by Δ, which eventually yields the self-consistency BCS equation (also called BCS gap equation).

Box 17 (BCS self-consistency equation) *The non-trivial value of the BCS order parameter is implicitly determined by the solution of*

$$1 = \frac{V}{2} \sum_{\boldsymbol{k}} \frac{1}{\sqrt{\epsilon_{\boldsymbol{k}}^2 + |\Delta|^2}} \tanh \frac{\beta \sqrt{\epsilon_{\boldsymbol{k}}^2 + |\Delta|^2}}{2} . \tag{4.108}$$

Nontrivial solutions of this equation do not always exist. For example, at high temperatures ($\beta \to 0$), the r.h.s. of the above equation will always be small, such that the equality cannot be fulfilled. To the contrary, for small temperatures, we can approximate the tanh function by one, and a non-trivial solution can exist

$$1 \approx \frac{V}{2} \int_{-\hbar\omega_D}^{\hbar\omega_D} \frac{\rho(\epsilon)}{\sqrt{\epsilon^2 + |\Delta|^2}} d\epsilon \approx V\rho(E_F) \int_0^{\hbar\omega_D} \frac{1}{\sqrt{\epsilon^2 + |\Delta|^2}} d\epsilon = V\rho(E_F) \text{arcsinh} \left(\frac{\hbar\omega_D}{|\Delta|} \right) . \tag{4.109}$$

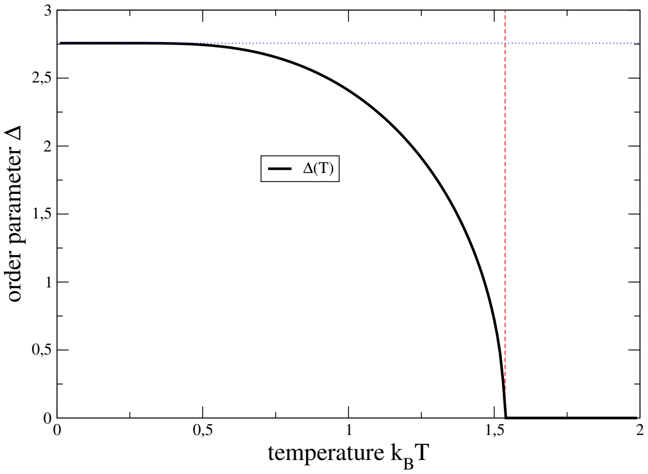

Figure 4.9: Plot of the order parameter $\Delta(T)$ (in arbitrary units) versus temperature $k_B T$ (in arbitrary units) for $V\rho(E_F) = 0.5$ and $\hbar\omega_D = 10$ a.u. Horizontal and vertical dashed lines represent analytical estimates (4.110) (with sinh) and (4.112), respectively.

Here, $\rho(E_F)$ is the unperturbed electronic density of states at the Fermi energy. Solving for the order parameter we get

$$|\Delta| = \frac{\hbar\omega_D}{\sinh(1/(V\rho(E_F)))} \approx 2\hbar\omega_D e^{-\frac{1}{V\rho(E_F)}} \,. \tag{4.110}$$

The fact that for large temperatures, Δ strictly vanishes, whereas for small temperatures, it may have a finite value, means that there must be some critical temperature, at which also the non-trivial solution for Δ vanishes. To find it, we consider $\Delta = 0$ in Eq. (4.108) and solve for the temperature

$$1 = V\rho(E_F) \int_0^{\hbar\omega_D} \frac{\tanh(\beta_c \epsilon/2)}{\epsilon} d\epsilon = \int_0^{\beta_c \hbar\omega_D} \frac{\tanh(x)}{x} dx \,. \tag{4.111}$$

Since $\beta_c \hbar\omega_D \gg 1$, we can solve this perturbatively, which eventually yields [3] with the Euler constant γ

$$k_B T_c \approx \frac{2e^\gamma}{\pi} \hbar\omega_D \exp\left\{-\frac{1}{V\rho(E_F)}\right\} \approx 1.14 \hbar\omega_D \exp\left\{-\frac{1}{V\rho(E_F)}\right\} \,. \tag{4.112}$$

First, we see that the critical temperature is proportional to the Debye frequency. This frequency in turn is proportional to the root of the inverse ion mass $\omega_D \propto M^{-1/2}$. When the ions in a crystal are replaced by a different isotope of the same element, the masses will change but all other things will remain the same – as the isotopes of an element have the same chemical properties. This dependence of the critical temperature on the ion mass is known as **isotope effect**, and it was a major success of BCS theory to explain it. Second, we also see that when the electron-phonon coupling $V\rho(E_F)$ is small, the critical temperature is exponentially suppressed. This explains that good metals (in the sense of good conductors) with a small electron-phonon coupling are bad superconductors (with a low critical temperature).

In the general case, the BCS self-consistency equation has to be solved numerically, see Fig. 4.9.

Eventually, we would like to compute the ground state energy of the effective Hamiltonian

$$\begin{aligned}
E_0^{\text{eff}} &= \sum_{\boldsymbol{k}} \left(\epsilon_{\boldsymbol{k}} - \sqrt{\epsilon_{\boldsymbol{k}}^2 + |\Delta|^2}\right) + \frac{|\Delta|^2}{V} \\
&\approx \rho(E_F) \int_{-\hbar\omega_D}^{\hbar\omega_D} \left(\epsilon - \sqrt{\epsilon^2 + |\Delta|^2}\right) d\epsilon + \frac{|\Delta|^2}{V} \\
&= \rho(E_F) \left[-\hbar\omega_D \sqrt{(\hbar\omega_D)^2 + |\Delta|^2} - |\Delta|^2 \text{arcsinh}\left(\frac{\hbar\omega_D}{|\Delta|}\right)\right] + \frac{|\Delta|^2}{V} \\
&= -\rho(E_F)(\hbar\omega_D)^2 \sqrt{1 + \frac{|\Delta|^2}{(\hbar\omega_D)^2}} \approx -\rho(E_F)(\hbar\omega_D)^2 \left(1 + 2e^{-\frac{2}{V\rho(E_F)}}\right) . \qquad (4.113)
\end{aligned}$$

This is not quite the same as our approximate result (4.92). Although we get the same non-analytic dependence on the electron-phonon coupling strength, the energy shift predicted by BCS theory is different from that which we obtained via minimizing the ground state energy with a variational ansatz. However, this is not too surprising as both approaches are approximate ones. When consistently applied however it is possible to get exactly the same ground state energy with both approaches [16].

4.5.3 Remarks on generalized Mean-Field approximations

We arrived at these results from the BCS Hamiltonian that was made plausible. On top of this, we performed the mean-field approximation by replacing the interacting part of the Hamiltonian with suitable single-particle operators (mean-field approximation). This procedure turned out successful later-on, but at that moment seemed a bit miraculous. Recalling the general approch of the Hartree-Fock treatment in Sec. 3.2.3, we see that the general strategy is to approximate the interacting BCS Hamiltonian (4.95)

$$H = \sum_{\boldsymbol{k}} \epsilon_{\boldsymbol{k}} \left[c_{\boldsymbol{k}\uparrow}^\dagger c_{\boldsymbol{k}\uparrow} + c_{\boldsymbol{k}\downarrow}^\dagger c_{\boldsymbol{k}\downarrow}\right] - V \sum_{\boldsymbol{k}\boldsymbol{k}'} c_{+\boldsymbol{k}'\uparrow}^\dagger c_{-\boldsymbol{k}'\downarrow}^\dagger c_{-\boldsymbol{k}\downarrow} c_{+\boldsymbol{k}\uparrow} \qquad (4.114)$$

by a non-interacting single-particle Hamiltonian – with respect to which all expectation values can be easily computed. In Sec. 3.2.3, we used a single-particle Hamiltonian in the same basis. Now, we simply use an a priori unknown single-particle basis

$$H_{\text{eff}} = \sum_{\boldsymbol{k}} \chi_{\boldsymbol{k}}^1 \alpha_{\boldsymbol{k}}^\dagger \alpha_{\boldsymbol{k}} + \chi_{\boldsymbol{k}}^2 \beta_{\boldsymbol{k}}^\dagger \beta_{\boldsymbol{k}} + \sigma \,. \qquad (4.115)$$

Here, we just need to relate the new operators $\alpha_{\boldsymbol{k}}$ and $\beta_{\boldsymbol{k}}$ to the old ones by some generalized Bogoliubov transform, and the single-particle energies $\chi_{\boldsymbol{k}}^i$ as well as the energy shift σ have to be determined self-consistently by minimizing the grand canonical potential. Fixing the Bogoliubov transform (4.105) and minimizing only with respect to the single-particle energies and the shift actually recovers the gap equation (4.108) and as a solution the mean-field Hamiltonian (4.106).

4.5.4 Magnetic field

An external magnetic field leads to a splitting of spin-up and spin-down contributions in the original Hamiltonian, which both in the original and in the effective Hamiltonian amounts to the additional term

$$\Delta H_{\text{eff}} = \mu B \sum_{\boldsymbol{k}} \left(c_{\boldsymbol{k}\uparrow}^\dagger c_{\boldsymbol{k}\uparrow} - c_{\boldsymbol{k}\downarrow}^\dagger c_{\boldsymbol{k}\downarrow}\right) . \qquad (4.116)$$

Using the very same Bogoliubov transform from Eq. (4.103) with coefficients (4.105) still diagonalizes the Hamiltonian, such that we can express the additional Hamiltonian also with the $\alpha_{\boldsymbol{k}}$ and $\beta_{\boldsymbol{k}}$ annihilation operators as

$$\Delta H_{\text{eff}} = \mu B \sum_{\boldsymbol{k}} \left(\alpha_{\boldsymbol{k}}^\dagger \alpha_{\boldsymbol{k}} - \beta_{\boldsymbol{k}}^\dagger \beta_{\boldsymbol{k}} \right) . \tag{4.117}$$

Apparently, this will split the single-particle energies of the quasiparticles, since the Hamiltonian (4.106) is now modified to

$$\begin{aligned} H_{\text{eff}} + \Delta H_{\text{eff}} &= \sum_{\boldsymbol{k}} \left(\sqrt{\epsilon_{\boldsymbol{k}}^2 + |\Delta|^2} + \mu B \right) \alpha_{\boldsymbol{k}}^\dagger \alpha_{\boldsymbol{k}} + \sum_{\boldsymbol{k}} \left(\sqrt{\epsilon_{\boldsymbol{k}}^2 + |\Delta|^2} - \mu B \right) \beta_{\boldsymbol{k}}^\dagger \beta_{\boldsymbol{k}} \\ &\quad + \sum_{\boldsymbol{k}} \left(\epsilon_{\boldsymbol{k}} - \sqrt{\epsilon_{\boldsymbol{k}}^2 + |\Delta|^2} \right) + \frac{|\Delta|^2}{V} . \end{aligned} \tag{4.118}$$

The gap equation (4.108) is now modified to

$$\Delta = \Delta \sum_{\boldsymbol{k}} \frac{V}{\sqrt{\epsilon_{\boldsymbol{k}}^2 + |\Delta|^2}} \left[\frac{1}{2} - \frac{1}{2} f\left(\sqrt{\epsilon_{\boldsymbol{k}}^2 + |\Delta|^2} - \mu B \right) - \frac{1}{2} f\left(\sqrt{\epsilon_{\boldsymbol{k}}^2 + |\Delta|^2} + \mu B \right) \right] . \tag{4.119}$$

Similar arguments as before apply. At vanishing external field $B = 0$, we reproduce the previous gap equation (4.108), such that – provided the temperature is also small enough – the superconducting phase exists. Going to strong fields now has qualitatively similar effects as going to high temperatures, since one of the Fermi functions approaches one and the other one vanishes

$$\begin{aligned} \lim_{B \to \infty} f\left(\sqrt{\epsilon_{\boldsymbol{k}}^2 + |\Delta|^2} - \mu B \right) &= 1 , \\ \lim_{B \to \infty} f\left(\sqrt{\epsilon_{\boldsymbol{k}}^2 + |\Delta|^2} + \mu B \right) &= 0 . \end{aligned} \tag{4.120}$$

This means that the r.h.s. of the above gap equation becomes vanishingly small, such that a nontrivial solution (associated to the superconducting phase) does not exist. This fully explains the observation that superconductivity breaks down above a critical field strength. In general however, the treatment of the gap equation can be made more precise by making the single-particle energy gap dependent on the mode $\Delta \to \Delta_{\boldsymbol{k}}$ [16].

4.5.5 Remarks on thermodynamic properties

We can directly compute the canonical potential

$$\begin{aligned} \Phi &= -k_B T \ln \operatorname{Tr} \left\{ e^{-\beta H_{\text{eff}}} \right\} \\ &= \frac{|\Delta|^2}{V} + \sum_{\boldsymbol{k}} \left(\epsilon_{\boldsymbol{k}} - \sqrt{\epsilon_{\boldsymbol{k}}^2 + |\Delta|^2} \right) - \frac{1}{\beta} \ln \operatorname{Tr} \left\{ e^{-\beta \sum_{\boldsymbol{k}} \sqrt{\epsilon_{\boldsymbol{k}}^2 + |\Delta|^2} (\alpha_{\boldsymbol{k}}^\dagger \alpha_{\boldsymbol{k}} + \beta_{\boldsymbol{k}}^\dagger \beta_{\boldsymbol{k}})} \right\} \\ &= \frac{|\Delta|^2}{V} + \sum_{\boldsymbol{k}} \left(\epsilon_{\boldsymbol{k}} - \sqrt{\epsilon_{\boldsymbol{k}}^2 + |\Delta|^2} \right) - \frac{2}{\beta} \sum_{\boldsymbol{k}} \ln \left(1 + e^{-\beta \sqrt{\epsilon_{\boldsymbol{k}}^2 + |\Delta|^2}} \right) . \end{aligned} \tag{4.121}$$

Here, we have first separated the shift of the effective Hamiltonian (4.106), and the factor of 2 resulted from the two particle species. As mentioned, the thermodynamic potential can be the starting point to obtain many useful quantities, and we will now demonstrate some of them explicitly. We will assume below that all parameters in the potential are real.

First, when we minimize the potential with respect to the order-parameter Δ (along the real axis)

$$\begin{aligned}\frac{\partial\Phi}{\partial\Delta} &= \frac{2\Delta}{V} + \sum_{\boldsymbol{k}} \frac{(-)\Delta}{\sqrt{\epsilon_{\boldsymbol{k}}^2+\Delta^2}} - \frac{2}{\beta}\sum_{\boldsymbol{k}} \frac{(-)\beta\Delta}{\sqrt{\epsilon_{\boldsymbol{k}}^2+\Delta^2}} f(\sqrt{\epsilon_{\boldsymbol{k}}^2+\Delta^2})\\ &= \frac{2\Delta}{V} - \sum_{\boldsymbol{k}} \frac{\Delta}{\sqrt{\epsilon_{\boldsymbol{k}}^2+\Delta^2}}\left[1-2f(\sqrt{\epsilon_{\boldsymbol{k}}^2+\Delta^2})\right]\\ &= \frac{2\Delta}{V}\left[1-\frac{V}{2}\sum_{\boldsymbol{k}}\frac{1}{\sqrt{\epsilon_{\boldsymbol{k}}^2+\Delta^2}}\tanh\left(\frac{\beta}{2}\sqrt{\epsilon_{\boldsymbol{k}}^2+\Delta^2}\right)\right] = 0\,, \end{aligned} \tag{4.122}$$

which precisely recovers the BCS gap equation (4.108). This is just a manifestation of the fact that the self-consistent determination of the gap Δ yields the best possible approximation (with a minimal potential) to the full dynamics.

Second, when we compute the mean particle number

$$\begin{aligned}\langle N\rangle &= \sum_{\boldsymbol{k}}\frac{\partial\Phi}{\partial\epsilon_{\boldsymbol{k}}} = \sum_{\boldsymbol{k}}\left[1-\frac{\epsilon_{\boldsymbol{k}}}{\sqrt{\epsilon_{\boldsymbol{k}}^2+\Delta^2}}\right] - \frac{2}{\beta}\sum_{\boldsymbol{k}}\left(-\beta\frac{\epsilon_{\boldsymbol{k}}}{\sqrt{\epsilon_{\boldsymbol{k}}^2+\Delta^2}}\right) f(\sqrt{\epsilon_{\boldsymbol{k}}^2+\Delta^2})\\ &= \sum_{\boldsymbol{k}}(1) - \sum_{\boldsymbol{k}}\frac{\epsilon_{\boldsymbol{k}}}{\sqrt{\epsilon_{\boldsymbol{k}}^2+\Delta^2}}\left[1-2f(\sqrt{\epsilon_{\boldsymbol{k}}^2+\Delta^2})\right] \to 2\hbar\omega_D\rho(E_F)\,, \end{aligned} \tag{4.123}$$

since the second term vanishes under the integral over the regime $-\hbar\omega_D \le \epsilon \le +\hbar\omega_D$. Therefore, the mean particle number does not depend on the order parameter Δ. Since the mean particle number therefore is related to $\hbar\omega_D\rho(E_F) = N/2$ we see that the ground state energy (4.113) actually describes the energy decrease due to $N/2$ Cooper pairs.

Third, by computing derivatives with respect to temperature k_BT, we get the entropy. To confirm this, we first write down the von-Neumann entropy (the thermodynamic entropy is obtained by multiplying with k_B)

$$S = -\mathrm{Tr}\left\{\rho_{\rm eff}\ln\rho_{\rm eff}\right\} = \mathrm{Tr}\left\{\rho_{\rm eff}(\beta H_{\rm eff}+\ln Z_{\rm eff})\right\} = \ln Z_{\rm eff} + \beta\left\langle H_{\rm eff}\right\rangle_{\rm eff}\,. \tag{4.124}$$

This can be equally obtained from the potential by computing derivatives with respect to k_BT

$$\begin{aligned}-\frac{\partial\Phi}{\partial k_BT} &= +\ln Z_{\rm eff} - k_BT\frac{\mathrm{Tr}\left\{-\frac{H_{\rm eff}}{(k_BT)^2}e^{-\beta H_{\rm eff}}\right\}}{Z_{\rm eff}} = +\ln Z_{\rm eff} + \beta\left\langle H_{\rm eff}\right\rangle_{\rm eff}\\ &= -\underbrace{\left(2\frac{\Delta}{V} - \sum_{\boldsymbol{k}}\frac{\Delta}{\sqrt{\epsilon_{\boldsymbol{k}}^2+\Delta^2}} + 2\sum_{\boldsymbol{k}}\frac{\Delta}{\sqrt{\epsilon_{\boldsymbol{k}}^2+\Delta^2}}f(\sqrt{\epsilon_{\boldsymbol{k}}^2+\Delta^2})\right)}_{=0}\frac{\partial\Delta}{\partial(k_BT)}\\ &\quad + 2\sum_{\boldsymbol{k}}\left[\ln\left(1+e^{-\beta\sqrt{\epsilon_{\boldsymbol{k}}^2+\Delta^2}}\right) + \beta\sqrt{\epsilon_{\boldsymbol{k}}^2+\Delta^2}f(\sqrt{\epsilon_{\boldsymbol{k}}^2+\Delta^2})\right]\\ &= -2\sum_{\boldsymbol{k}}\left[(1-f(E_k))\ln(1-f(E_k)) + f(E_k)\ln f(E_k)\right]\,. \end{aligned} \tag{4.125}$$

Here, we have used the gap equation (4.108) in the first line and the last line can be checked by inserting $E_k = \sqrt{\epsilon_{\boldsymbol{k}}^2 + \Delta^2}$ and the definition of the Fermi function. This is the entropy that one would naively write down for independent two-level systems with single-particle energies E_k and occupations $f(E_k)$ – the probability of the empty state is simply $1 - f(E_k)$. Furthermore, the factor of 2 just arises from the two particle species considered.

Fourth, by computing the derivative of the potential with respect to the inverse temperature β, we get the internal energy

$$\begin{aligned} U = \frac{\partial \Phi}{\partial \beta} &= \frac{|\Delta|^2}{V} + \sum_{\boldsymbol{k}} \left(\epsilon_{\boldsymbol{k}} - \sqrt{\epsilon_{\boldsymbol{k}}^2 + |\Delta|^2} \right) + 2 \sum_{\boldsymbol{k}} \sqrt{\epsilon_{\boldsymbol{k}}^2 + |\Delta|^2} f(\sqrt{\epsilon_{\boldsymbol{k}}^2 + |\Delta|^2}) \\ &= \frac{|\Delta|^2}{V} + \sum_{\boldsymbol{k}} \epsilon_{\boldsymbol{k}} - \sum_{\boldsymbol{k}} \sqrt{\epsilon_{\boldsymbol{k}}^2 + |\Delta|^2} \tanh\left(\frac{\beta}{2} \sqrt{\epsilon_{\boldsymbol{k}}^2 + |\Delta|^2} \right) . \end{aligned} \tag{4.126}$$

We could have guessed the first line of this expression from the effective Hamiltonian (4.106). Computing the derivative of the energy with respect to temperature, we get the specific heat. However, this is a bit lengthy, it is more convenient to calculate the specific heat from the derivative of the entropy with respect to temperature.

4.5.6 Specific heat capacity

We can alternatively compute the specific heat capacity from

$$C = T \frac{dS}{dT} = -\beta \frac{dS}{d\beta} . \tag{4.127}$$

Here, the thermodynamic entropy needs to be used, i.e., we multiply our previous result by k_B via $S = k_B S_{vN}$

$$S = -2 k_B \sum_{\boldsymbol{k}} \left[(1 - f(E_k)) \ln(1 - f(E_k)) + f(E_k) \ln f(E_k) \right] . \tag{4.128}$$

This is a bit simpler since the ground state (condensate) contribution to the internal energy does not vanish. We get

$$\begin{aligned} C &= +2\beta k_B \sum_{\boldsymbol{k}} \frac{d}{d\beta} \left[(1 - f(E_{\boldsymbol{k}})) \ln(1 - f(E_{\boldsymbol{k}})) + f(E_{\boldsymbol{k}}) \ln f(E_{\boldsymbol{k}}) \right] \\ &= 2\beta k_B \sum_{\boldsymbol{k}} \left[- \ln(1 - f(E_{\boldsymbol{k}})) - 1 + \ln f(E_{\boldsymbol{k}}) + 1 \right] \frac{df(E_{\boldsymbol{k}})}{d\beta} \\ &= 2\beta k_B \sum_{\boldsymbol{k}} \ln e^{-\beta E_{\boldsymbol{k}}} \frac{df(E_{\boldsymbol{k}})}{d\beta} = -2 k_B \beta^2 \sum_{\boldsymbol{k}} E_{\boldsymbol{k}} \frac{df(E_{\boldsymbol{k}})}{d\beta} . \end{aligned} \tag{4.129}$$

Here, we have used that $f(E_{\boldsymbol{k}})/(1 - f(E_{\boldsymbol{k}})) = e^{-\beta E_{\boldsymbol{k}}}$. To further evaluate this expression, it is important to note that the Fermi functions depend both explicitly on β but also implicitly (via the temperature-dependence of the single-particle energies $E_{\boldsymbol{k}} = \sqrt{\epsilon_{\boldsymbol{k}}^2 + \Delta^2}$). Therefore, we get

$$\begin{aligned} C &= -2 k_B \beta^2 \sum_{\boldsymbol{k}} E_{\boldsymbol{k}} \left(\frac{\partial f(E_{\boldsymbol{k}})}{\partial \beta} + \frac{\partial f(E_{\boldsymbol{k}})}{\partial E_{\boldsymbol{k}}} \frac{1}{2 E_{\boldsymbol{k}}} 2\Delta \frac{d\Delta}{d\beta} \right) \\ &= -2 k_B \beta \sum_{\boldsymbol{k}} \frac{\partial f(E_{\boldsymbol{k}})}{\partial E_{\boldsymbol{k}}} \left(E_{\boldsymbol{k}}^2 + \beta \Delta \frac{d\Delta}{d\beta} \right) . \end{aligned} \tag{4.130}$$

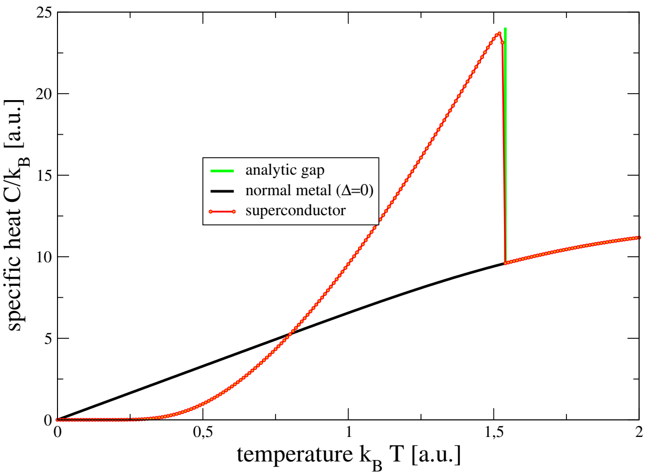

Figure 4.10: Heat capacity (4.130) in the continuum limit, where sums become integrals, versus temperature. Whereas the heat capacity of the normal metal varies smoothly (black), the superconducting phase heat capacity (red curve sampled at symbols) has a jump discontinuity (4.139) at the critical temperature (green bar) and is exponentially suppressed at low temperatures. Other parameters $\hbar\omega_D = 10$ a.u., $V\rho(E_F) = 0.5$.

Here, we have replaced $\frac{\partial f(E_{\boldsymbol{k}})}{\partial\beta} = \frac{\partial f(E_{\boldsymbol{k}})}{\partial E_{\boldsymbol{k}}}\frac{E_{\boldsymbol{k}}}{\beta}$.

First, we see that the prefactor in this sum

$$\frac{\partial f(E_{\boldsymbol{k}})}{\partial E_{\boldsymbol{k}}} = -\beta f(E_{\boldsymbol{k}})[1 - f(E_{\boldsymbol{k}})] \tag{4.131}$$

is at low temperatures where $E_{\boldsymbol{k}} = \sqrt{\epsilon_{\boldsymbol{k}}^2 + \Delta^2} \gg k_B T$ exponentially suppressed everywhere: It would for $T \to 0$ become a δ-function $-\delta(E_{\boldsymbol{k}})$ in continuum representation. However, in the superconducting phase the single particle energies $E_{\boldsymbol{k}} = \sqrt{\epsilon_{\boldsymbol{k}}^2 + |\Delta|^2}$ are always strictly positive, such that we conclude for this regime, all terms in the sum, and therefore the complete specific heat capacity is exponentially suppressed. As we learned already in our discussion of the specific heat of insulators and semiconductors in Sec. 3.1.9, this is a general and typical feature of systems with an excitation gap above their ground state.

Second, by forcing the gap Δ to vanish throughout, only a simplified variant of the first contribution remains, and we recover the electronic heat capacity of a normal metal that we already discussed in Sec. 3.1.8.

We can numerically calculate the specific heat contribution, which reveals a jump at the critical temperature, see Fig. 4.10. Although through the non-analytic gap solution both terms are non-analytic at the critical temperature, the first term is continuous at the critical point. Therefore, the second term must be responsible for the jump

$$\Delta C = \frac{1}{k_B^2 T^3} \sum_{\boldsymbol{k}} f(E_{\boldsymbol{k}})[1 - f(E_{\boldsymbol{k}})] \lim_{T \to T_c - \epsilon} \frac{d\Delta^2}{d\beta} \,. \tag{4.132}$$

We can compute the height of the jump analytically by looking at the behaviour of the gap Δ near the critical point. To get this behaviour, we insert the deviation from the critical temperature

$$\beta = \frac{1}{k_B T} = \frac{1}{k_B(T_c - \Delta T)} \tag{4.133}$$

into the gap equation [16] and expand for small ΔT as well as for the critical gap Δ^2. Up to first order in ΔT and Δ^2 one gets

$$\begin{aligned}1 &= V\rho(E_F)\int_0^{\hbar\omega_D}\frac{\tanh\left(\frac{\beta}{2}\sqrt{\epsilon^2+\Delta^2}\right)}{\sqrt{\epsilon^2+\Delta^2}}d\epsilon \\ &= V\rho(E_F)\int_0^{\hbar\omega_D}\frac{\tanh\left(\frac{\epsilon}{2k_BT_c}\right)}{\epsilon}d\epsilon + \frac{V\rho(E_F)\Delta T}{2k_BT_c^2}\int_0^{\hbar\omega_D}\frac{d\epsilon}{\cosh^2\left(\frac{\epsilon}{2k_BT_c}\right)} \\ &\quad + \frac{V\rho(E_F)\Delta_c^2}{4k_BT_c}\int_0^{\hbar\omega_D}\frac{d\epsilon}{\epsilon^2}\left(\frac{1}{\cosh^2\left(\frac{\epsilon}{2k_BT_c}\right)} - \frac{2k_BT_c\tanh\left(\frac{\epsilon}{2k_BT_c}\right)}{\epsilon}\right) + \ldots . \end{aligned} \tag{4.134}$$

In the second line, the first term on the r.h.s. must equal one as it yields the usual gap equation at the critical point, such that the other terms have to add up to zero. The second term results from the explicit dependence on temperature and can be analytically estimated using that $k_BT_c \ll \hbar\omega_D$

$$I_1 = \int_0^{\hbar\omega_D}\frac{d\epsilon}{\cosh^2\left(\frac{\epsilon}{2k_BT_c}\right)} \approx 2k_BT_c\int_0^\infty\frac{dx}{\cosh^2(x)} = 2k_BT_c\,. \tag{4.135}$$

The last term comes from the implicit dependence via the gap Δ, and it can be estimated with the same assumptions as

$$\begin{aligned}I_2 &= \int_0^{\hbar\omega_D}\frac{d\epsilon}{\epsilon^2}\left(\frac{1}{\cosh^2\left(\frac{\epsilon}{2k_BT_c}\right)} - \frac{2k_BT_c\tanh\left(\frac{\epsilon}{2k_BT_c}\right)}{\epsilon}\right) \\ &\approx \frac{1}{2k_BT_c}\int_0^\infty\frac{dx}{x^2}\left(\frac{1}{\cosh^2(x)} - \frac{\tanh(x)}{x}\right) = \frac{1}{2k_BT_c}\frac{7\zeta(3)}{\pi^2}\,.\end{aligned} \tag{4.136}$$

Here, $\zeta(3)$ is the Riemann-Zeta function. Since the last terms have to cancel, the resulting constraint yields a relation between Δ_c^2 and ΔT

$$\Delta_c^2 \approx \frac{8\pi^2}{7\zeta(3)}k_BT_ck_B\Delta T\,. \tag{4.137}$$

From this, we get the desired derivative

$$\lim_{\Delta T\to 0}\frac{d\Delta_c^2}{d\beta} = \lim_{\Delta T\to 0}\frac{\frac{d\Delta_c^2}{d\Delta T}}{\frac{d\beta}{d\Delta T}} = \frac{\frac{8\pi^2}{7\zeta(3)}k_BT_ck_B}{\frac{1}{k_BT_c^2}} = \frac{8\pi^2}{7\zeta(3)}k_B^3T_c^3\,. \tag{4.138}$$

Eventually inserting this into the specific heat we obtain

$$\Delta C \approx \frac{8\pi^2}{7\zeta(3)}k_B\int_{-\hbar\omega_D}^{+\hbar\omega_D}f(\epsilon)[1-f(\epsilon)]d\epsilon \approx \frac{8\pi^2}{7\zeta(3)}k_B\int_{-\infty}^{+\infty}f(\epsilon)[1-f(\epsilon)]d\epsilon = \frac{8\pi^2}{7\zeta(3)}k_B^2T_c\,. \tag{4.139}$$

Accordingly, the jump in the specific heat is linear in the critical temperature. This is the vertical green line shown in Fig. 4.10. It should be noted that we computed here the specific heat per mode, to get the specific heat per volume we need to multiply by the particle density.

Chapter 5

Magnetism

Being composed of magnetically active components (nuclei, electrons), all matter somehow reacts on the presence of an external magnetic field. For the case of superconductors, we already mentioned that they are perfect diamagnets. **Diamagnetic** materials tend to reduce the externally applied field in the medium. In contrast, in **paramagnetic** materials the magnetic moments align with the magnetic field, such that the field inside the medium is enhanced. **Ferromagnetism** is a special case where the magnetic moments inside a medium align with themselves, i.e., a magnetic field may exist inside the medium without an externally applied field (as is the case in permanent magnets). Therefore, in a ferromagnet the field inside a medium may be directed in any direction – depending on the orientation. Ferromagnetism breaks down beyond a critical field strength.

5.1 Interactions with the magnetic field

An external magnetic field can couple in two ways to matter. First, we have the coupling via the minimal coupling procedure used to include the electromagnetic field, where the momentum is shifted by the vector potential $\boldsymbol{A}$

$$\boldsymbol{p} \to \boldsymbol{p} - \frac{q}{c}\boldsymbol{A} \tag{5.1}$$

with electron charge q (for electrons $q = -e$) and velocity of light c. The magnetic field is related to the vector potential via $\boldsymbol{B} = \nabla \times \boldsymbol{A}$. This minimal coupling is sometimes termed diamagnetic coupling.

Additionally, an electron has a magnetic moment, linked to the spin $\boldsymbol{S}$ via

$$\boldsymbol{\mu} = g\frac{e}{2mc}\boldsymbol{S}\,, \qquad g = 2.002\ldots \tag{5.2}$$

Here, m is the electron mass and g the electronic g-factor. This leads to an additional term in the Hamiltonian, which for electrons with $g \approx 2$ becomes

$$\Delta H = -\boldsymbol{\mu}\boldsymbol{B} = \mu_B\boldsymbol{\sigma}\boldsymbol{B}\,, \qquad \mu_B = \frac{|e|\hbar}{2mc}\,. \tag{5.3}$$

Here, μ_B is the Bohr magneton and the electronic spin operator can be expressed with the vector of Pauli matrices via $\boldsymbol{S} = \frac{\hbar}{2}\boldsymbol{\sigma}$. This coupling leads to a Zeemann [1] splitting, which is responsible for paramagnetism. Here, we note that $\Delta H = -\boldsymbol{\mu}\boldsymbol{B}$ is the general Zeemann coupling in the Hamiltonian for arbitrary magnetic moments.

---

[1] P. Zeemann (1865–1943) was a dutch physist and Nobel laureate.

5.2 Paramagnetism of localized magnetic moments

Let us assume that we have N atoms and that the electrons are tightly bound to the atoms. Then, the total angular momentum $\boldsymbol{J}$ for an electron at each site is obtained by coupling the electronic spin $\boldsymbol{S}$ and the angular momentum $\boldsymbol{L}$

$$\boldsymbol{J} = \boldsymbol{L} + \boldsymbol{S}\,, \tag{5.4}$$

which implies a total magnetic moment

$$\boldsymbol{\mu} = g\frac{e}{2mc}\boldsymbol{J}\,, \tag{5.5}$$

where according to the rules of quantum mechanics the g-factor is computed via

$$g = 1 + \frac{J(J+1) + S(S+1) - L(L+1)}{2J(J+1)}\,. \tag{5.6}$$

Since this can depend on the position, the total Hamilton operator is given by

$$H = -\sum_{i=1}^{N} \boldsymbol{\mu}_i \boldsymbol{B}(\boldsymbol{R}_i)\,, \tag{5.7}$$

where $\boldsymbol{B}(\boldsymbol{R}_i)$ is the magnetic field at the position of the ith atom. It is now conventional to choose the magnetic field in z-direction, such that

$$H = \sum_{i=1}^{N} g_i \mu_B B J_z^i\,, \tag{5.8}$$

where J_z is a large-spin operator for the i-th lattice position and g_i denotes the corresponding g-factor of site i.

Since these magnetic moments do not interact, we can compute the partition function from that of the individual components

$$Z = \mathrm{Tr}\left\{e^{-\beta H}\right\} = \prod_i \mathrm{Tr}\left\{e^{-\beta g \mu_B B J_z^i}\right\} = \prod_i Z_i\,, \tag{5.9}$$

which we best evaluate in the angular momentum eigenbasis. This can be done also for different magnetic moments and site-dependent magnetic fields, but for simplicity we will be content with the homogeneous case. For a single-component partition function we get (we abbreviate $b = g\mu_B B$ below)

$$\begin{aligned} Z_i &= \sum_{m=-J}^{+J} e^{-\beta b m} = e^{+\beta b J} \sum_{\ell=0}^{2J} e^{-\beta b \ell} = e^{+\beta b J} \frac{1 - e^{-\beta b(2J+1)}}{1 - e^{-\beta b}} \\ &= \frac{e^{+\beta b(J+1/2)} - e^{-\beta b(J+1/2)}}{e^{+\beta b/2} - e^{-\beta b/2}}\,. \end{aligned} \tag{5.10}$$

Therefore, the logarithm of the partition function (related to the free energy via $F = -k_B T \ln Z$) becomes

$$\ln Z = N \ln \frac{\sinh(\beta g \mu_B B (J+1/2))}{\sinh(\beta g \mu_B B/2)}\,. \tag{5.11}$$

The total magnetization can be computed via (recall that $\Delta H_i = -\boldsymbol{\mu_i B(R_i)}$)

$$\begin{aligned} M &= g\mu_B \left\langle \sum_i J_z^i \right\rangle = k_B T \partial_B \ln Z \\ &= N g \mu_B \left[\left(J + \frac{1}{2} \right) \coth\left(\beta g \mu_B B (J + \frac{1}{2}) \right) - \frac{1}{2} \coth\left(\frac{\beta}{2} g \mu_B B \right) \right] . \end{aligned} \tag{5.12}$$

Specifically, for electrons without angular momentum that just have the electron spin $J = 1/2$, this would further reduce to $M = \frac{g\mu_B N}{2} \tanh\left(\frac{\beta g \mu_B B}{2}\right) \approx N\mu_B \tanh(\beta \mu_B B)$.

Generally however, we see that the magnetization is linear at small external fields ($\coth(x) = 1/x + x/3 + \ldots$)

$$\lim_{B\to 0} M = \frac{NJ(J+1)}{3} (g\mu_B)^2 \beta B \equiv \chi_M B , \tag{5.13}$$

and becomes saturated for strong external fields

$$\lim_{B\to\infty} M = N g \mu_B J . \tag{5.14}$$

Since the magnetic susceptibility χ_M is positive, this is paramagnetic. Hence, coupling the magnetic field directly to the localized magnetic moments induces paramagnetic behaviour.

5.3 Paramagnetism of delocalized electrons

For delocalized electrons – e.g. the conduction band electrons in metals, we can consider the paramagnetic Zeeman coupling as well, we just use $g = 2$ and $J = 1/2$, and the z-component of the total spin becomes

$$S_z = \frac{\hbar}{2} \sum_{\boldsymbol{R}} \left(c^\dagger_{\boldsymbol{R}\uparrow} c_{\boldsymbol{R}\uparrow} - c^\dagger_{\boldsymbol{R}\downarrow} c_{\boldsymbol{R}\downarrow} \right) = \frac{\hbar}{2} \sum_{\boldsymbol{k}} \left(c^\dagger_{\boldsymbol{k}\uparrow} c_{\boldsymbol{k}\uparrow} - c^\dagger_{\boldsymbol{k}\downarrow} c_{\boldsymbol{k}\downarrow} \right) , \tag{5.15}$$

where we used that the diagonalization leaves the total particle number operator invariant. Eventually, the Hamiltonian becomes

$$H = \sum_{\boldsymbol{k}} \left(\epsilon_{\boldsymbol{k}} + \mu_B B \right) c^\dagger_{k\uparrow} c_{k\uparrow} + \sum_{\boldsymbol{k}} \left(\epsilon_{\boldsymbol{k}} - \mu_B B \right) c^\dagger_{k\downarrow} c_{k\downarrow} , \tag{5.16}$$

such that a magnetic field just breaks the degeneracy of the single-particle energies. The magnetization is just given by the expectation value of

$$\begin{aligned} M = \langle \mu_z \rangle &= -\mu_B \left\langle \sum_{\boldsymbol{k}} \left(c^\dagger_{k\uparrow} c_{k\uparrow} - c^\dagger_{k\downarrow} c_{k\downarrow} \right) \right\rangle \\ &= -\mu_B \int \left[\rho(\epsilon + \mu_B B) f(\epsilon + \mu_B B) - \rho(\epsilon - \mu_B B) f(\epsilon - \mu_B B) \right] d\epsilon \\ &\approx -\mu_B \int \rho(\epsilon) \left[f(\epsilon + \mu_B B) - f(\epsilon - \mu_B B) \right] d\epsilon . \end{aligned} \tag{5.17}$$

Now, linearizing for small magnetic fields yields

$$M = -2\mu_B^2 B \int \rho(\epsilon) \frac{df}{d\epsilon} d\epsilon \overset{T\to 0}{\to} +2\mu_B^2 \rho(E_F) B , \tag{5.18}$$

where we have used that at low temperatures the derivative of the Fermi function becomes a negative Dirac-Delta function. Accordingly, the magnetic susceptibility becomes

$$\chi_{\mathrm{p}} = 2\mu_B^2 \rho(E_F) , \tag{5.19}$$

and the free conduction band electrons behave paramagnetically. However, there is also another contribution coming from the diamagnetic coupling to the vector potential.

5.4 Landau diamagnetism

We now consider the effect of minimal coupling [3], best treated in first quantization. A homogeneous magnetic field in z direction is generated by the vector potential

$$\boldsymbol{A} = \begin{pmatrix} 0 \\ Bx \\ 0 \end{pmatrix}, \qquad \boldsymbol{B} = \begin{pmatrix} 0 \\ 0 \\ B \end{pmatrix}. \tag{5.20}$$

Since we will not consider interactions, we just include one electron and in the end will extrapolate the result to many. The Hamiltonian of a single electron reads

$$\begin{aligned} H &= \frac{1}{2m}\left(\boldsymbol{p} - \frac{e}{c}\boldsymbol{A}\right)^2 = \frac{1}{2m}\left(p_x^2 + p_z^2 + p_y^2 - \frac{eB}{c}p_y x - \frac{eB}{c}x p_y + \frac{e^2B^2}{c^2}x^2\right) \\ &= \frac{p_x^2}{2m} + \frac{m}{2}\omega_0^2\left(x - \frac{p_y}{m\omega_0}\right)^2 + \frac{p_z^2}{2m}, \end{aligned} \tag{5.21}$$

where we have introduced the cyclotron frequency

$$\omega_0 = \frac{eB}{mc}. \tag{5.22}$$

The stationary Schrödinger equation can now be solved with the ansatz

$$\Psi(\boldsymbol{r}) = c\phi(x)e^{+\mathrm{i}k_y y}e^{-\mathrm{i}k_z z}, \tag{5.23}$$

which yields

$$\left(\frac{p_x^2}{2m} + \frac{m}{2}\omega_0^2\left(x - \frac{\hbar k_y}{m\omega_0}\right)^2 + \frac{\hbar^2 k_z^2}{2m}\right)c\phi(x)e^{+\mathrm{i}k_y y}e^{-\mathrm{i}k_z z} = Ec\phi(x)e^{+\mathrm{i}k_y y}e^{-\mathrm{i}k_z z}. \tag{5.24}$$

This is apparently just a 1d Schrödinger equation for $\phi(x)$

$$\left(\frac{p_x^2}{2m} + \frac{m}{2}\omega_0^2\left(x - \frac{\hbar k_y}{m\omega_0}\right)^2 + \frac{\hbar^2 k_z^2}{2m}\right)\phi(x) = E\phi(x). \tag{5.25}$$

However, there is a shift term $\hbar^2 k_z^2/(2m)$ (which does of course affect the energies), and there is also a displacement of the equilibrium position (which does not affect the energies). Therefore, the energies are degenerate in the quantum number k_y

$$E_{n,k_y,k_z} = E_{n,k_z} = \hbar\omega_0\left(n + \frac{1}{2}\right) + \frac{\hbar^2 k_z^2}{2m}. \tag{5.26}$$

However, this solution holds strictly speaking only when there are no spatial constraints in x-direction. Assuming periodic boundary conditions in y and z directions yields quantization of k_y and k_z

$$k_y = \frac{2\pi l_y}{L_y}, \qquad k_z = \frac{2\pi l_z}{L_z}, \qquad l_{y/z} \in \mathbb{Z}. \tag{5.27}$$

However, whereas the number of k_z values leading to different physics is finite, this is different for k_y. As it enters also in the Schrödinger equation displacement, we have to demand that the equilibrium position of the oscillator is inside the considered volume

$$x_0 = \frac{\hbar k_y}{m\omega_0} = \frac{2\pi\hbar l_y}{m\omega_0 L_y} \le L_x, \tag{5.28}$$

which constrains the possible values of k_y via

$$l_y \le \frac{m\omega_0 L_x L_y}{2\pi\hbar}\,. \tag{5.29}$$

Strictly speaking, since we have used the free solution of the infinitely extended harmonic oscillator, we are not allowed to impose periodic boundary conditions in x direction. However, the eigenfunctions of the harmonic oscillator decay exponentially in the far-field, such that it should be justified to perform this approximation when L_x is large. Therefore, the degeneracy of the energies resulting from the quantization of k_y is roughly given by (an integer approximation of)

$$N_y = \frac{m\omega_0 L_x L_y}{2\pi\hbar}\,. \tag{5.30}$$

It should be noted that the energies $E_{nk_yk_z}$ are the excitation energies of a single electron – if it is present. Quite generally, the electronic Hamiltonian in second quantization can therefore be written as (this now includes many non-interacting electrons)

$$H = \sum_{n=0}^{\infty}\sum_{k_y=1}^{N_y}\sum_{k_z\in 1.\mathrm{BZ}}\sum_{\sigma} E_{n,k_z} c^\dagger_{nk_yk_z\sigma} c_{nk_yk_z\sigma}\,. \tag{5.31}$$

The grand potential is now defined via the log of the partition function, where we can use the degeneracy in k_y and convert the sum over the allowed k_z values into an integral

$$\begin{aligned}\Phi &= -k_BT\ln\mathrm{Tr}\left\{e^{-\beta(H-\mu N)}\right\}\\ &= -2k_BT\sum_{n=0}^{\infty}\frac{L_z}{2\pi}\int_{-\pi}^{+\pi}dk_z\frac{m\omega_0L_xL_y}{2\pi\hbar}\ln\left(1+e^{-\beta(E_{nk_z}-\mu)}\right)\end{aligned} \tag{5.32}$$

Here, the factor of 2 results from the spin, and we have converted the sum over k_z into an integral in the usual way. The dependence on the magnetic field is via the cyclotron frequency ω_0 and the energy E_{nk_z} (which also depends on ω_0). Making this explicit, we can write the grand potential with $V = L_xL_yL_z$ as

$$\Phi = -\frac{k_BTVm\omega_0}{2\pi^2\hbar}\sum_{n=0}^{\infty} g\left(\mu-\hbar\omega_0\left(n+\frac{1}{2}\right)\right)\,,\qquad g(\mu-x) = \int_{-\pi}^{+\pi}\ln\left(1+e^{\beta(\mu-x-\frac{\hbar^2k_z^2}{2m})}\right)dk_z\,. \tag{5.33}$$

To evaluate the sum over n we can use the Euler-McLaurin summation formula [17]

$$\sum_{n=0}^{\infty} f(n) = \frac{f(0)}{2} + \int_0^\infty f(x)dx - \frac{f'(0)}{12} + \ldots\,, \tag{5.34}$$

which holds when the derivatives of $f(x)$ vanish at infinity. However, we actually need a relation for $f(n+1/2)$

$$\begin{aligned}\sum_{n=0}^{\infty} f(n+1/2) &= \frac{f(1/2)}{2} + \int_0^\infty f(x+1/2)dx - \frac{f'(1/2)}{12} + \ldots\\ &= \int_0^\infty f(x)dx - \int_0^{1/2} f(x)dx + \frac{f(1/2)}{2} - \frac{f'(1/2)}{12} + \ldots\\ &= \int_0^\infty f(x)dx - f(0)\frac{1}{2} - f'(0)\int_0^{1/2} xdx + f(0)\frac{1}{2} + f'(0)\frac{1}{4} - f'(0)\frac{1}{12} + \mathcal{O}\{f''(0)\}\\ &= \int_0^\infty f(x)dx + \frac{f'(0)}{24} + \mathcal{O}\{f''(0)\}\,,\end{aligned} \tag{5.35}$$

where we have taylor expanded all terms around $x = 0$ (except under the infinite integral).

Applying it to our case we have

$$\begin{aligned}\sum_{n=0}^{\infty} g\left(\mu - \hbar\omega_0(n+1/2)\right) &= \int_0^{\infty} dx g(\mu - \hbar\omega_0 x)dx + \frac{1}{24}\frac{d}{dx}g(x)\Big|_{x=0} \\ &= \frac{1}{\hbar\omega_0}\int_{-\infty}^{\mu} g(y)dy - \frac{\hbar\omega_0}{24}\frac{d}{dy}g(y)\Big|_{y=\mu}, \end{aligned} \tag{5.36}$$

where we have transformed variables to $y = \mu - \hbar\omega_0 x$. The potential accordingly becomes

$$\begin{aligned}\Phi &= -\frac{k_B T V m\omega_0}{2\pi^2\hbar}\left[\frac{1}{\hbar\omega_0}\int_{-\infty}^{\mu} g(y)dy - \frac{\hbar\omega_0}{24}\frac{d}{dy}g(y)\Big|_{y=\mu}\right], \\ &= -\frac{k_B T V m}{2\pi^2\hbar^2}\left[\int_{-\infty}^{\mu} g(y)dy - \frac{(\hbar\omega_0)^2}{24}\frac{d}{dy}g(y)\Big|_{y=\mu}\right], \end{aligned} \tag{5.37}$$

and we see that the dependence on ω_0 (and hence, the magnetic field) will drop out in the first term. Using that

$$g'(\mu) = \frac{\partial^2}{\partial\mu^2}\int_{-\infty}^{\mu} g(y)dy\,, \tag{5.38}$$

we can write the potential also as

$$\Phi = \Phi_0 - \frac{\hbar^2 e^2 B^2}{24 m^2 c^2}\frac{\partial^2}{\partial\mu^2}\Phi_0\,, \tag{5.39}$$

where Φ_0 denotes the grand potential in absence of any field. This can be calculated explicitly, and for our purposes it is more convenient to represent the potential using the usual k summation

$$\Phi_0 = -2k_B T\sum_{\boldsymbol{k}} \ln\left(1 + e^{-\beta(\epsilon_{\boldsymbol{k}}-\mu)}\right)\,. \tag{5.40}$$

Performing the derivative with respect to μ yields

$$\frac{\partial\Phi_0}{\partial\mu} = -2\sum_{\boldsymbol{k}}\frac{e^{-\beta(\epsilon_{\boldsymbol{k}}-\mu)}}{1+e^{-\beta(\epsilon_{\boldsymbol{k}}-\mu)}} = -2\sum_{\boldsymbol{k}} f(\epsilon_{\boldsymbol{k}})\,, \tag{5.41}$$

and for the second derivative we get

$$\frac{\partial^2\Phi_0}{\partial\mu^2} = -2\sum_{\boldsymbol{k}}\frac{\partial f(\epsilon_{\boldsymbol{k}})}{\partial\mu} = +2\sum_{\boldsymbol{k}}\frac{\partial f(\epsilon_{\boldsymbol{k}})}{\partial\epsilon_{\boldsymbol{k}}} = 2\int\rho(\epsilon)\frac{df}{d\epsilon}d\epsilon \overset{T\to 0}{\to} -2\rho_0(E_F)\,, \tag{5.42}$$

where in the last step we have again used that the Fermi function becomes (reversed) Heaviside function, such that its derivative converges to a δ function at the Fermi energy.

Now, we can compute the magnetization

$$\begin{aligned} M = -\frac{\partial\Phi}{\partial B} &= +\frac{e^2\hbar^2}{12m^2c^2}B\frac{\partial^2\Phi_0}{\partial\mu^2} \\ &= -2\rho(E_F)\frac{e^2\hbar^2}{12m^2c^2}B\,. \end{aligned} \tag{5.43}$$

We can read off the corresponding susceptibility

$$\chi = -2\rho(E_F)\frac{e^2\hbar^2}{12m^2c^2} = -2\rho(E_F)\frac{1}{3}\mu_B^2 = -\frac{1}{3}\chi_p\,, \tag{5.44}$$

where we have inserted the Bohr magneton $\mu_B = |e|\hbar/(2mc)$ and compared with Eq. (5.19). Accordingly, the minimal coupling procedure leads for otherwise free electrons to a diamagnetic behaviour. If one considers the conduction band electrons as quasi-free and adds up both couplings, the total susceptibility at low temperatures is still paramagnetic, since the paramagnetic contribution is larger, and one gets $\chi_{\rm total} = 2/3\chi_{\rm p}$.

5.5 Interaction of magnetic moments

To explain ferromagnetism, one may easily be tempted to simply write down a Hamiltonian of the form $H = -g_{ij}\boldsymbol{\mu}_i\boldsymbol{\mu}_j$, where g_{ij} would depend on the distance of the magnetic moments. From electrodynamics, we could conjecture that a dipolar interaction $H = \frac{1}{r^3}\left[\boldsymbol{\mu_i\mu_j} - 3(\boldsymbol{\mu_i e})(\boldsymbol{\mu_j e})\right]$ could lead to similar dynamics. However, this would lead to anti-aligned magnetic moments and for realistic parameters this interaction is too weak to explain the observed ferromagnetism. The real origin of interaction of localized magnetic moments is the exchange interaction.

To motivate it, we consider two electrons [3] in tight-binding representation (similar arguments hold when solving the H_2 problem [1])

$$\begin{aligned}
H = {} & \epsilon_a\left(c_{a\uparrow}^\dagger c_{a\uparrow} + c_{a\downarrow}^\dagger c_{a\downarrow}\right) + \epsilon_b\left(c_{b\uparrow}^\dagger c_{b\uparrow} + c_{b\downarrow}^\dagger c_{b\downarrow}\right) + U_a c_{a\uparrow}^\dagger c_{a\uparrow} c_{a\downarrow}^\dagger c_{a\downarrow} + U_b c_{b\uparrow}^\dagger c_{b\uparrow} c_{b\downarrow}^\dagger c_{b\downarrow} \\
& + V\left(c_{a\uparrow}^\dagger c_{a\uparrow} + c_{a\downarrow}^\dagger c_{a\downarrow}\right)\left(c_{b\uparrow}^\dagger c_{b\uparrow} + c_{b\downarrow}^\dagger c_{b\downarrow}\right) \\
& + J\left(+c_{a\uparrow}^\dagger c_{b\uparrow}^\dagger c_{a\uparrow} c_{b\uparrow} + c_{a\downarrow}^\dagger c_{b\downarrow}^\dagger c_{a\downarrow} c_{b\downarrow} + c_{a\uparrow}^\dagger c_{b\downarrow}^\dagger c_{a\downarrow} c_{b\uparrow} + c_{a\downarrow}^\dagger c_{b\uparrow}^\dagger c_{a\uparrow} c_{b\downarrow} + c_{a\uparrow}^\dagger c_{a\downarrow}^\dagger c_{b\downarrow} c_{b\uparrow} + c_{b\uparrow}^\dagger c_{b\downarrow}^\dagger c_{a\downarrow} c_{a\uparrow}\right)\,.
\end{aligned} \tag{5.45}$$

Here, the first line describes the individual Hamiltonian of the two sites with on-site energies ϵ_a and ϵ_b as well as intra-orbital Coulomb interactions U_a and U_b. We are mainly interested in the case $\epsilon = \epsilon_a = \epsilon_b$ and $U = U_a = U_b$, but for the purpose of bookkeeping it is convenient to keep the distinction for now. The second line includes the inter-orbital Coulomb interaction V, and the third line is an exchange term J, which describes all exchange processes under which the resulting wave function must be anti-symmetric. The Hamiltonian commutes with the total particle number operator, and therefore we can group the eigenstates of the different particle numbers into blocks. In principle, we have 16 eigenstates, since the total basis is constructed by the Fock states

$$|n_{a\uparrow}n_{a\downarrow}n_{b\uparrow}n_{b\downarrow}\rangle\,, \qquad n_{i\sigma} \in \{0,1\}\,. \tag{5.46}$$

- There is just one eigenvector with zero particles $|v_1\rangle \equiv |0000\rangle$ with energy $E_1 = 0$.
- Then, there are four eigenstates with a single electron

$$\begin{aligned}
|v_2\rangle &= c_{a\uparrow}^\dagger|0\rangle\,, & |v_3\rangle &= c_{a\downarrow}^\dagger|0\rangle & &\text{with} & E_2 &= E_3 = \epsilon_a\,, \\
|v_4\rangle &= c_{b\uparrow}^\dagger|0\rangle\,, & |v_5\rangle &= c_{b\downarrow}^\dagger|0\rangle & &\text{with} & E_4 &= E_5 = \epsilon_b\,.
\end{aligned} \tag{5.47}$$

- The nontrivial part of the Hamiltonian is in the subspace where we have two electrons, since this block is not diagonal. The basis of the two-electron subspace is spanned by the states $c_{a\uparrow}^\dagger c_{b\uparrow}^\dagger|0\rangle$, $c_{a\downarrow}^\dagger c_{b\downarrow}^\dagger|0\rangle$, $c_{b\uparrow}^\dagger c_{b\downarrow}^\dagger|0\rangle$, $c_{a\uparrow}^\dagger c_{a\downarrow}^\dagger|0\rangle$, $c_{a\uparrow}^\dagger c_{b\downarrow}^\dagger|0\rangle$, $c_{a\downarrow}^\dagger c_{b\uparrow}^\dagger|0\rangle$. Of these, the first two are already eigenstates with energies $E_6 = E_7 = \epsilon_a + \epsilon_b + V - J$, since two terms of the exchange interaction are already diagonal. In the remaining four states $\{c^\dagger_{b\uparrow} c^\dagger_{b\downarrow} \left|0\right\rangle, c^\dagger_{a\uparrow} c^\dagger_{a\downarrow} \left|0\right\rangle, c^\dagger_{a\uparrow} c^\dagger_{b\downarrow} \left|0\right\rangle, c^\dagger_{a\downarrow} c^\dagger_{b\uparrow} \left|0\right\rangle\}$, the Hamiltonian has the matrix representation

$$H_4 = \begin{pmatrix} 2\epsilon_b + U_b & J & & \\ J & 2\epsilon_a + U_a & & \\ & & \epsilon_a + \epsilon_b + V & -J \\ & & -J & \epsilon_a + \epsilon_b + V \end{pmatrix}, \tag{5.48}$$

which again further decomposes into two blocks that can be diagonalized. Altogether, we get the states

$$\begin{aligned}
\left|v_6\right\rangle &= c^\dagger_{a\uparrow} c^\dagger_{b\uparrow} \left|0\right\rangle , \qquad E_6 = \epsilon_a + \epsilon_b + V - J , \\
\left|v_7\right\rangle &= c^\dagger_{a\downarrow} c^\dagger_{b\downarrow} \left|0\right\rangle , \qquad E_7 = \epsilon_a + \epsilon_b + V - J , \\
\left|v_8\right\rangle &\propto \left(2\epsilon_b - 2\epsilon_a + U_b - U_a + \sqrt{4J^2 + (U_a - U_b + 2\epsilon_a - 2\epsilon_b)^2}\right) c^\dagger_{a\uparrow} c^\dagger_{a\downarrow} \left|0\right\rangle - 2J c^\dagger_{b\uparrow} c^\dagger_{b\downarrow} \left|0\right\rangle , \\
E_8 &= \epsilon_a + \epsilon_b + \frac{1}{2}\left(U_a + U_b - \sqrt{4J^2 + (U_a - U_b + 2\epsilon_a - 2\epsilon_b)^2}\right) , \\
\left|v_9\right\rangle &\propto 2J c^\dagger_{a\uparrow} c^\dagger_{a\downarrow} \left|0\right\rangle + \left(2\epsilon_b - 2\epsilon_a + U_b - U_a + \sqrt{4J^2 + (U_a - U_b + 2\epsilon_a - 2\epsilon_b)^2}\right) c^\dagger_{b\uparrow} c^\dagger_{b\downarrow} \left|0\right\rangle , \\
E_9 &= \epsilon_a + \epsilon_b + \frac{1}{2}\left(U_a + U_b + \sqrt{4J^2 + (U_a - U_b + 2\epsilon_a - 2\epsilon_b)^2}\right) , \\
\left|v_{10}\right\rangle &= \frac{1}{\sqrt{2}}\left[c^\dagger_{a\uparrow} c^\dagger_{b\downarrow} + d^\dagger_{a\downarrow} c^\dagger_{b\uparrow}\right] \left|0\right\rangle , \qquad E_{10} = \epsilon_a + \epsilon_b + V - J , \\
\left|v_{11}\right\rangle &= \frac{1}{\sqrt{2}}\left[c^\dagger_{a\uparrow} c^\dagger_{b\downarrow} - d^\dagger_{a\downarrow} c^\dagger_{b\uparrow}\right] \left|0\right\rangle , \qquad E_{11} = \epsilon_a + \epsilon_b + V + J .
\end{aligned} \tag{5.49}$$

Specifically in the limit $\epsilon = \epsilon_a = \epsilon_b$ and $U = U_a = U_b$ one can now see that

$$E_{8/9} = 2\epsilon + U \pm J , \tag{5.50}$$

and when we assume that the on-site Coulomb interaction is significantly larger than the intra-orbital and exchange interaction $U \gg V, J$, we can completely neglect the states $\left|v_8\right\rangle$ and $\left|v_9\right\rangle$ from the dynamics, since due to their large energy, they can never be occupied and hardly particate in the dynamics. The remaining, relevant, four states form a degenerate triplett

$$\left|v_6\right\rangle = c^\dagger_{a\uparrow} c^\dagger_{b\uparrow} \left|0\right\rangle , \qquad \left|v_7\right\rangle = c^\dagger_{a\downarrow} c^\dagger_{b\downarrow} \left|0\right\rangle , \qquad \left|v_{10}\right\rangle = \frac{1}{\sqrt{2}}\left[c^\dagger_{a\uparrow} c^\dagger_{b\downarrow} + c^\dagger_{a\downarrow} c^\dagger_{b\uparrow}\right] \left|0\right\rangle , \tag{5.51}$$

with the energy $E_6 = E_7 = E_{10} = \epsilon_a + \epsilon_b + V - J$ and a singlett

$$\left|v_{11}\right\rangle = \frac{1}{\sqrt{2}}\left[c^\dagger_{a\uparrow} c^\dagger_{b\downarrow} - c^\dagger_{a\downarrow} c^\dagger_{b\uparrow}\right] \left|0\right\rangle \tag{5.52}$$

with energy $E_{11} = \epsilon_a + \epsilon_b + V + J$.

- Again, there are four eigenstates with three electrons (or a single hole)

$$\begin{aligned}
\left|v_{12}\right\rangle &= c^\dagger_{a\downarrow} c^\dagger_{b\uparrow} c^\dagger_{b\downarrow} \left|0\right\rangle , \qquad \left|v_{13}\right\rangle = c^\dagger_{a\uparrow} c^\dagger_{b\uparrow} c^\dagger_{b\downarrow} \left|0\right\rangle \qquad \text{with} \qquad E_{12} = E_{13} = \epsilon_a + 2\epsilon_b + U_b + 2V - J , \\
\left|v_{14}\right\rangle &= c^\dagger_{a\uparrow} c^\dagger_{a\downarrow} c^\dagger_{b\downarrow} \left|0\right\rangle , \qquad \left|v_{15}\right\rangle = c^\dagger_{a\uparrow} c^\dagger_{a\downarrow} c^\dagger_{b\uparrow} \left|0\right\rangle \qquad \text{with} \qquad E_{14} = E_{15} = 2\epsilon_a + \epsilon_b + U_a + 2V - J ,
\end{aligned} \tag{5.53}$$

which we can neglect for large $U_a = U_b = U$.

- Finally, there is one eigenstate with four electrons $\left|v_{16}\right\rangle = c^\dagger_{a\uparrow} c^\dagger_{a\downarrow} c^\dagger_{b\uparrow} c^\dagger_{b\downarrow} \left|0\right\rangle$ with energy $E_{16} = 2\epsilon_a + 2\epsilon_b + U_a + U_b + 4V - 2J$, which can be neglected as well.

We will now concentrate on the subspace with two electrons, assuming that the number of particles is fixed. Further, we will eliminate the states with on-site Coulomb interaction ($U \to \infty$), leaving only the triplett and the singlett states. Our observation is that when $J > 0$, the energetically degenerate triplett states are energetically lower than the singlett state. We are now looking for an interaction between local magnetic moments that reproduces this behaviour.

We can introduce spin operators for every site $\alpha \in \{a, b\}$

$$\begin{aligned} S^x_\alpha &= \frac{1}{2}\left(d^\dagger_{\alpha\uparrow} d_{\alpha\downarrow} + d^\dagger_{\alpha\downarrow} d_{\alpha\uparrow}\right) \hat{=} \frac{1}{2}\sigma^x_\alpha\,, \\ S^y_\alpha &= \frac{-\mathrm{i}}{2}\left(d^\dagger_{\alpha\uparrow} d_{\alpha\downarrow} - d^\dagger_{\alpha\downarrow} d_{\alpha\uparrow}\right) \hat{=} \frac{1}{2}\sigma^y_\alpha\,, \\ S^z_\alpha &= \frac{1}{2}\left(d^\dagger_{\alpha\uparrow} d_{\alpha\uparrow} - d^\dagger_{\alpha\downarrow} d_{\alpha\downarrow}\right) \hat{=} \frac{1}{2}\sigma^z_\alpha\,, \end{aligned} \tag{5.54}$$

which fulfil the known commutation relations

$$[S^i_\alpha, S^j_\beta] = \delta_{\alpha\beta} \mathrm{i} \epsilon_{ijk} S^k_\alpha \tag{5.55}$$

and yield for the total spin in the allowed subspace an eigenvalue of $\boldsymbol{S_\alpha}^2 = (S^x_\alpha)^2 + (S^y_\alpha)^2 + (S^z_\alpha)^2 = 3/4 = 1/2(1/2+1)$. Of course, these operators are – when represented on the basis for a single site – 4×4 matrices, but since we consider only the singly occupied sector per site (via $U \to \infty$), they become Pauli matrices in the allowed subspace.

By direct inspection we can now compute the eigenvalues of $\boldsymbol{S_a S_b}$. However, we can also obtain it from the rules of angular momentum coupling: The total spin of both sites reads

$$S^2 = \boldsymbol{S^2} = (\boldsymbol{S}_a + \boldsymbol{S}_b)^2 = \boldsymbol{S_a}^2 + \boldsymbol{S_b}^2 + 2\boldsymbol{S_a S_b}\,, \tag{5.56}$$

and it can have eigenvalues $s(s+1)$ with $s = 0$ or $s = 1$. In fact, one can check explicitly with Eq. (5.51) and Eq. (5.52) that the triplett corresponds to total angular momentum $s = 1$ and the singlett to angular momentum $s = 0$

$$\left\langle v_6\right| S^2 \left|v_6\right\rangle = \left\langle v_7\right| S^2 \left|v_7\right\rangle = \left\langle v_{10}\right| S^2 \left|v_{10}\right\rangle = 1 \cdot 2\,, \qquad \left\langle v_{11}\right| S^2 \left|v_{11}\right\rangle = 0 \cdot 1\,. \tag{5.57}$$

We can solve for the scalar product as $\boldsymbol{S_a S_b} = \frac{1}{2}\left[S^2 - S_a^2 - S_b^2\right]$, which can have eigenvalues

$$\frac{1}{2}\left[s(s+1) - \frac{1}{2}\left(1 + \frac{1}{2}\right) - \frac{1}{2}\left(1 + \frac{1}{2}\right)\right] \tag{5.58}$$

where the s assumes the values $s \in \{0, 1\}$. Therefore, the operator $\boldsymbol{S_a S_b}$ assigns the $s = 1$ states the eigenvalue $+1/4$ and the $s = 0$ state the eigenvalue $-3/4$.

We want the precise opposite, such that eventually, we conclude that the exchange interaction between localized spins can be written as

$$H_{\text{eff}} = -\tilde{J} \boldsymbol{S}_a \cdot \boldsymbol{S}_b\,, \qquad \tilde{J} > 0\,, \tag{5.59}$$

which tends to align the spins. Often, this is further generalized for many sites and supplemented by an external field (which can be chosen in a particular direction). The resulting Hamiltonian

$$H_{\text{Hs}} = -\sum_{ij} J_{ij} \boldsymbol{S}_i \cdot \boldsymbol{S}_j + g\mu_B \sum_i \boldsymbol{B S}_i \tag{5.60}$$

is known as **Heisenberg** model. Variants of this model are an important playground in statistical physics. Below, we will consider a reduced version of the Heisenberg model.

5.6 The 1d quantum Ising model in a transverse field

The quantum Ising chain in a transverse field for N spins

$$H=-g\sum_{i=1}^{N}\sigma_i^x-J\sum_{i=1}^{N}\sigma_i^z\sigma_{i+1}^z\,,\qquad N\ \text{even} \tag{5.61}$$

where $g\propto B$ describes the coupling to an external magnetic field in $\boldsymbol{x}$-direction, J the inter-chain coupling to nearest neighbors, and periodic boundary conditions are assumed $\sigma_{N+1}^z\equiv\sigma_1^z$ is a paradigmatic model to describe quantum-critical behaviour [18]. Although rather a technical constraint, we note explicitly that we consider here only the case where N is even. The model is analytically diagonalizable for finite N and displays a second order quantum phase transition at $g=J$. One can distinguish easily the behaviour in the simple cases where one coefficient vanishes

- When $J=0$, the model behaves either paramagnetic or diamagnetic, depending on how the magnetic field enters the constant g.
- When $g=0$, the model may describe ferromagnetic behaviour when $J>0$ (in the ground state, all spins are aligned) or anti-ferromagnetic behaviour when $J<0$ (all spins tend to anti-align)

We will just consider the paramagnetic-ferromagnetic transition here by assuming $g\geq 0$ and $J\geq 0$.

We can introduce a dimensionless phase parameter by fixing $\Omega s=J$ and $\Omega(1-s)=g$ with energy scale Ω

$$H_{\rm S}=-\Omega(1-s)\sum_{i=1}^{N}\sigma_i^x-\Omega s\sum_{i=1}^{N}\sigma_i^z\sigma_{i+1}^z\,. \tag{5.62}$$

The successive application of Jordan-Wigner, Fourier-, and Bogoliubov transforms maps the system Hamiltonian into two mutually commuting parts $H=H^-+H^+$ with

$$H^\pm=\sum_k\epsilon_k^\pm\gamma_{k\pm}^\dagger\gamma_{k\pm}+\sigma^\pm \tag{5.63}$$

with fermionic annihilation operators γ_k that describe quasi-particles and shifts $\sigma^\pm$. Here, the quasi-momentum k may assume discrete values only, and the single-particle energies – that correspond to excitation energies of the full model – can be explicitly computed.

5.6.1 Mean-field approximation

Although the mean-field approximation does not work well with the Ising model, we can apply it to the quantum Ising model to get some first ideas on the model dynamics. With the mean-field replacement (4.96) applied to the Pauli matrix products, we represent the Ising model by an effective Hamiltonian

$$\begin{aligned}H_{\rm eff}&=-\Omega(1-s)\sum_{i=1}^{N}\sigma_i^x-\Omega s\sum_{i=1}^{N}\left<\sigma_i^z\right>_{\rm eff}\sigma_{i+1}^z-\Omega s\sum_{i=1}^{N}\left<\sigma_{i+1}^z\right>_{\rm eff}\sigma_i^z+\Omega s\sum_{i=1}^{N}\left<\sigma_i^z\right>_{\rm eff}\left<\sigma_{i+1}^z\right>_{\rm eff}\\&=-\Omega(1-s)\sum_{i=1}^{N}\sigma_i^x-\Omega s\sum_{i=1}^{N}\left[\left<\sigma_{i-1}^z\right>_{\rm eff}+\left<\sigma_{i+1}^z\right>_{\rm eff}\right]\sigma_i^z+\Omega s\sum_{i=1}^{N}\left<\sigma_i^z\right>_{\rm eff}\left<\sigma_{i+1}^z\right>_{\rm eff}\,.\end{aligned} \tag{5.64}$$

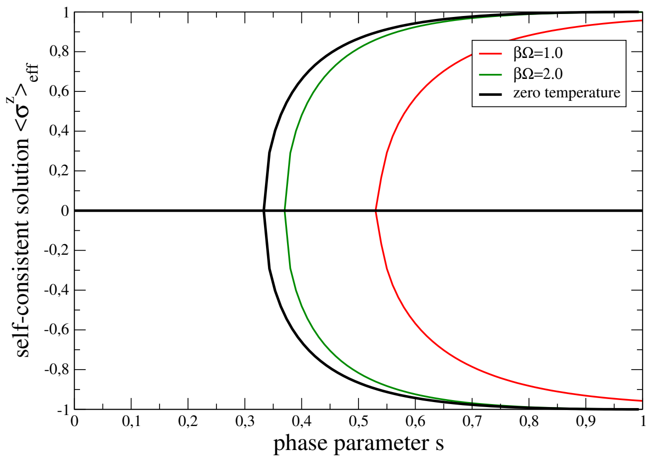

Figure 5.1: Self-consistent solutions of Eq. (5.66) versus scale parameter s for different temperatures. At zero temperature, we see at $s^* = 1/3$ a bifurcation, where two solutions with $\left<\sigma^z\right>_{\rm eff} \neq 0$ emerge. At larger temperatures, the bifurcation point moves to the right.

Here, the expectation value $\left<\sigma_i^z\right>_{\rm eff}$ has to be determined self-consistently from

$$\left<\sigma_i^z\right>_{\rm eff} = {\rm Tr}\left\{\sigma_i^z \frac{e^{-\beta H_{\rm eff}}}{{\rm Tr}\left\{e^{-\beta H_{\rm eff}}\right\}}\right\} . \tag{5.65}$$

The periodic boundary conditions imply that $\left<\sigma_i^z\right>_{\rm eff} = \left<\sigma^z\right>_{\rm eff}$ is homogeneous, which eventually yields

$$\begin{aligned}
\left<\sigma^z\right>_{\rm eff} &= {\rm Tr}\left\{\sigma^z \frac{e^{+\beta\Omega(1-s)\sigma^x + 2\beta\Omega s\left<\sigma^z\right>_{\rm eff}\sigma^z}}{{\rm Tr}\left\{e^{+\beta\Omega(1-s)\sigma^x + 2\beta\Omega s\left<\sigma^z\right>_{\rm eff}\sigma^z}\right\}}\right\}\\
&= 2s\left<\sigma^z\right>_{\rm eff} \frac{\tanh\left(\beta\Omega\sqrt{1+s(4s\left<\sigma^z\right>_{\rm eff}^2+s-2)}\right)}{\sqrt{1+s(4s\left<\sigma^z\right>_{\rm eff}^2+s-2)}} .
\end{aligned} \tag{5.66}$$

Here, we have on the r.h.s. computed the matrix exponential and normalized it for general expectation values $\left<\sigma^z\right>_{\rm eff}$. This resulting equation is always trivially solved by $\left<\sigma^z\right>_{\rm eff} = 0$, but further nontrivial solutions can be found numerically. At high temperatures, $\beta\Omega \ll 1$, we only have the trivial solution $\left<\sigma^z\right>_{\rm eff} = 0$. At zero temperatures, we can approximate the tanh by one, and we additionally have the two solutions $\left<\sigma^z\right>_{\rm eff} = \pm\frac{1}{2s}\sqrt{(1+s)(3s-1)}$. This nonanalytic behaviour is found for zero temperatures at $s = 1/3$. For finite temperatures, we have to solve the self-consistency equation numerically, and we also observe the additional nontrivial branches, see Fig. 5.1. Since the non-analytic behaviour of the σ^z-observable is found even at zero temperature as a function of the parameter s describing the competition between external field and spin-spin interaction, the mean-field treatment thus predicts a **quantum phase transition**. We will see that it is indeed correct that a quantum phase transition exists for this model but that the correct position is at $s^* = 1/2$, unlike the value obtained from the mean-field treatment.

5.6.2 Exact Diagonalization of the closed system

First, we note that since

$$\begin{aligned}
\left[\sigma_i^z\sigma_{i+1}^z, \sigma_i^x\sigma_{i+1}^x\right] &= \sigma_i^x\left[\sigma_i^z\sigma_{i+1}^z, \sigma_{i+1}^x\right] + \left[\sigma_i^z\sigma_{i+1}^z, \sigma_i^x\right]\sigma_{i+1}^x\\
&= \sigma_i^x\sigma_i^z(2{\rm i}\sigma_{i+1}^y) + (2{\rm i}\sigma_i^y)\sigma_{i+1}^z\sigma_{i+1}^x\\
&= (-{\rm i}\sigma_i^y)(2{\rm i}\sigma_{i+1}^y) + (2{\rm i}\sigma_i^y)(+{\rm i}\sigma_{i+1}^y) = 0 ,
\end{aligned} \tag{5.67}$$

it follows that the full Ising model Hamiltonian commutes with the operator

$$\Sigma^x = \bigotimes_{\ell=1}^{N} \sigma_\ell^x \,, \tag{5.68}$$

which means that H and Σ^x must have a common system of eigenvectors. Since the eigenvalues of Σ^x are just ± 1, we conclude that it must be possible to classify the eigenvalues of the Hamiltonian into two groups.

Jordan-Wigner transform

We could directly use the representation of the Pauli matrices by fermions (5.54), to embed the Ising model in a fermionic system of higher dimension. This procedure however would introduce (unnecessary) degrees of freedom and – more problematic – would introduce interactions between the fermions, inhibiting an exact solution. The mapping discussed below also maps to fermionic particles, but in a different non-local way.

The Jordan-Wigner transform (JWT)

$$\sigma_n^x = \mathbf{1} - 2c_n^\dagger c_n \,, \qquad \sigma_n^z = -(c_n + c_n^\dagger)\prod_{m=1}^{n-1}\left(\mathbf{1} - 2c_m^\dagger c_m\right) \tag{5.69}$$

maps the spin-1/2 Pauli matrices non-locally to spinless fermionic operators c_m. Inserting the JWT into the Ising Hamiltonian, one has to treat the boundary term with special care

$$\begin{aligned} H &= -g\sum_{n=1}^{N}(\mathbf{1} - 2c_n^\dagger c_n) - J\sum_{n=1}^{N-1}(c_n + c_n^\dagger)(c_{n+1} + c_{n+1}^\dagger)(\mathbf{1} - 2c_n^\dagger c_n) \\ &\quad - J(c_N + c_N^\dagger)\left[\prod_{n=1}^{N-1}(\mathbf{1} - 2c_n^\dagger c_n)\right](c_1 + c_1^\dagger) \\ &= -g\sum_{n=1}^{N}(\mathbf{1} - 2c_n^\dagger c_n) - J\sum_{n=1}^{N-1}(c_n^\dagger - c_n)(c_{n+1}^\dagger + c_{n+1}) \\ &\quad + J(c_N^\dagger - c_N)(c_1^\dagger + c_1)\left[\prod_{n=1}^{N}(\mathbf{1} - 2c_n^\dagger c_n)\right] , \end{aligned} \tag{5.70}$$

where we have extensively used the fermionic anticommutation relations. Introducing the projection operators on the subspaces with even (+) and odd (-) total number of fermion quasiparticles

$$\mathcal{P}^\pm \equiv \frac{1}{2}\left[\mathbf{1} \pm \Sigma^x\right] = \frac{1}{2}\left[\mathbf{1} \pm \prod_{m=1}^{N}(\mathbf{1} - 2c_m^\dagger c_m)\right] , \tag{5.71}$$

we may also write the Hamiltonian (5.70) as $H = (\mathcal{P}^+ + \mathcal{P}^-)H(\mathcal{P}^+ + \mathcal{P}^-)$. It is straightforward to see that terms with different projectors and with $n < N$ vanish

$$\begin{aligned} 0 &= \mathcal{P}^+(\mathbf{1} - 2c_n^\dagger c_n)\mathcal{P}^- = \mathcal{P}^-(\mathbf{1} - 2c_n^\dagger c_n)\mathcal{P}^+ \,, \\ 0 &= \mathcal{P}^+(c_n^\dagger - c_n)(c_{n+1}^\dagger + c_{n+1})\mathcal{P}^- = \mathcal{P}^-(c_n^\dagger - c_n)(c_{n+1}^\dagger + c_{n+1})\mathcal{P}^+ \,. \end{aligned} \tag{5.72}$$

For the boundary terms one finds similarly

$$\begin{aligned} &(\mathcal{P}^+ + \mathcal{P}^-)(c_N^\dagger - c_N)(c_1^\dagger + c_1)\left[\prod_{n=1}^{N}(\mathbf{1} - 2c_n^\dagger c_n)\right](\mathcal{P}^+ + \mathcal{P}^-) \\ &= (\mathcal{P}^+ + \mathcal{P}^-)(c_N^\dagger - c_N)(c_1^\dagger + c_1)(2\mathcal{P}^+ - \mathbf{1})(\mathcal{P}^+ + \mathcal{P}^-) \\ &= \mathcal{P}^+(c_N^\dagger - c_N)(c_1^\dagger + c_1)\mathcal{P}^+ - \mathcal{P}^-(c_N^\dagger - c_N)(c_1^\dagger + c_1)\mathcal{P}^- \,. \end{aligned} \tag{5.73}$$

The prefactor of the last term with the $\mathcal{P}^-$ is negative as it should be, but the first is positive. We can correct for this by demanding anti-periodic boundary conditions in the even subspace. Eventually, we can write the Hamiltonian (5.70) as the sum of two non-interacting parts with either an even or an odd total number of fermionic quasiparticles

$$\begin{aligned} H &= \mathcal{P}^+ H^+ \mathcal{P}^+ + \mathcal{P}^- H^- \mathcal{P}^- \\ &= \mathcal{P}^+ \left[-g \sum_{n=1}^N (\mathbf{1} - 2c_n^\dagger c_n) - J \sum_{n=1}^N (c_n^\dagger - c_n)(c_{n+1}^\dagger + c_{n+1}) \right] \mathcal{P}^+ \\ &\quad + \mathcal{P}^- \left[-g \sum_{n=1}^N (\mathbf{1} - 2c_n^\dagger c_n) - J \sum_{n=1}^N (c_n^\dagger - c_n)(c_{n+1}^\dagger + c_{n+1}) \right] \mathcal{P}^- . \end{aligned} \tag{5.74}$$

Although the Hamiltonians in the brackets look formally identical, we stress that to arrive at this expression, we need to demand antiperiodic boundary conditions in the even (+) subspace and periodic boundary conditions in the odd (-) subspace

$$c_{N+1,(+)} \equiv -c_{1,(+)} , \qquad c_{N+1,(-)} \equiv +c_{1,(-)} . \tag{5.75}$$

Even subspace diagonalization

We first seek to diagonalize the even part of the Hamiltonian

$$H^+ = -g \sum_{n=1}^N (\mathbf{1} - 2c_n^\dagger c_n) - J \sum_{n=1}^N (c_n^\dagger - c_n)(c_{n+1}^\dagger + c_{n+1}) \tag{5.76}$$

with antiperiodic boundary conditions $c_{N+1} = -c_1$. This is often the only part considered, since it contains the ground state (with zero quasi-particles). Translational invariance suggests to use the discrete Fourier transform (DFT, preserving the anticommutation relations due to its unitarity by construction)

$$c_n = \frac{e^{-\mathrm{i}\pi/4}}{\sqrt{N}} \sum_k \tilde{c}_k e^{+\mathrm{i}kn\frac{2\pi}{N}} , \tag{5.77}$$

which is a specific case of a Bogoliubov transformation. By construction, the DFT is unitary and since it does not mix between annihilation and creation operators, it leaves the fermionic anticommutation relations invariant (as one can check). The factor $e^{-\mathrm{i}\pi/4}$ in front has just been inserted for convenience (to obtain real-valued Bogoliubov coefficients later-on). The DFT is compatible with the antiperiodic boundary conditions $c_{N+1} = -c_1$ when k takes half-integer values

$$k \in \{\pm\frac{1}{2}, \pm\frac{3}{2}, \pm\frac{5}{2}, \ldots\} , \qquad \text{where} \qquad |k| \le \frac{N-1}{2} . \tag{5.78}$$

Therefore, for even N, we get N different k values. The DFT maps the Hamiltonian into

$$H^+ = -gN\mathbf{1} + \sum_k \left\{ 2[g - J\cos(k2\pi/N)]\tilde{c}_k^\dagger \tilde{c}_k + J\sin(k2\pi/N) \left[\tilde{c}_k^\dagger \tilde{c}_{-k}^\dagger + \tilde{c}_{-k}\tilde{c}_k \right] \right\} . \tag{5.79}$$

Now, the observation that only positive and negative frequencies couple (conservation of one-dimensional quasi-momentum), suggests to use the reduced Bogoliubov transform

$$\tilde{c}_k = u_{+k}\gamma_{+k} + v_{-k}^* \gamma_{-k}^\dagger , \tag{5.80}$$

which mixes positive and negative momenta and where the a priori unknown coefficients have already been labeled suggestively (a more general ansatz would eventually of course yield the same solution). Since the new operators γ_k should be fermionic, we obtain from the orthonormality conditions and the fermionic anticommutation relations

$$1 = \left|u_{+k}\right|^2 + \left|v_{-k}\right|^2 , \qquad 0 = u_{+k}v_{+k}^* + u_{-k}v_{-k}^* = (v_{+k}^*, v_{-k}^*) \begin{pmatrix} u_{+k} \\ u_{-k} \end{pmatrix} . \tag{5.81}$$

Demanding that the Bogoliubov transform eliminates all non-diagonal terms (of the form $\gamma_{-k}\gamma_{+k}$ etc.) yields (by combining positive and negative k) the equation

$$\begin{aligned} 0 &= 2\left[g - J\cos\left(k\frac{2\pi}{N}\right)\right](u_{+k}v_{-k} - u_{-k}v_{+k}) + 2J\sin\left(k\frac{2\pi}{N}\right)(u_{-k}u_{+k} + v_{-k}v_{+k}) \\ &= (v_{-k}, u_{-k}) \begin{pmatrix} +2\left[g - J\cos\left(k\frac{2\pi}{N}\right)\right] & +2J\sin\left(k\frac{2\pi}{N}\right) \\ +2J\sin\left(k\frac{2\pi}{N}\right) & -2\left[g - J\cos\left(k\frac{2\pi}{N}\right)\right] \end{pmatrix} \begin{pmatrix} u_{+k} \\ v_{+k} \end{pmatrix} \\ &\equiv (v_{-k}, u_{-k})\,\mathcal{M} \begin{pmatrix} u_{+k} \\ v_{+k} \end{pmatrix} . \end{aligned} \tag{5.82}$$

All equations can be fulfilled when we choose $(u_{+k}, v_{+k})^T$ as the normalized positive energy eigenstate of the matrix $\mathcal{M}$ with eigenvalue

$$\varepsilon_k^+ = +2\sqrt{g^2 + J^2 - 2gJ\cos(k2\pi/N)} \equiv \epsilon_k \tag{5.83}$$

and $(v_{-k}^*, u_{-k}^*)^T = (-v_{+k}^*, +u_{+k}^*)^T$ as its negative energy eigenstate with eigenvalue $\varepsilon_k^- = -2\sqrt{g^2 + J^2 - 2gJ\cos(k2\pi/N)}$. To be more explicit, we have

$$\begin{aligned} u_k &= \frac{g - J\cos(k2\pi/N) + \sqrt{g^2 + J^2 - 2gJ\cos(k2\pi/N)}}{\sqrt{\left[g - J\cos(k2\pi/N) + \sqrt{g^2 + J^2 - 2gJ\cos(k2\pi/N)}\right]^2 + \left[J\sin(k2\pi/N)\right]^2}} , \\ v_k &= \frac{J\sin(k2\pi/N)}{\sqrt{\left[g - J\cos(k2\pi/N) + \sqrt{g^2 + J^2 - 2gJ\cos(k2\pi/N)}\right]^2 + \left[J\sin(k2\pi/N)\right]^2}} . \end{aligned} \tag{5.84}$$

As a sanity check, we see that when the interaction vanishes $J \to 0$, we get that the modes no longer mix $u_k \to 1$ and $v_k \to 0$.

Using these solutions, we obtain when N is even

$$H^+ = \sum_k 2\sqrt{g^2 + J^2 - 2gJ\cos\left(k\frac{2\pi}{N}\right)}\left(\gamma_k^\dagger\gamma_k - \frac{1}{2}\right) . \tag{5.85}$$

From this, we conclude the single-particle energies

$$\epsilon_k^+ = 2\sqrt{g^2 + J^2 - 2gJ\cos\left(k\frac{2\pi}{N}\right)} = 2\Omega\sqrt{(1-s)^2 + s^2 - 2s(1-s)\cos\left(k\frac{2\pi}{N}\right)} . \tag{5.86}$$

The ground state has zero quasi-particles, and we can compute the ground state energy for large chain lengths N explicitly by converting the sum into an integral

$$E_0 = -\frac{1}{2}\sum_k \epsilon_k^+ \overset{N\to\infty}{\to} -\Omega\frac{N}{2}\int_{-1}^{+1} d\kappa\sqrt{(1-s)^2 + s^2 - 2s(1-s)\cos(\pi\kappa)} , \tag{5.87}$$

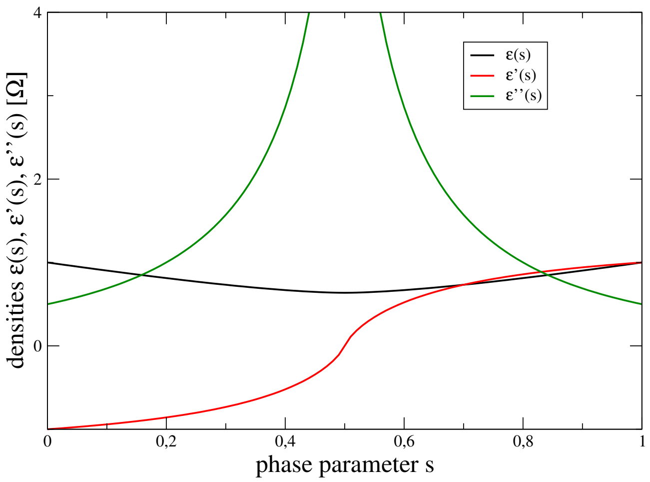

Figure 5.2: Plot of the (negative) ground state energy density $\varepsilon(s)$ (black) and its first two derivatives versus s. At the critical point $s^* = 1/2$, the second derivative diverges.

where $\kappa = 2k/N$. Accordingly, the ground state energy density per spin becomes

$$\varepsilon(s) = \frac{E_0}{N} = -\Omega \int_0^1 d\kappa \sqrt{(1-s)^2 + s^2 - 2s(1-s)\cos(\pi\kappa)} = -\frac{2\Omega}{\pi}\epsilon(4s(1-s))\,, \tag{5.88}$$

where $\epsilon(x)$ is an elliptic integral of the second kind. This function has the peculiar property that although its value at $s = 1/2$ is continuous, its second derivative diverges there logarithmically, see Fig. 5.2. The next excited state in the subspace of an even quasiparticle number would be to put two quasiparticles. To get the lowest excitation, we take the quasiparticles with $k = \pm 1/2$, which yields for the excitation gap

$$G(s) = E_1(s) - E_0(s) = 2\epsilon_{1/2}^+ = 4\Omega\sqrt{s^2 + (1-s)^2 - 2s(1-s)\cos\left(\frac{\pi}{N}\right)}\,. \tag{5.89}$$

By expanding the cos for large N and considering only the value of the gap at the critical point $s \to 1/2$, the critical gap becomes

$$G_{\rm crit} \approx 2\Omega\frac{\pi}{N}\,. \tag{5.90}$$

It is a general feature of quantum-critical models that the gap above the ground state vanishes as $N \to \infty$. The scaling for the Ising model is rather mild, connected to the fact that it has a second order quantum phase transition.

Odd subspace diagonalization

The procedure for the odd subspace is essentially analogous, except that the Fourier transform should now be compatible with periodic boundary conditions $c_{N+1} = +c_1$. The DFT

$$c_n = \frac{1}{\sqrt{N}}\sum_k \tilde{c}_k e^{+ikn\frac{2\pi}{N}} \tag{5.91}$$

is compatible with the periodic boundary conditions when k takes only integer values

$$k \in \{0, \pm 1, \pm 2, \pm 3, \ldots, \pm\left(\frac{N}{2} - 1\right), +\frac{N}{2}\}\,, \tag{5.92}$$

which holds for even values of N (we treat only this case) and then yields N different k-values. From this choice, it also follows that $\tilde{c}_{-N/2} = \tilde{c}_{+N/2}$. We get in analogy to the even subspace calculations the relations

$$\begin{aligned}
\sum_{i=1}^{N-1} c_i c_{i+1} + c_N c_1 &= \sum_k \tilde{c}_{+k}\tilde{c}_{-k} e^{-\mathrm{i}k\frac{2\pi}{N}}\,, & \sum_{i=1}^{N-1} c_{i+1}^\dagger c_i^\dagger + c_1^\dagger c_N^\dagger &= \sum_k \tilde{c}_{-k}^\dagger \tilde{c}_{+k}^\dagger e^{+\mathrm{i}k\frac{2\pi}{N}}\,,\\
\sum_{i=1}^{N-1} c_i^\dagger c_{i+1} + c_N^\dagger c_1 &= \sum_k \tilde{c}_{+k}^\dagger \tilde{c}_{+k} e^{-\mathrm{i}k\frac{2\pi}{N}}\,, & \sum_{i=1}^{N-1} c_{i+1}^\dagger c_i + c_1^\dagger c_N &= \sum_k \tilde{c}_{+k}^\dagger \tilde{c}_{+k} e^{+\mathrm{i}k\frac{2\pi}{N}}\,,
\end{aligned} \tag{5.93}$$

and inserting them into the Hamiltonian H^- we get

$$\begin{aligned}
H^- &= gN\mathbf{1} - 2g\sum_k \tilde{c}_{+k}^\dagger \tilde{c}_{+k} - J\sum_k \left[\tilde{c}_{+k}\tilde{c}_{-k} e^{-\mathrm{i}k\frac{2\pi}{N}} + \tilde{c}_{-k}^\dagger \tilde{c}_{+k}^\dagger e^{+\mathrm{i}k\frac{2\pi}{N}}\right]\\
&\qquad + J\sum_k \tilde{c}_{+k}^\dagger \tilde{c}_{+k}\left(e^{+\mathrm{i}k\frac{2\pi}{N}} + e^{-\mathrm{i}k\frac{2\pi}{N}}\right)\\
&= gN\mathbf{1} - 2(g-J)c_0^\dagger c_0 - 2(g+J)c_{N/2}^\dagger c_{N/2} + \sum_{k=1}^{N/2-1} H_k^-\,.
\end{aligned} \tag{5.94}$$

Here, the two additional terms arise from $k = 0$ and $k = N/2$, which is due to the different boundary conditions in the odd subspace. The excitation energies of these modes can become negative. The diagonalization of the quasimomentum pair Hamiltonian H_k^- proceeds in full analogy to H_k^+, we only have to take the different values of k into account

$$\begin{aligned}
H_k^- &= \left[2J\cos\left(\frac{2\pi k}{N}\right) - 2g\right] c_{+k}^\dagger c_{+k} + \left[2J\cos\left(\frac{2\pi k}{N}\right) - 2g\right] c_{-k}^\dagger c_{-k}\\
&\qquad - 2\mathrm{i}J\sin\left(\frac{2\pi k}{N}\right) c_{-k}c_{+k} + 2\mathrm{i}J\sin\left(\frac{2\pi k}{N}\right) c_{+k}^\dagger c_{-k}^\dagger\\
&= \epsilon_k^- \left[\gamma_{-k}^\dagger\gamma_{-k} + \gamma_{+k}^\dagger\gamma_{+k}\right] + \omega_k^-\mathbf{1}\,,\\
\omega_k^- &= -2\left(\sqrt{g^2 + J^2 - 2gJ\cos\left(\frac{2\pi k}{N}\right)} + g - J\cos\left(\frac{2\pi k}{N}\right)\right)\,,\\
\epsilon_k^- &= 2\sqrt{g^2 + J^2 - 2gJ\cos\left(\frac{2\pi k}{N}\right)}\,.
\end{aligned} \tag{5.95}$$

After some rewriting, we can write the total Hamiltonian in the odd subspace as

$$\begin{aligned}
H^- &= -2(g-J)\left(\gamma_0^\dagger\gamma_0 - \frac{1}{2}\right) - 2(g+J)\left(\gamma_{N/2}^\dagger\gamma_{N/2} - \frac{1}{2}\right)\\
&\qquad + \sum_{k=1}^{N/2-1} \epsilon_k^- \left[\left(\gamma_{+k}^\dagger\gamma_{+k} - \frac{1}{2}\right) + \left(\gamma_{-k}^\dagger\gamma_{-k} - \frac{1}{2}\right)\right]\,.
\end{aligned} \tag{5.96}$$

From these excitation energies we can succesively compute the full spectrum in the odd subspace. First, we compute the lowest energy eigenstate by putting a single (odd subspace) quasiparticle with minimum energy (this is for our parameters the one with $k = +N/2$) into the system. Further energies can be computed by putting quasiparticles with larger energies, always obeying the constraint that in this subspace, the total number of quasi-particles must be odd. Other odd branches are obtained by inserting three quasi-particles and so on.

Fig. 5.3 illustrates the analytic calculation of the eigenvalues for both even and odd subspaces by comparing with a full-scale numerical solution for $N = 10$ spins, which yields in total $2^N = 1024$ eigenvalues. One can see that by knowing the single-quasiparticle energies and the ground state energy in the separate subspaces, we can successively build up the complete spectrum of the model – which numerically (dashed curves) requires the diagonalization of a $2^N \times 2^N$ matrix.

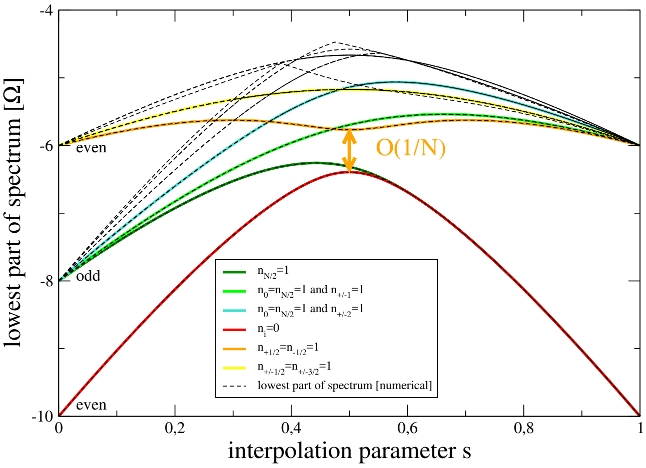

Figure 5.3: Comparison of analytical (bold, colored) predictions with numerical (thin dashed, black) results for the lower part of the spectrum for $N = 10$. Other parameters have been chosen as $g = \Omega(1-s)$ and $J = \Omega s$. At the critical point $s^* = 1/2$, the indicated gap between ground state and first excited state of the even subspace closes in the continuum limit $N \to \infty$.

5.6.3 Equilibrium

To compute the heat capacity in the continuum limit, we do for simplicity only consider the even subspace

$$H^+ = E_0 + \sum_{k:\text{even}} \epsilon_k^+ \gamma_{k+}^\dagger \gamma_{k+} \,,$$
$$E_0 = -\frac{N}{2} \int_{-1}^{+1} d\kappa \sqrt{g^2 + J^2 - 2gJ\cos(\pi\kappa)} = -\frac{2N(g+J)}{\pi} \varepsilon\left(\frac{4gJ}{(g+J)^2}\right) . \tag{5.97}$$

From this, we can evaluate the logarithm of the partition function

$$\begin{aligned}\ln Z_+(\beta) &= -\beta E_0 + \sum_{k:\text{even}} \ln\left[1 + e^{-\beta\epsilon_k^+}\right] \\ &= -\beta E_0 + \frac{N}{2}\int_{-1}^{+1} \ln\left[1 + e^{-\beta\epsilon(\kappa)}\right] d\kappa \,,\end{aligned} \tag{5.98}$$

where we have used an asymptotic convergence to an integral for large N with $\kappa = 2k/N$ in the last step and introduced continuous excitation energies

$$\epsilon(\kappa) = 2\sqrt{g^2 + J^2 - 2gJ\cos(2\pi\kappa)} \,. \tag{5.99}$$

Now, the mean energy can be expressed by the derivative of the partition function with respect to the inverse temperature

$$\begin{aligned}\langle E_+ \rangle &= -\partial_\beta \ln Z(\beta) \\ &= E_0 + \frac{N}{2}\int_{-1}^{+1} \frac{\epsilon(\kappa)}{1 + e^{+\beta\epsilon(\kappa)}} d\kappa \,,\end{aligned} \tag{5.100}$$

and we see that at zero temperature $\beta \to \infty$ it simply becomes the ground state energy of the Ising model, which we computed before.

The heat capacity is given by the derivative of the energy with respect to temperature, where the

$$C_+ = \frac{\partial \langle E_+ \rangle}{\partial T} = -\beta^2 \frac{\partial \langle E_+ \rangle}{\partial \beta} \,. \tag{5.101}$$

Here, the contribution from the ground state drops out and we get an expression for the specific heat capacity (per spin)

$$\frac{C_+}{N} = \frac{1}{2}\int_{-1}^{+1} \frac{\left(\frac{\beta\epsilon(\kappa)}{2}\right)^2}{\cosh^2\left(\frac{\beta\epsilon(\kappa)}{2}\right)} d\kappa \,. \tag{5.102}$$

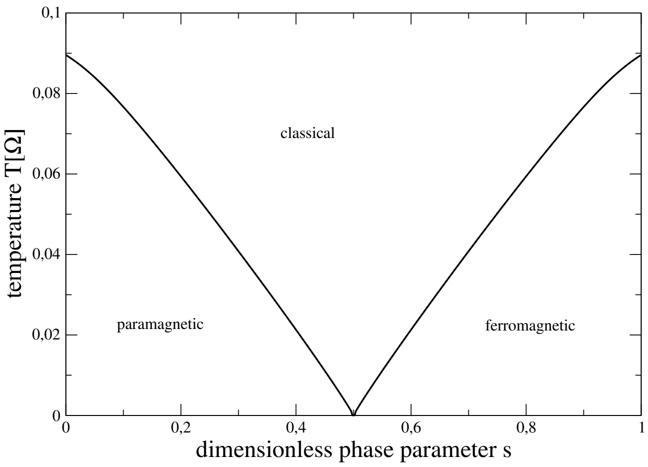

Figure 5.4: Plot of the crossover temperature versus the paramagnetic-ferromagnetic transition parameter s, obtained by solving $C(T^*) = C^*$ for very small C^*. Below the curve, the heat capacity vanishes exponentially, whereas it becomes finite above the curve.

As $\cosh(x) \geq 1$, the integral is well-defined everywhere, and the specific heat capacity is a continuous function e.g. of s and also of temperature (no jump discontinuities). We can plot the heat capacity versus temperature and we see that away from the critical point ($s \neq 1/2$), it vanishes at low temperatures exponentially. Again, we see in the spectra that the system always has an energy gap of order Ω there, so this does not come as a surprise. At the critical point $s^* = 1/2$ however, the spectrum becomes gapless, and the heat capacity is finite already at the smallest achievable temperatures. When we consider finite temperatures, the heat capacity vanishes for low temperatures in the gapped phase but rises above a certain critical temperature. This extends the zero-temperature phase diagram by a classical phase on top of the quantum phase, see Fig. 5.4. At finite temperatures, there is no longer a true phase transition as a function of temperature, but we still see that the heat capacity behaviour can be classified in distinct regimes.

Similarly, we can compute other order parameters such as

$$\begin{aligned} \frac{1}{N}\left\langle \sum_i \sigma_i^x \right\rangle &= \frac{1}{N\beta}\partial_g \ln Z_+ \,, \\ \frac{1}{N}\left\langle \sum_i \sigma_i^z \sigma_{i+1}^z \right\rangle &= \frac{1}{N\beta}\partial_J \ln Z_+ \,. \end{aligned} \tag{5.103}$$

These are shown in Fig. 5.5. The behaviour of these order parameters mimics the phases defined in Fig. 5.4.

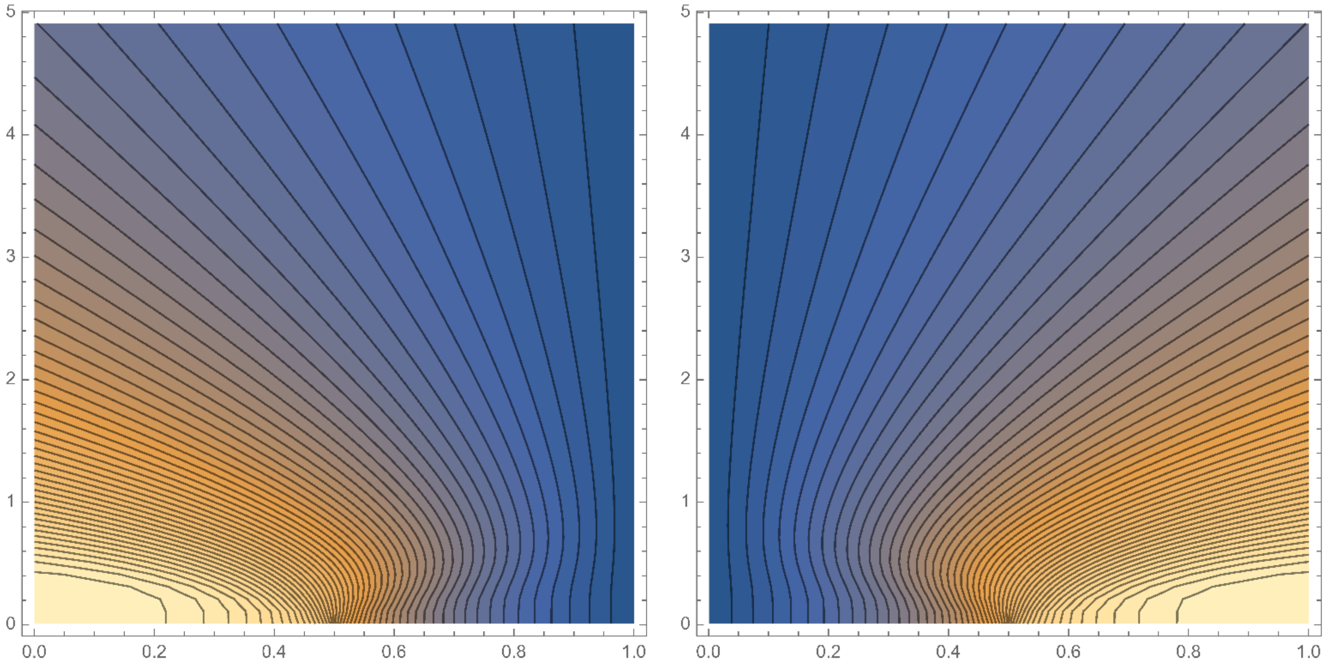

Figure 5.5: Contour plots of magnetization per spin (left) and spin-spin correlation (right) as defined in Eq. (5.103) versus scale parameter s (horizontal axis) and temperature $k_B T/(\hbar\Omega)$ (vertical axis). Contours range from 0.02 (blue) to 0.98 (yellow). Other parameters $g = \Omega(1-s)$, $J = \Omega s$.

Chapter 6

Open Quantum Systems

6.1 Mathematical Prerequisites

Master equations are often used to describe the dynamics of systems interacting with one or many large reservoirs (baths). To derive them from microscopic models – including the Hamiltonian of the full system – requires to review some basic mathematical concepts.

6.1.1 Tensor Product

The greatest advantage of the density matrix formalism is visible when quantum systems composed of several subsystems are considered. Roughly speaking, the tensor product represents a way to construct a larger vector space from two (or more) smaller vector spaces.

Box 18 (Tensor Product) *Let V and W be Hilbert spaces (vector spaces with scalar product) of dimension m and n with basis vectors $\{\left|v\right>\}$ and $\{\left|w\right>\}$, respectively. Then $V \otimes W$ is a Hilbert space of dimension $m \cdot n$, and a basis is spanned by $\{\left|v\right> \otimes \left|w\right>\}$, which is a set combining every basis vector of V with every basis vector of W.*

Mathematical properties

- *Bilinearity* $(z_1 \left|v_1\right> + z_2 \left|v_2\right>) \otimes \left|w\right> = z_1 \left|v_1\right> \otimes \left|w\right> + z_2 \left|v_2\right> \otimes \left|w\right>$
- *operators acting on the combined Hilbert space* $A \otimes B$ *act on the basis states as* $(A \otimes B)(\left|v\right> \otimes \left|w\right>) = (A \left|v\right>) \otimes (B \left|w\right>)$
- *any linear operator on* $V \otimes W$ *can be decomposed as* $C = \sum_i c_i A_i \otimes B_i$
- *the scalar product is inherited in the natural way, i.e., one has for* $\left|a\right> = \sum_{ij} a_{ij} \left|v_i\right> \otimes \left|w_j\right>$ *and* $\left|b\right> = \sum_{k\ell} b_{k\ell} \left|v_k\right> \otimes \left|w_\ell\right>$ *the scalar product* $\left<a|b\right> = \sum_{ijk\ell} a_{ij}^* b_{k\ell} \left<v_i|v_k\right> \left<w_j|w_\ell\right> = \sum_{ij} a_{ij}^* b_{ij}$

If more than just two vector spaces are combined to form a larger vector space, the dimension of the joint vector space grows rapidly, as e.g. exemplified by the case of a qubit: Its Hilbert space is just spanned by two vectors $\left|0\right>$ and $\left|1\right>$. The joint Hilbert space of two qubits is four-dimensional, of three qubits 8-dimensional, and of n qubits 2^n-dimensional. Eventually, this exponential growth of the Hilbert space dimension for composite quantum systems is at the heart of quantum computing.

Since the scalar product is inherited, this typically enables a convenient calculation of the trace in case of a few operator decomposition, e.g., for just two operators

$$\begin{aligned}\mathrm{Tr}\left\{A\otimes B\right\} &= \sum_{n_A,n_B} \left\langle n_A, n_B\right| A\otimes B \left|n_A, n_B\right\rangle \\ &= \left[\sum_{n_A} \left\langle n_A\right| A \left|n_A\right\rangle\right]\left[\sum_{n_B} \left\langle n_B\right| B \left|n_B\right\rangle\right] \\ &= \mathrm{Tr}_A\{A\}\mathrm{Tr}_B\{B\}\,, \end{aligned} \tag{6.1}$$

where $\mathrm{Tr}_{A/B}$ denote the trace in the Hilbert space of A and B, respectively.

6.1.2 The partial trace

For composite systems, it is usually not necessary to keep all information of the complete system in the density matrix. Rather, one would like to have a density matrix that encodes all the information on a particular subsystem only. Obviously, the map $\rho \to \mathrm{Tr_B}\left\{\rho\right\}$ to such a reduced density matrix should leave all expectation values of observables A acting only on the considered subsystem invariant, i.e.,

$$\mathrm{Tr}\left\{A\otimes \mathbf{1}\rho\right\} = \mathrm{Tr}\left\{A\mathrm{Tr_B}\left\{\rho\right\}\right\}\,. \tag{6.2}$$

If this basic condition was not fulfilled, there would be no point in defining such a thing as a reduced density matrix: Measurement would yield different results depending on the Hilbert space of the experimenters feeling.

Box 19 (Partial Trace) *Let $\left|a_1\right\rangle$ and $\left|a_2\right\rangle$ be vectors of state space A and $\left|b_1\right\rangle$ and $\left|b_2\right\rangle$ vectors of state space B. Then, the partial trace over state space B is defined via*

$$\mathrm{Tr_B}\left\{\left|a_1\right\rangle\left\langle a_2\right|\otimes\left|b_1\right\rangle\left\langle b_2\right|\right\} = \left|a_1\right\rangle\left\langle a_2\right| \mathrm{Tr}\left\{\left|b_1\right\rangle\left\langle b_2\right|\right\}\,. \tag{6.3}$$

The partial trace is linear, such that the partial trace of arbitrary operators is calculated similarly. By choosing the $\left|a_\alpha\right\rangle$ and $\left|b_\gamma\right\rangle$ as an orthonormal basis in the respective Hilbert space, one may therefore calculate the most general partial trace via

$$\begin{aligned}\mathrm{Tr_B}\left\{C\right\} &= \mathrm{Tr_B}\left\{\sum_{\alpha\beta\gamma\delta} c_{\alpha\beta\gamma\delta}\left|a_\alpha\right\rangle\left\langle a_\beta\right|\otimes\left|b_\gamma\right\rangle\left\langle b_\delta\right|\right\} \\ &= \sum_{\alpha\beta\gamma\delta} c_{\alpha\beta\gamma\delta}\mathrm{Tr_B}\left\{\left|a_\alpha\right\rangle\left\langle a_\beta\right|\otimes\left|b_\gamma\right\rangle\left\langle b_\delta\right|\right\} \\ &= \sum_{\alpha\beta\gamma\delta} c_{\alpha\beta\gamma\delta}\left|a_\alpha\right\rangle\left\langle a_\beta\right| \mathrm{Tr}\left\{\left|b_\gamma\right\rangle\left\langle b_\delta\right|\right\} \\ &= \sum_{\alpha\beta\gamma\delta} c_{\alpha\beta\gamma\delta}\left|a_\alpha\right\rangle\left\langle a_\beta\right| \sum_\epsilon \left\langle b_\epsilon|b_\gamma\right\rangle\left\langle b_\delta|b_\epsilon\right\rangle \\ &= \sum_{\alpha\beta}\left[\sum_\gamma c_{\alpha\beta\gamma\gamma}\right]\left|a_\alpha\right\rangle\left\langle a_\beta\right|\,. \end{aligned} \tag{6.4}$$

The definition 19 is the only linear map that respects the invariance of expectation values.

As an example, we can compute the partial trace of a pure density matrix $\rho = \left|\Psi\right>\left<\Psi\right|$ in the bipartite state

$$\left|\Psi\right> = \frac{1}{\sqrt{2}}\left(\left|01\right> + \left|10\right>\right) \equiv \frac{1}{\sqrt{2}}\left(\left|0\right>\otimes\left|1\right> + \left|1\right>\otimes\left|0\right>\right) . \tag{6.5}$$

The reduced density matrix becomes

$$\rho_A = \mathrm{Tr}_{\mathrm{B}}\left\{\left|\Psi\right>\left<\Psi\right|\right\} = \frac{1}{2}\left|0\right>\left<0\right| + \frac{1}{2}\left|1\right>\left<1\right| . \tag{6.6}$$

6.2 Coarse-Graining derivation of a Master Equation

In some cases, it is possible to derive a master equation rigorously based only on a few assumptions. Open quantum systems for example are mostly treated as part of a much larger closed quantum system (the union of system and bath), where the partial trace is used to eliminate the unwanted (typically many) degrees of freedom of the bath [19, 20]. Technically speaking, we will consider Hamiltonians of the form

$$H = H_{\mathrm{S}}\otimes\mathbf{1} + \mathbf{1}\otimes H_{\mathrm{B}} + H_{\mathrm{I}} , \tag{6.7}$$

where the system and bath Hamiltonians act only on the system and bath Hilbert space, respectively. Since the index clearly defines on which space the respective Hamiltonian is acting, we often also write

$$H = H_{\mathrm{S}} + H_{\mathrm{B}} + H_{\mathrm{I}} . \tag{6.8}$$

It is important to note that the interaction Hamiltonian acts on both Hilbert spaces

$$H_{\mathrm{I}} = \sum_\alpha A_\alpha \otimes B_\alpha , \tag{6.9}$$

where the summation boundaries are in the worst case limited by the dimension of the system Hilbert space $\alpha < N^2 - 1$. As we consider physical observables here, it is required that all Hamiltonians of system, bath, and interaction are self-adjoint. This enables one to find representations where even all individual system and bath operators in the coupling Hamiltonian are self-adjoint $A_\alpha = A_\alpha^\dagger$ and $B_\alpha = B_\alpha^\dagger$, we will however not assume this here.

Here, we will derive the master equation generally, for an arbitrary system coupled to a thermal environment. This will at first appear a bit technical but may prove useful later-on, since it also allows us to show general properties for later reference.

6.2.1 Interaction Picture

When the interaction H_{I} is small, it is justified to apply perturbation theory. The von-Neumann equation in the joint total quantum system

$$\dot\rho = -\mathrm{i}\left[H_{\mathrm{S}} + H_{\mathrm{B}} + H_{\mathrm{I}}, \rho\right] \tag{6.10}$$

describes the full evolution of the combined density matrix. This equation can be formally solved by the unitary evolution $\rho(t) = e^{-\mathrm{i}Ht}\rho_0 e^{+\mathrm{i}Ht}$, which however is impractical to compute as H involves too many degrees of freedom.

Transforming to the interaction picture

$$\boldsymbol{\rho}(t) = e^{+\mathrm{i}(H_{\mathrm{S}}+H_{\mathrm{B}})t}\rho(t)e^{-\mathrm{i}(H_{\mathrm{S}}+H_{\mathrm{B}})t} , \tag{6.11}$$

which will be denoted by bold symbols throughout, the von-Neumann equation transforms into

$$\dot{\boldsymbol{\rho}} = -\mathrm{i}\left[\boldsymbol{H_I}(t), \boldsymbol{\rho}\right] , \tag{6.12}$$

where the in general time-dependent interaction Hamiltonian

$$\begin{aligned}\boldsymbol{H_I}(t) &= e^{+\mathrm{i}(H_\mathrm{S}+H_\mathrm{B})t} H_\mathrm{I} e^{-\mathrm{i}(H_\mathrm{S}+H_\mathrm{B})t} = \sum_\alpha e^{+\mathrm{i}H_\mathrm{S}t} A_\alpha e^{-\mathrm{i}H_\mathrm{S}t} \otimes e^{+\mathrm{i}H_\mathrm{B}t} B_\alpha e^{-\mathrm{i}H_\mathrm{B}t} \\ &= \sum_\alpha \boldsymbol{A_\alpha}(t) \otimes \boldsymbol{B_\alpha}(t)\end{aligned} \tag{6.13}$$

allows to perform perturbation theory.

Coarse-graining provides a possibility to obtain valid short-time approximations of the density matrix with a generator that is of Lindblad form. We start with the von-Neumann equation in the interaction picture (6.12). For factorizing initial density matrices, it is formally solved by $\boldsymbol{U}(t)\rho_\mathrm{S}^0 \otimes \bar{\rho}_\mathrm{B} \boldsymbol{U}^\dagger(t)$, where the time evolution operator

$$\boldsymbol{U}(t) = \hat{\tau} \exp\left\{-\mathrm{i}\int\limits_0^t \boldsymbol{H_I}(t')dt'\right\} \tag{6.14}$$

obeys the evolution equation

$$\dot{\boldsymbol{U}} = -\mathrm{i}\boldsymbol{H_I}(t)\boldsymbol{U}(t) , \tag{6.15}$$

which defines the time-ordering operator $\hat{\tau}$. Formally integrating this equation with the evident initial condition $\boldsymbol{U}(0) = \boldsymbol{1}$ yields

$$\begin{aligned}\boldsymbol{U}(t) &= \boldsymbol{1} - \mathrm{i}\int\limits_0^t \boldsymbol{H_I}(t')\boldsymbol{U}(t')dt' \\ &= \boldsymbol{1} - \mathrm{i}\int\limits_0^t \boldsymbol{H_I}(t')dt' - \int\limits_0^t dt' \boldsymbol{H_I}(t') \left[\int\limits_0^{t'} dt'' \boldsymbol{H_I}(\boldsymbol{t''})\boldsymbol{U}(t'')\right] \\ &= \sum_{n=0}^\infty (-\mathrm{i})^n \int\limits_0^t dt_1 \int\limits_0^{t_1} dt_2 \ldots \int\limits_0^{t_{n-1}} dt_n \boldsymbol{H_I}(t_1) \ldots \boldsymbol{H_I}(t_n) .\end{aligned} \tag{6.16}$$

In particular, we can define the truncated operator to second order

$$\boldsymbol{U}_2(t) = \boldsymbol{1} - \mathrm{i}\int\limits_0^t \boldsymbol{H_I}(t_1)dt_1 - \int\limits_0^t dt_1 dt_2 \boldsymbol{H_I}(t_1)\boldsymbol{H_I}(t_2)\Theta(t_1 - t_2) , \tag{6.17}$$

where we have introduced the Heaviside function to account for the ordering of the integral bounds. For the Hermitian conjugate operator we obtain

$$\boldsymbol{U}_2^\dagger(t) = \boldsymbol{1} + \mathrm{i}\int\limits_0^t \boldsymbol{H_I}(t_1)dt_1 - \int\limits_0^t dt_1 dt_2 \boldsymbol{H_I}(t_1)\boldsymbol{H_I}(t_2)\Theta(t_2 - t_1) . \tag{6.18}$$

To keep the discussion at a moderate level, we assume $\mathrm{Tr}\left\{\boldsymbol{H_I}\bar{\rho}_\mathrm{B}\right\} = 0$ from the beginning. The exact solution $\boldsymbol{\rho_S(t)} = \mathrm{Tr}_\mathrm{B}\left\{\boldsymbol{U}(t)\rho_\mathrm{S}^0 \otimes \bar{\rho}_\mathrm{B}\boldsymbol{U}^\dagger(t)\right\}$ is then approximated by

$$
\begin{aligned}
\boldsymbol{\rho_S^{(2)}}(t) \approx \rho_\mathrm{S}^0 &+ \mathrm{Tr}_\mathrm{B}\left\{\int\limits_0^t dt_1 \int\limits_0^t dt_2 \boldsymbol{H_I}(t_1)\rho_\mathrm{S}^0 \otimes \bar{\rho}_\mathrm{B}\boldsymbol{H_I}(t_2)\right\} \qquad (6.19)\\
&- \int\limits_0^t dt_1 dt_2 \mathrm{Tr}_\mathrm{B}\left\{\Theta(t_1-t_2)\boldsymbol{H_I}(t_1)\boldsymbol{H_I}(t_2)\rho_\mathrm{S}^0\otimes\bar{\rho}_\mathrm{B} + \Theta(t_2-t_1)\rho_\mathrm{S}^0\otimes\bar{\rho}_\mathrm{B}\boldsymbol{H_I}(t_1)\boldsymbol{H_I}(t_2)\right\} .
\end{aligned}
$$

We introduce the bath correlation functions with two time arguments

$$
C_{\alpha\beta}(t_1,t_2) = \mathrm{Tr}\left\{\boldsymbol{B_\alpha}(t_1)\boldsymbol{B_\beta}(t_2)\bar{\rho}_\mathrm{B}\right\} , \qquad (6.20)
$$

such that we have

$$
\begin{aligned}
\boldsymbol{\rho_S^{(2)}}(t) = \rho_\mathrm{S}^0 + \sum_{\alpha\beta}\int\limits_0^t dt_1 \int\limits_0^t dt_2 C_{\alpha\beta}(t_1,t_2)\Big[&\boldsymbol{A_\beta}(t_2)\rho_\mathrm{S}^0\boldsymbol{A_\alpha}(t_1)\\
&- \Theta(t_1-t_2)\boldsymbol{A_\alpha}(t_1)\boldsymbol{A_\beta}(t_2)\rho_\mathrm{S}^0 - \Theta(t_2-t_1)\rho_\mathrm{S}^0\boldsymbol{A_\alpha}(t_1)\boldsymbol{A_\beta}(t_2)\Big] . \qquad (6.21)
\end{aligned}
$$

Typically, in the interaction picture, the system coupling operators $\boldsymbol{A_\alpha}(t)$ will simply carry some oscillatory time dependence. In the worst case, they may remain time-independent. Therefore, the decay of the correlation function is essential for the convergence of the above integrals. In this way, Markovian approximation and weak-coupling assumptions are related. In particular, we note that the truncated density matrix may remain finite even when $t \to \infty$, rendering the expansion convergent also in the long-term limit.

6.2.2 Coarse-Graining

The basic idea of **coarse-graining** is to match this approximate expression for the system density matrix at time $t = \tau$ with one resulting from a Markovian generator

$$
\boldsymbol{\rho_S}^\mathrm{CG}(\tau) = e^{\mathcal{L}_\tau^\mathrm{CG}\cdot\tau}\rho_\mathrm{S}^0 \approx \rho_\mathrm{S}^0 + \tau\mathcal{L}_\tau^\mathrm{CG}\rho_\mathrm{S}^0 , \qquad (6.22)
$$

such that we can infer the action of the generator on an arbitrary density matrix

$$
\begin{aligned}
\mathcal{L}_\tau^\mathrm{CG}\boldsymbol{\rho_S} &= \frac{1}{\tau}\sum_{\alpha\beta}\int\limits_0^\tau dt_1 \int\limits_0^\tau dt_2 C_{\alpha\beta}(t_1,t_2)\Big[\boldsymbol{A_\beta}(t_2)\boldsymbol{\rho_S}\boldsymbol{A_\alpha}(t_1)\\
&\qquad - \Theta(t_1-t_2)\boldsymbol{A_\alpha}(t_1)\boldsymbol{A_\beta}(t_2)\boldsymbol{\rho_S} - \Theta(t_2-t_1)\boldsymbol{\rho_S}\boldsymbol{A_\alpha}(t_1)\boldsymbol{A_\beta}(t_2)\Big]\\
&= -\mathrm{i}\left[\frac{1}{2\mathrm{i}\tau}\int\limits_0^\tau dt_1 \int\limits_0^\tau dt_2 \sum_{\alpha\beta} C_{\alpha\beta}(t_1,t_2)\mathrm{sgn}(\mathrm{t}_1-\mathrm{t}_2)\boldsymbol{A_\alpha}(\mathrm{t}_1)\boldsymbol{A_\beta}(\mathrm{t}_2), \boldsymbol{\rho_S}\right]\\
&\qquad + \frac{1}{\tau}\int\limits_0^\tau dt_1 \int\limits_0^\tau dt_2 \sum_{\alpha\beta} C_{\alpha\beta}(t_1,t_2)\left[\boldsymbol{A_\beta}(t_2)\boldsymbol{\rho_S}\boldsymbol{A_\alpha}(t_1) - \frac{1}{2}\left\{\boldsymbol{A_\alpha}(t_1)\boldsymbol{A_\beta}(t_2), \boldsymbol{\rho_S}\right\}\right] ,
\end{aligned}
\qquad (6.23)
$$

where we have inserted $\Theta(x) = \frac{1}{2}\left[1 + \mathrm{sgn(x)}\right]$ – in order to separate unitary and dissipative effects of the system-reservoir interaction.

Box 20 (CG Master Equation) *In the weak coupling limit, an interaction Hamiltonian of the form* $H_{\rm I} = \sum_\alpha A_\alpha \otimes B_\alpha$ *leads to the Lindblad-form master equation in the interaction picture*

$$\dot{\boldsymbol{\rho}}_{\mathbf{S}} = -\mathrm{i}\left[\frac{1}{2\mathrm{i}\tau}\int\limits_0^\tau dt_1 \int\limits_0^\tau dt_2 \sum_{\alpha\beta} C_{\alpha\beta}(t_1,t_2)\mathrm{sgn}(\mathrm{t}_1-\mathrm{t}_2)\boldsymbol{A}_{\boldsymbol{\alpha}}(\mathrm{t}_1)\boldsymbol{A}_{\boldsymbol{\beta}}(\mathrm{t}_2), \boldsymbol{\rho}_{\mathbf{S}}\right]$$
$$+\frac{1}{\tau}\int\limits_0^\tau dt_1 \int\limits_0^\tau dt_2 \sum_{\alpha\beta} C_{\alpha\beta}(t_1,t_2)\left[\boldsymbol{A}_{\boldsymbol{\beta}}(t_2)\boldsymbol{\rho}_{\mathbf{S}}\boldsymbol{A}_{\boldsymbol{\alpha}}(t_1) - \frac{1}{2}\left\{\boldsymbol{A}_{\boldsymbol{\alpha}}(t_1)\boldsymbol{A}_{\boldsymbol{\beta}}(t_2), \boldsymbol{\rho}_{\mathbf{S}}\right\}\right],$$

where the bath correlation functions are given by

$$C_{\alpha\beta}(t_t,t_2) = \mathrm{Tr}\left\{e^{+\mathrm{i}H_{\rm B}t_1}B_\alpha e^{-\mathrm{i}H_{\rm B}t_1}e^{+\mathrm{i}H_{\rm B}t_2}B_\beta e^{-\mathrm{i}H_{\rm B}t_2}\bar{\rho}_{\rm B}\right\}. \tag{6.24}$$

We have not used Hermiticity of the coupling operators nor that the bath correlation functions do typically only depend on a single argument. However, if the coupling operators were chosen Hermitian, it is easy to show the Lindblad form. For completeness, we also note there that a Lindblad form is also obtained for non-Hermitian couplings. Obtaining the master equation requires the calculation of bath correlation functions and the evolution of the coupling operators in the interaction picture. This master equation is now always of Lindblad form.

Thus, we have found that the best approximation to the exact solution can be written as $\rho(t) = e^{\mathcal{L}_t^{\rm CG}t}\rho_0$. Unfortunately, this is not the solution to a (single) master equation only. By acting with a time-derivative, we can see that $\dot\rho \neq \mathcal{L}_t^{\rm CG}\rho(t)$. Rather, if interested in the solution at a specific time t, we would have to derive the Liouville superoperator and then exponentiate it.

6.2.3 Correspondence to the quantum-optical master equation

Let us make once more the time-dependence of the coupling operators explicit, which is most conveniently done in the system energy eigenbasis. Now, we also assume that the bath correlation functions only depend on the difference of their time arguments $C_{\alpha\beta}(t_1,t_2) = C_{\alpha\beta}(t_1-t_2)$, such that we may use their Fourier transforms to obtain

$$\dot{\boldsymbol{\rho}}_{\mathbf{S}} = -\mathrm{i}\left[\frac{1}{2\mathrm{i}\tau}\sum_{abc}\int\limits_0^\tau dt_1 \int\limits_0^\tau dt_2 \sum_{\alpha\beta} C_{\alpha\beta}(t_1-t_2)\mathrm{sgn}(\mathrm{t}_1-\mathrm{t}_2)\left|\mathrm{a}\right\rangle\left\langle\mathrm{a}\right|\boldsymbol{A}_{\boldsymbol{\alpha}}(\mathrm{t}_1)\left|\mathrm{c}\right\rangle\left\langle\mathrm{c}\right|\boldsymbol{A}_{\boldsymbol{\beta}}(\mathrm{t}_2)\left|\mathrm{b}\right\rangle\left\langle\mathrm{b}\right|, \boldsymbol{\rho}_{\mathbf{S}}\right]$$
$$+\frac{1}{\tau}\int\limits_0^\tau dt_1 \int\limits_0^\tau dt_2 \sum_{\alpha\beta}\sum_{abcd} C_{\alpha\beta}(t_1-t_2)\Big[\left|a\right\rangle\left\langle a\right|\boldsymbol{A}_{\boldsymbol{\beta}}(t_2)\left|b\right\rangle\left\langle b\right|\boldsymbol{\rho}_{\mathbf{S}}\left|d\right\rangle\left\langle d\right|\boldsymbol{A}_{\boldsymbol{\alpha}}(t_1)\left|c\right\rangle\left\langle c\right|$$
$$-\frac{1}{2}\left\{\left|d\right\rangle\left\langle d\right|\boldsymbol{A}_{\boldsymbol{\alpha}}(t_1)\left|c\right\rangle\left\langle c\right|\cdot\left|a\right\rangle\left\langle a\right|\boldsymbol{A}_{\boldsymbol{\beta}}(t_2)\left|b\right\rangle\left\langle b\right|, \boldsymbol{\rho}_{\mathbf{S}}\right\}\Big]$$
$$= -\mathrm{i}\frac{1}{4\mathrm{i}\pi\tau}\int d\omega\sum_{abc}\int\limits_0^\tau dt_1 \int\limits_0^\tau dt_2 \sum_{\alpha\beta}\sigma_{\alpha\beta}(\omega)e^{-\mathrm{i}\omega(t_1-t_2)}e^{+\mathrm{i}(E_a-E_c)t_1}e^{+\mathrm{i}(E_c-E_b)t_2}A_\beta^{cb}A_\alpha^{ac}\left[L_{ab}, \boldsymbol{\rho}_{\mathbf{S}}\right]$$
$$+\frac{1}{2\pi\tau}\int d\omega\int\limits_0^\tau dt_1 \int\limits_0^\tau dt_2 \sum_{\alpha\beta}\sum_{abcd}\gamma_{\alpha\beta}(\omega)e^{-\mathrm{i}\omega(t_1-t_2)}e^{+\mathrm{i}(E_a-E_b)t_2}e^{+\mathrm{i}(E_d-E_c)t_1}A_\beta^{ab}A_\alpha^{dc}\times$$
$$\times\left[L_{ab}\boldsymbol{\rho}_{\mathbf{S}}L_{cd}^\dagger - \frac{1}{2}\left\{L_{cd}^\dagger L_{ab}, \boldsymbol{\rho}_{\mathbf{S}}\right\}\right]. \tag{6.25}$$

Here, the FTs of the reservoir correlation functions read

$$\gamma_{\alpha\beta}(\omega) = \int C_{\alpha\beta}(\tau) e^{+\mathrm{i}\omega\tau} d\tau\,, \qquad \sigma_{\alpha\beta}(\omega) = \int C_{\alpha\beta}(\tau)\mathrm{sgn}(\tau) e^{+\mathrm{i}\omega\tau} d\tau\,. \tag{6.26}$$

In particular, the matrix formed by $\gamma_{\alpha\beta}(\omega)$ at fixed ω is positive semidefinite, as a consequence of Bochner's theorem [17].

We perform the temporal integrations by invoking

$$\int\limits_0^\tau e^{\mathrm{i}\alpha_k t_k} dt_k = \tau e^{\mathrm{i}\alpha_k\tau/2}\mathrm{sinc}\left[\frac{\alpha_\mathrm{k}\tau}{2}\right] \tag{6.27}$$

with the bandfilter function sinc(x) = sin(x)/x to obtain

$$\begin{aligned}
\dot{\boldsymbol{\rho}}_{\mathbf{S}} &= -\mathrm{i}\frac{\tau}{4\mathrm{i}\pi}\int d\omega \sum_{abc}\sum_{\alpha\beta}\sigma_{\alpha\beta}(\omega) e^{\mathrm{i}\tau(E_a-E_b)/2}\mathrm{sinc}\left[\frac{\tau}{2}(\mathrm{E_a}-\mathrm{E_c}-\omega)\right]\mathrm{sinc}\left[\frac{\tau}{2}(\mathrm{E_c}-\mathrm{E_b}+\omega)\right]\times\\
&\quad\times \langle c|A_\beta|b\rangle\langle c|A_\alpha^\dagger|a\rangle^* \left[|a\rangle\langle b|, \boldsymbol{\rho}_{\mathbf{S}}\right]\\
&\quad+\frac{\tau}{2\pi}\int d\omega\sum_{\alpha\beta}\sum_{abcd}\gamma_{\alpha\beta}(\omega) e^{\mathrm{i}\tau(E_a-E_b+E_d-E_c)/2}\mathrm{sinc}\left[\frac{\tau}{2}(\mathrm{E_d}-\mathrm{E_c}-\omega)\right]\mathrm{sinc}\left[\frac{\tau}{2}(\omega+\mathrm{E_a}-\mathrm{E_b})\right]\times\\
&\quad\times\langle a|A_\beta|b\rangle\langle c|A_\alpha^\dagger|d\rangle^*\left[|a\rangle\langle b|\boldsymbol{\rho}_{\mathbf{S}}(|c\rangle\langle d|)^\dagger - \frac{1}{2}\left\{(|c\rangle\langle d|)^\dagger|a\rangle\langle b|, \boldsymbol{\rho}_{\mathbf{S}}\right\}\right]\,.
\end{aligned} \tag{6.28}$$

Therefore, the coefficients in the master equation depend on the coarse-graining time

$$\begin{aligned}
\dot{\boldsymbol{\rho}}_{\mathbf{S}} &= -\mathrm{i}\left[\sum_{ab}\sigma_{ab}^\tau|a\rangle\langle b|, \boldsymbol{\rho}_{\mathbf{S}}\right]\\
&\quad+\sum_{abcd}\gamma_{ab,cd}^\tau\left[|a\rangle\langle b|\boldsymbol{\rho}_{\mathbf{S}}(|c\rangle\langle d|)^\dagger-\frac{1}{2}\left\{(|c\rangle\langle d|)^\dagger|a\rangle\langle b|, \boldsymbol{\rho}_{\mathbf{S}}\right\}\right]
\end{aligned} \tag{6.29}$$

with the coefficients

$$\begin{aligned}
\sigma_{ab}^\tau &= \frac{1}{2\mathrm{i}}\int d\omega\sum_c e^{\mathrm{i}\tau(E_a-E_b)/2}\frac{\tau}{2\pi}\mathrm{sinc}\left[\frac{\tau}{2}(\mathrm{E_a}-\mathrm{E_c}-\omega)\right]\mathrm{sinc}\left[\frac{\tau}{2}(\mathrm{E_b}-\mathrm{E_c}-\omega)\right]\times\\
&\quad\times\left[\sum_{\alpha\beta}\sigma_{\alpha\beta}(\omega)\langle c|A_\beta|b\rangle\langle c|A_\alpha^\dagger|a\rangle^*\right]\,,\\
\gamma_{ab,cd}^\tau &= \int d\omega e^{\mathrm{i}\tau(E_a-E_b+E_d-E_c)/2}\frac{\tau}{2\pi}\mathrm{sinc}\left[\frac{\tau}{2}(\mathrm{E_d}-\mathrm{E_c}-\omega)\right]\mathrm{sinc}\left[\frac{\tau}{2}(\mathrm{E_b}-\mathrm{E_a}-\omega)\right]\times\\
&\quad\times\left[\sum_{\alpha\beta}\gamma_{\alpha\beta}(\omega)\langle a|A_\beta|b\rangle\langle c|A_\alpha^\dagger|d\rangle^*\right]\,.
\end{aligned} \tag{6.30}$$

Most important, in the limit of large coarse-graining times $\tau\to\infty$, these dampening coefficients converge to a finite limit

$$\lim_{\tau\to\infty}\tau\mathrm{sinc}\left[\frac{\tau}{2}(\Omega_\mathrm{a}-\omega)\right]\mathrm{sinc}\left[\frac{\tau}{2}(\Omega_\mathrm{b}-\omega)\right] = 2\pi\delta_{\Omega_\mathrm{a},\Omega_\mathrm{b}}\delta(\Omega_\mathrm{a}-\omega)\,. \tag{6.31}$$

With defining

$$\lim_{\tau\to\infty}\sigma_{ab}^\tau \equiv \sigma_{ab}\,, \qquad \lim_{\tau\to\infty}\gamma_{ab,cd}^\tau\equiv\gamma_{ab,cd}\,, \tag{6.32}$$

we eventually arrive at the quantum-optical master equation

Box 21 (BMS master equation) *In the weak coupling limit, an interaction Hamiltonian of the form* $H_\mathrm{I} = \sum_\alpha A_\alpha \otimes B_\alpha$ *with system coupling operators* A_α *and bath coupling operators* B_α *and* $[H_\mathrm{B}, \bar{\rho}_\mathrm{B}] = 0$ *and* $\mathrm{Tr}\left\{B_\alpha \bar{\rho}_\mathrm{B}\right\} = 0$ *leads in the system energy eigenbasis* $H_\mathrm{S} \left|a\right> = E_a \left|a\right>$ *to the Lindblad-form master equation*

$$\begin{aligned}
\dot{\rho_\mathrm{S}} &= -\mathrm{i}\left[H_\mathrm{S} + \sum_{ab} \sigma_{ab} \left|a\right>\left<b\right|, \rho_\mathrm{S}(t)\right] \\
&\quad + \sum_{a,b,c,d} \gamma_{ab,cd} \left[\left|a\right>\left<b\right| \rho_\mathrm{S}(t) \left(\left|c\right>\left<d\right|\right)^\dagger - \frac{1}{2}\left\{\left(\left|c\right>\left<d\right|\right)^\dagger \left|a\right>\left<b\right|, \rho_\mathrm{S}(t)\right\}\right], \\
\gamma_{ab,cd} &= \sum_{\alpha\beta} \gamma_{\alpha\beta}(E_b - E_a)\delta_{E_b-E_a, E_d-E_c} \left<a\right| A_\beta \left|b\right> \left<c\right| A_\alpha^\dagger \left|d\right>^*, \qquad (6.33)
\end{aligned}$$

where $\gamma_{ab,cd}$ *is a positive semidefinite matrix and the Lamb-shift Hamiltonian* $H_\mathrm{LS} = \sum_{ab} \sigma_{ab} \left|a\right>\left<b\right|$ *matrix elements read*

$$\sigma_{ab} = \sum_{\alpha\beta}\sum_c \frac{1}{2\mathrm{i}} \sigma_{\alpha\beta}(E_b - E_c)\delta_{E_b,E_a} \left<c\right| A_\beta \left|b\right> \left<c\right| A_\alpha^\dagger \left|a\right>^* \qquad (6.34)$$

and the constants are given by even and odd Fourier transforms

$$\begin{aligned}
\gamma_{\alpha\beta}(\omega) &= \int\limits_{-\infty}^{+\infty} C_{\alpha\beta}(\tau) e^{+\mathrm{i}\omega\tau} d\tau, \\
\sigma_{\alpha\beta}(\omega) &= \int\limits_{-\infty}^{+\infty} C_{\alpha\beta}(\tau)\mathrm{sgn}(\tau)\mathrm{e}^{+\mathrm{i}\omega\tau}\mathrm{d}\tau = \frac{\mathrm{i}}{\pi}\mathcal{P}\int\limits_{-\infty}^{+\infty} \frac{\gamma_{\alpha\beta}(\omega')}{\omega - \omega'}\mathrm{d}\omega' \qquad (6.35)
\end{aligned}$$

of the bath correlation functions

$$C_{\alpha\beta}(\tau) = \mathrm{Tr}\left\{e^{+\mathrm{i}H_\mathrm{B}\tau} B_\alpha e^{-\mathrm{i}H_\mathrm{B}\tau} B_\beta \bar{\rho}_\mathrm{B}\right\}. \qquad (6.36)$$

The coarse-graining approach provides an alternative to the standard derivation of the quantum-optical master equation [19], replacing three subsequent approximations (Born-, Markov- and secular) by just one (perturbative expansion in the interaction). Also note that it does not require the coupling operators to be explicitly hermitian.

The above definition may serve as a recipe to cook a Lindblad type master equation in the weak-coupling limit. It is expected to yield good results in the weak coupling and Markovian limit (continuous and nearly flat bath spectral density), when $[\bar{\rho}_\mathrm{B}, H_\mathrm{B}] = 0$ and additionally the level splittings of the system is large in comparison to the coupling strength to the reservoir. It requires to rewrite the coupling operators tensor product form, to calculate the bath correlation function Fourier transforms, and to diagonalize system Hamiltonian. The above quantum-optical master equation is heavily used since it has many favorable properties.

- In the case that the spectrum of the system Hamiltonian is non-degenerate, we have a further simplification, since the δ-functions simplify further, e.g. $\delta_{E_b,E_a} \to \delta_{ab}$. By taking matrix elements of Eq. (6.33) in the energy eigenbasis $\rho_{aa} = \left<a\right| \rho_\mathrm{S} \left|a\right>$, we obtain an effective rate equation for the populations only

$$\dot{\rho}_{aa} = +\sum_b \gamma_{ab,ab}\rho_{bb} - \left[\sum_b \gamma_{ba,ba}\right]\rho_{aa} \equiv \sum_b W_{ab}\rho_{bb} \,. \tag{6.37}$$

This means that in the energy eigenbasis, the coherences decouple from the evolution of the populations. The transition rates from state b to state a reduce in this case to

$$\begin{aligned} W_{a\neq b} &= \gamma_{ab,ab} = \sum_{\alpha\beta} \gamma_{\alpha\beta}(E_b - E_a) \left\langle a\right| A_\beta \left|b\right\rangle \left\langle a\right| A_\alpha^\dagger \left|b\right\rangle^* \geq 0 \,, \\ W_{aa} &= -\sum_{b\neq a} W_{ba} \,, \end{aligned} \tag{6.38}$$

which – after inserting all definitions – condenses basically to Fermis Golden Rule. The negative entries on the diagonals just enforce the conservation of the trace. Therefore, with such a rate equation description, open quantum systems can be described with the same complexity as closed quantum systems, since only N dynamical variables have to be evolved.

- First, for a bath that is in thermal equilibrium

$$\bar{\rho}_{\rm B} = \frac{e^{-\beta H_{\rm B}}}{{\rm Tr}\left\{e^{-\beta H_{\rm B}}\right\}} \tag{6.39}$$

with inverse temperature β one can show that the reservoir correlation functions obey analytic properties such as the Kubo-Martin-Schwinger (KMS) condition (we now use $\bar{\alpha}$ for the indices in order to avoid confusion with the inverse temperature)

$$C_{\alpha\bar{\alpha}}(\tau) = C_{\bar{\alpha}\alpha}(-\tau - {\rm i}\beta) \,. \tag{6.40}$$

For the Fourier transform, this shift property implies

$$\begin{aligned} \gamma_{\alpha\bar{\alpha}}(-\omega) &= \int\limits_{-\infty}^{+\infty} C_{\alpha\bar{\alpha}}(\tau) e^{-{\rm i}\omega\tau} d\tau = \int\limits_{-\infty}^{+\infty} C_{\bar{\alpha}\alpha}(-\tau - {\rm i}\beta) e^{-{\rm i}\omega\tau} d\tau \\ &= \int\limits_{+\infty-{\rm i}\beta}^{-\infty-{\rm i}\beta} C_{\bar{\alpha}\alpha}(\tau') e^{+{\rm i}\omega(\tau'+{\rm i}\beta)} (-d\tau)' = \int\limits_{-\infty-{\rm i}\beta}^{+\infty-{\rm i}\beta} C_{\bar{\alpha}\alpha}(\tau') e^{+{\rm i}\omega\tau'} d\tau' e^{-\beta\omega} \\ &= \int\limits_{-\infty}^{+\infty} C_{\bar{\alpha}\alpha}(\tau') e^{+{\rm i}\omega\tau'} d\tau' e^{-\beta\omega} = \gamma_{\bar{\alpha}\alpha}(+\omega) e^{-\beta\omega} \,, \end{aligned} \tag{6.41}$$

where in the last line we have used that the bath correlation functions are analytic in τ in the complex plane and vanish at infinity, such that we may safely deform the integration contour. Finally, the KMS condition can thereby be used to prove that for a reservoir with inverse temperature β, the density matrix

$$\bar{\rho}_{\rm S} = \frac{e^{-\beta H_{\rm S}}}{{\rm Tr}\left\{e^{-\beta H_{\rm S}}\right\}} \tag{6.42}$$

is one stationary state of the BMS master equation (and the $\tau \to \infty$ limit of the CG appraoch). In orther words, the system thermalizes with the reservoir.

- Things become a bit more complicated when the reservoir is in the grand-canonical equilibrium state

  $$\bar{\rho}_{\rm B} = \frac{e^{-\beta(H_{\rm B}-\mu N_{\rm B})}}{{\rm Tr}\left\{e^{-\beta(H_{\rm B}-\mu N_{\rm B})}\right\}}\,, \tag{6.43}$$

  with the chemical potential μ and the particle number operator N_B of the bath. Then, the normal KMS condition is not fulfilled anymore by the correlation function. Chemical potentials become relevant for models discussing particle transport. To talk about transport, it is natural to assume that the total particle number $N = N_{\rm S} + N_{\rm B}$ is a conserved quantity $[H_{\rm S}, N_S] = [H_{\rm B}, N_B] = [H_{\rm I}, N_S + N_B] = 0$. In this case one can show that the KMS relation is generalized according to

  $$\sum_{\bar\alpha} A_{\bar\alpha} C_{\alpha\bar\alpha}(\tau) = \sum_{\bar\alpha} e^{+\beta\mu N_S} A_{\bar\alpha} e^{-\beta\mu N_S} C_{\bar\alpha\alpha}(-\tau - {\rm i}\beta)\,. \tag{6.44}$$

  This modifies the detailed-balance relation of the master equation coefficients to

  $$\frac{\gamma_{ab,cd}}{\gamma_{dc,ba}} = e^{\beta[(E_b-E_a)-\mu(N_b-N_a)]}\,. \tag{6.45}$$

  In the end, these modified relations can be used to show that a stationary state of the BMS master equation is given by

  $$\bar{\rho}_{\rm S} = \frac{e^{-\beta(H_{\rm S}-\mu N_{\rm S})}}{{\rm Tr}\left\{e^{-\beta(H_{\rm S}-\mu N_{\rm S})}\right\}}\,, \tag{6.46}$$

  i.e., both temperature β and chemical potential μ must equilibrate with the reservoir.

6.3 Multiple reservoirs

For multiple reservoirs, the bath is often modeled as a tensor product of stationary local thermal equilibrium states

$$\bar{\rho}_{\rm B} = \bigotimes_\ell \frac{e^{-\beta_\ell(H_{\rm B}^{(\ell)}-\mu_\ell N_B^{(\ell)})}}{Z_\ell} \tag{6.47}$$

with local inverse temperatures β_ℓ and chemical potentials μ_ℓ and Hamiltonian $H_{\rm B}^{(\ell)}$ and particle number operator $N_B^{(\ell)}$ of the l-th bath, respectively. We can then similarly decompose the interaction Hamiltonian as

$$H_{\rm I} = \sum_\alpha \sum_\nu A_\alpha \otimes B_\alpha^{(\nu)}\,. \tag{6.48}$$

Together with the already stated properties of the single-operator expectation values

$${\rm Tr}\left\{B_\alpha^{(\nu)}\bar{\rho}_{\rm B}\right\} = 0\,, \tag{6.49}$$

it follows that to leading order there are no interferences between the reservoirs, i.e., one has for the correlation functions

$$C_{\alpha,\nu;\beta,\nu'} = \delta_{\nu\nu'} C_{\alpha\beta}^{\nu}(t-t')\,. \tag{6.50}$$

Through their FTs, this maps to the full generator of the reduced evolution, such that the evolution of the reduced density matrix can be formally written as

$$\dot{\rho_{\rm S}} = \mathcal{L}_0 \rho_{\rm S} + \sum_\nu \mathcal{L}_\nu \rho_{\rm S} \,, \tag{6.51}$$

where $\mathcal{L}_0\rho_{\rm S} \hat{=} -{\rm i}[H_{\rm S}, \rho_{\rm S}]$ is the free evolution of the system (calligraphic symbols denote superoperator notation) and $\mathcal{L}_\nu$ is the dissipator associated with the νth reservoir.

For an additive decomposition of the dissipator, it is straightforward to associate the energy and matter flows from a reservoir into the system via looking at the energy and matter balance of the system, respectively

$$\begin{aligned}
\frac{d}{dt}\left\langle E\right\rangle &= {\rm Tr}\left\{H_{\rm S}\dot{\rho}\right\} = \sum_\nu {\rm Tr}\left\{H_{\rm S}\left(\mathcal{L}_\nu\rho_{\rm S}\right)\right\} = \sum_\nu I_E^{(\nu)} \,, \\
\frac{d}{dt}\left\langle N\right\rangle &= {\rm Tr}\left\{N_S\dot{\rho}\right\} = \sum_\nu {\rm Tr}\left\{N_S\left(\mathcal{L}_\nu\rho_{\rm S}\right)\right\} = \sum_\nu I_M^{(\nu)} \,,
\end{aligned} \tag{6.52}$$

which defines the energy and matter currents entering the system from reservoir ν, respectively

$$I_E^{(\nu)} = {\rm Tr}\left\{H_{\rm S}\left(\mathcal{L}_\nu\rho_{\rm S}\right)\right\} \,, \qquad I_M^{(\nu)} = {\rm Tr}\left\{N_S\left(\mathcal{L}_\nu\rho_{\rm S}\right)\right\} \,. \tag{6.53}$$

Such a simple treatment only holds for driven Markovian systems in the weak-coupling system and they can only be used to infer the currents entering the system. For other observables, higher moments, or driven and strongly-coupled system, the Full Counting Statistics [20] can be used. These are defined positive when energy and matter enter the system. Note that the bracket notation above enforces that the superoperator notation is evaluated first. In particular, when $\mathcal{L}_\nu$ couples only the populations in the energy eigenbasis to each other, e.g. the energy current becomes

$$\begin{aligned}
I_E^{(\nu)} &= \sum_i E_i\left(\mathcal{L}_\nu\rho_{\rm S}\right)_{ii} = \sum_{ij} E_i W_{ij}^{(\nu)}\rho_{jj} = \sum_{i\neq j} E_i W_{ij}^{(\nu)}\rho_{jj} + \sum_i E_i W_{ii}^{(\nu)}\rho_{ii} \\
&= \sum_{i\neq j} E_i W_{ij}^{(\nu)}\rho_{jj} - \sum_{i\neq j} E_i W_{ji}^{(\nu)}\rho_{ii} = \sum_{i\neq j}(E_i - E_j) W_{ij}^{(\nu)}\rho_{jj} = \sum_{ij}(E_i - E_j) W_{ij}^{(\nu)}\rho_{jj} \,.
\end{aligned} \tag{6.54}$$

Above, we have used the rate equation properties (6.38). This is precisely the value that one would naively assign to a rate equation through a system with discrete energy eigenstates E_i, and an analogous discussion holds for the matter current, assuming that the energy eigenstates are also eigenstates of the particle number operator.

6.4 Application: Transport spectroscopy

We now consider a rate equation in the energy eigenbasis of the system, generated by a two-terminal system

$$\dot{\rho_{\rm S}} = \left(\mathcal{W}^L + \mathcal{W}^R\right)\rho_{\rm S} \,. \tag{6.55}$$

The steady-state energy and matter currents (at steady state, we have $I_{M/E}^{(R)} = -I_{M/E}^{(L)}$) are then given by

$$I_E = \sum_{ij}(E_i - E_j) W_{ij}^{(L)}\bar{\rho}_{jj} \,, \qquad I_M = \sum_{ij}(N_i - N_j) W_{ij}^{(L)}\bar{\rho}_{jj} \,. \tag{6.56}$$

Specifically, we had for a decomposition of the interaction Hamiltonian of the form $H_{\rm I}^\nu = A_\alpha \otimes B_\alpha^\nu$ transition rates of the form

$$W_{ij}^{(\nu)} = \sum_{\alpha\beta} \gamma_{\alpha\beta}^{(\nu)}(E_j - E_i) \langle i| A_\beta |j\rangle \langle i| A_\alpha^\dagger |j\rangle^* \,. \tag{6.57}$$

We now consider the case of a fermionic interaction Hamiltonian of the tunneling type

$$H_{\rm I} = c_0 \sum_{k=1}^\infty t_k c_k^\dagger - c_0^\dagger \sum_{k=1}^\infty t_k^* c_k \,, \tag{6.58}$$

where $c_0^\dagger$ creates a fermion inside the system and $c_k^\dagger$ one in the reservoir in mode k. The sign in the second term exemplifies the problem: Products of fermionic system-bath operators are not tensor products! However, similar to the Jordan-Wigner transform (5.69), we can represent the fermions by (tensor) products of Pauli matrices

$$c_0 = \sigma_0^- \,, \qquad c_k = \sigma_0^z \left[\prod_{\ell=1}^{k-1} \sigma_\ell^z\right] \sigma_k^- \,, \tag{6.59}$$

and in terms of these operators we can write the interaction as

$$\begin{aligned} H_{\rm I} &= \sigma_0^- \sigma_0^z \otimes \sum_{k=1}^\infty t_k \left[\prod_{\ell=1}^{k-1} \sigma_\ell^z\right] \sigma_k^+ - \sigma_0^+ \sigma_0^z \otimes \sum_{k=1}^\infty t_k^* \left[\prod_{\ell=1}^{k-1} \sigma_\ell^z\right] \sigma_k^- \,, \\ &= \tilde{c}_0 \otimes \sum_{k=1}^\infty t_k \tilde{c}_k^\dagger + \tilde{c}_0^\dagger \otimes \sum_{k=1}^\infty t_k^* \tilde{c}_k \,. \end{aligned} \tag{6.60}$$

Within the system and within the bath, the new operators $\tilde{c}_0$ and $\tilde{c}_k$ obey standard fermionic statistics, and we identify the coupling operators $A_1 = \tilde{c}_0$ and $A_2 = \tilde{c}_0^\dagger$ as well as $B_1 = \sum_{k=1}^\infty t_k \tilde{c}_k^\dagger$ and $B_2 = \sum_{k=1}^\infty t_k^* \tilde{c}_k$.

The calculation of a typical correlation function now proceeds along standard routes

$$C_{12}(\tau) = {\rm Tr}\left\{\sum_{k=1}^\infty t_k \tilde{c}_k^\dagger e^{+{\rm i}\epsilon_k \tau} \sum_{q=1}^\infty t_q^* \tilde{c}_q \bar{\rho}_{\rm B}\right\} = \sum_k |t_k|^2 f(\epsilon_k) e^{+{\rm i}\epsilon_k\tau} = \frac{1}{2\pi} \int \Gamma(\omega) f(\omega) e^{+{\rm i}\omega\tau} d\omega \,, \tag{6.61}$$

where we have introduced the spectral (coupling) density

$$\Gamma(\omega) = 2\pi \sum_k |t_k|^2 \delta(\omega - \epsilon_k) \,. \tag{6.62}$$

From this representation, we can immediately read off the FT of the correlation function

$$\gamma_{12}(\omega) = \Gamma(-\omega) f(-\omega) \,. \tag{6.63}$$

A similar calculation (exercise) shows that the FT of the other non-vanishing correlation function becomes

$$\gamma_{21}(\omega) = \Gamma(+\omega)[1 - f(+\omega)] \,. \tag{6.64}$$

Inserting this into the rates, we get

$$\begin{aligned} W_{ij}^{(\nu)} &= \gamma_{12}^{(\nu)}(E_j - E_i) \left|\langle i| \tilde{c}_0^\dagger |j\rangle\right|^2 + \gamma_{21}^{(\nu)}(E_j - E_i) |\langle i| \tilde{c}_0 |j\rangle|^2 \\ &= \Gamma(E_i - E_j) f(E_i - E_j) \left|\langle i| \tilde{c}_0^\dagger |j\rangle\right|^2 + \Gamma(E_j - E_i)[1 - f(E_j - E_i)] |\langle i| \tilde{c}_0 |j\rangle|^2 \,. \end{aligned} \tag{6.65}$$

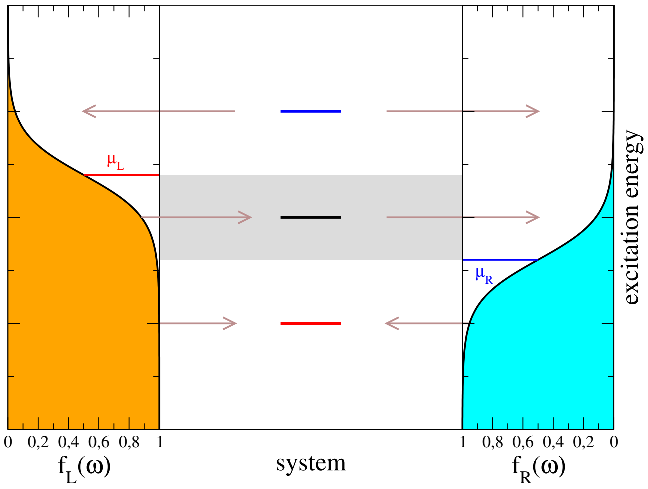

Figure 6.1: Visualization of the transport window. The central panel contains the transition energies of the system, whereas left and right panels visualize the Fermi functions of the leads. Transport is only supported by a transition energy when it is inside the transport window (grey). Transition energies significantly outside this window will essentially just be driven once, corresponding to filling or emptying one particular energy level in the system. Afterwards (at steady state) these transition energies no longer participate in transport.

These rates have a simple interpretation. The matrix elements apparently do not vanish when state i and j differ by the single fermion described by the mode $\tilde{c}_0$. The first term describes a process where a fermion is entering the system from the reservoir, bringing in the energy difference $E_i - E_j$. The second term describes a process of a fermion leaving the system and taking away the energy difference $E_j - E_i$.

This now – together with the property that at low temperatures the Fermi functions behave similar to step functions – enables transport spectroscopy. By connecting an electronic quantum system (quantum dots) to two reservoirs and measuring the current through it, we can learn about its internal states. Essentially, at steady state only those transitions in the rate equation can contribute to transport, when the corresponding Fermi functions are somewhere between zero and one: Let ϵ denote the transition energy between two energy eigenstates of the system, where the higher-energy state is occupied. When the Fermi function of both leads at the transition energy is zero $f_\alpha(\epsilon) = 0$ and consequently $1 - f_\alpha(\epsilon) = 1$, the filled state will just empty to one of the reservoirs via performing the transition to the empty one. A re-occupation of this state is improbable since $f_\alpha(\epsilon) = 0$ for both reservoirs. Conversely, when the Fermi function of both leads at the transition is one, the state will be filled. The particle cannot jump out again, since all reservoir states at this energy are occupied. Only if one of the Fermi functions (called drain) vanishes at the transition energy $f_R(\epsilon) \ll 1/2$ and the other one is large $f_L(\epsilon) \gg 1/2$, the transition will be continuously driven, corresponding to a transport situation where the source continuously provides particles and the drain continuously consumes particles. It is this case where the corresponding transition participates in transport. This defines a window of transport – in particular for low temperatures – visualized in Fig. 6.1. When one increases the bias voltage (defined by the difference of chemical potentials), more excitation energies enter the transport window, which will result in steps of the current, see Fig. 6.2. Here, spectroscopy of a double quantum dot

$$H_S = \epsilon(d_R^\dagger d_R - d_L^\dagger d_L) + T_c(d_L^\dagger d_R + d_R^\dagger d_L) + U d_L^\dagger d_L d_R^\dagger d_R \tag{6.66}$$

has been performed. The eigenenergies of the system equate to

$$E_0 = 0\,, \qquad E_2 = U\,, \qquad E_\pm = \pm\sqrt{\epsilon^2 + T_c^2}\,, \tag{6.67}$$

which explains why the two single-particle states enter the transport window simultaneously (single step in the figure). Therefore, by finding these steps, one can get information about the intrinsic properties of the system. The height of the plateaus can also be calculated by reducing the dimension of the rate equation under Coulomb blockade assumptions.

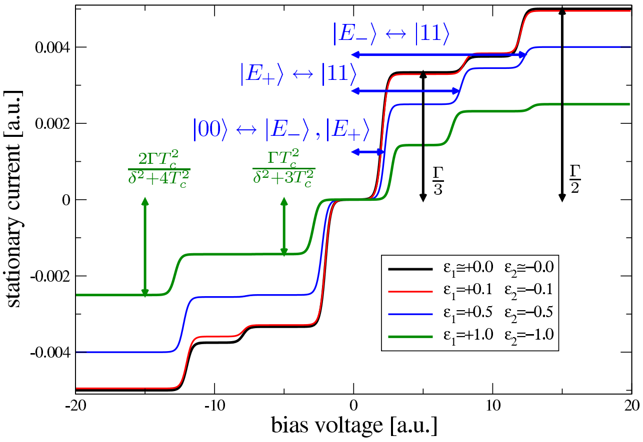

Figure 6.2: Plot of the current through a double quantum dot versus bias voltage $V = \mu_L - \mu_R$, taken from Ref. [21]. For sufficiently low temperatures, position and height of the current steps allow to infer microscopic parameters of the system: As transition energies enter the transport window, this is manifest in steps in the current.

Chapter 7

An introduction to topological Insulators

In brief, a topological insulator is an insulator that however has metallic edge or surface states. These surface states are topologically protected against particular perturbations.

This topological protection has raised some attention since it may be useful to construct quantum devices that are intrinsically protected against the (normally devastating) influence of particular perturbations. The field has become quite huge and many different developments are being observed. We will approach the topic here first from a phenomenological perspective and afterwards study particular models where topological effects are important. There is further reading material available e.g. in Ref. [28].

7.1 Phenomenology: The integer quantum Hall effect

The integer quantum Hall effect is very often used as the simplest manifestation of topological state. Discovered in 1980 by von Klitzing [1], it is a very robust effect observed for sufficiently strong magnetic fields and sufficiently low temperatures.

To understand the setting, we first consider the ordinary Hall [2] effect, which is observed in a piece of conductor subject to a magnetic field. By applying an electric field perpendicular to the magnetic field, one can induce a current in the conductor. The electrons in the conductor start to move and experience a Lorentz force

$$\boldsymbol{F} = e\left(\boldsymbol{E} + \boldsymbol{v} \times \boldsymbol{B}\right) , \tag{7.1}$$

which has components longitudinal with the electric field $\boldsymbol{E}$ and perpendicular to the magnetic field $\boldsymbol{B}$. Initially, the electric field just points in x-direction $\boldsymbol{E}_{\rm i} = E_{\rm ext}\boldsymbol{e_x}$, and electrons will start moving in this direction, building up a velocity component in x-direction. Since $\boldsymbol{B} = B\boldsymbol{e_z}$, the Lorentz force will have a component in y-direction, leading to the accumulation of electrons along the edges of the conductor. The charge imbalance induces a transverse electric field $E_{\rm ind}\boldsymbol{e_y}$ in y direction, which counter-acts this component. At steady state, the velocity of electrons on average points in x direction, and the force from the induced electric field must compensate the force arising from the magnetic field,

$$E_{\rm ind}\boldsymbol{e_y} + vB\boldsymbol{e_x} \times \boldsymbol{e_z} = 0\,, \tag{7.2}$$

which yields a relation between the transverse voltage and the magnetic field, see Fig. 7.1 for an illustration. The Hall voltage measured in perpendicular direction can then be used as a

---

[1] Klaus von Klitzing (born 1943) is a German physicist and Nobel laureate (1985).

[2] Edwin Hall (1855–1938) was an American physicist who discovered the effect during his PhD.

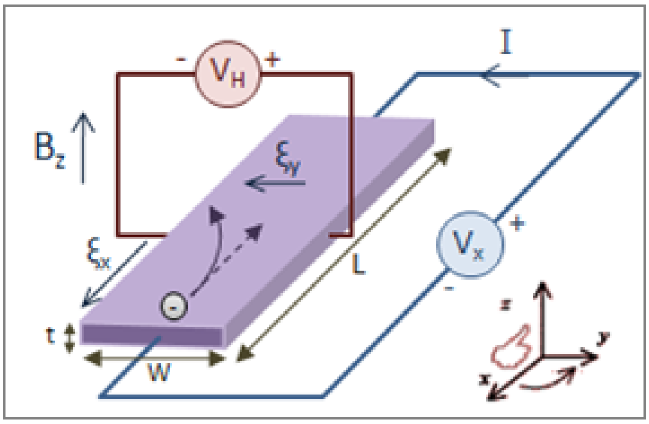

Figure 7.1: Illustration of the ordinary Hall effect. Due to the perpendicular magnetic field, a charge difference along the edges aligned with the applied voltage builds up. It can be measured to deduce the strength of the magnetic field. Source: Wikipedia.

sensitive detector to measure the strength of a magnetic field.

Now, the integer quantum Hall effect is essentially a quantum version that develops as one approaches low temperatures and strong magnetic fields. One measures the perpendicular (Hall) voltage and the longitudinal current along the conductor. Their ratio is the Hall conductivity

$$\sigma_{xy} = \frac{I_\parallel}{V_\perp} = C\frac{e^2}{h}\,. \tag{7.3}$$

At sufficiently low temperatures and strong fields, one now observes – with strikingly good accuracy – that the Hall conductivity is integer-quantized

$$C \in \{1, 2, 3, \ldots\} \tag{7.4}$$

Here, the constant C is known as Chern [3] number (which can be microscopically calculated). The inverse of the Hall conductivity defines the transverse (Hall) resistance

$$\rho_{xy} = \frac{V_\perp}{I_\parallel}\,. \tag{7.5}$$

One observes that it is quantized accordingly and shows plateaus, see Fig. 7.2. At the plateaus of the transverse resistance, the transport through the system is mediated by edge states, which in pictorial representations often drawn as electrons bouncing in semicircles along the boundaries, see Fig. 7.3. At the same time, the longitudinal resistance

$$\rho_{xx} = \frac{V_\parallel}{I_\parallel} = \frac{1}{\sigma_{xx}} \tag{7.6}$$

nearly vanishes at these regions. Only when the magnetic field is fine-tuned to particular values, one observes that the system suddenly behaves quite differently. Then, the longitudinal resistance ρ_{xx} shows finite peaks, and the transversal resistance ρ_{xy} switches from one plateau to another. This can be seen as a topological phase transition. Quantum-mechanically, the steps in the resistance can be understood from the formation of Landau levels in 2d electron gases subject to a magnetic field. As we discussed in Sec. 5.4, the energy levels in an electron gas become quantized. To induce transitions between the Landau levels, one therefore has to provide the energy of the cyclotron frequency

$$\hbar\omega_0 = \frac{|e|\hbar B}{mc}\,. \tag{7.7}$$

The extreme accuracy of this effect has led to a new standard of electrical resistance $R_K = \frac{h}{e^2}$ (the Klitzing constant), but it its robustness has puzzled scientists. In this chapter, we would like to approach this robustness qualitatively.

---

[3] Shiing-Shen Chern (1911–2004) was a chinese-american mathematician.

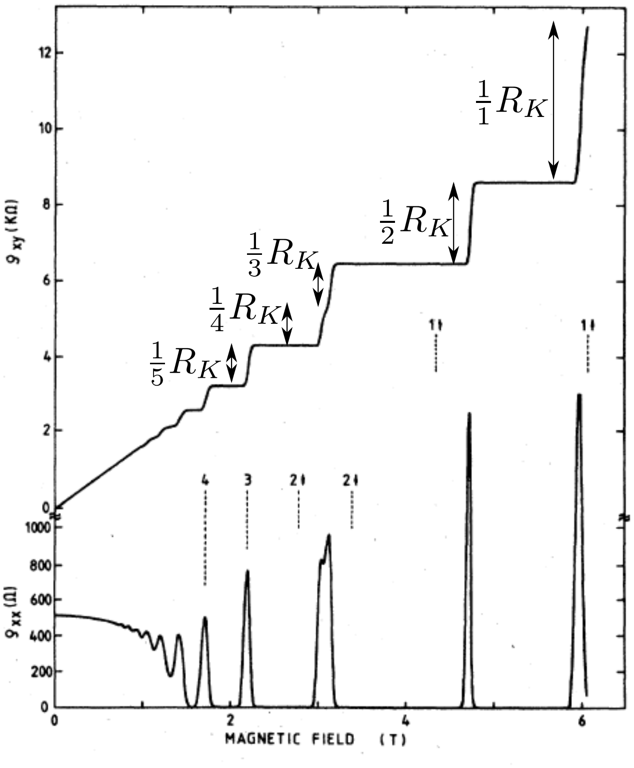

Figure 7.2: Plot of Plot of measured transverse (top) and longitudinal (bottom) resistance versus magnetic field strength. The height of the plateaus in the transverse resistance changes according to $\rho_n = \frac{h}{e^2}\frac{1}{C}$ with integer C. For small B, the classical Hall effect is recovered. Figure adapted from Ref. [24].

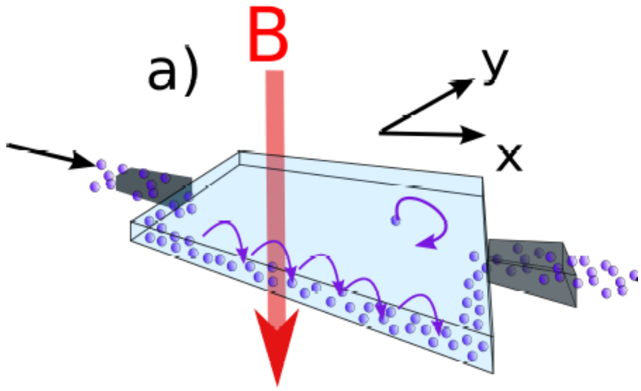

Figure 7.3: Classical understanding of transport in the quantum Hall effect. During the transversal resistance plateaus, the electronic transport is dominated by edge states, which are represented by electrons being reflected from the boundaries. Figure taken from Ref. [22].

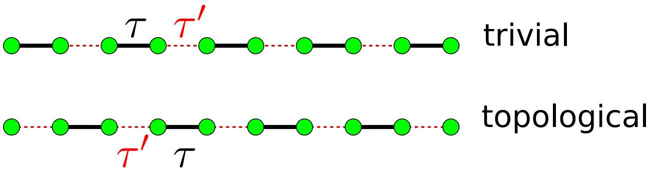

Figure 7.4: Illustration of the SSH model Hamiltonian with alternating tunnel couplings τ and τ' for $M = 5$ dimers. Depending on the ratio of τ and τ' (thickness of connections), there are two different phases, corresponding to two monomers at the edges and $(M-1)$ dimers (topological) or just M dimers (trivial).

7.2 The 1d Su-Schrieffer-Heeger model

Probably the simplest model displaying topological effects is the Su-Schrieffer-Heeger (SSH) model. First introduced to describe the electron dynamics on polyacethylene-chains, it is nowadays widely studied as a sample model for topological protection. The Hamiltonian describes the hopping of fermions along a chain of M dimers

$$H = -\sum_{n=1}^{M} \left[\tau \left(c_{n,1}^\dagger c_{n,2} + c_{n,2}^\dagger c_{n,1} \right) + \tau' \left(c_{n,2}^\dagger c_{n+1,1} + c_{n+1,1}^\dagger c_{n,2} \right) \right] . \tag{7.8}$$

Here, $c_{n,\alpha}$ annihilates a fermion on the site $\alpha \in \{1,2\}$ of the dimer n. Alternative ways of writing this Hamiltonian include using only a single annihilation operator type on $N = 2M$ sites, the essential ingredient however is that the tunnel couplings between neighboring sites alternate, see Fig. 7.4.

7.2.1 Diagonalization for periodic boundary conditions

For periodic boundary conditions (where $c_{M+1} = c_1$ and similar for the creation operator) (or an infinitely long chain), the spectrum of the chain can be obtained analytically. The translational invariance suggests to use separate discrete Fourier transform for every α

$$c_{n,\alpha} = \frac{1}{\sqrt{M}} \sum_{k \in \tilde{M}} d_{k,\alpha} e^{+\mathrm{i}k\frac{2\pi n}{M}} . \tag{7.9}$$

Here, the discretization in k needs to be chosen such that periodic boundary conditions are obeyed. Upon insertion, the Hamiltonian becomes

$$\begin{aligned} H &= -\tau \sum_k \left(d_{k,1}^\dagger d_{k,2} + d_{k,2}^\dagger d_{k,1} \right) - \tau' \sum_k \left(d_{k,2}^\dagger d_{k,1} e^{+\mathrm{i}k\frac{2\pi}{M}} + d_{k,1}^\dagger d_{k,2} e^{-\mathrm{i}k\frac{2\pi}{M}} \right) \\ &= \sum_k \left(d_{k,1}^\dagger, d_{k,2}^\dagger \right) \begin{pmatrix} 0 & -\tau - \tau' \cos(\frac{2\pi k}{M}) + \mathrm{i}\tau' \sin(\frac{2\pi k}{M}) \\ -\tau - \tau' \cos(\frac{2\pi k}{M}) - \mathrm{i}\tau' \sin(\frac{2\pi k}{M}) & 0 \end{pmatrix} \begin{pmatrix} d_{k,1} \\ d_{k,2} \end{pmatrix} \end{aligned} \tag{7.10}$$

We have M different k modes, and for every k value, we get two quasiparticle energies, obtained by diagonalizing the matrix

$$H_k = \left[-\tau - \tau' \cos(\frac{2\pi k}{M}) \right] \sigma^x - \tau' \sin(\frac{2\pi k}{M}) \sigma^y = h_x(k) \sigma^x + h_y(k) \sigma^y . \tag{7.11}$$

The eigenvalues of this 2×2 matrix become

$$E_{k,\pm} = \pm \sqrt{h_x^2(k) + h_y^2(k)} = \pm \sqrt{\tau^2 + (\tau')^2 + 2\tau\tau' \cos(\frac{2\pi k}{M})} , \tag{7.12}$$

and the corresponding eigenvectors read

$$v_{k,\pm} = \frac{1}{\sqrt{2}} \begin{pmatrix} \frac{E_{k,\pm}}{h_x(k) + \mathrm{i}h_y(k)} \\ 1 \end{pmatrix} \tag{7.13}$$

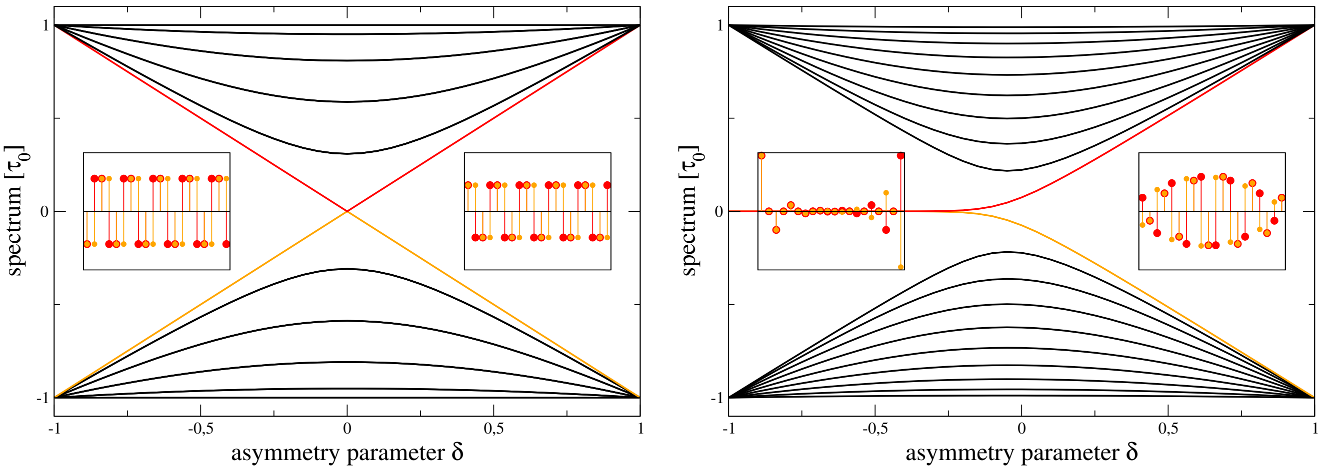

Figure 7.5: SSH spectrum for $\tau = \tau_0(1+\delta)/2$ and $\tau' = \tau_0(1-\delta)/2$ versus δ for periodic boundary conditions (left panel) and open boundary conditions (right panel) for $M = 10$. In both cases, we have two bulk bands (black) which for most values of δ are separated by a band gap (insulator). For periodic boundary conditions, some of the energies are two-fold degenerate. However, for the case of open boundary conditions we additionally observe that two eigenvalues (red and orange) separate from the bulk bands for $\delta < 0$ and form midgap states, nearly completely fixed to energy zero. These midgap states are for $\delta < 0$ localized at the ends of the chain and can therefore be called edge states. Insets show exemplary wave functions at $\delta = -0.5$ (left inset) and $\delta = +0.5$ (right inset).

7.2.2 Diagonalization and symmetry for open boundary conditions

Instead, when we consider open boundary conditions

$$H = -\sum_{n=1}^{M}\left[\tau\left(c_{n,1}^\dagger c_{n,2} + c_{n,2}^\dagger c_{n,1}\right)\right] - \sum_{n=1}^{M-1}\left[\tau'\left(c_{n,2}^\dagger c_{n+1,1} + c_{n+1,1}^\dagger c_{n,2}\right)\right] , \qquad (7.14)$$

we can no longer use a simple Fourier transform to compute the spectrum. Instead, one can use numerical methods, leading to a numerical spectrum. One finds that the spectra of the two chains are very different, even when $M \to \infty$, see Fig. 7.5. We see that one always has two bulk bands, which become more and more dense as M increases. However, for open boundary conditions two separate state emerge – topologically protected boundary modes.

It is simple to understand the extreme cases: For $\tau' = 0$ ($\delta = +1$), we just have a chain of M decoupled dimers

$$H_n = -\tau c_{n,1}^\dagger c_{n,2} - \tau c_{n,2}^\dagger c_{n,1} \, . \qquad (7.15)$$

These individual dimers have eigenvalues $\pm\tau$. Also, when $\tau = \tau'$ ($\delta = 0$), we have the example of the homogeneous chain with an analytically computable spectrum, compare Sec. 4.2.3. In contrast, for $\tau = 0$ ($\delta = -1$), two monomers at the end of the chain arise. The edge states associated with these monomers

$$\left|\Psi_0^L\right\rangle = \left|1, 0, \ldots, 0, 0\right\rangle \, , \qquad \left|\Psi_0^R\right\rangle = \left|0, 0, \ldots, 0, 1\right\rangle \qquad (7.16)$$

have energy 0, and then we have $M-1$ decoupled dimers with the same energies as before. However, why are the two edge states so much pinned to energy zero also for $\tau \neq 0$, i.e., why are they somehow protected against the perturbation from that Hamiltonian? The answer lies in the combination of the fact that the two edge states are chiral symmetry partners and at the same time they are so "distant" from each other. A perturbation ΔH that respects the symmetry of the model (we see below what this means) is not able to lift their degeneracy.

To understand the characteristics of the spectrum, it is helpful to introduce the concept of chirality.

Box 22 (chirality) *A Hamiltonian H is* **chiral** *if there is a hermitian $\Gamma = \Gamma^\dagger$ and unitary $\Gamma^2 = \mathbf{1}$ chiral symmetry operator, such that*

$$\Gamma H \Gamma = -H\,. \tag{7.17}$$

From this definition it also follows that the Hamiltonian must anti-commute with the chiral symmetry operator $\{H, \Gamma\} = \mathbf{0}$. For a chiral Hamiltonian we can conclude that the spectrum must be symmetrically distributed around $E = 0$, since for any eigenvector with a non-vanishing eigenvalue

$$H \left|v_n\right\rangle = E_n \left|v_n\right\rangle \tag{7.18}$$

there must be an associated eigenvector $\left|w_n\right\rangle = \Gamma \left|v_n\right\rangle$ with the negative eigenvalue

$$\Gamma H \left|v_n\right\rangle = E_n \Gamma \left|v_n\right\rangle = -H\Gamma \left|v_n\right\rangle\,. \tag{7.19}$$

Such a chiral symmetry may imply a sublattice symmetry as well. We can introduce the projectors related to the chiral symmetry

$$P_\pm = \frac{1}{2}\left[\mathbf{1} \pm \Gamma\right]\,. \tag{7.20}$$

Since we can express $\Gamma = P_+ - P_-$, it follows that the eigenstates of a chiral Hamiltonian must be equally distributed over the two subspaces

$$0 = \left\langle v_n | w_n \right\rangle = \left\langle v_n \right| \Gamma \left|v_n\right\rangle = \left\langle v_n \right| P_+ \left|v_n\right\rangle - \left\langle v_n \right| P_- \left|v_n\right\rangle\,. \tag{7.21}$$

In addition, when $E = 0$ for chiral partners $\left|v\right\rangle$ and $\left|w\right\rangle = \Gamma \left|v\right\rangle$, the symmetric and antisymmetric superpositions

$$\left|v_\pm\right\rangle = \frac{1}{\sqrt{2}}\left[\left|v\right\rangle \pm \left|w\right\rangle\right] \tag{7.22}$$

of the chiral partner states are also an eigenstate of the Hamiltonian.

For the SSH model, the chiral symmetry operator becomes

$$\Gamma = \exp\left\{\mathrm{i}\pi \sum_j c_{j,1}^\dagger c_{j,1}\right\} = \exp\left\{\mathrm{i}\pi \sum_k d_{k,1}^\dagger d_{k,1}\right\}\,, \tag{7.23}$$

and we can check that

$$\begin{aligned}
\Gamma^\dagger &= \exp\left\{-\mathrm{i}\pi \sum_j c_{j,1}^\dagger c_{j,1}\right\} = \exp\left\{\mathrm{i}\pi \sum_j c_{j,1}^\dagger c_{j,1}\right\} = \Gamma\,,\\
\Gamma^2 &= \exp\left\{\mathrm{i}2\pi \sum_j c_{j,1}^\dagger c_{j,1}\right\} = \mathbf{1}\,.
\end{aligned} \tag{7.24}$$

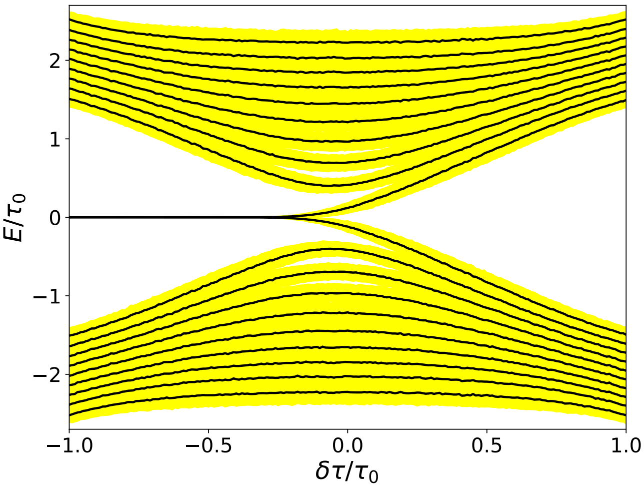

Figure 7.6: Plot of the averaged SSH spectrum for $\tau = (1+\frac{\delta\tau}{\tau_0})\tau_0+\delta\tau_m$ and $\tau' = (1-\frac{\delta\tau}{\tau_0})\tau_0+\delta\tau'_m$ versus δ for 1000 disorder realizations (black lines), where both $\delta\tau_m$ and $\delta\tau'_m$ were chosen uniformly within the interval $[-0.1, +0.1]\tau_0$. The yellow background shows one standard deviation: Only the edge states are robust with respect to the perturbation. Taken from Ref. [23].

Furthermore, the chiral symmetry holds both for open or closed (periodic) boundary conditions. From this, we get

$$\begin{aligned} &\Gamma c_{j,1}\Gamma = [\mathbf{1}]\, c_{j,1}\left[\mathbf{1} + \left(e^{+\mathrm{i}\pi}-1\right) c_{j,1}^\dagger c_{j,1}\right] = +e^{+\mathrm{i}\pi} c_{j,1} = -c_{j,1}\,, \qquad \Gamma c_{j,1}^\dagger\Gamma = -c_{j,1}^\dagger \\ &\Gamma c_{j,2}\Gamma = c_{j,2}\,, \qquad \Gamma c_{j,2}^\dagger\Gamma = c_{j,2}^\dagger\,. \end{aligned} \tag{7.25}$$

From this, we can see directly that for the SSH model $\Gamma H\Gamma = -H$, and it explains the symmetry observed in the spectrum in Fig. 7.5 for both periodic and open boundary conditions. Perturbations respecting the chiral symmetry only allow for changes of the corresponding eigenstates when they have a non-negligible effect within the subspace of the chiral symmetry partners. For example, the chiral symmetry partners from the bulk are just either distributed on the even or on the odd sites. In particular, deeply in the topological phase, they are sitting on the same dimer, any small local perturbation will couple them, and correspondingly, these eigenvalues are not robust against symmetry-preserving perturbations. However, the edge states are located far away from each other, their overlap matrix element

$$\langle L|\,\Delta H^k\,|R\rangle = \langle v_+|\,\Delta H^k\,|v_-\rangle = 0 \qquad : \qquad k \ll M \tag{7.26}$$

vanishes for sufficiently small k, such that any ΔH respecting the chiral symmetry, i.e.

$$\Gamma\Delta H\Gamma = -\Delta H \tag{7.27}$$

will leave the edge states and their eigenvalues invariant as long as it is not totally dominating the Hamiltonian. In fact, the chiral symmetry in the SSH model is not only robust with respect to perturbations that can be parametrized by $\delta\tau$ or $\delta\tau'$, but also to arbitrary next-neighbour tunnel disorder perturbations

$$\Delta H = \sum_m \delta\tau_m\left(c_{m,1}^\dagger c_{m,2} + c_{m,2}^\dagger c_{m,1}\right) + \sum_m \delta\tau'_m\left(c_{m,2}^\dagger c_{m+1,1} + c_{m+1,1}^\dagger c_{m,2}\right)\,. \tag{7.28}$$

This robustness is exemplified in Fig. 7.6. In contrast, if we would add a perturbation that does not respect the chiral symmetry, the edge states would not just interact with themselves, but also with the bulk states, and their robustness would soon be lost.

Finally, we just mention that the the current through such SSH chains allows to extract the single-particle excitation spectrum. For this purpose, one connects the SSH chain at its ends to fermionic reservoirs and considers the dependence of the current versus the bias voltage. When the temperature of the reservoirs is below the energy gaps of the chain, as discussed in Sec. 6.4, the current exhibits steps at the transition energies of the system, see Fig. 7.7. Here, at weak system-reservoir coupling, the term "transition energy" means the single-particle excitation energy of the SSH spectrum. The existence or non-existence of boundary modes in the gap thereby allows to distinguish between the phases.

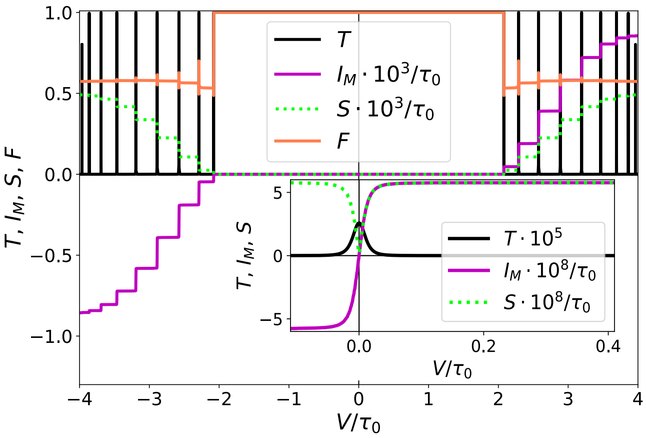

Figure 7.7: Plot of matter current I_M (red, and associated noise and Fano factor) and transmission through an SSH chain of $M = 10$ dimers versus bias voltage in the topological phase. The single-particle excitation energies map to steps in the current. The edge states are strongly localized to the ends, and correspondingly the current through them is significantly smaller (inset) than through the bulk states. Figure taken from Ref. [23].

7.2.3 Topological invariants

To classify the different topological phases, one defines topological invariants, which may within particular phases assume only integer values and are for this reason also called topological quantum numbers. For the example of the SSH model, we would have the value zero in the trivial phase and the value plus one in the topological phase. Revisiting the spectra of the SSH chain with periodic boundary conditions, we see that in the topological phase, the origin is encircled by the 2d curve parametrized by

$$h_x(k) = -\tau - \tau' \cos(2\pi k/M) \,, \qquad h_y(k) = -\tau' \sin(2\pi k/M) \,. \tag{7.29}$$

Here, $2\pi k/M$ runs over the 1. BZ, such that the above equation defines a circle with radius τ' and with center at $(-\tau, 0)$. When we increase τ', the origin is included when $\tau' = \tau$, which marks the point of the topological phase transition. At this point, the excitation energies vanish $E_\pm = \sqrt{h_x^2(k) + h_y^2(k)} \to 0$ for a particular value of k, and the full spectrum therefore becomes gapless. We can therefore characterize the phase by asking if the curve defined by $h_x(k)$ and $h_y(k)$ encloses the origin or not. Formally, this is defined by the **winding number**

$$W = \frac{1}{2\pi\mathrm{i}} \oint_\gamma \frac{dz}{z - z_0} \tag{7.30}$$

of the complex closed curve γ, defined by $z(\kappa) = h_x(\kappa) + \mathrm{i} h_y(\kappa)$ around the origin $z_0 = 0$ in the complex plane as the topological invariant. Functional calculus tells us that the above integral counts the number of windings around the pole at z_0. Inserting these definitions, the winding number becomes

$$W = \frac{1}{2\pi\mathrm{i}} \int_{-\pi}^{+\pi} \frac{dz}{d\kappa} \frac{1}{z} d\kappa = \frac{1}{2\pi\mathrm{i}} \int_{-\pi}^{+\pi} \frac{d \ln z(\kappa)}{d\kappa} d\kappa = \frac{1}{2\pi\mathrm{i}} \int_{-\pi}^{+\pi} \frac{d}{d\kappa} \ln \left[h_x(\kappa) + \mathrm{i} h_y(\kappa)\right] d\kappa \,. \tag{7.31}$$

Indeed, recalling that $h_x(\kappa) = -\tau - \tau' \cos(\kappa)$ and $h_y(\kappa) = -\tau' \sin(\kappa)$, we can solve the integral for some special cases and obtain the value $W = 0$ for the trivial phase $\tau' < \tau$ and the value $W = 1$ for the topological phase $\tau' > \tau$.

Although a winding number is very intuitive to define, it has the disadvantage that we may not always be able to express the Hamiltonian by a curve in the complex plane. Therefore, one considers often other ways of defining topological quantum numbers. One is via the Berry [4] phase, which appears in the context of adiabatically driven quantum systems. For a Hamiltonian that depends on some parameters $\boldsymbol{\kappa}$ we consider a closed curve in time $\boldsymbol{\kappa}(t_i) = \boldsymbol{\kappa}(t_f)$. At each point in time, we can define the instantaneous set of eigenstates via

$$H(\boldsymbol{\kappa}) \left|\Psi_n(\boldsymbol{\kappa})\right\rangle = E_n(\boldsymbol{\kappa}) \left|\Psi_n(\boldsymbol{\kappa})\right\rangle \,, \tag{7.32}$$

---

[4] Sir Michael Victor Berry, (born 1941) is a british physicist.

where n is the corresponding quantum number. If we would consider a quantum system subject to the time-dependent parameter $\boldsymbol{\kappa}$, initialized in one of the initial eigenstates, and evolve it slowly from t_i to t_f, the adiabatic theorem tells us that – if the evolution is slow in comparison to the energy gaps of the system – we remain in the instantaneous energy eigenstates up to a phase factor [17]

$$\left|\Psi(t_i)\right\rangle = \left|\Psi_n(\boldsymbol{\kappa}(t_i))\right\rangle \qquad \Longrightarrow \qquad \left|\Psi(t_f)\right\rangle \approx e^{+\mathrm{i}(\gamma_n^{\mathrm{Berry}}-\gamma_n^{\mathrm{dyn}})} \left|\Psi_n(\boldsymbol{\kappa}(t_i))\right\rangle . \tag{7.33}$$

Here, we have completely neglected the transition to other instantaneous eigenstates. The phases are the dynamical phase

$$\gamma_n^{\mathrm{dyn}} = \int_{t_i}^{t_f} E_n(\boldsymbol{\kappa}(t'))dt' , \tag{7.34}$$

which does depend on the speed of the evolution. For our purposes however, the celebrated Berry phase is important

$$\gamma_n^{\mathrm{Berry}} = \mathrm{i} \int_{t_i}^{t_f} \left\langle \Psi_n(\boldsymbol{\kappa}(t)) \right| \frac{d}{dt} \left|\Psi_n(\boldsymbol{\kappa}(t))\right\rangle dt = \mathrm{i} \oint \left\langle \Psi_n(\boldsymbol{\kappa}) \right| \nabla_{\boldsymbol{\kappa}} \left|\Psi_n(\boldsymbol{\kappa})\right\rangle d\boldsymbol{\kappa} . \tag{7.35}$$

The second equality sign of the above equation demonstrates that the Berry phase is an intrinsically geometric phase, it does only depend on the characteristics of the curve $\boldsymbol{\kappa}$ and not on the speed at which this curve is traversed. With introducing the Berry vector potential for each eigenstate

$$\boldsymbol{A}_n(\boldsymbol{\kappa}) = \mathrm{i} \left\langle \Psi_n(\boldsymbol{\kappa}) \right| \nabla_{\boldsymbol{\kappa}} \left|\Psi_n(\boldsymbol{\kappa})\right\rangle = \boldsymbol{A}_n^*(\boldsymbol{\kappa}) \tag{7.36}$$

(this follows from the normalization $\langle \Psi_n(\boldsymbol{\kappa}) | \Psi_n(\boldsymbol{\kappa}) \rangle = 1$) we can also write the Berry phase as

$$\gamma_n^{\mathrm{Berry}} = \oint \boldsymbol{A}_n(\boldsymbol{\kappa}) d\boldsymbol{\kappa} . \tag{7.37}$$

As an example, let us consider a spin-1/2 model

$$H = \boldsymbol{\kappa} \cdot \boldsymbol{\sigma} = \kappa_x \sigma_x + \kappa_y \sigma_y + \kappa_z \sigma_z , \qquad \boldsymbol{\kappa} = \kappa \begin{pmatrix} \sin(\theta)\cos(\phi) \\ \sin(\theta)\sin(\phi) \\ \cos(\theta) \end{pmatrix} . \tag{7.38}$$

The eigenvalues are $\pm\kappa$

$$H \left|\Psi_\pm(\boldsymbol{\kappa})\right\rangle = \pm\kappa \left|\Psi_\pm(\boldsymbol{\kappa})\right\rangle , \tag{7.39}$$

with the eigenstates

$$\left|\Psi_-(\boldsymbol{\kappa})\right\rangle = \begin{pmatrix} \sin(\theta/2)e^{-\mathrm{i}\phi} \\ -\cos(\theta/2) \end{pmatrix} , \qquad \left|\Psi_+(\boldsymbol{\kappa})\right\rangle = \begin{pmatrix} \cos(\theta/2)e^{-\mathrm{i}\phi} \\ \sin(\theta/2) \end{pmatrix} . \tag{7.40}$$

As a curve parametrization, we consider a rotation (e.g. of the external field steering the spin Hamiltonian) around the z axis

$$\theta(t) = \theta_0 , \qquad \phi(t) = \frac{2\pi t}{T} , \qquad 0 \le t \le T . \tag{7.41}$$

The Berry phases become

$$\gamma_-^{\mathrm{Berry}} = 2\pi \sin^2(\theta_0/2) , \qquad \gamma_+^{\mathrm{Berry}} = 2\pi \cos^2(\theta_0/2) . \tag{7.42}$$

For example, when $\theta_0 = \pi/2$ ($\boldsymbol{\kappa}$ circles around the equator), the Berry phase becomes maximal $\gamma_\pm^{\rm Berry} \to \pi$, which is an often-used example to demonstrate that a spin 1/2- rotation leads to a sign. We observe that the sum of the two Berry phases is just 2π, which is equivalent to zero. In general, one can prove that

$$\sum_n \gamma_n^{\rm Berry} \qquad \mathrm{mod} \qquad 2\pi = 0\,. \tag{7.43}$$

Now, for a system with energy bands one defines the macroscopic polarization

$$P_{\rm mac}(E) = \frac{1}{2\pi} \sum_{n:E_n \le E} \gamma_n^{\rm Berry}\,. \tag{7.44}$$

For electronic systems, this could in principle be related to expectation values at zero temperature, where all states below the energy $E = \mu$ are occupied and all other states are empty. Since it is defined in terms of the Berry phase, we clearly see that also $P_{\rm mac}$ is a geometric quantity. Furthermore, for an insulator with chiral symmetry, which in quasi-momentum representation reads

$$\Gamma H_k \Gamma = -H_k\,, \tag{7.45}$$

we can denote the eigenstate of the chiral partner state by $|\Psi_{\bar n}\rangle = \Gamma |\Psi_n\rangle$. The Berry phases of these chiral partners are identical (using that $\Gamma^2 = \mathbf{1}$)

$$\gamma_n = \mathrm{i} \oint \langle \Psi_n(\boldsymbol{\kappa})| \, \Gamma \nabla_{\boldsymbol{\kappa}} \Gamma \, \langle \Psi_n(\boldsymbol{\kappa})| \, d\boldsymbol{\kappa} = \gamma_{\bar n}\,. \tag{7.46}$$

Therefore, if in addition there is an energy gap at $E = 0$, we have the condition

$$0 = \left(\frac{1}{2\pi} \sum_{n:E_n<0} \gamma_n^{\rm Berry} + \frac{1}{2\pi} \sum_{n:E_n>0} \gamma_n^{\rm Berry} \right) \qquad \mathrm{mod} \qquad 1\,. \tag{7.47}$$

This implies that the macroscopic polarization defined for the lower part of the spectrum is half-integer quantized

$$P_{\rm mac}(0) = \frac{1}{2\pi} \sum_{n:E_n<0} \gamma_n^{\rm Berry} = \frac{m}{2} \qquad m \in \mathbb{Z}\,, \tag{7.48}$$

and a corresponding quantity similar to a winding number can be defined by

$$W = 2P_{\rm mac}(0). \tag{7.49}$$

We can check the consistency of this for the SSH model: Here, it suffices to consider the extreme cases as $P_{\rm mac}$ can only change at critical points. For $\tau' = 0$, the Hamiltonian in momentum space does not depend on k, and all the Berry phases vanish. Consequently, the macroscopic polarization vanishes and the associated winding number becomes $W = 0$, as we have already computed. For $\tau = 0$, the Hamiltonian for the excitation energies of the dimers becomes

$$H_k = -\tau' \cos(\kappa)\sigma^x - \tau' \sin(\kappa)\sigma^y\,, \tag{7.50}$$

which is equivalent to the previously discussed example when $\theta_0 = \pi/2$. Therefore, the Berry phases become $\gamma_- = \gamma_+ = \pi$, which means for the macroscopic polarization for a single-particle Hamiltonian $P_{\rm mac} = \frac{1}{2}$, and we recover the winding number $W = 1$ of the topological phase.

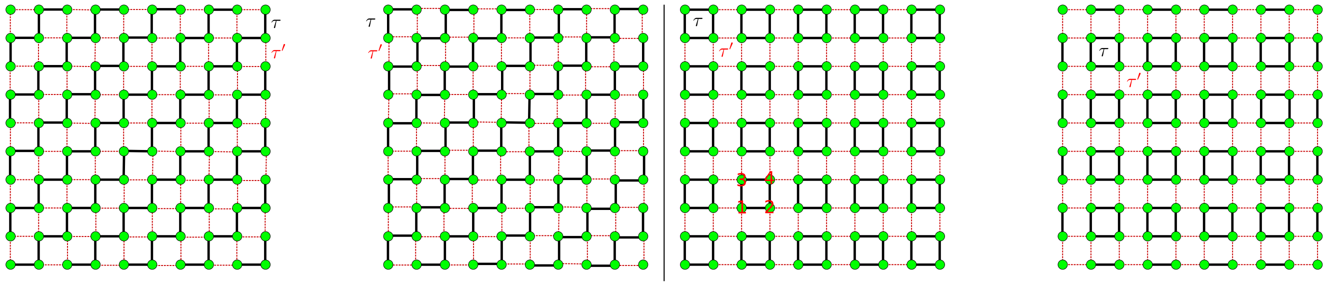

Figure 7.8: Illustration of two 2d generalizations of the SSH model. The first variant (left) alternates between SSH chains in the topological and trivial phase in transverse direction, and the resulting model cannot exhibit a topological phase transition: Exchanging red and black links yields another variant, which is related to the previous one by a simple rotation. The second one (right) in contrast leads to a non-trivial transformation, where one can expect edge states to exist in the right phase.

7.2.4 Towards higher dimensions

In two dimensions, we can construct different generalizations of the SSH model. One can consider parallel SSH chains and add crosslinks between them, such that in transverse direction one also recovers SSH models. This can be done in different ways, and already by symmetry considerations one can see that one of them will not lead to a topological phase transition, see Fig. 7.8. The Hamiltonian of the model reads

$$\begin{aligned} H = &-\tau \sum_{ij} \left[c^\dagger_{ij;1} c_{ij;2} + c^\dagger_{ij;1} c_{ij,3} + c^\dagger_{ij;2} c_{ij;4} + c^\dagger_{ij;3} c_{ij;4} + \text{h.c.} \right] \\ &- \tau' \sum_{ij} \left[c^\dagger_{ij;2} c_{i+1j;1} + c^\dagger_{ij;3} c_{ij+1,1} + c^\dagger_{ij;4} c_{i+1j;3} + c^\dagger_{ij;4} c_{ij+1;2} + \text{h.c.} \right] , \end{aligned} \tag{7.51}$$

and we can distinguish open or closed boundary conditions. For open boundary consitions we simply have to use

$$c_{ij} = 0 \qquad \text{for} i < 1, i > m_x, j < 1, j > M_y \,. \tag{7.52}$$

A numerical calculation of the spectrum shows that edge states – and some chiral symmetry – exist, see Fig. 7.9. However, the edge states are not topologically protected agains perturbations, since they are not degenerate with their chiral partners. This only holds true for the corner states.

For periodic boundary conditions, we can as before use a DFT to obtain a representation in terms of quasimomentum operators

$$c_{ij,\alpha} = \frac{1}{\sqrt{M_x M_y}} \sum_{k_x,k_y} d_{k_x k_y,\alpha} e^{+\mathrm{i}k_x \frac{2\pi i}{M_x}} e^{+\mathrm{i}k_y \frac{2\pi j}{M_y}} \,. \tag{7.53}$$

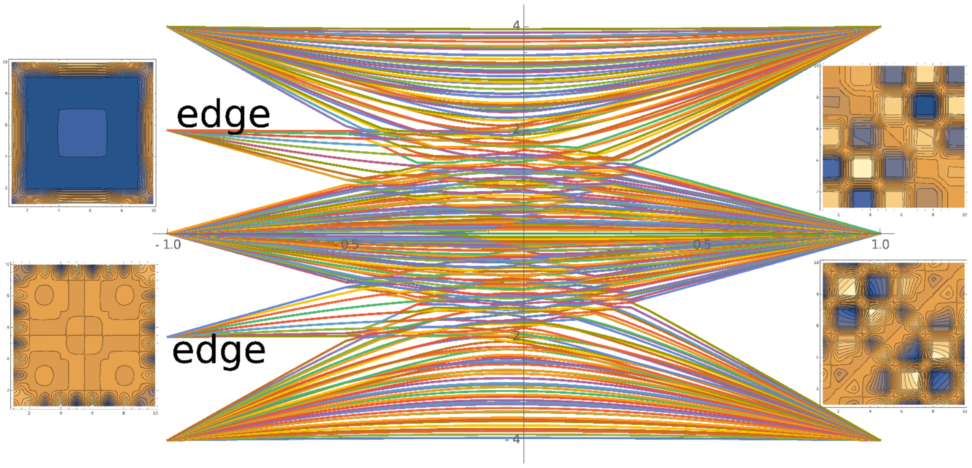

Figure 7.9: Plot of the 2d SSH spectrum for a 10×10 lattice from Eq. (7.51) in units of τ_0 versus asymmetry parameter δ for $\tau = (1+\delta)\tau_0$ and $\tau' = (1-\delta)\tau_0$. The two additional bands on the left part correspond to modes localized along the edges, but in addition modes from the outside bands on the right converge to degenerate corner modes at energy zero on the left, hidden by the central bulk band. Panels show exemplary wave functions that in the two intermediate bands on the left are localized on the edges.

The transformed Hamiltonian reads

$$\begin{aligned}
H &= -\tau \sum_{k_x,k_y} \left[d^\dagger_{k_xk_y;1} d_{k_xk_y;2} + d^\dagger_{k_xk_y;1} d_{k_xk_y,3} + d^\dagger_{k_xk_y;2} d_{k_xk_y;4} + d^\dagger_{k_xk_y;3} d_{k_xk_y;4} + \text{h.c.} \right] \\
&\quad - \tau' \sum_{k_x,k_y} \Big[d^\dagger_{k_xk_y;2} d_{k_xk_y;1} e^{+\mathrm{i}\frac{2\pi k_x}{M_x}} + d^\dagger_{k_xk_y;3} d_{k_xk_y,1} e^{+\mathrm{i}\frac{2\pi k_y}{M_y}} \\
&\qquad + d^\dagger_{k_xk_y;4} d_{k_xk_y;3} e^{+\mathrm{i}\frac{2\pi k_x}{M_x}} + d^\dagger_{k_xk_y;4} d_{k_xk_y;2} e^{+\mathrm{i}\frac{2\pi k_y}{M_y}} + \text{h.c.} \Big] = \sum_{k_x,k_y} H(k_x,k_y) \\
&= \sum_{\boldsymbol{k}} \left(d^\dagger_{\boldsymbol{k},1}, d^\dagger_{\boldsymbol{k},2}, d^\dagger_{\boldsymbol{k},3}, d^\dagger_{\boldsymbol{k},4} \right) A_{\boldsymbol{k}} \begin{pmatrix} d_{\boldsymbol{k},1} \\ d_{\boldsymbol{k},2} \\ d_{\boldsymbol{k},3} \\ d_{\boldsymbol{k},4} \end{pmatrix} , \\
A_{\boldsymbol{k}} &= \begin{pmatrix} 0 & -\tau - \tau' e^{-2\pi\mathrm{i}\frac{k_x}{M_x}} & -\tau - \tau' e^{-2\pi\mathrm{i}\frac{k_y}{M_y}} & 0 \\ -\tau - \tau' e^{+2\pi\mathrm{i}\frac{k_x}{M_x}} & 0 & 0 & -\tau - \tau' e^{-2\pi\mathrm{i}\frac{k_y}{M_y}} \\ -\tau - \tau' e^{+2\pi\mathrm{i}\frac{k_y}{M_y}} & 0 & 0 & -\tau - \tau' e^{-2\pi\mathrm{i}\frac{k_x}{M_x}} \\ 0 & -\tau - \tau' e^{+2\pi\mathrm{i}\frac{k_y}{M_y}} & -\tau - \tau' e^{+2\pi\mathrm{i}\frac{k_x}{M_x}} & 0 \end{pmatrix} \\
&= \left[-\tau - \tau' \cos(\kappa_y)\right] \sigma_1^x \otimes \mathbf{1}_2 + \left[-\tau' \sin(\kappa_y)\right] \sigma_1^y \otimes \mathbf{1}_2 \\
&\quad + \left[-\tau - \tau' \cos(\kappa_x)\right] \mathbf{1}_1 \otimes \sigma_2^x + \left[-\tau' \sin(\kappa_x)\right] \mathbf{1}_1 \otimes \sigma_2^y , \qquad (7.54)
\end{aligned}$$

where $\kappa_\alpha = 2\pi/M_\alpha k_\alpha \in (-\pi, +\pi]$. The individual four-fermion Hamiltonians can be exactly diagonalized and yields the excitation spectra

$$\begin{aligned}
E(\kappa_x, \kappa_y) = \pm\sqrt{2} \Big[& \tau^2 + (\tau')^2 + \tau\tau'(\cos(\kappa_x) + \cos(\kappa_y)) \\
& \pm \sqrt{(\tau^2 + (\tau')^2 + 2\tau\tau'\cos(\kappa_x))\,(\tau^2 + (\tau')^2 + 2\tau\tau'\cos(\kappa_y))} \Big]^{1/2} . \qquad (7.55)
\end{aligned}$$

The excitation energy may now vanish all values of τ and τ', so it may be difficult to detect a topological phase transition here. However, from the second decomposition of the matrix we see that for $\tau = \tau'$ we have a topological phase transition.

7.3 Peierls substitution

We have discussed that a magnetic field can be coupled in two ways to magnetic moments: Via the Zeemann splitting and also via the minimal coupling. Whereas it was straightforward to represent the Zeemann splitting within second quantization, this is less obvious for the minimal coupling procedure. Let us assume that for a single electron, the Hamiltonian in absence of a magnetic field is given by the kinetic term and the periodic lattice potential

$$H = \frac{\boldsymbol{p}^2}{2m} + U(\boldsymbol{r})\,, \qquad U(\boldsymbol{r}+\boldsymbol{R}) = U(\boldsymbol{r})\,. \tag{7.56}$$

Then, Bloch's theorem holds and the eigenstates can be expanded in terms of Wannier functions $\Phi_{\boldsymbol{R}}(\boldsymbol{r})$

$$\Psi_{\boldsymbol{k}}(\boldsymbol{r}) = \frac{1}{\sqrt{N}} \sum_{\boldsymbol{R}} e^{+\mathrm{i}\boldsymbol{k}\boldsymbol{R}} \Phi_{\boldsymbol{R}}(\boldsymbol{r})\,, \tag{7.57}$$

where N is the number of lattice sites and $\boldsymbol{R}$ denotes the positions of the nuclei. The energies are then obtained by

$$E_{\boldsymbol{k}} = \langle \Psi_{\boldsymbol{k}} | H | \Psi_{\boldsymbol{k}} \rangle = \int \Psi^*_{\boldsymbol{k}}(\boldsymbol{r}) H \Psi_{\boldsymbol{k}}(\boldsymbol{r}) d^3r = \frac{1}{N} \sum_{\boldsymbol{R}\boldsymbol{R}'} e^{+\mathrm{i}\boldsymbol{k}(\boldsymbol{R}-\boldsymbol{R}')} \int \Phi^*_{\boldsymbol{R}}(\boldsymbol{r}) H \Phi_{\boldsymbol{R}'}(\boldsymbol{r}) d^3r\,. \tag{7.58}$$

Similarly, the hopping matrix element between sites $\boldsymbol{R}$ and $\boldsymbol{R}'$ are computed via

$$t_{\boldsymbol{R}\boldsymbol{R}'} = \int \Phi^*_{\boldsymbol{R}}(\boldsymbol{r}) H \Phi_{\boldsymbol{R}'}(\boldsymbol{r}) d^3r\,. \tag{7.59}$$

Now, under the minimal coupling substitution, the Hamiltonian becomes

$$H \to \tilde{H} = \frac{(\boldsymbol{p} - e\boldsymbol{A})^2}{2m} + U(\boldsymbol{r})\,, \tag{7.60}$$

where $\boldsymbol{A}$ is the vector potential from which we can derive the magnetic field $\boldsymbol{B} = \nabla \times \boldsymbol{A}$ (we now use SI units, therefore the $1/c$-factor is missing). However, the vector potential is not uniquely determined, as any gauge transformation $\boldsymbol{A} \to \boldsymbol{A} + \nabla\Phi$ with arbitrary Φ leaves the magnetic field invariant. To account for the effect of the minimal coupling substitution, we introduce new, transformed Wannier functions

$$\tilde{\Phi}_{\boldsymbol{R}}(\boldsymbol{r}) = \exp\left\{\mathrm{i}\frac{e}{\hbar}\int_{\boldsymbol{R}}^{\boldsymbol{r}} A(\boldsymbol{r}')d\boldsymbol{r}'\right\} \Phi_{\boldsymbol{R}}(\boldsymbol{r})\,, \tag{7.61}$$

which can be obtained from the old ones (without magnetic field) by multiplying with a phase factor. Here, the integral in the exponential may depend on the path chosen between $\boldsymbol{R}$ and $\boldsymbol{r}$. We consider the shortest connection here (straight-line). Now, we can – with using that

$\boldsymbol{p} = -\mathrm{i}\hbar\nabla$ – compute the action of the Hamiltonian on the transformed Wannier functions

$$\begin{aligned}\tilde{H}\tilde{\Phi}_{\boldsymbol{R}}(\boldsymbol{r}) &= \left[\frac{(-\mathrm{i}\hbar\nabla - e\boldsymbol{A})^2}{2m} + U(\boldsymbol{r})\right]\exp\left\{\mathrm{i}\frac{e}{\hbar}\int_{\boldsymbol{R}}^{\boldsymbol{r}} A(\boldsymbol{r}')d\boldsymbol{r}'\right\}\Phi_{\boldsymbol{R}}(\boldsymbol{r})\\ &= \exp\left\{\mathrm{i}\frac{e}{\hbar}\int_{\boldsymbol{R}}^{\boldsymbol{r}} A(\boldsymbol{r}')d\boldsymbol{r}'\right\}\left[\frac{(-\mathrm{i}\hbar\nabla - e\boldsymbol{A} + e\boldsymbol{A})^2}{2m} + U(\boldsymbol{r})\right]\Phi_{\boldsymbol{R}}(\boldsymbol{r})\\ &= \exp\left\{\mathrm{i}\frac{e}{\hbar}\int_{\boldsymbol{R}}^{\boldsymbol{r}} A(\boldsymbol{r}')d\boldsymbol{r}'\right\}H\Phi_{\boldsymbol{R}}(\boldsymbol{r})\,. \end{aligned}\tag{7.62}$$

This means that the new Bloch functions

$$\tilde{\Psi}_{\boldsymbol{k}}(\boldsymbol{r}) = \frac{1}{\sqrt{N}}\sum_{\boldsymbol{R}} e^{+\mathrm{i}\boldsymbol{k}\boldsymbol{R}}\tilde{\Phi}_{\boldsymbol{R}}(\boldsymbol{r}) \tag{7.63}$$

are now eigenstates of $\tilde{H}$ with the same energies as before. Therefore, we have to compute the hopping matrix elements with the phase-transformed Wannier functions

$$\begin{aligned}\tilde{t}_{\boldsymbol{R}\boldsymbol{R}'} &= \int \tilde{\Phi}^*_{\boldsymbol{R}}(\boldsymbol{r})\tilde{H}\tilde{\Phi}_{\boldsymbol{R}'}(\boldsymbol{r})d^3r\\ &= \int \exp\left\{-\mathrm{i}\frac{e}{\hbar}\int_{\boldsymbol{R}}^{\boldsymbol{r}} A(\boldsymbol{r}')d\boldsymbol{r}' + \mathrm{i}\frac{e}{\hbar}\int_{\boldsymbol{R}'}^{\boldsymbol{r}} A(\boldsymbol{r}')d\boldsymbol{r}'\right\}\Phi^*_{\boldsymbol{R}}(\boldsymbol{r})H\Phi_{\boldsymbol{R}'}(\boldsymbol{r})d^3r\\ &= \exp\left\{\mathrm{i}\frac{e}{\hbar}\int_{\boldsymbol{R}'}^{\boldsymbol{R}} \boldsymbol{A}(\boldsymbol{r}')d\boldsymbol{r}'\right\}\int \exp\left\{-\mathrm{i}\frac{e}{\hbar}\oint_{\boldsymbol{R}\to\boldsymbol{r}\to\boldsymbol{R}'\to\boldsymbol{R}} A(\boldsymbol{r}')d\boldsymbol{r}'\right\}\Phi^*_{\boldsymbol{R}}(\boldsymbol{r})H\Phi_{\boldsymbol{R}'}(\boldsymbol{r})d^3r\,. \end{aligned}\tag{7.64}$$

Here, we have taken the first factor out of the integral as it does not depend on $\boldsymbol{r}$, and the convention that we take the shortest connection path still holds. Since the Wannier functions are strongly localized, we can now approximate the integrand in the following way: Taking only nearest-neighbour couplings into account, the length of the vector $\boldsymbol{R} - \boldsymbol{R}'$ is bounded by the lattice constant from the beginning. Furthermore, the integrand will only for small distances between $\boldsymbol{r}$ and $\boldsymbol{R}$ and $\boldsymbol{R}'$ contribute significantly, since the Wannier functions are highly localized. Assuming that the magnetic flux is approximately uniform over the small triangle defined by $\boldsymbol{R}$, $\boldsymbol{R}'$, and $\boldsymbol{r}$ (i.e., over a lattice constant), we can approximate

$$\begin{aligned}\Phi(\boldsymbol{R},\boldsymbol{R}',\boldsymbol{r}) &= \oint_{\boldsymbol{R}\to\boldsymbol{r}\to\boldsymbol{R}'\to\boldsymbol{R}} A(\boldsymbol{r}')d\boldsymbol{r}' = \int\int_{(\boldsymbol{R},\boldsymbol{r},\boldsymbol{R}')} (\nabla\times\boldsymbol{A})\cdot d\boldsymbol{A}\\ &\approx 0\,. \end{aligned}\tag{7.65}$$

Here, we have used Stokes integral theorem, and the approximation holds when the total flux is negligible, i.e., when the product of the homogeneous magnetic field and the area spanned by the triangle $(\boldsymbol{R},\boldsymbol{r},\boldsymbol{R}')$ are small (which is determined by the localization of the Wannier functions). This eventually leads to the Peierls [5] substitution.

Box 23 (Peierls substitution) *In presence of a weak magnetic field described by vector potential $\boldsymbol{A}$, the effect of the minimal coupling procedure can be approximately taken into account by substituting*

$$t_{\boldsymbol{R}\boldsymbol{R}'} \to \tilde{t}_{\boldsymbol{R}\boldsymbol{R}'} = \exp\left\{\mathrm{i}\frac{e}{\hbar}\int_{\boldsymbol{R}'}^{\boldsymbol{R}} \boldsymbol{A}(\boldsymbol{r}')d\boldsymbol{r}'\right\}t_{\boldsymbol{R}\boldsymbol{R}'} \tag{7.66}$$

---

[5] Sir Rudolph Ernst Peierls (1907–1995) was a german-british physicist.

in the electronic tunneling amplitudes, where the path is the shortest connection between $\boldsymbol{R}$ *and* $\boldsymbol{R'}$.

Such substitutions lead on a square lattice subject to a perpendicular magnetic field to a **Hofstadter Hamiltonian**. Here, the constraint of the shortest path came from the approximations done before. We note that a gauge transformation of the form $\boldsymbol{A} \to \boldsymbol{A} + \nabla\Phi$ changes all the phases in the Hamiltonian but must leave the physics invariant.

7.4 The 2d Hofstadter model

Now, we want to make the model explicit. Consider a 2d square lattice with positions denoted by

$$\boldsymbol{R}_{ab} = \begin{pmatrix} a\Delta \\ b\Delta \\ 0 \end{pmatrix}, \qquad a, b \in \mathbb{Z} \tag{7.67}$$

and where $\Delta > 0$ is a lattice constant. The system is subject to to a magnetic field in z-direction, which is described by the vector potential

$$\boldsymbol{A} = \begin{pmatrix} 0 \\ Bx \\ 0 \end{pmatrix}. \tag{7.68}$$

The points $\boldsymbol{R}$ and $\boldsymbol{R'}$ are on the square lattice, whereas $\boldsymbol{r}$ is arbitrary but within the neihboring elementary cells, such that we write

$$\boldsymbol{R'} = \boldsymbol{R} + \begin{pmatrix} \Delta x \\ \Delta y \\ 0 \end{pmatrix}, \qquad \boldsymbol{r} = \boldsymbol{R} + \begin{pmatrix} \delta x \\ \delta y \\ 0 \end{pmatrix}, \tag{7.69}$$

where we have $\Delta x, \Delta y = \pm\Delta$ and $|\delta x|, |\delta y| \le \Delta$. Accordingly, we can parametrize the curves by

$$\boldsymbol{\gamma_1}(t) = \boldsymbol{R} + \begin{pmatrix} \delta x \\ \delta y \\ 0 \end{pmatrix} t, \qquad \boldsymbol{\gamma_2}(t) = \boldsymbol{r} + \begin{pmatrix} \Delta x - \delta x \\ \Delta y - \delta y \\ 0 \end{pmatrix} t, \qquad \boldsymbol{\gamma_3}(t) = \boldsymbol{R'} + \begin{pmatrix} -\Delta x \\ -\Delta y \\ 0 \end{pmatrix} t,$$
$$t \in [0, 1]. \tag{7.70}$$

The magnetic flux becomes

$$\begin{aligned} \Phi = \oint_{\boldsymbol{R}\to\boldsymbol{r}\to\boldsymbol{R'}\to\boldsymbol{R}} A(\boldsymbol{r'})d\boldsymbol{r'} &= \int_0^1 \boldsymbol{A}(\boldsymbol{\gamma_1}) \cdot \begin{pmatrix} \delta x \\ \delta y \\ 0 \end{pmatrix} dt + \int_0^1 \boldsymbol{A}(\boldsymbol{\gamma_2}) \cdot \begin{pmatrix} \Delta x - \delta x \\ \Delta y - \delta y \\ 0 \end{pmatrix} dt \\ &+ \int_0^1 \boldsymbol{A}(\boldsymbol{\gamma_3}) \cdot \begin{pmatrix} -\Delta x \\ -\Delta y \\ 0 \end{pmatrix} dt \\ &= \frac{B}{2}(\delta x \Delta y - \delta y \Delta x) \approx 0. \end{aligned} \tag{7.71}$$

This is just the (homogeneous field) times the area spanned by the triangle $(\boldsymbol{R}, \boldsymbol{r}, \boldsymbol{R'})$. For moderate magnetic fields and highly-localized Wannier functions – limiting the maximum range

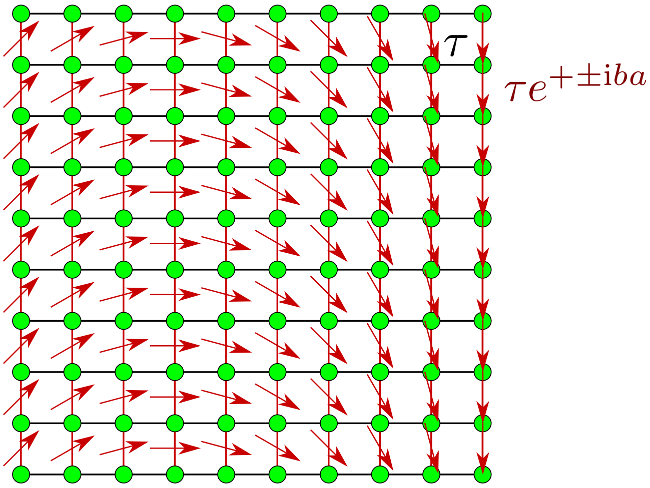

Figure 7.10: Visualization of the Hofstadter Hamiltonian for a magnetic field in z direction (perpendicular to the plane). Horizontal tunneling amplitudes do not have a relative phase, but vertical tunneling amplitudes are equipped with a phase factor that depends on the horizontal position (arrows).

of δ_x and δ_y, this contribution is negligible. Accordingly, we just use the Peierls substitution for originally (in absence of a magnetic field fully homogeneous hopping amplitudes)

$$\begin{aligned}\tau_{(a,b)(a+1,b)} &= \tau \exp\left\{ \mathrm{i}\frac{e}{\hbar}\int_{R_{a,b}}^{R_{a+1,b}} \boldsymbol{A}(\boldsymbol{r'})d\boldsymbol{r'} \right\} = \tau\,,\\ \tau_{(a,b)(a,b+1)} &= \tau \exp\left\{ \mathrm{i}\frac{e}{\hbar}\int_{R_{a,b}}^{R_{a,b+1}} \boldsymbol{A}(\boldsymbol{r'})d\boldsymbol{r'} \right\} = \tau e^{\mathrm{i}\frac{e}{\hbar}B\Delta a\Delta}\,. \end{aligned} \tag{7.72}$$

Here, we have just solved the trivial integrals along the x and y directions, which correspond to the shortest paths on the lattice.

Altogether, we arrive at a variant of the Hofstadter [6] Hamiltonian.

$$H = \tau\sum_{ab}\left[c_{a,b}^\dagger c_{a+1,b} + c_{a+1,b}^\dagger c_{a,b} + e^{+\mathrm{i}\frac{e}{\hbar}B\Delta^2 a} c_{a,b}^\dagger c_{a,b+1} + e^{-\mathrm{i}\frac{e}{\hbar}B\Delta^2 a} c_{a,b+1}^\dagger c_{a,b}\right]\,. \tag{7.73}$$

This Hamiltonian has trivial hopping amplitudes in x-direction and phase-modified hopping amplitudes in y-direction, see Fig. 7.10. It has a chiral symmetry, which can be constructed similar to the SSH chain (7.23) from computing the occupation of the even lattice sites only like in a checkerboard pattern

$$\Gamma = \exp\left\{ \mathrm{i}\pi \sum_{ij\,:\,i+j=\text{even}} c_{ij}^\dagger c_{ij} \right\}\,. \tag{7.74}$$

This will flip the sign of operatos on even sites and leave the sign of operators on odd sites invariant, such that we can immediately deduce $\Gamma H \Gamma = -H$. In addition, it will of course conserve the total particle number. Furthermore, there are symmetries related to the gauge freedom of the vector potential: Adding the gradient of any function $\boldsymbol{A} \to \boldsymbol{A} + \nabla\Phi(\boldsymbol{r}, t)$ will not change the magnetic field and must therefore have no observable effect. Within the Peierls substitution, we would get by defining $\Phi_{ab} = \Phi(a\Delta, b\Delta, 0, t)$ the fully equivalent Hamiltonian

$$\begin{aligned} H = \tau\sum_{ab}\Big[& e^{+\mathrm{i}\frac{e}{\hbar}(\Phi_{a+1,b}-\Phi_{a,b})} c_{a,b}^\dagger c_{a+1,b} + e^{-\mathrm{i}\frac{e}{\hbar}(\Phi_{a+1,b}-\Phi_{a,b})} c_{a+1,b}^\dagger c_{a,b}\\ &+ e^{+\mathrm{i}\frac{e}{\hbar}B\Delta^2 a} e^{+\mathrm{i}\frac{e}{\hbar}(\Phi_{a,b+1}-\Phi_{ab})} c_{a,b}^\dagger c_{a,b+1} + e^{-\mathrm{i}\frac{e}{\hbar}B\Delta^2 a} e^{-\mathrm{i}\frac{e}{\hbar}(\Phi_{a,b+1}-\Phi_{ab})} c_{a,b+1}^\dagger c_{a,b}\Big]\,, \end{aligned} \tag{7.75}$$

---

[6] D. R. Hofstadter (born 1945) is a US-american physicist and cognition scientist and the son of the Nobel laureate Robert Hofstadter (1915–1990).

and we see that this gauge transformation just induces a local phase on the creation and annihilation operators, which can be transformed away easily with a local rotation

$$c_{ab} \to c_{ab} e^{-\mathrm{i}\frac{e}{\hbar}\Phi_{ab}}\,, \tag{7.76}$$

which recovers Eq. (7.73).

When we assume **periodic boundary conditions**, the model becomes translationally invariant in y direction, but not in x direction. In y direction, one will only observe periodicity when $b/(2\pi) = \frac{e}{\hbar}B\Delta^2$ is a rational number: Then, some integer multiple of it will be integer again, leading to a reproduction of phases in the Hofstadter Hamiltonian. In contrast, when $b/(2\pi)$ is irrational, one will not be able to find a periodicity in x direction. Therefore, the complexity of the Hofstadter model can be reduced with a partial DFT of the second variable

$$c_{ab} = \frac{1}{\sqrt{N_y}} \sum_{k_y} d_{ak_y} e^{+\mathrm{i}k_y \frac{2\pi b}{N_y}}\,, \tag{7.77}$$

which allows to map it into a chain-like model with k_y-dependent on-site energies (we use $b = \frac{e}{\hbar}B\Delta^2$)

$$\begin{aligned}
H &= +\tau \sum_{ak_y} \left[d_{ak_y}^\dagger d_{a+1,k_y} + d_{a+1,k_y}^\dagger d_{a,k_y} + e^{+\mathrm{i}ba} d_{a,k_y}^\dagger d_{a,k_y} e^{+\mathrm{i}k_y \frac{2\pi}{N_y}} + e^{-\mathrm{i}ba} d_{a,k_y}^\dagger d_{a,k_y} e^{-\mathrm{i}k_y \frac{2\pi}{N_y}}\right] \\
&= \sum_{k_y} H_{k_y}\,, \\
H_{k_y} &= \sum_a 2\tau \cos\left(ba + k_y \frac{2\pi}{N_y}\right) d_{ak_y}^\dagger d_{ak_y} + \tau \sum_a \left[d_{ak_y}^\dagger d_{a+1k_y} + d_{a+1k_y}^\dagger d_{ak_y}\right]\,.
\end{aligned} \tag{7.78}$$

computing the eigenvalues of the H_{k_y} Hamiltonian now requires only the numerical diagonalization of an $N_x \times N_x$ matrix – sometimes called Harper problem (who studied this before Hofstadter). Obviously, as $a \in \mathbb{Z}$, the Harper problem is periodic under

$$b \to b + 2\pi m\,, \qquad m \in \mathbb{Z}\,. \tag{7.79}$$

Also here, its solution similarly strongly depends on whether $\Phi = \frac{1}{2\pi}b$ is a rational or irrational number. For example, when the magnetic field assumes particular values such that $bN_x/(2\pi)$ is an integer value, the Hamiltonian becomes periodic again, and we can apply an FT also in x direction. For sufficiently large N_x (corresponding to the realistic experimental situation) this condition can be satisfied by a dense set of b-values. In such cases, we may apply also a DFT in x direction

$$d_{ak_y} = \frac{1}{\sqrt{N_x}} \sum_{k_x} d_{k_x k_y} e^{+\mathrm{i}k_x \frac{2\pi a}{N_x}}\,. \tag{7.80}$$

This further maps the Hamiltonian into

$$H = \sum_{k_x,k_y} \left[2\tau \cos(k_x \frac{2\pi}{N_x}) d_{k_x k_y}^\dagger d_{k_x k_y} + \tau e^{+\mathrm{i}k_y \frac{2\pi}{N_y}} d_{k_x + \frac{N_x b}{2\pi},k_y}^\dagger d_{k_x k_y} + \tau e^{-\mathrm{i}k_y \frac{2\pi}{N_y}} d_{k_x - \frac{N_x b}{2\pi},k_y}^\dagger d_{k_x k_y}\right]\,. \tag{7.81}$$

Now, one particular possibility could be that $k_x \pm \frac{N_x b}{2\pi}$ is folded back onto k_x. Then, we just have decoupling modes. Another one would be that $k_x \pm \frac{N_x b}{2\pi}$ is equivalent to $-k_x$. Then we can decompose it into pairs of coupling modes. The next iteration would involve tripletts of coupled modes and so on. Every time we can ask how often the origin is enclosed by the surface

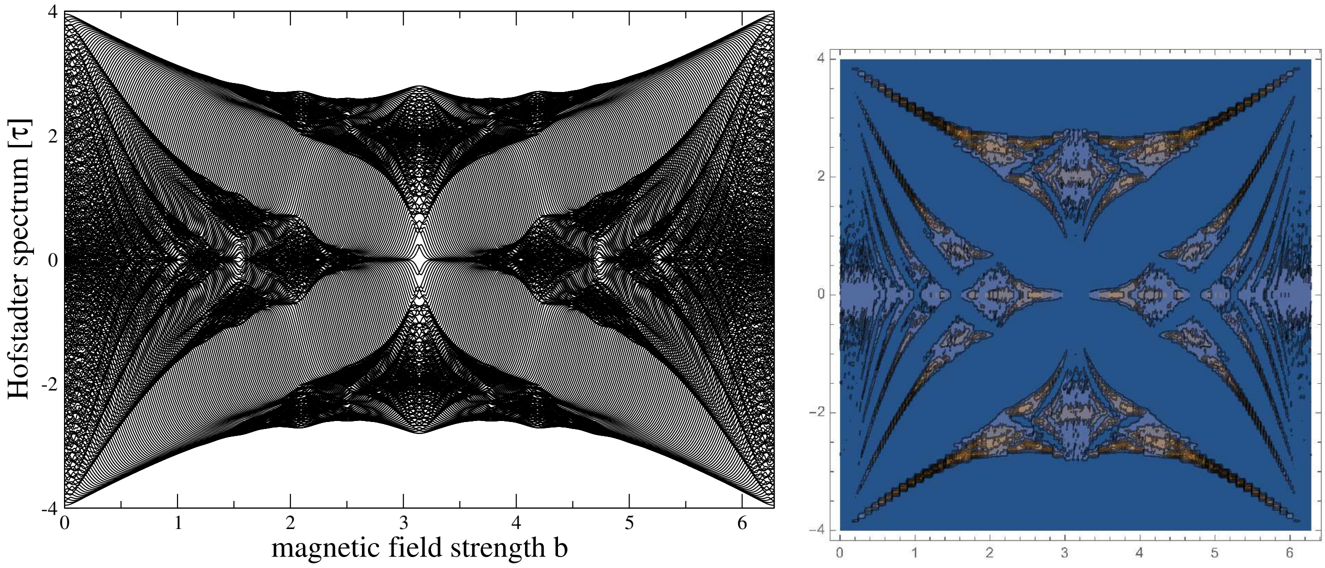

Figure 7.11: Left panel: Plot of energy levels versus dimensionless field strength $b = \frac{e}{\hbar}B\Delta^2$ and $\epsilon = 0$ resulting from Eq. (7.73) for a patch of 20 × 20 sites. The right panel shows the corresponding level density. The spectrum – known as Hofstadter butterfly – has in the infinite size limit a fractal structure and shows self-similarity.

parametrized by k_x and k_y, which provides some winding number classifying the topological phase.

However, for **open boundary conditions** translational invariance does not hold, and we need to set up the full matrix. The numerically calculated spectrum and corresponding level density for open boundary conditions is shown in Fig. 7.11 We can numerically add disorder to the Hamiltonian

$$\epsilon \to \epsilon + \delta\epsilon_{ab} \,, \qquad \tau e^{+\mathrm{i}\phi} \to \tau e^{+\mathrm{i}\phi}(1 + \delta_{ab}) \tag{7.82}$$

and compute the resulting Hofstadter butterfly spectrum again for tunnel disorder δ_{ab}, onsite-disorder $\delta\epsilon_{ab}$ and both types of disorder. One observes that some of the Hamiltonians eigenstates are quite inert to these perturbations, see Fig. 7.12.

7.5 Sketch: Connection to the Hall conductivity

To relate the spectral characteristics model to the Hall conductivity, one has to take the additional electric field along the probe into account. As before, we include it into the Hamiltonian by the minimal coupling procedure $p_\mu \to p_\mu - eA_\mu$ with the four-momentum $p_\mu = (\frac{E}{c}, \boldsymbol{A})$ and the four-vector potential $A_\mu = (\frac{\Phi}{c}, \boldsymbol{A})$, from which we can obtain electric and magnetic fields via

$$\boldsymbol{E} = -\nabla\Phi - \frac{\partial \boldsymbol{A}}{\partial t} = -\nabla\Phi \,, \qquad \boldsymbol{B} = \nabla \times \boldsymbol{A} \,. \tag{7.83}$$

Here, the first equation holds since we assume that the applied magnetic field is time-independent and so is the vector potential. As outlined in Ref. [25], the basic idea here is to transform the electric field away by a time-dependent gauge transformation of the vector potential

$$\boldsymbol{A} \to \boldsymbol{A'} = \boldsymbol{A} - (\nabla\Phi)t = \boldsymbol{A} + \boldsymbol{E}t \,, \tag{7.84}$$

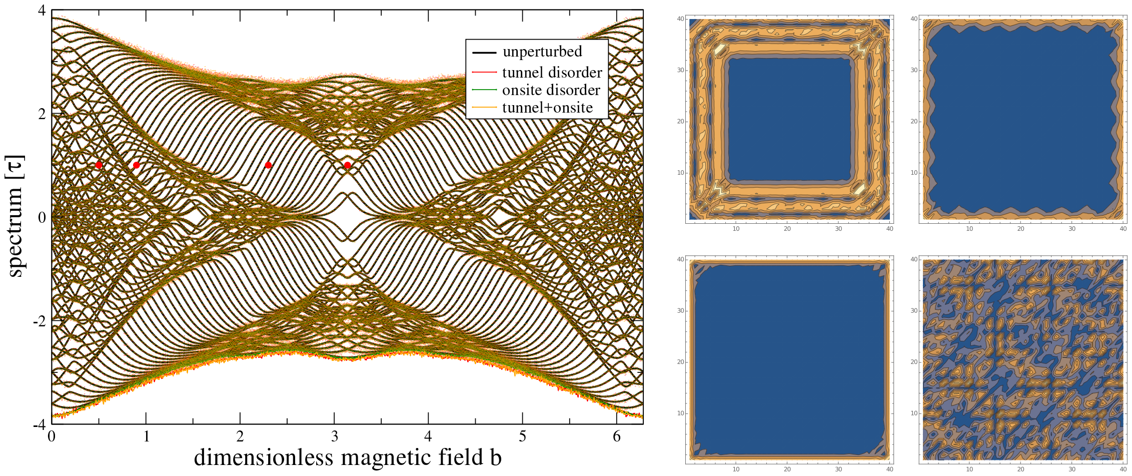

Figure 7.12: Plot of the Hofstadter spectrum versus dimensionless field strength b for a patch of $N_x = N_y = 10$. For various kinds of disorder, some parts of the spectrum – those where the level density is low – are remarkably robust, due to strong topological protection. As the wave functions (right, for a 40×40 grid without disorder, computed at the red dots on the left) demonstrate, these modes are localized at the boundaries (right).

such that one effectively goes into a frame where $\boldsymbol{E'} = 0$. The Hamiltonian under minimal coupling substitution now looks like

$$H = \frac{(\boldsymbol{p} - e\boldsymbol{A} - e\boldsymbol{E}t)^2}{2m} + V(\boldsymbol{r})\,. \tag{7.85}$$

In this case, we still have the Bloch theorem, just with time-dependent $\boldsymbol{k}$ vectors

$$|\Psi(\boldsymbol{k},t)\rangle = e^{+\mathrm{i}\boldsymbol{kr}} |u(\boldsymbol{k},t)\rangle\ , \tag{7.86}$$

where the $|u(\boldsymbol{k},t)\rangle$ satisfy the time-dependent Schrödinger equation

$$\mathrm{i}\hbar\partial_t |u(\boldsymbol{k},t\rangle = \left[\frac{1}{2m}\left(-\mathrm{i}\hbar\nabla + \hbar\boldsymbol{k}(t)\right)^2 + V(\boldsymbol{r})\right] |u(\boldsymbol{k},t)\rangle\ , \qquad \boldsymbol{k}(t) = \boldsymbol{k} - \frac{e}{\hbar}\boldsymbol{E}t\,. \tag{7.87}$$

The momentum is thus shifted accordingly. These equations are in principle valid for an arbitrary strength of the electric field. However, when the field is small, the transformation in the time-dependent Schrödinger equation is slow, such that we may use the adiabatic theorem. Let for fixed time the corresponding eigenvector problem be given by

$$H(\boldsymbol{k}) |u_n(\boldsymbol{k})\rangle = \epsilon_n(\boldsymbol{k}) |u_n(\boldsymbol{k})\rangle \tag{7.88}$$

and let the applied field as in the Hall effect point in the x direction. When we start the evolution in the n-th eigenstate at time $t = 0$, the time-dependent solution can be written as

$$|u(\boldsymbol{k}(t))\rangle = |u_n(\boldsymbol{k}(t)\rangle + \mathrm{i}eE_x \sum_{n'\neq n} \frac{|u_{n'}(\boldsymbol{k}(t))\rangle \langle u_{n'}(\boldsymbol{k}(t))| \frac{\partial}{\partial k_x} |u_n(\boldsymbol{k}(t))\rangle}{\epsilon_n(\boldsymbol{k}) - \epsilon_{n'}(\boldsymbol{k})}\,. \tag{7.89}$$

To obtain the velocity in y direction (perpendicular to both magnetic field and electric field), we calculate the expectation value to linear order in E_x

$$\begin{aligned} \langle v_y \rangle &= \langle u(\boldsymbol{k})| v_y |u(\boldsymbol{k})\rangle \\ &= \langle u_n| v_y |u_n\rangle + \left[\mathrm{i}eE_x \sum_{n'\neq n} \frac{\langle u_n| v_y |u_{n'}\rangle \langle u_{n'}| \frac{\partial}{\partial k_x} |u_n\rangle}{\epsilon_n - \epsilon_{n'}} + h.c.\right] + \ldots \end{aligned} \tag{7.90}$$

Now, we can express the velocity operator as

$$\boldsymbol{v} = \frac{1}{\hbar}\frac{\partial H(\boldsymbol{k})}{\partial \boldsymbol{k}} , \tag{7.91}$$

and specifically $v_y = \frac{1}{\hbar}\partial_{k_y} H(k_x, k_y)$. By performing suitable derivatives of the eigenvalue equation (7.88), we get identities like

$$\langle u_n| \nabla_{\boldsymbol{k}} H(\boldsymbol{k}) |u_{n'}\rangle = (\epsilon_n - \epsilon_{n'}) \left\langle \frac{\partial u_n}{\partial \boldsymbol{\kappa}} | u_{n'} \right\rangle , \tag{7.92}$$

which we can insert in the expectation value of the velocity operator

$$\langle v_y\rangle = \frac{1}{\hbar}\frac{\partial \epsilon_n}{\partial k_y} - \mathrm{i}\frac{eE_x}{\hbar}\left[\left\langle \frac{\partial u_n}{\partial k_x}|\frac{\partial u_n}{\partial k_y}\right\rangle - \left\langle \frac{\partial u_n}{\partial k_y}|\frac{\partial u_n}{\partial k_x}\right\rangle\right] \tag{7.93}$$

Each volume element in k space contributes to the total velocity, such that we get the Hall current

$$\langle j_y\rangle = \int \frac{dk_x dk_y}{(2\pi)^2} \langle v_y(k_x, k_y)\rangle , \tag{7.94}$$

and to get the Hall conductivity, we have to divide by the longitudinal electric field E_x, which yields [26]

$$\sigma_H = \frac{e^2}{h}\int \frac{\mathrm{i} dk_x dk_y}{2\pi}\left[\left\langle \frac{\partial u_n}{\partial k_x}|\frac{\partial u_n}{\partial k_y}\right\rangle - \left\langle \frac{\partial u_n}{\partial k_y}|\frac{\partial u_n}{\partial k_x}\right\rangle\right] . \tag{7.95}$$

The integral on the r.h.s. is the Chern number

$$C = \int \frac{\mathrm{i} dk_x dk_y}{2\pi}\left[\left\langle \frac{\partial u_n}{\partial k_x}|\frac{\partial u_n}{\partial k_y}\right\rangle - \left\langle \frac{\partial u_n}{\partial k_y}|\frac{\partial u_n}{\partial k_x}\right\rangle\right] . \tag{7.96}$$

Since it is a topological invariant, it can only assume integer values.

7.6 The 2d Haldane model

Another celebrated but simple model at which topological effects can be discussed is the Haldane [7] model [27]. It is based on a model for graphene and thereby corresponds to a 2d hexagonal lattice. The formal difference to the Hofstadter Hamiltonian is that in the Haldane model, one does not determine the phases from a Peierls substitution. (If one would want to motivate these phases from a Peierls substitution, it would require a periodic magnetic field.) The formal difference is therefore that the phases in the Hamiltonian are also always strictly periodic,see Fig. 7.13 Thus, any sublattice (i.e. red or blue) is constructed from integer combinations of the two basis vectors

$$\boldsymbol{w}_1 = \frac{\Delta}{2}\begin{pmatrix} +\sqrt{3} \\ 3 \\ 0 \end{pmatrix} , \qquad \boldsymbol{w}_2 = \frac{\Delta}{2}\begin{pmatrix} -\sqrt{3} \\ 3 \\ 0 \end{pmatrix} . \tag{7.97}$$

Here, Δ denotes the next-neighbour distance, which can be parametrized as

$$\boldsymbol{a}_1 = \Delta\begin{pmatrix} 0 \\ 1 \end{pmatrix} , \qquad \boldsymbol{a}_2 = \Delta\begin{pmatrix} -\sqrt{3}/2 \\ -1/2 \end{pmatrix} , \qquad \boldsymbol{a}_3 = \Delta\begin{pmatrix} +\sqrt{3}/2 \\ -1/2 \end{pmatrix} . \tag{7.98}$$

---

[7] Frederick Duncan Michael Haldane (born 1951) is a british physicist and Nobel laureate.

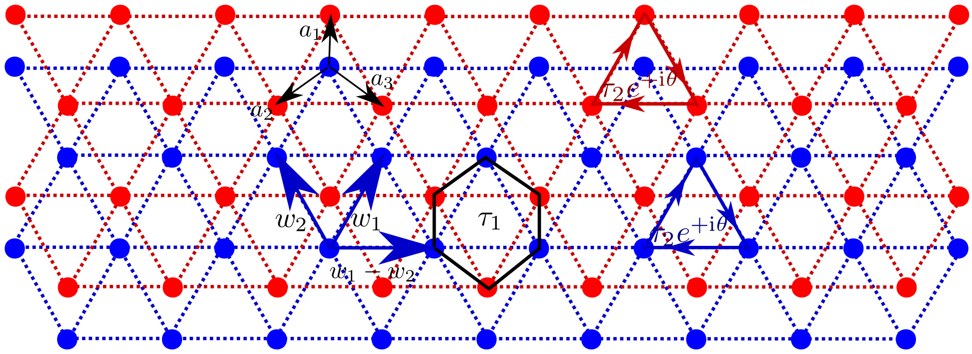

Figure 7.13: Visualization of the Haldane model. It is implemented on a honeycomb lattice that is constructed from two trigonal sublattices (blue and red), spanned by basis vectors $\boldsymbol{w}_i$. The vectors $\boldsymbol{a}_i$ connect the next neighbours, and in particular one gets the red sublattice by adding $\boldsymbol{a}_1$ to the blue sublattice sites. The model includes next-neighbour τ_1 (solid black) and next-next neighbour $\tau_2 e^{\pm i\theta}$ (dotted red and blue) hopping interactions, where the latter come with a + phase when the corresponding triangle is traversed clockwise, and with the negative phase when it is traversed counter-clockwise.

To generate the full honeycomb lattice, we need to consider the basis by adding e.g. the vector $\boldsymbol{a}_1$ to each of the blue lattice sites. Formally, we can parametrize the positions of all lattice points of one sublattice (e.g. blue) by a double index (ij), where

$$\boldsymbol{R}_{ij}^{(1)} = i\boldsymbol{w}_1 + j\boldsymbol{w}_2 \,, \tag{7.99}$$

and the other lattice points (then red) by

$$\boldsymbol{R}_{ij}^{(2)} = \boldsymbol{R}_{ij}^{(1)} + \boldsymbol{a}_1 \,. \tag{7.100}$$

Let $a_{ij,1}$ denote the annihilation operator for an electron at site $i\boldsymbol{w}_1 + j\boldsymbol{w}_2$ (blue lattice sites) and $a_{ij,2}$ the annihilation operator for an electron at site $i\boldsymbol{w}_1 + j\boldsymbol{w}_2 + \boldsymbol{a}_1$. Then, the Haldane model Hamiltonian reads

$$\begin{aligned} H = & -\tau_1 \sum_{ij} \left[a_{ij,2}^\dagger a_{ij,1} + a_{ij,1}^\dagger a_{ij,2} \right] \\ & - \tau_2 \sum_{ij} \left[e^{+i\theta} a_{i+1,j,1}^\dagger a_{ij,1} + e^{-i\theta} a_{i,j+1,1}^\dagger a_{ij,1} + e^{-i\theta} a_{i+1,j-1,1}^\dagger a_{ij,1} + \text{h.c.} \right] \\ & - \tau_2 \sum_{ij} \left[e^{+i\theta} a_{i+1,j,2}^\dagger a_{ij,2} + e^{-i\theta} a_{i,j+1,2}^\dagger a_{ij,2} + e^{-i\theta} a_{i+1,j-1,2}^\dagger a_{ij,2} + \text{h.c.} \right] \\ & + \epsilon \sum_{i,j} \left[a_{ij,1}^\dagger a_{ij,1} - a_{ij,2}^\dagger a_{ij,2} \right] \,. \end{aligned} \tag{7.101}$$

Here, τ_1 denotes the next-neighbor tunneling amplitude, and τ_2 the next-to-next neighbour tunneling amplitude. The phase θ in the next-to-next neighbour tunneling amplitude will be considered as $\theta = \pi/2$ in the following, such that the next-neighbor hopping amplitudes are purely imaginary.

Since the Hamiltonian of the model is always periodic, we can – for periodic boundary conditions – use a 2d Fourier transform

$$a_{ij,\alpha} = \frac{1}{\sqrt{N}} \sum_{\boldsymbol{k} \in 1.\text{BZ}} b_{\boldsymbol{k},\alpha} e^{i\boldsymbol{k}\cdot\boldsymbol{R}_{ij,\alpha}} \,. \tag{7.102}$$

Figure 7.14: Plot of the dispersion relation for for $\epsilon = 0$ and $\tau_2 = 0$ (graphene limit) in quasi-momentum space. At the degenerate points, the dispersion relation is linear, and electrons behave like massless Dirac fermions.

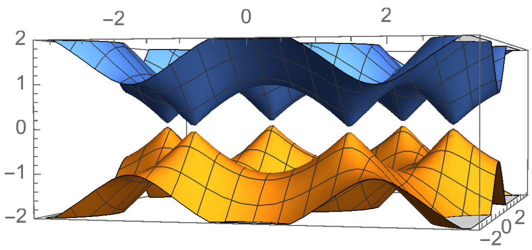

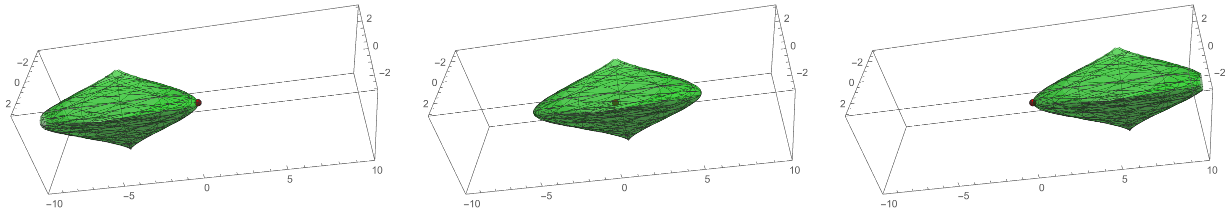

Figure 7.15: Plot of the surface parametrized by (7.105) for $\epsilon = -3\sqrt{3}\tau_2$ (left), $\epsilon = 0$ (middle), and $\epsilon = +3\sqrt{3}\tau_2$ (right). The red ball marks the origin. Other parameters $\tau_1 = \tau_2$, $\theta = \pi/2$. The phase which includes the origin is topologically non-trivial.

Here, $\boldsymbol{k} = (k_x, k_y)$ runs over the Brillouin zone of the reciprocal lattice. Inserting this in the Hamiltonian yields a complete decoupling, such that only the A and B sublattices couple to each other

$$H = \sum_{\boldsymbol{k}} (b^\dagger_{\boldsymbol{k},1} b^\dagger_{\boldsymbol{k},2}) H_k \begin{pmatrix} b_{\boldsymbol{k},1} \\ b_{\boldsymbol{k},2} \end{pmatrix} , \tag{7.103}$$

where

$$H_{\boldsymbol{k}} = h_0(\boldsymbol{k}) + h_x(\boldsymbol{k})\sigma^x + h_y(\boldsymbol{k})\sigma^y + h_z(\boldsymbol{k})\sigma^z \tag{7.104}$$

with specifically

$$\begin{aligned} h_x(\boldsymbol{k}) &= -\tau_1 \left[\cos(\boldsymbol{k}\boldsymbol{a}_1) + \cos(\boldsymbol{k}\boldsymbol{a}_2) + \cos(\boldsymbol{k}\boldsymbol{a}_3)\right] , \\ h_y(\boldsymbol{k}) &= -\tau_1 \left[\sin(\boldsymbol{k}\boldsymbol{a}_1) + \sin(\boldsymbol{k}\boldsymbol{a}_2) + \sin(\boldsymbol{k}\boldsymbol{a}_3)\right] , \\ h_z(\boldsymbol{k}) &= \epsilon - 2\tau_2 \left[\sin(\boldsymbol{k}(\boldsymbol{w}_1 - \boldsymbol{w}_2)) + \sin(\boldsymbol{k}\boldsymbol{w}_2) - \sin(\boldsymbol{k}\boldsymbol{w}_1))\right] . \end{aligned} \tag{7.105}$$

Here, we have used the vectors defined in Eqns. (7.98) and (7.97).

When $\tau_2 = 0$, and $\epsilon = 0$, we can recover the Dirac-cones known for graphene, see Fig. 7.14.

In general, i.e., also for finite ϵ and τ_2, this defines a surface as a function of $\boldsymbol{k}$ in $\mathbb{R}^3$, which may or may not wind around the origin. In Fig. 7.15 this surface is shown as a function of $\boldsymbol{k}$, where one can see that the topological phase transition occurs when the surface encloses the origin.

We are also free to choose other phases than $\phi = \pi/2$ (not shown). Then, the topological phase transition occurs when

$$\epsilon = \pm 3\sqrt{3}\tau_2 \sin(\theta) . \tag{7.106}$$

Then, one observes that the parametrized surface becomes flatter and flatter. When it intersects itself at $\phi = 0$, it changes its orientation, and thereby the corresponding Chern number may assume negative values. This means that, for the present example, it can assume values $C \in \{-1, 0, +1\}$.

Bibliography

[1] T. Brandes, Theoretische Festkörperphysik, Vorlesungsskript, TU Berlin (2014). http://www1.itp.tu-berlin.de/brandes/fk2010.pdf

[2] T. Brandes, Quantenmechanik II, Vorlesungsskript, TU Berlin (2012). http://www1.itp.tu-berlin.de/brandes/qm2011.pdf

[3] G. Czycholl, Theoretische Festkörperphysik, Springer, Berlin Heidelberg (2008).

[4] N. W. Ashcroft and N. D. Mermin, Solid State Physics, Holt Sounders (1987).

[5] L. van Hove, Phys. Rev. **89**, 1189 (1953).

[6] L. D. Landau and J. M. Lifschitz, Elastizitätstheorie, Akademie-Verlag Berlin (1983).

[7] D. J. Griffiths, Introduction to Electrodynamics, Prentice-Hall New Jersey (1999).

[8] J. D. Jackson, Classical Electrodynamics, Wiley New York (1999).

[9] J. Lindhard, On the properties of a gas of charged particles, Dan. Mat. Fys. Medd. **28** (1954).

[10] F. Stern, Polarizability of a Two-Dimensional Electron Gas, Phys. Rev. Lett. **18**, 546 (1967).

[11] P. J. Hirschfeld, Solid State Physics II, lecture notes (2013). http://www.phys.ufl.edu/~pjh/teaching/phz7427/

[12] G. Schaller, T. Krause, T. Brandes, and M. Esposito, Single-electron transistor strongly coupled to vibrations: counting statistics and fluctuation theorem, New Journal of Physics **15**, 033032 (2013).

[13] C. Kittel, Quantum Theory of Solids, Wiley (1987).

[14] L. N Cooper, Bound Electron Pairs in a Degenerate Fermi Gas, Physical Review **104**, 1189 (1956).

[15] J. Bardeen, L. N Cooper, J. R. Schrieffer, Theory of Superconductivity, Physical Review **108**, 1175 (1957).

[16] C. Timm, Theory of Superconductivity, lecture notes (2012). https://www.physik.tu-dresden.de/~timm/personal/teaching/thsup_w11/Theory_of_Superconductivity.pdf

[17] G. Schaller, Advanced Mathematical Methods in Theoretical Physics, lecture notes (2017). http://www1.itp.tu-berlin.de/schaller/download/FMMTP.pdf

[18] S. Sachdev, Quantum Phase Transitions, Cambridge University Press, (2000).

[19] H.-P. Breuer and F. Petruccione, The Theory of Open Quantum Systems, Oxford University Press, (2002).

[20] G. Schaller, Theory of non-equilibrium quantum systems, lecture notes (2017). `http://www1.itp.tu-berlin.de/schaller/download/TQSNE.pdf`

[21] G. Schaller, G. Kießlich, and T. Brandes, Transport statistics of interacting double dot systems: Coherent and non-Markovian effects, Physical Review B **80**, 245107 (2009).

[22] G. Engelhardt, Topology in weakly and strongly nonlinear bosonic systems, dissertation TU Berlin (2017).

[23] S. Böhling, G. Engelhardt, G. Platero, and G. Schaller, Thermoelectric performance of topological boundary modes, Physical Review B **98**, 035132, (2018).

[24] K. von Klitzing, The quantized Hall effect, Rev. Mod. Phys. **58**, 519 (1986).

[25] A. Bohm, A. Mostafazadeh, H. Koizumi, Q. Niu, and J. Zwanziger, The Geometric Phase in Quantum Systems, Springer, Berlin (2003).

[26] D. Thouless, M. Kohmoto, N. Nightingale, and N. de Nijs, Quantized Hall Conductance in a Two-Dimensional Periodic Potential, Physical Review Letters **49**, 405 (1982).

[27] F. D. M. Haldane, Model for a Quantum Hall Effect without Landau Levels, Physical Review Letters **61**, 2015 (1988).

[28] lecture material Topology in Condensed Matter, `http://topocondmat.org/`.